Redox regulation of the cell cycle in *Arabidopsis thaliana*

Ambra De Simone

Submitted in accordance with the requirements for the degree of
Doctor of Philosophy

The University of Leeds

Faculty of Biological Sciences

June 2016

I confirm that the work submitted is my own and that appropriate credit has been given where reference has been made to the work of others.

Acknowledgements

I thank my mentor and supervisor Prof Christine H. Foyer, for her guidance during these years and encouragement to become a better scientist.

I thank my co-supervisor Dr Chris West, for his help, patience and priceless advice.

I thank Dr Yoselin Benitez Alfonso, for looking after me and caring about my work and heart.

I thank Dr Rob Hancock, for his support and hosting at the James Hutton Institute, Dundee.

I thank Dr Wim J. J. Soppe, Natanael Viñegra and Wozny from Max Planck Institute for Plant Breeding Research, Cologne, Germany, for providing raw RNAseq data.

I thank Michael Wilson, for his precious bioinformatics expertise.

I thank my fellow lab mates, Barbara, Gloria, Yat, Danny and James, for sharing ideas, excitement and all the laughs.

I thank my friends, Gloria, Kasia, Mercedes, Rocio and Rupesh for making my time even sweeter.

I thank the Ecoseed consortium for funding my PhD studies.

Finally, I thank my family for being there anytime.

Abstract

Seed germination is critical for plant establishment but little is known about how the reduction-oxidation (redox) environment of the cells in the emerging root meristem influences cell division. The glutathione redox potentials of the nuclei and cytosol were determined using redox-sensitive green fluorescent protein (roGFP2) in the Arabidopsis root apical meristem, in which cell cycle had been synchronised using hydroxyurea, within the period immediately after germination, in order to characterise the relationships between cellular redox status and cell cycle progression. The average glutathione redox potentials of the nuclei and cytosol were -297.5 mV ± 0.7 and -292.8 mV ± 0.6 respectively. However, a transient oxidation occurred in compartments during the G1 phase of the cell cycle, as determined by the expression of cell cycle markers (*CYCB1;1-GUS*, cytrap and cyclins). The effect of low antioxidant buffering capacity on the gene expression profiles of dry and imbibed seeds as well as the redox potentials of the nuclei and cytosol was determined using the ascorbate deficient *vtc2-1* and *vtc2-4* mutants. The glutathione redox potentials of the nuclei in the proliferation zone of *vtc2-1* radicles expressing roGPF2 were -282.3 mV ± 0.5 and the cytosol was -282.9 mV ± 0.5. These increased levels of oxidation persisted throughout the period of measurement, a feature that was linked to changes in cell cycle progression. The transcriptome profiles of *vtc2-1* and *vtc2-4* dry seeds compared with that of wild-type seeds revealed large changes in the abundance of transcripts encoding transcription factors, redox components, and proteins involved in cell cycle and secondary metabolism. Fewer differences were shown for the transcriptome profiles of *vtc2-1* and *vtc2-4* imbibed seeds. Taken together these data show that antioxidant buffering capacity exerts a strong influence on cell cycle progression and gene expression without having marked effects on germination.

Contents

List of Figures

List of Tables

List of Abbreviations

½ MS	Half strength Murashige and Skoog medium
ABA	Abscisic acid
APX	Ascorbate peroxidase
ATP	Adenosine triphosphate
Bcl-2	B-cell lymphoma 2
BR	Brassinosteroid
BSO	L-buthionine (S,R)-sulfoximine
BY-2	Bright yellow cell lines
cad2	Cadmium sensitive mutant
CAK	Cyclin A kinase
CDK	Cyclin-dependent kinase
CI	Mitochondrial respiratory chain complex I
CLSM	Confocal laser scanning microscopy
CLT	Chloroquine resistance like transporter
Col-0	Wild type ecotype Columbia-0
Cytrap	Cell cycle tracking in plant cells
DAPI	4',6-diamidino-2-phenylindole
DHA	Dehydroascorbate
DHAR	Dehydroascorbate reductase
DNA	Deoxyribonucleic acid
DTT	Dithiothreitol
EDTA	Ethylenediaminetetraacetic acid
EdU	5-ethynyl-2'-deoxyuridine
EMS	Ethyl-methanesulfonate
Fru-6P	Fructose 6 phosphate
GA	Gibberellic acid
GCL	Glutamate cysteine ligase
GFP	Green fluorescent protein
GLDH	L-Galactose dehydrogenase
GMP	GDP-Man pyrophosphorylase
GSH	Glutathione
GMP	GDP-D-Mannose-3’,5’ epimerase

GSH-S	Glutathione synthetase
GSSG	Glutathione disulphide
GST	Glutathione transferase
GT	Glycosyltransferases
GUS	β-Glucuronidase
GR	Glutathione reductase
GRX	Glutaredoxin
H_2O_2	Hydrogen peroxide
H3	Histone 3
HCl	Hydrogen chloride
HTR2	Histone three related 2
HU	Hydroxyurea
ICK	Cyclin-dependent kinase inhibitor
JA	Jasmonic acid
K3[Fe(CN)^6]	Potassium ferricyanide
KCl	Potassium chloride
KH_2PO_4	Monopotassium phosphate
LEA	Late embryogenesis abundant protein
MDHA	Monodehydroascorbate
MES	2-ethanesulfonic acid
MS	Murashige and Skoog
$Na2HPO_4$	Sodium phosphate dibasic
NaCl	Sodium chloride
NADPH	Nicotinamide adenine dinucleotide phosphate
ND	NADH-ubiquinone oxidoreductase chain
NIH3T3	Fibroblast 3T3 cell line
O^{2-}	Superoxide
PBS	Phosphate-buffered saline
PCA	Principal component analysis
PCR	Polymerase chain reaction
PER	Peroxidase
PGI	Phosphoglucose isomerase
PI	Propidium iodide

PLT3	PLETHORA3
PMI	Phosphomannose isomerase
PMM	Phosphomannomutase
QC	Quiescent centre
RB	Retinoblastoma
rml1	Root meristemless1 mutants
RNA	Ribonucleic acid
roGFP2	Redox sensitive GFP2
ROS	Reactive oxygen species
SA	Salicylic acid
SAM	Shoot apical meristem
SAR	Systemic acquired resistance
SCF	F-box containing complex
TAE	Tris-acetate-EDTA
TRX/NTR	NADPH-thioredoxin reductases
TPM	Transcripts per kilobase million
Tyr	Tyrosine
VTC	Vitamin C
vtc2-1	Ascorbate deficient *vtc2-1* EMS mutants
vtc2-4	Ascorbate deficient *vtc2-4* T-DNA mutants
WOL	WOODEN LEG
WOX5	WUSCHEL related homeobox

Chapter 1. Introduction

The availability of high quality seeds is pivotal to the sustainability of agriculture, food security and conservation of wild species. The seeds of crop plants are used directly or indirectly to fulfil the needs of the human diet. Seeds are used for plant propagation and crop breeding, as well as for animal feed and the generation of a wide range of chemicals such as oils. The life cycle of flowering plants relies on seeds, which contain the embryo of the next generation (Figure 1.1). The embryo is surrounded by the endosperm and the seed coat. The endosperm controls embryo growth by supplying nutrients and together with the seed coat acts as a physical and chemical barrier during germination (Yan et al 2014). If favourable environmental conditions are present, the growth of the embryo will result in the break of the coat and once the cell division has started the establishment of the seedling (Figure 1.1). This process is called germination and it depends on different internal and external factors (Bashandy et al 2010). Moreover, environmental conditions sensed during the seed formation on the mother plant will influence the future germination response. Environmental stresses sensed by the mother plant will also strongly influence seed quality undermining seed performance and leading to economic losses. For example, drought conditions during seed maturation on the mother plant changes the properties of the maternal tissue that will form the seed coat affecting in this way the seed longevity and the ability to germinate (Caron et al 2015, Hoyle et al 2008). The quantity and quality of seeds produced by crop species are crucial for agricultural productivity, while the seeds of wild species are essential to ecosystems. Seed yield is the major factor determining the commercial success of grain crops. However, significant seed wastage occurs worldwide because of a range of determinants from inherent seed traits and sub-optimal seed performance to poor storage conditions. Furthermore, increases in seed wastage losses are likely to occur as a result of climate change (Foyer & Noctor 2009). The

predicted higher global temperatures and increased periods of drought will have a strong impact on the agricultural productivity, at least in part through effects on seed production and quality. High temperature and drought conditions lead to reactive oxygen species accumulation, imbalance of the redox homeostasis and undermines plant growth (Sharma et al 2012). Redox changes perceived by the mother plant will affect the redox state of the seed and therefore, its development and germination (Garnczarska et al 2009). Because these mechanisms have been poorly studied, the aim of my project will be to understand what determines the cellular redox state during seed germination. I will focus the attention on the onset of the cell cycle and in particular, how changes in the redox state influences the cell cycle in the early stages of germination.

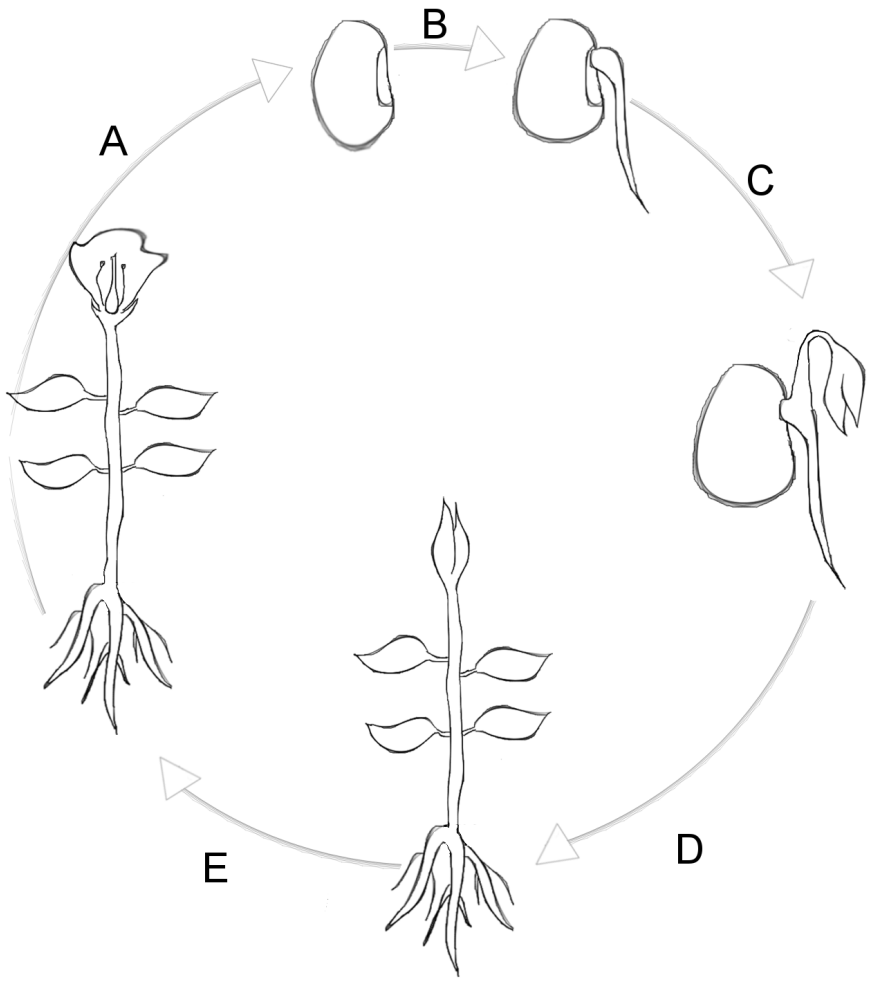

Figure 1.1 Diagram of the life cycle in flowering plants.

(A) Embryogenesis and seed maturation. The embryo develops on the mother plant. Seeds undergo a set of morphological and biochemical changes to become physiologically independent from the mother plant. (B) Germination. Non-dormant mature seeds germinate upon water uptake in permissive conditions of light and temperature. The seed coat breaks and the embryonic root protrudes. (C) Appearance of cotyledons. In the case of hypogeal germination cotyledon remains under the soil and the epicotyl elongates pushing the plumule upwards. (D) Vegetative growth. Plants photosynthesise and accumulate mass before entering the reproductive phase. (E) Flowering. The reproductive organs are formed. The male and female gametes fuse to produce a zygote, which develops into an embryo.

1.1 Seed biology in Arabidopsis

Arabidopsis thaliana (Arabidopsis) is a frequently used model in plant biology and genetics because of its small genome size and rapid life cycle. Arabidopsis seeds have an endospermic structure with the embryo surrounded by a single layer of endosperm. In Arabidopsis the seed is formed through double fertilization during which one ovule receives two sperm cells. One sperm cell produces a zygote, which develops into the embryo, while the second sperm cell fuses with two maternal nuclei to produce the triploid endosperm. The embryo contains the organs required for the early stages of seedling development including the shoot apical meristem (SAM), cotyledons (the embryonic leaves), hypocotyl, the radicle (the embryonic root) and the root meristem. In Arabidopsis the endosperm is one cell layer, which protects and feeds the embryo during its development but it also regulates the embryo growth at later stages (Kondou et al 2008). The maternal layers that form the seed coat enclose the embryo and endosperm. Upon exposure to water mucilage is secreted from the seed coat and surrounds the seed. Mucilage in Arabidopsis is not necessary for seed viability and germination (Haughn & Western 2012). During germination, the embryo contained within a seed expands and grows resulting in the establishment of the seedling (Figure 1.2) (Maia et al 2011).

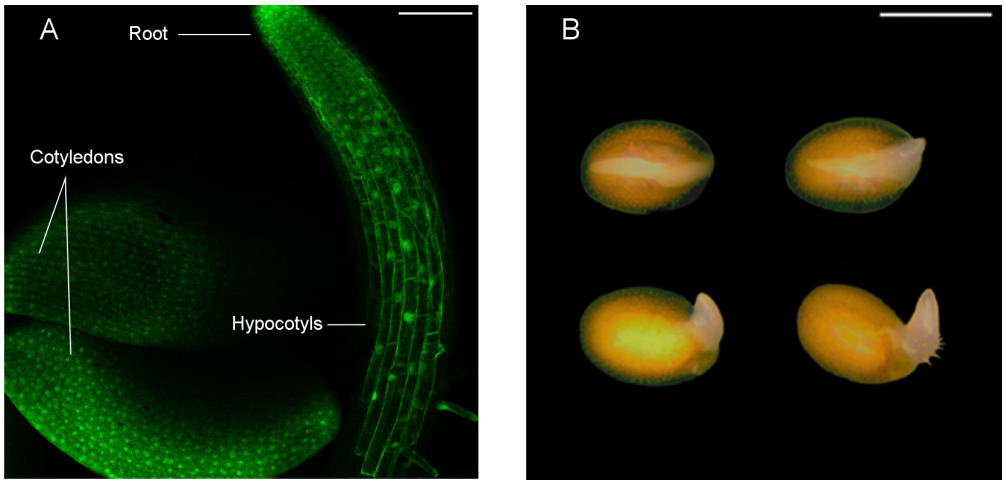

Figure 1.2. Embryo structure and seed developmental stages during germination in Arabidopsis.

(A) Confocal laser scanning microscope (CLSM) image of Arabidopsis imbibed embryo expressing roGFP2 in the root, cotyledons and hypocotyls. Scale bar 100 µm. (B) Arabidopsis seed germination showing testa rupture (top left), protrusion of the emerging radicle (top right), end of germination (bottom left) and first root hair appearance (bottom right). Scale bar 1 mm. Figure B taken from Maia et al (2011)

1.2 Seed germination and dormancy in Arabidopsis

Seed germination requires viable seeds and favourable environmental conditions including water, temperature, oxygen and light (Chory 1997). Germination begins with imbibition and changes in the fresh weight due to water uptake. Imbibition is followed by ATP and protein synthesis; increase in metabolic and mitochondrial activity and metabolism of storage reserves (Dong et al 2015, Logan et al 2001, Weitbrecht et al 2011). The early phase of seed germination in Arabidopsis is also characterized by biochemical changes, alteration in transcripts, proteins and hormone levels that contribute to the plant establishment. Moreover, changes in the redox state of proteins in cereals have been shown (Alkhalfioui et al 2007). In dry seeds proteins are present in oxidized form which are converted in a more reduce state after imbibition. In wheat the reduction of disulphide groups of the storage proteins has been shown to increase during seed germination (Yano et al 2001). Studies in Medicago have shown that a large number of proteins, which are oxidized or partly reduced in dry seeds become more reduced upon germination (Alkhalfioui et al 2007). Germination is a complex physiological process started by triggers such as temperature, light or alteration in the hormonal balance between inhibitors and promoters of germination, which lead to the break of the state of quiescence (El-Maarouf-Bouteau & Bailly 2008). An important function of most seeds is the ability to control or delay germination, a property that permits seed to germinate when conditions are favourable. Many species of plants have “orthodox seeds” that can withstand desiccation and thus delay germination for prolonged periods by entering a process called dormancy. Orthodox seeds are able to tolerate desiccation to very low water contents. These seeds can be stored in a dry state at low temperatures for many years (Berjak & Pammenter 2013). In contrast, recalcitrant seeds are sensitive to desiccation. Recalcitrant seeds are characterized by high initial water contents and they are extremely difficult to store without rapid loss of

viability. Often germination starts after the break of dormancy, a period during which plant slows down the metabolic process and does not grow in order to retain resources until conditions are favourable. The transition between seed dormancy and germination is an important ecological and commercial trait because it represents a critical stage in the plant life cycle.

Seed dormancy is important because it prevents or delays germination. While seed dormancy is useful because it inhibits pre-harvest sprouting or vivipary it can also cause problems, especially in the horticultural and forest industries because it can be deep and difficult to break. In some cases, chemical treatments may be required to promote germination. Two plant hormones, abscisic acid (ABA) and gibberellic acid (GA) are the major endogenous regulators of the transition from dormancy to germination, and they regulate this process in an antagonistic fashion (Kucera et al 2005). However, many endogenous triggers and environmental signals such as phytohormones, nutrients, temperature and light also affect seed dormancy. Hence, dormancy is an important determinant of the seed and plant fate. Dormancy-germination transition can be regulated by itself or by environmental factors (Holdsworth et al 2008). Internal regulation includes inhibitory factors due to the seed coat or endogenous dormancy. On the other hand, adverse environmental conditions include improper temperature, oxygen and in some cases light factors. Seed quality depends on external factors such as storage conditions and maternal effects and internal factors such as dormancy. GSH is the major buffer for reactive oxygen species (ROS) contributing to maintain the intracellular redox balance (Foyer & Noctor 2011). GSH is involved also in flowering process and in release of dormancy signalling (El-Maarouf-Bouteau & Bailly 2008, Ogawa et al 2001). In dry seeds the antioxidant enzyme activity is limited by a lack of water so that glutathione is the major antioxidant for ROS. Reactive oxygen species oxidize GSH to GSSG with an accumulation of the latter in dry seeds (Grill 1993, Weitbrecht et al 2011). Oxidative processes are required for after ripening and loss of dormancy but

prolonged oxidations lead to oxidative damage (Bailly 2004). Changes in intracellular redox state may have a role in signalling of dormancy release and germination. In addition, metabolic arrest and reactivation of metabolism, the first characterizing dormancy and the second taking place during germination; both involve arrest and reactivation of the cell cycle (Barroco et al 2005).

1.3 Root structure and the control of root development after germination

Roots are crucial for plants because they fulfil function of anchorage, mechanical support, absorption of water and nutrients. They are also important for humans and other life forms because they provide food (carrots, parsnip etc.), fuel and materials. Roots represent a major system of sensing and responding to many biotic and abiotic stresses and they help to overcome limitations imposed by the sessile condition of the plant. Most of the time plant fitness improvement focuses on the aboveground part of the plant. Indeed, no interest was given to roots during the first green revolution (Waines & Ehdaie 2007). However, recent studies have suggested that root architecture can affect yields and seed production and improving root growth could be a new strategy to increase plant fitness and yields. Arabidopsis root system is a key model for development and environmental adaptation. However, the information obtained on Arabidopsis will be needed to be transferred to crop models that have slightly different root systems. Arabidopsis primary root is defined as the embryonically developed root and it has an organised structure (Dolan et al 1993). At the very tip of the root there is the root cap, which includes the columella cap and lateral root cap (Figure 1.3). Columella cells are implicated in gravitropism by a redistribution of amyloplasts contained in these cells and changes in auxin efflux (Swarup et al 2005). Just above the columella cells there is the quiescent centre (QC), which is essential for root architecture and for maintaining the stem cells population (vandenBerg et al 1997). The QC sends signals to inhibit differentiation via expression of the *WUSCHEL* related homeobox (*WOX5*) (Sarkar et al 2007, Zhang et al 2015). The cells proximal to the QC form the stem niche, which actively divide and accumulate in the meristem. Once reached the elongation zone the cells of the stem niche exit the cell cycle and start to differentiate (Sarkar et al 2007). The cortex layer is sited between epidermis and endodermis and it is unspecialised. The endodermis is

the inner part of the cortex, which differentiates in a single cell layer and regulates water flow between outer layers and the vascular cylinder. Between the endodermis and the central cylinder there is the pericycle, which is the site of lateral roots branching. Lateral root are formed by a progression of the cell cycle driven by auxin (Sabatini et al 1999). In the central cylinder there is the meristematic zone which spans 250 μm of the root. The meristem is a layer of undifferentiated cells capable to grow and divide. The meristematic zone is responsible for the growth of the primary root and for this reason it is also known as the primary meristem. Root development is affected by different factors from soil composition and moisture, water and nutrients availability, light and hormones. Light can penetrate several millimetres in the soil and affects soil composition. Differential phytochromes are responsible for light perception in roots affecting root growth (Galen et al 2007). Light also regulates the expression of many genes involved in root development (Molas et al 2006). Moreover, phytochromes deficiency is correlated to root inhibition by jasmonic acid (JA) (Zhai et al 2007). JA is a hormone largely studied in plant responses to biotic stresses but it also has implication in root development by inhibiting root growth. It has been shown that elongated hypocotyl mutants show less sensitivity to JA and present longer primary roots (Costigan et al 2011). The most studied hormone is auxin, which regulates patterning, cell division and differentiation; it mediates gravitropism, environmental stimuli and induces lateral roots formation. It has been demonstrated the auxin gradient in the root apex is maximal in the QC (Petersson et al 2009). Moreover, auxins have a crucial role in cell division induction and are required to enter in the G1/S phase of the cell cycle (Inze & De Veylder 2006).

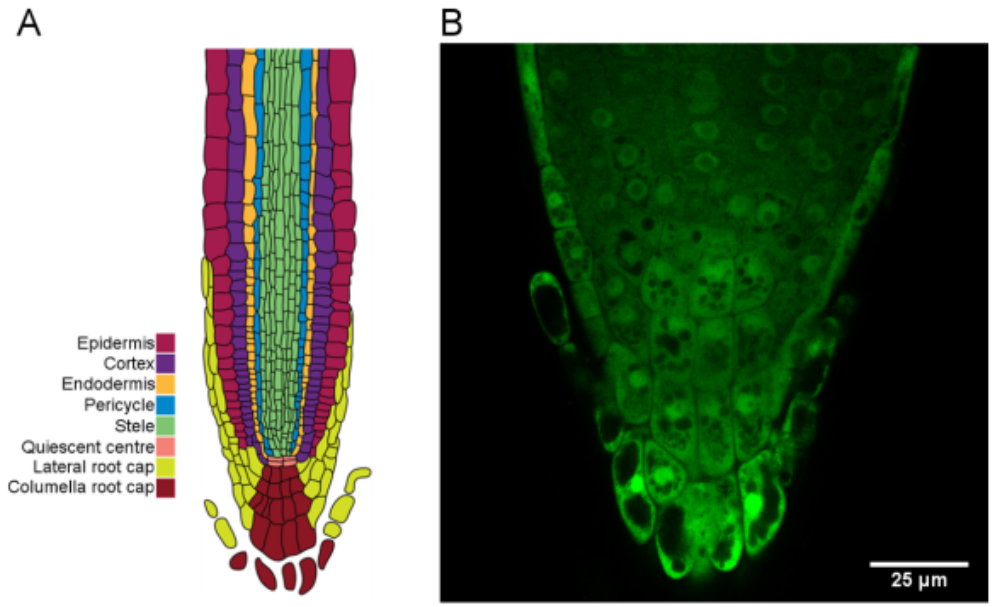

Figure 1.3 A comparison of a diagram of Arabidopsis root structure with roGFP2 CLSM image of Arabidopsis root tip *in vivo*.

(A) Diagram of Arabidopsis root structure. (B) roGFP2 fluorescence image showing the Arabidopsis root structure *in vivo*. Confocal image was taken by LSM700 with excitation at 488 nm. Courtesy of Dr. Rupesh Paudyal (University of Leeds, UK)

1.4 The impact of environmental stresses on plant productivity and seed production

The conditions used for seed storage are important for agriculture because they can lead to a loss of viability, particularly in the long term. Seed longevity and vigour can be related to various seed properties such as weight, composition and moisture. The ability of seeds to withstand stresses that occur while stored is a key aspect of seed longevity, as it is the ability to germinate and begin prompt to grow. However, the effects of the environmental stresses experienced during seed set and development on the mother plant may also have a significant impact on seed longevity and vigour (Carrera et al 2008, Job et al 2005). Arabidopsis has been studied intensively with regard to seed drying and it is widely used as a model specie for the identification of genes controlling seed longevity (Nguyen et al 2015). In the natural environment, plants are constantly exposed to a variety of biotic and abiotic stresses that perturb plant growth and development, leading to reduced vigour and yield losses, usually in terms of number and viability of seed production. All abiotic stress conditions such as cold, drought and excess of light that impair plant growth lead to reactive oxygen species (ROS) accumulation and a perturbation of the redox homeostasis. This is responsible for changes in the expression of numerous genes associated to oxidative signalling which is central in the regulation of plant physiology, such as development and response to stresses. These stress-induced changes in gene expression will not only alter the processes within the mother plant but they will also influence the pathways of seed development and factors that affect the dormancy and ability of the seeds to germinate. However, while it is widely accepted that stress limits the ability of plants to produce seed, little information is available in the literature concerning how seed quality and longevity is modified by the stresses experienced by the parent plant. Most importantly, little is known about how the stress experienced by the mother plant influences the redox state of the

seeds, the ability to germinate and initiate the cell cycle. Once seeds are mature, the desiccation process starts. Drying seeds is an important step because it maintains seed viability and vigour avoiding mould growth, heating and increased microorganism activity. It permits also early harvest and long-term storage. The proteins and membranes of orthodox seeds are protected during desiccation by water replacement with sugars at the hydrogen bonding sites. This process preserves the native structure of proteins and the spacing between phospholipids (Bryant et al 2001, Xiao & Koster 2001). In addition to sugars, other proteins such as the hydrophilic proteins called late-embryogenesis abundant (LEA) proteins, dehydrins and small heat shock proteins are considered to play important roles in protein and membrane stabilization during seed drying (Tolleter et al 2010). This is important because seed drying is accompanied by the accumulation of reactive oxygen species (ROS) such as the superoxide radical ($O2^{\bullet -}$) and hydrogen peroxide (H_2O_2) (Gomes & Garcia 2013). The production and accumulation of ROS has to be tightly controlled because these oxidants can perturb the reduction-oxidation (redox) homeostasis if they are not rapidly removed by the cellular antioxidant network. The network is comprised of low molecular weight antioxidants such as ascorbate and glutathione and antioxidant enzymes such as catalase (Foyer 2005). The antioxidant capacities of recalcitrant and orthodox seeds are known to change during seed drying and storage. Uncontrolled oxidation contributes to the loss of seed viability particularly during storage (Bailly et al 2001). ROS and antioxidant systems have a crucial role in the redox signalling and therefore in the regulation of plant development and responses to stress. Moreover, reduction in antioxidant levels compromises cell division with a result in a decrease of the plant growth rate and yield. The cell cycle has been widely studied, however limited information about the communication between internal signals and external stimuli are available (Inze & De Veylder 2006).

1.5 Ascorbate

Ascorbic acid (vitamin C) is the most abundant low molecular weight antioxidant in plant cells (Foyer & Noctor 2011). It accumulates to high concentrations (20-300 mM) in the chloroplasts and the cytosol (Foyer et al 1983, Pallanca & Smirnoff 2000). The ascorbate pool has a high turnover rate, with about 13% of the total pool being degraded per hour (Pallanca & Smirnoff 2000). About 90% of the ascorbate pool is localised in the cytoplasm but a significant amount is transported to the apoplast where it functions as the first defence response against external oxidants (Kiddle et al 2003). A major role of ascorbate is to scavenge ROS (Conklin et al 1996) and to prevent uncontrolled oxidation (Noctor & Foyer 1998). In this reaction ascorbate is first oxidised to monodehydroascorbate (MDHA) and then dehydroascorbate (DHA). Ascorbate is an excellent antioxidant because these oxidised are rapidly re-reduced within the cell to the reduced form ascorbate.

In addition to its antioxidant functions, ascorbate has important roles in cell growth and expansion influencing for example root growth and development (Arrigoni 1994, Cordoba-Pedregosa et al 1996). Ascorbate is required for the progression of the cell cycle (Potters et al 2002, Potters et al 2004). The addition of DHA to tobacco cells delayed the cell cycle when this oxidant was added during the G1 phase (Potters et al 2000). However, the mechanisms of cell cycle regulation by ascorbate are poorly understood.

The D-mannose/L-galactose (D-Man/L-Gal) pathway of ascorbate synthesis is essential in Arabidopsis leaves. However, in other organs and species ascorbate can be produced by other mechanisms, such as the guanosine diphosphate-mannose pathway (Running et al 2003, Wolucka & Van Montagu 2003), or from D-galacturonic acid (Agius et al 2003) or D-glucuronic acid (Lorence et al 2004). In the D-Man/L-Gal

pathway, GDP-D-Mannose is produced from D-fructose-6-phosphate (Fru-6P) in reactions catalysed by phosphomannose isomerase (PMI), phosphomannomutase (PMM) and GDP-Man pyrophosphorylase (GMP) (Bartoli et al 2005, Dowdle et al 2008) (Figure 1.4). GDP-D-Mannose is then converted to GDP-L-Galactose, L-Galactose-1-P, L-Galactose, L-galactono-1,4-lactone, and finally to ascorbic acid (Dowdle et al 2008, Ishikawa et al 2007). The last step is catalysed by L-Galactose dehydrogenase (GLDH), which is localised in the mitochondria and associated with the respiratory electron transport chain (Bartoli et al 2005, Heazlewood et al 2003).

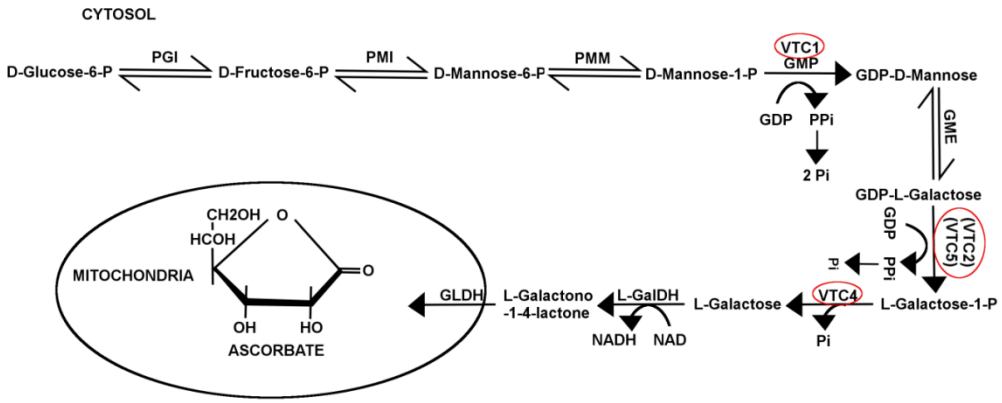

Figure 1.4 Ascorbic acid biosynthetic pathway.

The first 8 steps of ascorbic acid biosynthesis occur in the cytosol. Phosphoglucose isomerase (PGI), phosphomannose isomerase (PMI), phosphomannose mutase (PMM), GTP-D-mannose phosphorylase (GMP) and GTP- mannose 3,5 epimerase (GME) convert D-Glucose-6-P to GDP-L-Galactose precursor. *VTC2* and *VTC5* genes encode GDP-L-galactose phosphorylase, which catalyses the conversion of GDP-L-galactose to L-Galactose-1-P in a reaction that consumes inorganic phosphate and produces GDP. The last step of the pathway in leaves is catalysed by the L-galactonolactone dehydrogenase (GLDH), which is localized in the respiratory electron transport chain in the mitochondria.

1.5.1 Ascorbic acid deficient mutants: *vtc2-1* and *vtc2-4*

Mutants have been useful tools to elucidate gene functions and metabolic pathways. A number of ascorbate (vitamin C)-defective (*vtc*) mutants were isolated from Arabidopsis (Conklin et al 1996) using ethyl methanesulfonate (EMS) and a screen using increased ozone sensitivity (Conklin et al 2000). Since then the *vtc2-1* mutant has been extensively characterised (Kerchev et al 2011, Pavet et al 2005) providing insight into the role of *VTC2*. Recently, a new *vtc2* T-DNA insertion mutant line was isolated by Robbie Gillett but this mutant has not been characterised yet. The *VTC2* gene has 7 exons with the *vtc2-1* single base substitution introduced a 3' splice site of the fifth intron. While in *vtc2-4* the T-DNA is inserted into the second exon, 620pb downstream the start codon (Figure 1.6).

All of these mutants, except for *vtc3*, are defective in components of the D-Man/L-Gal pathway. The *VTC2 and VTC5* genes encode GDP-L-galactose phosphorylase, which catalyses the rate limiting step of the D-Man/L-Gal pathway (Conklin et al 1996, Dowdle et al 2008, Laing et al 2007, Linster et al 2007). Double knockout mutants that are defective in both the *VTC2* and *VTC5* genes have a seedling lethal phenotype (Dowdle et al 2008). However, seedling growth was restored in the *vtc2vtc5* double mutants by the addition of L-galactose or ascorbate (Dowdle et al 2008). The abundance of transcripts encoding enzymes of the ascorbate biosynthesis pathway, including *VTC2* are higher in the light than the dark (Yabuta et al 2007). Moreover, ascorbate accumulation in leaves increases in the light and decreases in the dark (Bartoli et al 2006, Pignocchi et al 2006). GDP-L-galactose phosphorylase activity was found to be higher in the light than the dark (Dowdle et al 2008). Inhibition of photosynthetic electron suppresses the expression of *VTC2* and other ascorbate biosynthetic genes leading to a decrease in leaf ascorbate (Yabuta et al 2008, Yabuta et al 2007).

These findings demonstrate that the ascorbate synthesis pathway is regulated by light.

The *VTC3* gene encodes a novel polypeptide called CSN5B that has a N-terminal protein kinase domain tethered covalently to a C-terminal protein phosphatase type 2C domain (Conklin et al 2013). The VTC3 protein is localized in the chloroplasts. The light-mediated accumulation of ascorbate was lost in the *vtc3* knockout mutants, suggesting that the VTC3 protein is important in the light-dependent regulation of the D-Man/L-Gal pathway. In addition, the 5B subunit of COP9 signalosome enhances the degradation of the VTC3 protein at night in Arabidopsis suggesting that this pathway negatively regulates ascorbate synthesis (Wang et al 2013).

The *VTC2* gene is considered to produce the predominant form of GDP-L-phosphorylase in Arabidopsis with *VTC5* gene product making only a relatively small contribution to leaf ascorbate production and accumulation (Dowdle et al 2008, Gao et al 2011). *VTC2* also appears to be controlled by the availability of ascorbate. High ascorbate concentrations lead to posttranscriptional repression of *VTC2* by down-regulating translation (Laing et al 2007). This control mechanism involves ribosome stalling on a conserved upstream open reading frame (uORF) in the long 59 untranslated region (UTR). The uORF is translated and encodes a peptide that functions in the ascorbate inhibition of translation.

Constitutive *VTC2* overexpression in tomato, strawberry or potato leads to significant increases in fruit or tuber ascorbate levels (Bulley et al 2012). Similarly, estrogen-induced overexpression of the *VTC2* gene increased the ascorbate levels of Arabidopsis seedlings (Yoshimura et al 2014). Overexpression of the kiwifruit GDP *VTC2* and GDP-D-Mannose-3',5'-epimerase genes in tobacco led to much higher levels of ascorbate in leaves than overexpression of *VTC2* alone (Bulley et al

2009). Ascorbate has an essential role in plant growth and establishment. Knock out mutants defective in ascorbate synthesis are lethal (Dowdle et al 2008). *vtc2-1* and *vtc2-2* have only 20-30% of the wild ascorbate content and show slow growth phenotype as well as hypersensitivity to abiotic stresses (Bartoli et al 2005, Conklin et al 2000, Pavet et al 2005) (Figure 1.5). *vtc1-1, vtc2-1, vtc3-1,* and *vtc4-1* flowered and senesced earlier than wild type (Kotchoni et al 2009). Recently, a new *vtc2* T-DNA insertion mutant line has been produced and not yet characterised. The *VTC2* gene has 7 exons with the *vtc2-1* (EMS) single base substitution from G to A in the fifth intron. The single base mutation introduced a splicing site and a premature stop codon (Muller-Moule 2008). In *vtc2-4* the T-DNA is inserted into the second exon, 620 pb downstream the start codon however this mutant has not been fully characterised yet (Figure 1.6).

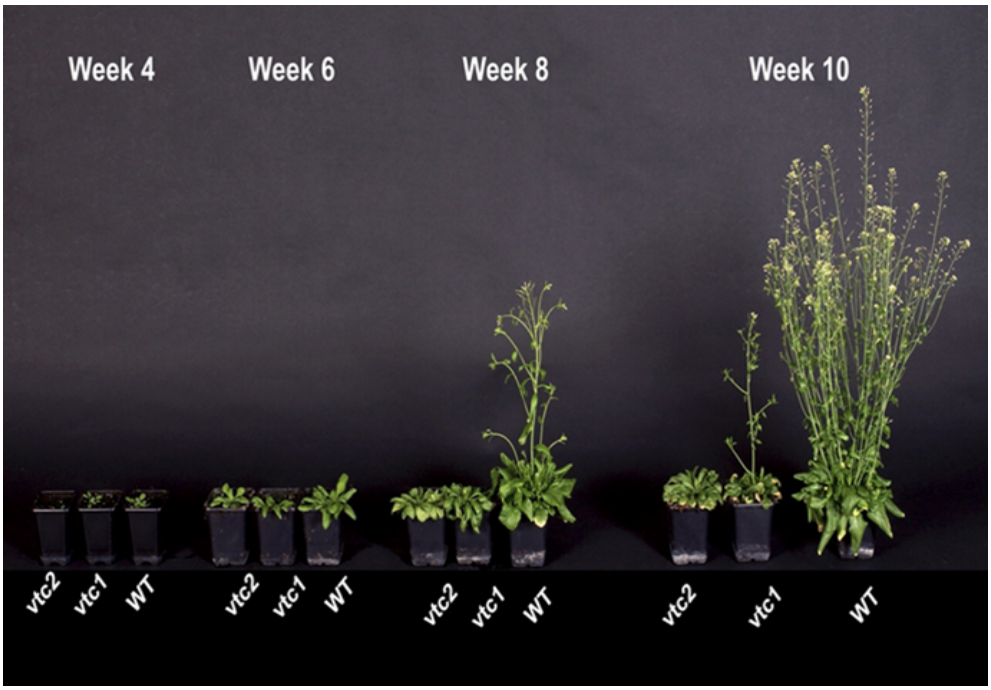

Figure 1.5 A comparison of plant development of *vtc1-1* and *vtc2-1* mutants compared to wild type (WT).

vtc1-1 and *vtc2-1* mutants showing a slow growth phenotype and delay in flowering over the 10 weeks experiment. Picture taken from Pavet et al (2005).

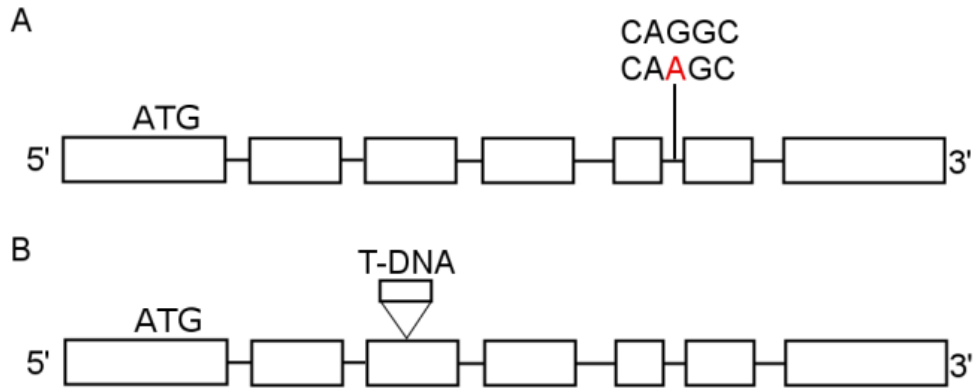

Figure 1.6 Diagram of *VTC2* gene showing the point mutation of (A) *vtc2-1* and the (B) *vtc2-4* T-DNA insertion mutant.

Start codon (ATG), exons (boxes), introns (lines) and position of the mutation are shown. (A) *vtc2-1* has a point mutation with a single base substitution (G to A) at the fifth intron as shown in red (Dowdle et al 2008). (B) In *vtc2-4* mutant the T-DNA is inserted in the third exon.

1.6 Glutathione

The thiol tripeptide glutathione, γ-glutamylcysteinylglycine (GSH) is one of the major soluble redox buffers in plant cells. GSH plays a central role in cellular redox homeostasis and prevents the oxidation of biomolecules such as proteins and nucleic acids. It also has diverse functions in detoxification, antioxidant defence, maintenance of cellular thiol status and regulation of cell proliferation (Foyer & Noctor 2011). In animals GSH concentration varies in the different phases of the cell cycle (Zuelke et al 2003) and plays a crucial role in the cell cycle regulation (Pajaud et al 2015). Nevertheless, the mechanisms of redox regulation of the cell cycle are poorly understood in plants.

Glutathione is synthesized from glutamate, cysteine and glycine, in two ATP dependent steps. In the first step, γ-glutamylcysteine is formed by glutamate cysteine ligase (GCL, also known as γ-EC synthetase). The second step is catalysed by glutathione synthetase (GSH-S), during which a glycine is added to form glutathione. In animal cells, GCL is a two subunits (catalytic and modifier) cytosolic enzyme (Griffith 1999). In plants, instead, GCL is localized in plastids although in Arabidopsis it is exclusively in chloroplasts (Galant et al 2011, Wachter et al 2005). GCL is encoded by the *GSH1* gene. The second step of glutathione synthesis occurs both in plastids and cytosol, and the GS enzyme is encoded by the *GSH2* gene (Noctor et al 2012). Glutathione exists in the thiol-reduced (GSH) and disulphide-oxidized (GSSG) forms. The reduced form is regenerated from GSSG by glutathione reductase (GR) using NADPH as a cofactor (Figure 1.7). Glutathione synthesis is controlled in multiple ways. However, the availability of cysteine and GCL activity are considered to be decisive factors limiting GSH synthesis. The production of γ-glutamylcysteine is considered to be the rate-limiting step of GSH synthesis (Griffith 1999) (Foyer & Noctor 2009). Over-expression of GSH biosynthesis enzymes or the enzymes involved in cysteine biosynthesis leads to an increase in the GSH pool (Noctor & Foyer 1998). GCL activity is negatively controlled by GSH

with important consequences for the regulation of cellular glutathione homeostasis. When the GSH pool is depleted or GSSG increases feedback inhibition is alleviated leading to enhanced rates of GSH synthesis (Bartoli et al 2006, Jez et al 2004, May et al 1998).

Mutants or transgenic plants with altered activities of GSH biosynthesis enzymes are useful tools in understanding GSH functions. For instance, *Arabidopsis thaliana* knockout mutants lacking *GSH1* are lethal. This shows that GSH is indispensable for plant survival as it is in animal and yeast cells. *Rootmeristemless1* (*rml1*) mutants have a knock down mutation in *GSH1* and as a consequence contain only about 5% of the wild type GSH contents. In *rml1* roots but not shoots, the cell cycle arrests at G1 phase soon after the embryonic root emerges. Buthionine sulfoximine (BSO) is a specific inhibitor of GCL. The addition of BSO to wild type Arabidopsis leads to a similar phenotype in the root meristem to that observed in *rml1* (Vernoux 2000). These studies demonstrate that GSH is required for the root meristem growth. Unlike the root, shoot meristem development is not impeded by the absence of GSH. Studies with mutants defective in the cytosolic NADPH-thioredoxin reductases (TRX/NTR) have revealed that loss of TRX/NTR function alone produces no phenotype (Bashandy et al 2010). However, when *trx/ntr* mutants were crossed with *rml1,* the *trx/ntr/rml1* mutants were impaired in both shoot and root development. This shows that TRX is required for meristem maintenance in shoots (Bashandy et al 2010).

GSH and γ-Glu-Cys are transported from plastids by a family of transporters that are homologous to the Chloroquine-Resistance-Like Transporters (CTL) family of transporter proteins of the malaria parasite (Maughan et al 2010). Single *clt1* mutants were first identified on a screen based on the ability of Arabidopsis seedlings to grow on media containing BSO (Maughan et al 2010). The *clt1clt3* double mutants show an enhanced BSO resistance but they have similar GSH contents to the wild type. The triple *clt1clt2clt3* mutant is deficient of GSH in root (but not in shoot) and it is hypersensitive to heavy metals such as cadmium and fungal infections (Maughan et al 2010). Moreover, the

triple mutants show an altered intracellular distribution of GSH having a lower cytosolic GSH pool and a higher chloroplast GSH pool (Maughan et al 2010).

Low levels of GSH are associated with a decreased ability to resist some forms of stress. For example, another knock down mutation in *GSH1* (*cad2)* resulted in a 60% of the wild type GSH contents and an enhanced sensitivity to cadmium. Conversely, GSH accumulation is considered to enhance abiotic stress responses. However, the regulated partitioning of GSH between the different cellular compartments will alter the redox state within each compartment and so influence stress tolerance and cell cycle regulation (Maughan et al 2010).

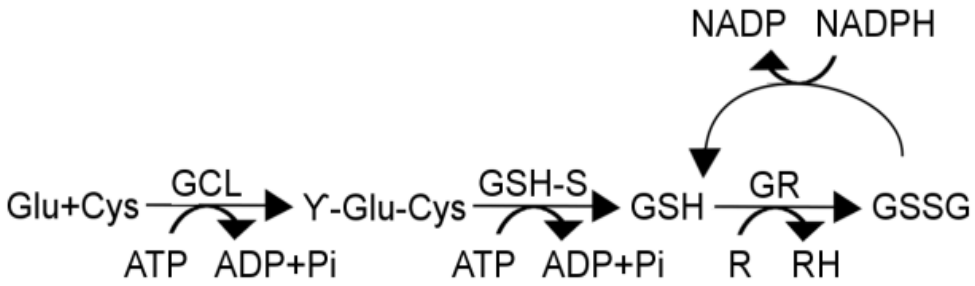

Figure 1.7 Two step GSH synthesis occurs through enzymatic process requiring ATP.

The first reaction is catalysed by glutamate cysteine ligase (GCL) and it is the rate limiting step of GSH synthesis. GCL conjugates cysteine with glutamate to form Y-glutamylcysteine (Y-Glu-Cys). During the second step, GSH is formed by glutathione synthetase (GSH-S), which adds glycine to Y-Glu-Cys to form γ-glutamylcysteinylglycine (GSH). Glutathione reductase (GR) catalyses glutathione reduction using NADPH.

1.6.1 Intra-cellular glutathione partitioning

Glutathione is distributed between the various cellular compartments. Recent studies have indicated that GSH is abundant in mitochondria of plant cells, as it is in animal mitochondria. In animals, the Bcl-2 protein, which directly binds GSH via the BH3 groove, is important in GSH transport into the mitochondria (Zimmermann K. 2007). The loss of the Bcl-2 protein can lead to neurodegenerative diseases in mammals (Zimmermann K. 2007). Over-expressing Bcl-2 leads to increased GSH levels while Bcl-2-deficient mice display enhanced sensitivity to mitochondrial oxidative stress (Maleki et al 2012, Merad-Saidoune M 1999). However, no Bcl-2 homologous sequences have been found in plants (Cacas 2010, Dion et al 1997). The mechanisms of glutathione transport and sequestration in the nucleus are unknown. However, both animals and plants present high level of nuclear glutathione in dividing cells, while quiescent and differentiated cells have similar glutathione content in nucleus and cytoplasm. In animal cells, a mechanism involving Bcl-2 proteins has been proposed. For example, an increase of nuclear glutathione in nuclear extract of NIH3T3 fibroblasts during the initial phase of proliferation has been observed (Markovic et al 2007). Bcl-2 proteins are more abundant during prophase and metaphase and they are associated with the chromosome during mitotic phase. Less Bcl-2 is bound to chromosome during telophase and undetectable level after separation of the daughter cells. Moreover, Bcl-2 is an important component in HeLa cells and it was associated to chromosome during metaphase (Barboule et al 2009). It has been seen that Bcl-2 is associated with H3 on some region of the mitotic chromosome (Barboule et al 2009). For this reasons it may be possible that Bcl-2 is an integral component of the mitotic chromosome and it mediates reduced glutathione (GSH) translocation into the nucleus (Barboule et al 2009). However, no information is available on the mechanisms that regulate glutathione into the nucleus in plants.

1.6.2 Glutathione recruitment into the nucleus during cell cycle

In animals, oxidation of proteins regulates the normal cell cycle progression. For instance, in HeLa cells oxidative stress leads to cyclin D1 depletion and cell cycle arrests in G2 phase (Pyo et al 2013). The G1-S and G2-M transition are regulated by Akt, which inhibits cyclin D1 degradation. It has been shown Akt2 has redox sensitive properties and that oxidation of Akt2 mediates the cell cycle (Wani et al 2011).

Recently, the existence of a redox cycle within the cell cycle has gained an increasing attention. An oxidation event is required in G1 phase for the activation of CDKs, stimulate the mitogenic cycle and enter in S phase (Menon et al 2003). After that a more reduced environment is required to progress to the G2/M phase. The recruitment of glutathione into the nucleus will have implications for the regulation of the abundance of reactive oxygen species (ROS) in the cytosol and on the redox state in the nucleus. Combining information from studies on animals and plants, a model for glutathione cycle has been proposed (Figure 1.8) (Vivancos et al 2010). In the early G1, glutathione is recruited into the nucleus with subsequent depletion of glutathione in the cytosol and changes in the redox state. The cytosolic decrease of glutathione stimulates glutathione synthesis so that the total reduced glutathione pool increases rapidly. When the nuclear envelope dissolves during the metaphase, the nuclear and cytosolic glutathione pool is equilibrated during G2 and M phase. As a final step, the nuclear envelope reforms and GSH is re-distributed between the two daughter cells.

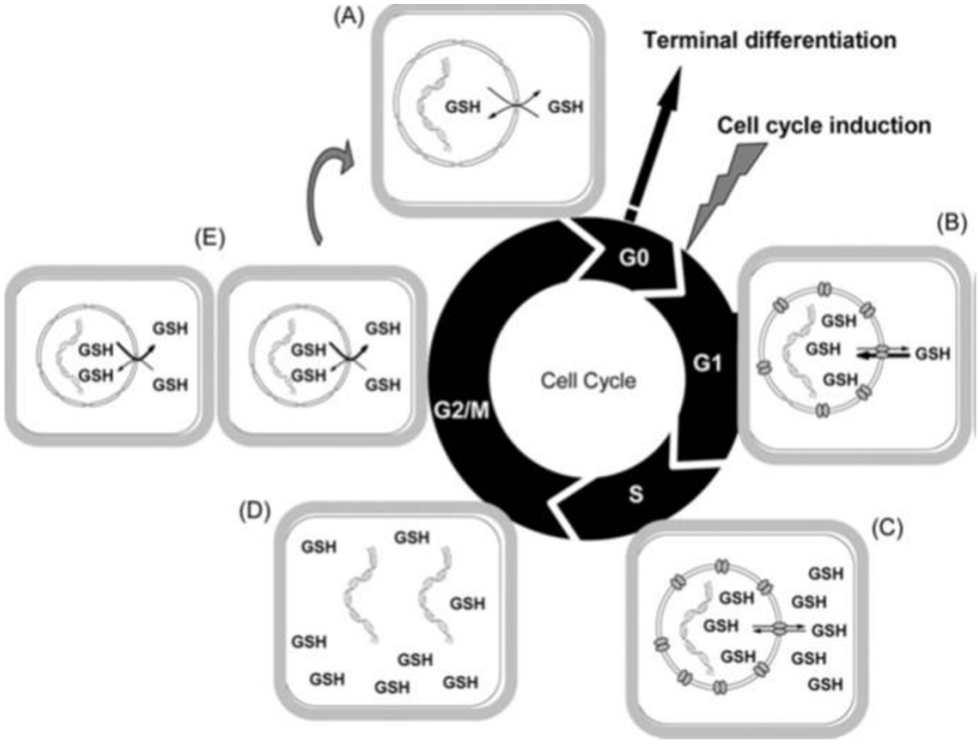

Figure 1.8 Glutathione cycle within the cell cycle model.

(A) Before the start of the cell cycle GSH is equally distributed between the cytoplasm and nucleus. (B) Changes in the nuclear envelope allow GSH recruitment into the nucleus. GSH is depleted from the cytoplasm with repercussion for GSH content in other organelles such as the mitochondria and chloroplasts. (C) GSH depletion stimulates GSH synthesis in the chloroplasts and cytosol until the GSH pools in the nucleus and cytoplasm reach similar levels. (D) The nuclear envelope disappears at the end of prophase and the beginning of G2/M phase. (E) At the end of the G2/M the nuclear envelope reforms and GSH pool is redistributed between the two newly formed daughter cells and GSH pools in the nucleus and cytoplasm are again in equilibrium. Figure from Vivacons at al (2010).

1.6.3 Estimation of Glutathione redox potential *in vivo*: roGFP2

Most of the metabolic reactions in biological processes involve exchange of electrons between compounds. One species will lose electrons and increase its oxidation state while the other will gain electrons decreasing its oxidation state. The redox potential of a substance is the electronegativity or the affinity for electrons. Intracellular glutathione redox state and in particular glutathione redox state fluctuations may have a role as regulators of the cell cycle progression. The redox potential of a redox couple is described by the Nernst equation and for the GSH/GSSG couple is:

$E=E_0\ (-(RT/nF))\ln([GSH]^2/[GSSG])$

where E is the glutathione redox potential, E_0, glutathione midpoint potential, R, gas constant, T, temperature, n, the number of electrons exchanged and F, the Faraday constant. Based on the Nernst equation and the property of glutathione (2 GSH are required to form 1 GSSG), both the total glutathione concentration and the GSH/GSSG ratio influence the redox potential.

While it would be very useful to have an accurate estimate of the redox state of the cell or a given organelle, such measurements are far from trivial because of the many redox-active compounds present. It is generally accepted however, that determinations of the redox potential of the glutathione pool, which interacts directly with protein thiol groups, provides a good estimate of cellular redox state. The cytosolic redox potential it has been estimated to be about -300 mV but using redox sensitive GPF probes it has been established that it could be even lower, being about -320 mV (Meyer et al 2007). *In vivo* probes have been developed to determine the redox potential of glutathione in a dynamic fashion. These are based on fluorescent proteins containing oxidizable thiol groups including redox-sensitive protein variants of the yellow (rxYFP) or green (roGFP) fluorescent protein (Hanson et al

2004, Maulucci et al 2009) used to monitor glutathione status in the cytosol (Jiang et al 2006, Meyer et al 2007). However, the roGFP that was developed for the cytosol also moves into the nucleus and so it can be used to monitor the glutathione status of the nucleus. Redox sensitive roGFP probes are therefore important tools for the *in vivo* measurement of glutathione redox potential in specific compartments, particularly the nucleus. However, although some data are available concerning the redox state of the nucleus in yeast (Dardalhon et al 2012), to date there are no measurements in the literature on the redox state of the nucleus in plant cells. Evidence from yeast suggests that redox states of the nuclei and cytosol are maintained independently and have distinct regulatory mechanisms (Dardalhon et al 2012). roGFP2 has been developed from the GFP of the jellyfish *Aquorea Victoria* with some modification in the structure. Crucially, two cysteines are introduced into the ß-barrel close enough to undergo thiol-disulphide exchange reactions (Figure 1.9). The formation of the disulphide bridge leads to a modification in the spectral properties allowing the discrimination between the reduced and oxidised form of the probe. roGFP2 probe has two excitation maxima related to the reduced and oxidised forms respectively with glutaredoxin (GRX) required to equilibrate the glutathione redox potential (Meyer et al 2007) (Figure 1.9). The roGFP2 probe therefore reports changes in the glutaredoxin redox potential that then modify roGFP2. Changes in the fluorescence profile can then be used to calculate changes in the redox potential. Dynamic monitoring of the glutathione redox potential of cellular compartments is possible because of the reversibility of the thiol-disulphide exchange reactions and because the roGFP2 probe has two excitation peaks that can be used for measurements (Figure 1.10). It is important to note that the glutathione redox potential not only depends on GSH: GSSG ratio but also on the overall concentration of glutathione. The actual glutathione redox potential is therefore related to $[GSH]^2/GSSG$. *In vivo* roGFP studies suggest that the glutathione redox potential in wild-type Arabidopsis is lower than -300 mV (Meyer et al

2007) suggesting that the glutathione and pyridine nucleotide couples are close to redox equilibrium in the cytosol, conferring a high sensitivity on the signalling functions of the glutathione redox potential mediated through GRX-dependent changes in protein thiol-disulphide status. For example, a change in redox potential of about 50 mV is sufficient to significantly alter the balance between oxidized and reduced forms of TRX-regulated proteins (Setterdahl et al 2003). roGFP2 can be used effectively to monitor *in vivo* changes in the redox potential in the nucleus and cytosol and this technology can be applied to the investigation of developmental processes such as germination, cell cycle regulation and the growth of the root meristem.

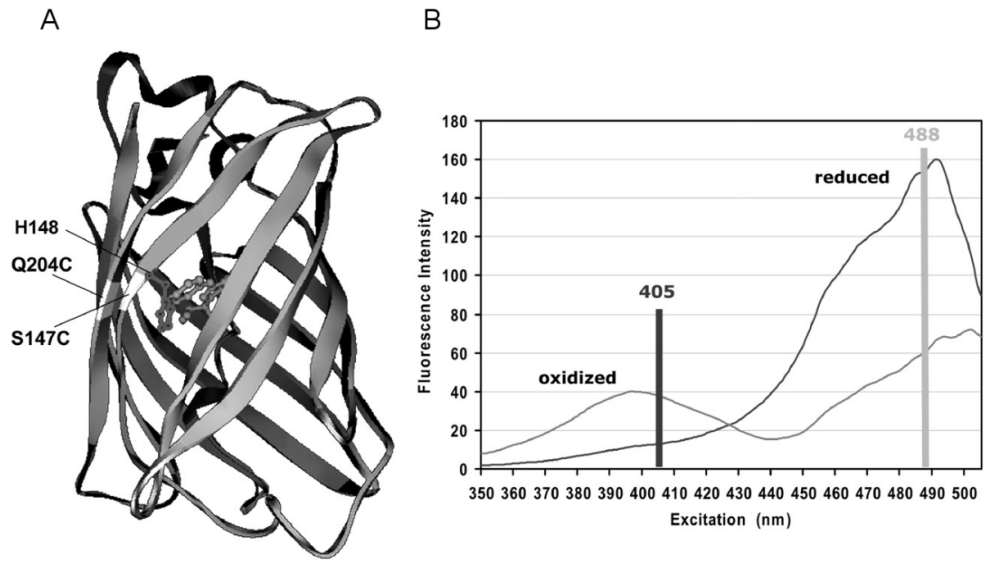

Figure 1.9 roGFP2 structure and excitation spectrum.

(A) The amino acid substitutions (Q204C and S147C) are shown in the GFP ß-barrel structure. (B) roGFP2 fluorescence spectrum showing the reduced form excited at 488 nm and the oxidised form excited at 405 nm. Figure from Meyer et al (2007).

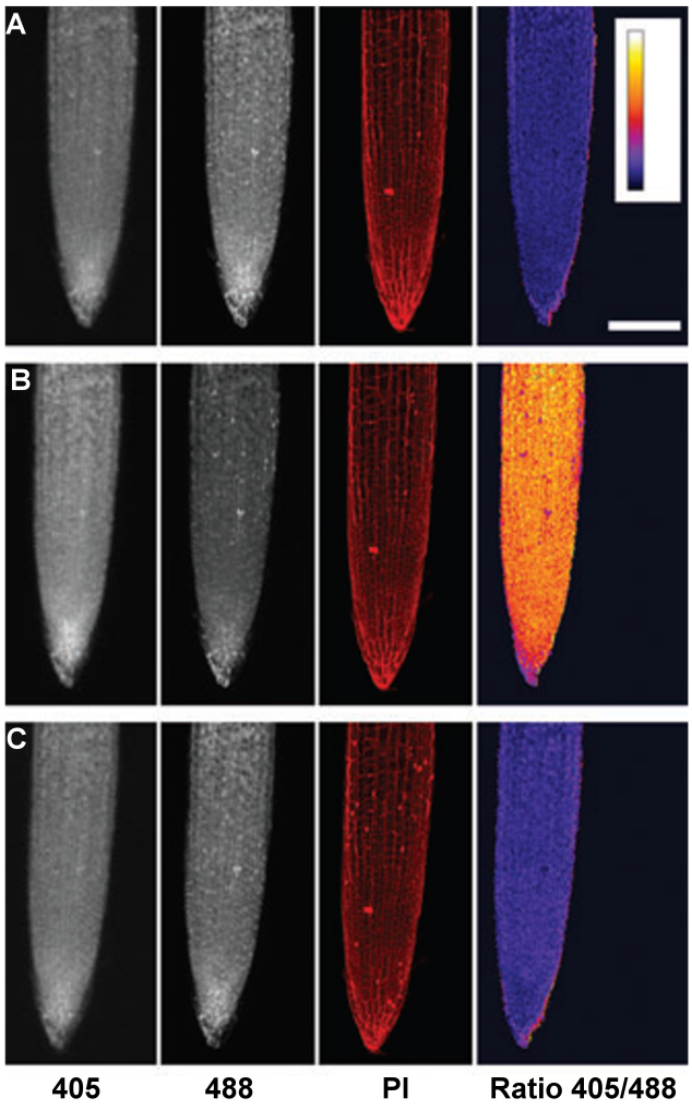

Figure 1.10 Redox-dependent fluorescence of redox-sensitive GFP2 (roGFP2) in the cytosol of Arabidopsis root cells is fully reversible.

Stack of CLSM images of Arabidopsis root tip excited at 405 nm (oxidised form of roGFP2), 488 nm (reduced form of roGFP2), PI staining (red) and 405/488 ratio. (A) Untreated Arabidopsis root tip expressing roGFP2. (B) Root tip after oxidation by treatment with 1 mM H_2O_2. (C) Addition of 2 mM DTT to the root tip previously oxidised with H_2O_2. Colour scale for the 405/488 nm ratio images indicate the reduced roGFP2 in blue and the oxidised roGFP2 in yellow. Figure from Meyer et al (2007).

1.7 Cell cycle and hydroxyurea

1.7.1 Cell cycle

The last two decades have seen great progress in our understanding of the molecular mechanisms that regulate cell proliferation and revealed that these pathways are highly conserved in all eukaryotes. However, the mechanisms that control the cell cycle appear to have evolved independently in plants and animals with plant cell cycle possessing some unique characteristics (Meyerowitz 2002). Plant development, in contrast to animal development is largely post-embryonic with numerous inhibitors of cyclin-dependent kinases modulating the postembryonic development. The cell division takes place at the meristems. The cells of the meristem are pluripotent, characteristic that confers high plasticity to plant cells, so that their progeny can perform a spectrum of developmental fates. Many plant cells can also replicate DNA in the absence of mitosis. This process is known as endoreduplication and it causes polyploidy. Although the cell cycle and its regulation have been widely studied, how the cell cycle is integrated with plant development still remains a great challenge. Arabidopsis with its fully sequenced genome may be a major contributor in understanding how external factor regulate the cell cycle.

The cell cycle is comprised of growth, mitosis and cell division phases that are ordered sequentially to allow the replication of the genetic material and its subsequent segregation in two daughter cells. For the cell cycle to progress, cellular components, such as organelles, genetic material and other macromolecular structures have to be duplicated in order to be delivered to the new formed daughter cells. The two daughter cells will be mostly identical to their mother cell. The cell cycle is a process divided in two stages, the interphase and mitosis. The interphase stage of the cell cycle includes three distinctive phases: the G1 phase, the S phase, and the G2 phase (Figure 1.11). The G1 phase, which is the first gap, separates the previous mitosis and the

next S phase during which DNA is replicated. In G1 or the “growth phase”, the cell is preparing for the replication of DNA and all the biosynthetic activities of the cell, which had been considerably slowed down during M phase, resume at a high rate. G1 is characterized by the synthesis of the various enzymes that are required in S phase, particularly those needed for DNA replication and by a growth in cellular dimension (Nurse 2003). During the G1 phase, the cell chooses if conditions are favourable to replicate the DNA or to exit the cell cycle entering in a quiescent state (G0 phase). During the G0 phase, the cell cycle machinery is disassembled and cyclins and cyclin-dependent kinases disappear (Dewitte & Murray 2003). Cells will remain in the G0 phase until there will be some changes favourable to divide. S phase follows the G1 phase and it is characterized by DNA synthesis. It is completed when all of the chromosomes have been replicated and the amount of DNA has effectively doubled, though the ploidy remains the same. Like RNA transcription, protein synthesis is very low during S phase, except for histone production, which occurs mainly in S phase (Chioda et al 2004, Nelson et al 2002). During S phase, each chromosome replicates exactly once to form a pair of physically linked sister chromatids. After completion of S phase, the cell enters the G2 phase, which lasts until the mitosis begins. Like G1, G2 is characterized by high rates of biosynthesis but in this case it supports the production of microtubules, which are required during the process of mitosis. Some cells can exit the cell cycle from G2 phase, just as the case of G1 phase. If this happens, protein synthesis is inhibited during G2 phase to prevent the cell from undergoing mitosis. Gap phases (G1 and G2) separate the replication of DNA (S phase, interphase) and the segregation of chromosomes (M phase). M phase includes the process of mitosis and cytokinesis. Mitosis is divided in stages, which are prophase, prometaphase, metaphase, anaphase, and telophase. The last stage of cell cycle is cytokinesis, during which the cytoplasm divides and two separate cells are formed. In animals the formation of the two new cells occurs by cell cleavage. In plant cells, because the

presence of a cell wall, cytokinesis occurs by assembling a new cell wall at the centre of the cell by vesicles from the Golgi body. A cell plate will form with phragmoplast and microtubules to supports its formation. Then the cell plate will fuse with the parental plasma membrane thus completing the cytokinesis. Regulation of the cell cycle is vital for the survival of the cells and is at the basis of many agronomic traits such as growth, vigour and germinability. Entry into the cell cycle and progression through the different phases is tightly controlled by the synthesis and turnover of regulatory proteins such as cyclins and cyclin-dependent kinases (CDKs), as discussed below.

1.7.2 Cell cycle regulation in Arabidopsis

Regulation of the cell cycle generally involves processes that are vital to the survival of a cell, such as the detection and repair of genetic damage and the prevention of uncontrolled cell division. The molecular events that control the cell cycle like the cell cycle itself also show a cyclic behaviour. Cyclins are proteins that activate the CDKs, which are the key regulatory molecules that determine the progress of a cell through the cell cycle and are coordinated in a unidirectional way. This means that once a transition has taken place, it is impossible to go back in the cell cycle. Different CDK-cyclin complexes phosphorylate diverse substrates at the vital G1/S and G2/M transition points, triggering the start of DNA replication and mitosis (Figure 1.11).

CDKs are constitutively expressed in cells, whereas, cyclins are synthesised at specific stages of the cell cycle, in response to molecular signals. Studies in Arabidopsis have confirmed that many of the genes encoding cyclins and CDKs are conserved among all eukaryotes (Vandepoele 2002). Arabidopsis contains a family of 12 CDKs classified from A to F groups, a large group of CDK-like genes and a large collection of cyclin genes. The catalytic CDK subunit recognizes the target motif present in the protein substrate and the cyclins discriminate distinct protein substrates. A single CDK regulating the G1/S and G2/M transitions is a common characteristic of plants and yeast. However, the regulatory machinery shows little similarity in plants and animals and many components are plant specific. Transcripts encoding CDKB proteins peak at G2 and at mitosis and the abundance of these proteins and their kinase activities are maximal during mitosis. CDKA has also a crucial role in the cell cycle progression. CDKA and CDKB cooperate to regulate the G2/M transition. CDKD and CDKF phosphorylate CDKA at the T161 producing a conformational modification that allows the substrate recognition. CDKD is related to human CAK while CDKF is plant specific.

The activity of CDK/cyclin complexes is negatively regulated by CDK inhibitors, ICKs. The transcription of ICKs is induced by the stress-responsive hormone ABA and they interact with D-type cyclins. The hormone GA, which acts antagonistically to ABA, up-regulates the CDK-activating kinase, CDKD;1 which induces CDKA phosphorylation of the Thr160 residue (Stals 2001). Some regulators such as CDKA;1 and CYCB1 are related to yeast, however in 1990s a plant homologue of the human tumour suppressor (RB) has been found. This strongly suggests that these components of cell cycle regulation are similar in plants to other multicellular organisms. The phosphorylation of retinoblastoma protein (RB) during late G1 phase is initiated by the active CDKA–CycD complex, resulting in the release of the E2F–DP complex that promotes the transcription necessary for progression into S phase. Members of the E2F family of transcription factors were also identified in Arabidopsis (Ramirez-Parra. E & Gutierrez. C 2000). E2F/DP factors regulate gene expression of genes required for the cell cycle progression but also other functional categories of genes. However, E2F-responsive promoters contain consensus E2F-binding sequence identical to animal cells (Gutierrez 2009). Other plant hormones in addition to ABA and GA also influence CDK and cyclin processes in the regulation of cell cycle. For example, cytokinins, auxin, and metabolites such as sucrose are important regulators of G1 phase progression and the G1/S transition. They positively regulate the expression of *CYCD* and *CDKA*. *CDKA* seems to be the only kinase required for the G1/S transition and it forms complexes with *CYCD*. As mitotic activators, auxin, cytokinin and GA regulate the kinase activity of A and B-type CDKs by activation of the transcription of CDKs and of A and B-type cyclins (Stals 2001). Cytokinins induce dephosphorylation of the inhibitory Tyr residue and phosphorylation of CDK at the Thr160 residue influencing the G2-M transition. Inhibitors of the cell cycle have been identified, such as the nuclear kinase *WEE1*, which blocks the CDK/cyclin complex activity (De Schutter et al 2007). When plant cells experience stress, *WEE1* expression is induced and this leads to an

arrest of the cell cycle at the G2 phase. This allows time for DNA repair before progression into mitosis.

In animal cells, the expression of cyclin genes that initiate the cell cycle is activated by an oxidative event. However, uncontrolled oxidation causes an arrest of the cell cycle. For example, the addition of the pro-oxidant menadione causes an arrest of the cell cycle in tobacco BY-2 cells at the G1/S and G2/M transitions, slowing DNA replication and mitosis and allowing synchronisation (Combettes et al 1999). Synchronisation techniques are important tools to study the cells progression trough the cell cycle. It can be obtained by adding compounds such as aphidicolin (Dolezel et al 1999), hydroxyurea (Cools et al 2010) and oryzalin (Baskin et al 1994), which block the cell cycle at different phases. Hydroxyurea is an inhibitor of the ribonucleotide reductase, which leads to a decrease in the deoxyribonucleotide triphosphate pool, the stall of the replicative fork and hence, to an arrest in S phase. Oxidant-induced arrest of the cell cycle is followed by activation of defence genes (Riechheld 1999).

A transient increase in ROS levels early in G1 has been demonstrated also in mouse embryos and shown to be required for the transition from G1 to S phase (Menon et al 2003). Regulated oxidation of the cytosol at G1 has also been linked to the recruitment to GSH into the nucleus in both animal and plant cells, as illustrated in (Vivancos et al 2010). This suggests that transport of glutathione is important in the control of the redox state of the cytosol and nucleus during the cell cycle. Moreover, the total GSH pool is significantly increased at the G2+M phase compared to G1, suggesting that overall the cells are more reduced at the G2+M phase than at G1 (Conour et al 2004). Depletion of the cellular GSH pool causes an arrest of the cell cycle at G1. Thus, accumulating evidence from studies on cell cycle regulation in animals and plants support the view that glutathione is a key regulator of cell proliferation (Vivancos et al 2010).

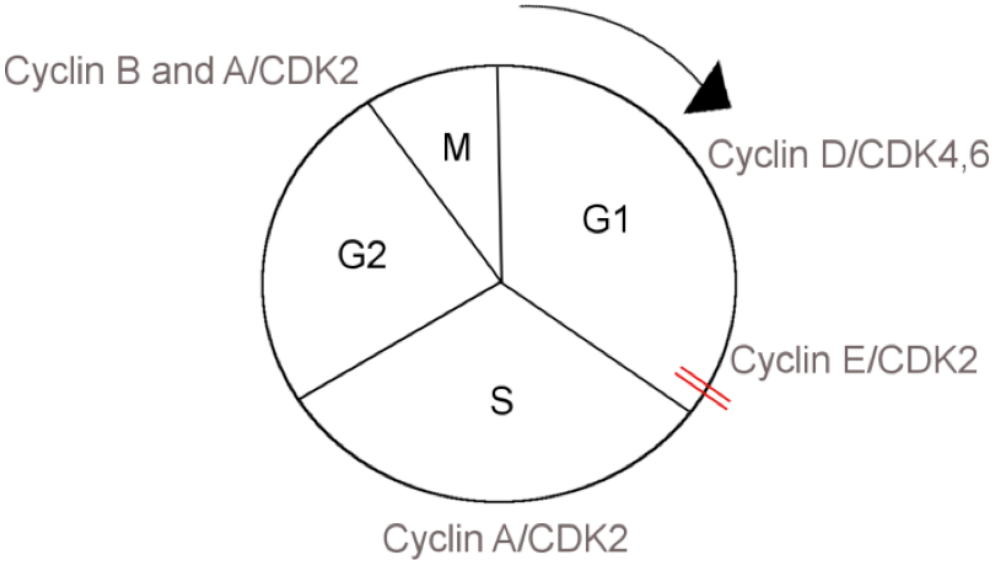

Figure 1.11 Schematic representation of cell cycle regulation in Arabidopsis root.

Cyclin D/CDK4,6 regulates G1 phase stimulating cell growth and cell cycle progression. Cyclin E/CDK2 is determinant for G1/S phase transition and entering in the S phase. Cyclin A/CDK2 complex inhibits cyclin E/CDK2 and activates DNA replication in the S phase. Moreover, A/CDK2 complex has also a role in the late G2 phase where it stimulates Cyclin B and regulates the timing of mitosis. Cyclin B is the main promoter of mitosis being part of the complex of the maturation promoting factor. Upon hydroxyurea (HU) treatment the cell cycle slows down before entering in S phase leading to an enrichment of cells in G1 as indicated by the red lines.

1.8 Aims of the thesis

Evidence suggests that oxidative processes and redox controls involving GSH and ascorbate are important determinants of developmental processes such as plant growth, seed germination and cell cycle control. Redox processes might therefore exert a significant influence over the fitness of the plant from germination to flowering. While many studies have focused on the role of oxidative events in responses to environmental stresses, little is known about the mechanisms of redox control of individual processes such as the cell cycle and how they affect early plant development. In particular, it is not clear how ROS, GSH, ascorbate and hormones interact to regulate germination and the cell cycle progression after germination. The following study is therefore designed to characterise the role of GSH and ascorbate in seed germination and the control of the initiation of the cell cycle after germination. The specific objectives were:

1. To use roGFP2 sensing system to determine the redox state of the nucleus and cytosol of germinated seeds in Arabidopsis.
2. To determine the changes in the redox state of the nucleus and cytosol during cell cycle progression in Arabidopsis radicles, in which cells were synchronised with hydroxyurea (HU).
3. To determine whether low redox capacity conditions alter the redox state of the nucleus and cytosol in the radicle of low ascorbate *vtc2-1* mutant.
4. To determine the changes in the redox state of the nucleus and cytosol during cell cycle progression in synchronised cells of *vtc2-1* mutant radicles.
5. To analyse the changes in the transcriptome of the dry and imbibed seeds of *vtc2-1* and *vtc2-4* mutant lines and investigate the relationships between cellular redox state, dormancy control and germination.

Chapter 2. Material and Methods

2.1 Plant material and growth analysis

2.1.1 *Arabidopsis thaliana* lines

2.1.1.1 Redox sensitive GFP (roGFP2) lines

Seeds of roGFP2 (Meyer et al 2007) and *vtc2-1* mutants expressing roGFP2 (*vtc2*-roGFP2; F2 generation) ecotype Columbia (Col-0) were provided by Till K. Pellny (Rothamsted Research, UK). roGFP2 line was previously cloned into the binary vector pBinAR (Figure 2.1) by Dr Andreas Meyer (University of Bonn, Germany).

2.1.1.2 Root structure markers

Seeds of *WUSCHEL* (*WOX5::GFP*), *WOODEN LEG 1* (*WOL::GFP*) and *PLETHORA 3* (*PLT3::GFP*) were provided by Dr Yoselin Beñitez Alfonso (University of Leeds, UK).

2.1.1.3 Cell cycle markers

Seeds of *CYCB1;1::GUS* reporter line (Di Donato et al 2004) was provided by Dr Chris West (University of Leeds, UK).

Seeds of the DUAL CORE MARKER SYSTEM (Cytrap) expressing *pHTR2::CDT1a (C3)-RFP* and *pCYCB1::CYCB1-GFP* was provided by Dr Masaaki Umeda (Nara Institute of Science and Technology, Japan). *pHTR2::CDT1a (C3)-RFP* and *pCYCB1::CYCB1-GFP* fluorescence was visualised by confocal laser scanning microscopy (CLSM) exciting at 488 nm and at 559 nm respectively.

2.1.1.4 Low ascorbate mutant lines

Arabidopsis wild type seeds ([L.] Heynh. Ecotype Columbia 0; Col-0) and ascorbate-deficient mutant lines *vtc2-1* EMS [*vtc2-1*] were obtained from the laboratory of Dr Robert Last and grown in our lab since 2003. Seeds of *vtc2-4* T-DNA insertion line [*vtc2-4*] was obtained from

Nottingham Arabidopsis stock (NASC; SAIL_769_H05 for At4g26850) and provided by Robbie Gillet (Dr Chris West lab, University of Leeds, UK).

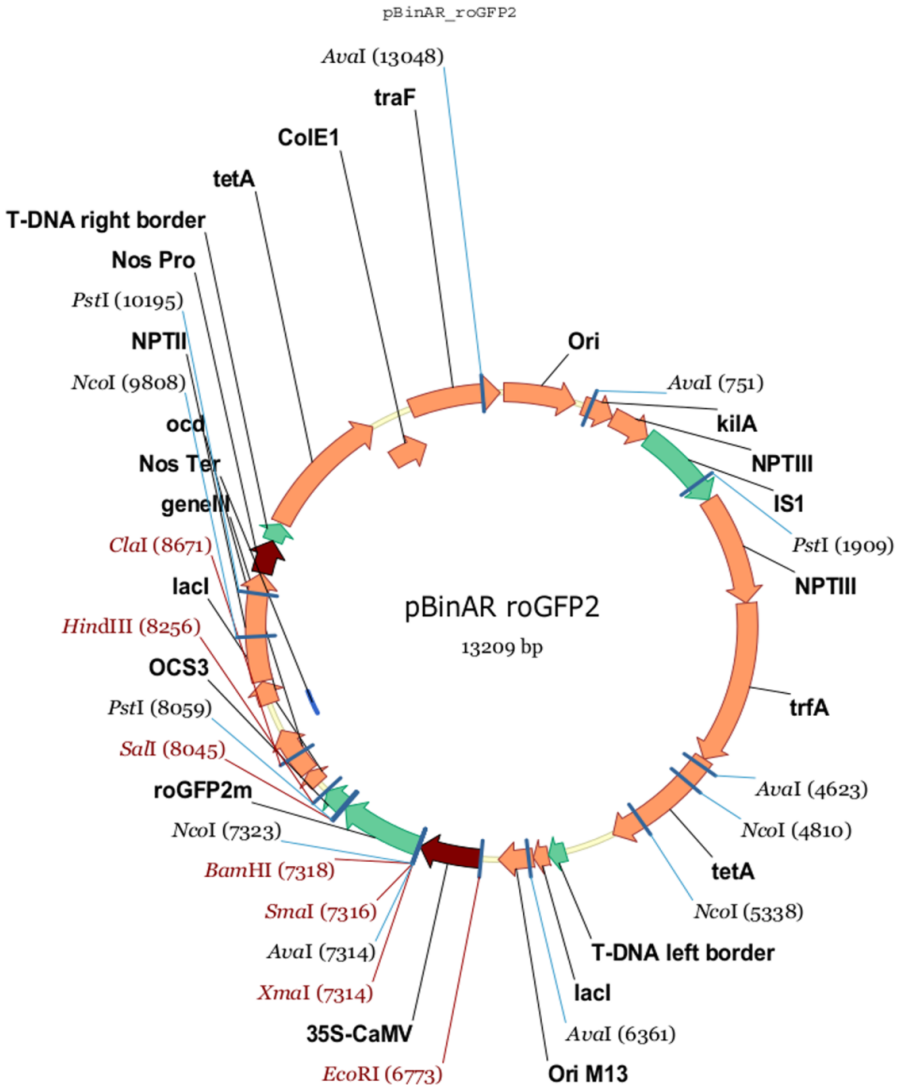

Figure 2.1 Map of the binary vector pBinAR used to clone roGFP2 T-DNA region.

The small green arrows show the right and left border of the T-DNA insertion. roGFP2m T-DNA sequence is inserted under the cauliflower mosaic virus 35S promoter (35S-CaMV, red arrow) and under the terminator sequence of octopine synthase (OCS3, green arrow). The map shows also nopaline synthase promoter (Nos Pro), neomycin phosphotransferase (NPTII) and the terminator sequence of nopaline synthase (Nos Ter).

2.1.2 Growth conditions

2.1.2.1 In vitro plant growth and synchronization treatment

All seeds were sterilised with 70% ethanol in water for 3 minutes (min). Seeds were then washed three times with sterile water and transferred to Half Strength Murashige and Skoog 1% Agar medium (½MS). ½MS was prepared as follows: 2.2 g/l Murashige and Skoog Basal Medium (Sigma-Aldrich), 0.1 g/l myo-Inositol, 0.5 g/l, MES, 10 g/l sucrose, adjusted to pH 5.7 with 1M KOH. 1% Agar was added prior to autoclave program at 121°C for 20 min.

½MS medium was poured into 12 cm^2 plates under sterile conditions. Seeds were sown and stratified for 48 hours at 4°C. Plates were then moved to controlled temperature conditions at 21°C for further 48 hours (Figure 2.2). In all cases, seeds were kept in dark by wrapping the plates with foil.

For cell cycle synchronization, following the stratification and germination steps described above, seedlings were transferred to fresh ½MS medium supplemented with 3 mM hydroxyurea (HU) and incubated at 21°C for 24 hours (Figure 2.2). In parallel, seedlings were transfer to fresh ½MS in the absence of HU as controls.

2.1.2.1 Shoot growth on soil

Arabidopsis plants were grown up to 4 weeks in controlled environment chambers with an irradiance of either 180 µmol m^{-2} s^{-2} or 250 µmol m^{-2} s^{-2}. Day length applied were 8h light/16h dark (short day), 16h light/8h dark (long day) and continuous light photoperiod, at a constant temperature of 21°C and a relative humidity of 60%.

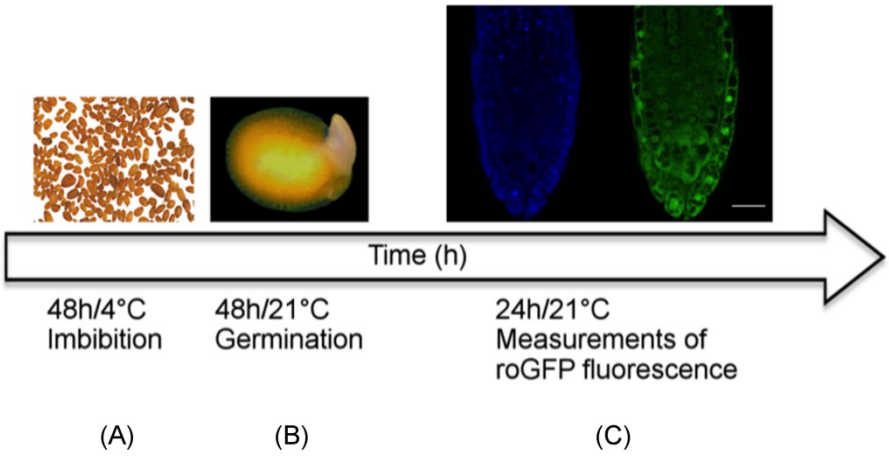

Figure 2.2 Diagram of the experimental plan of roGFP2 fluorescence measurements.

(A) Seeds were imbibed for 48 hours at 4ºC. (B) Germination was allowed for 48 hours at 21ºC. (C) Measurements of roGFP2 fluorescence were taken each hour for 24 hours. The entire experiment was performed under dark conditions.

2.2 Shoot phenotype analysis

2.2.1 Rosette diameter, number of leaves and biomass

Measurements of the rosette diameter, number of leaves and rosette biomass (fresh weight) were performed on the third week for plants grown under short day conditions and on the second week for plants grown under continuous light photoperiod. Measurements involved a minimum of 10 plants per genotype analysed per experiment. In all cases, photographs of the shoot were taken using a canon EOS 450D digital camera and using a ruler for scaling. Images were analysed by Fiji Image J (v1.46r) (Schindelin et al 2012).

2.2.1.1 Rosette biomass

Fresh rosettes were weighed on two days old plants using microbalance and immediately stored at -80°C. A minimum of 4 plants per time-point per experiment were used for analysis.

2.3 Ascorbate content estimation

Total ascorbate measurements were performed on whole rosettes that had been harvested midday through the photoperiod. Samples were frozen immediately in liquid nitrogen and stored at -80 °C until analysis. Ascorbate was measured using a FLUOstar Omega multi-detection microplate reader (BMG LABTECH) and Corning Costar 96-well UV transparent plates as previously described (Foyer et al 1983, Queval & Noctor 2007).

2.3.1 Total ascorbate extraction

Leaf tissue was ground to a fine powder in liquid nitrogen. 1 M $HClO_4$ (1 ml per 0.1 g fresh weight) was added to the sample and mixed. The homogenate was centrifuged 10 minutes at 16000g and 4ºC. 200 µl of the supernatant was transferred to a new tube and pH was neutralised to 5-6 adding 5M K_2CO_3. The mixture was centrifuged at 14000g for 2

minutes at 4ºC and ascorbate assay was performed as previously described by Foyer et al (1983).

2.4 Selection on kanamycin

Seeds were surface sterilised and stratified as described in section 2.1.2. Plants were selected on ½MS medium supplemented with 50 µg/ml kanamycin according to the rapid method of selection shown in Figure 2.3 (Harrison et al 2006). Following the step of stratification, a treatment of light/dark alternate conditions was performed. Seeds were exposed to 6 hours light, incubated for two days in dark conditions followed by 1-day light exposure and selection.

Figure 2.3 Diagram of the rapid method of kanamycin selection according to Harrison (2006).

In order to induce kanamycin resistance single individuals were treated with alternate light/dark conditions. Firstly, seeds were stratified for two days to allow synchronization of germination. Stratified seeds were exposed to light for 6 hours before being incubated in dark conditions for other two days at 21ºC. Seedlings were then transfer to light at 21ºC and selection of resistant individuals was performed.

2.5 Standard PCR

2.5.1 DNA extraction

Leaf samples were ground in liquid nitrogen and DNA was extracted in 0.4 ml of lysis buffer prepared as follows: 200 mM Tris HCl (pH 7.5), 25 mM EDTA, 250 mM NaCl and 0.5% SDS. The lysate was centrifuged at 10000g for 10 minutes at 4ºC and 0.2 ml of the supernatant was transferred to a new tube. A precipitation step was performed by treating the lysate with 0.2 ml of ice-cold isopropanol followed by centrifugation at 10000g for 10 minutes at 4ºC. At least two washing steps were performed by adding 0.5 ml of ice-cold 70% ethanol, centrifugation at 10000g for 10 minutes at 4ºC. Ethanol was allowed to evaporate and the pellet (DNA extracted) was resuspended in 0.1 ml of TE prepared as follows: 10 mM Tris HCl (pH 8) and 1 mM EDTA.

2.5.2 PCR reaction mix and program

Standard PCR was performed using BioMix^{TM} Red (Bioline) with a 1x final working concentration. PCR was performed in 0.2 ml PCR tubes with 20 µl of final volumes of the reaction mix. Oligonucleotide primers were designed to have 25 bp homology with the sequence to be amplified. A 100 µM stock of each oligonucleotide primer was made in TE from which a 10 µM working solution was prepared in dH20. A final concentration of 1 µM was used for each primer. Reactions were run in a thermal cycler with the following conditions: An initial denaturation step at 95 ºC 5:00 minutes, an annealing step at 60 ºC for 30 seconds and an extension step at 72 ºC for 1 minute, repeated for 30 cycles. A final extension step was performed at 72 ºC for 10 minutes.

2.5.3 Agarose gel electrophoresis

Agarose gel was prepared by dissolving Agarose in 1x Tris-acetate-EDTA (TAE) buffer at a final concentration of 1% (w/v). TAE was prepared as follows: 40 mM Tris, 20 mM acetic acid and 1mM EDTA. Once cooled, ethidium bromide was added to allow visualization of DNA under ultra violet (UV) light. Samples to be loaded were treated with 6x loading buffer and electrophoresis was performed at a constant voltage of 100V in 1x TAE buffer.

2.6 Quantitative Real-Time Reverse Transcription PCR

2.6.1 RNA isolation and cDNA synthesis

RNA for quantitative transcriptase real time was isolated from 20-30 mg of Arabidopsis seedlings. RNA extraction was performed using RNAqueous Small scale phenol-free total RNA isolation kit (Ambion; catalog #AM1912) with minor correction of the manufacturer's protocol. These consisted in grinding samples in liquid nitrogen to a fine powder and immediately suspend them in 0.8 ml of lysis/binding solution and 0.1 ml of plant RNA isolation aid. The homogenate was centrifuged 5 to 10 min at 15000 g at room temperature. The supernatant was transferred to a new 1.5 ml tube and the centrifugation step was repeated until the supernatant was clear. The pellet was treated with 2.5 M ammonium acetate, 2.5 volumes of 100% ice-cold ethanol and an overnight incubation was performed at -80ºC. The precipitated was washed three times with ice-cold 75% ethanol and eluted in 50 µl RNase free dH_20. The isolated RNA was quantified by Nanodrop ND-1000 (Thermo) and the QuantiTect Reverse Transcription Kit (Qiagen) was used for reverse transcription of 0.5 µg of RNA according to manufacturer's protocol.

2.6.2 Quantitative Real-Time RT-PCR

Quantitative Real-Time RT-PCR (qRT-PCR) was performed on cDNA synthesised from the RNA of harvested samples. QuantiFast SYBR® Green PCR Kit (Qiagen) was used according to manufacturer's protocol on a C100™ Thermal Cycler (BIO-RAD) real-time PCR system. A total of 20 µl PCR reaction mixture consisted in 10 µl SYBR Green, 1 µl 10 µM primer mix, 4 µl 10 ng cDNA and 5 µl RNAse free water.
The reaction conditions were as follows: An initial denaturation step at 95ºC for 5 min, 40 cycles of denaturation/amplification consisting of 95ºC for 10 sec, 60ºC for 30 sec and 55°C to 95°C by increment of 0,5°C for 5 sec. A melting curve analysis was performed to monitor possible primer dimer artefacts.

2.6.3 Primer design

Primers were designed using sequence viewer at TAIR (http://arabidopsis.org). To design primers based on the sequence of target genes the *primer3* software (http://primer3.ut.ee) was used. The sequences of primers of target genes are listed in Table 1. The sequences of primers of housekeeping genes are listed in Table 2.

Table 1 List of primers sequence used for qRT-PCR in cell cycle studies.

Primers	Sequence	Target
CYCB1;2 Fwd	5'-TTCTTGGAAACCTCGAATGG-3'	At5g06150
CYCB1;2 Rev	5'-TCTGGATCAGACATCGAAGC-3'	
CYCB2;1 Fwd	5'-CCTCAGTTCCAAGTGCTAACG-3'	At2g17620
CYCB2;1 Rev	5'-GGTTTCTCAAGCGACATTGG-3'	
CYCA1;1 Fwd	5'-CGTTAATGCCAGTTTCTCTAGC-3'	At1g44110
CYCA1;1 Rev	5'-TGAGCCATCATCAGATTTGC-3'	
CYCA3;1 Fwd	5'-CTAGGTTCATCATCCGTCCA-3'	At5g43080
CYCA3;1 Rev	5'-CATTCTTTCAAATCACCCGC-3'	
CYCD3;1 Fwd	5'-AACAGTCCTTCATCTGGGAG-3	At4g34160
CYCD3;1 Rev	5'-CTGCTATGTGCATCAGCCAT-3'	
CYCD5;1 Fwd	5'-GACACCTCCACCGGAAATAG-3'	At4g37630
CYCD5;1 Rev	5'-CTACGCATTCTCTTGGCTGG-3'	
VTC5 Fwd	5'-AATGTGAGTCCGATTGAGTATGG-3'	At5g55120
VTC5 Rev	5'-TAAGCCTGAAAGTGAAGATGG-3'	

Table 2 Primers sequence used for housekeeping genes transcripts.

Primers	Sequence	Target
TIP41 FWD	5'-GGCGAAGATGAGGCACCAA-3'	At4g34270
TIP41 REV	5'-GCCTCTGACTGATGGAGCT-3'	
PP2A2 FWD	5'ACAGATGTGGAAACATGGCCGC-3'	At1g13320
PP2A2 REV	5'GCGTGGTATCGGGTTCGACTTG-3'	
TUBUL FWD	5'-CCACAAACTGCAGGTCGCTCC-3'	At3g57890
TUBUL REV	5'-ACACCGGCAGGATGTGACAGG-3'	
PHOS2C FWD	5'-ATGAGGCCGAGTTGCTTGTGC-3'	At5g53140
PHOS2C REV	5'-ATGTTGTCTGCACTGCCACGG-3'	
SAND FWD	5'-GAAGTTTGCGCGTCTGGTGTCT-3'	At2g28390
SAND REV	5'-GCAAGTCATCGGGATGGAGAGA-3'	
PP2A3 FWD	5'-TAACGTGGCCAAAATGATGC-3'	At1g13320
PP2A3 REV	5'-GTTCTCCACAACCGCTTGGT-3'	
PDF2 Fwd	5'-TAACGTGGCCAAAATGATGC-3'	At1g13320
PDF2 Rev	5'-GTTCTCCACAACCGCTTGGT-3'	

2.7 Confocal laser scanning microscope (CLSM) imaging

2.7.1 Propidium iodide (PI) staining

Seedlings were stained with 50 µM of propidium iodide (PI) on microscope slide and visualised using 40x/1.3 Oil DIC M27 lens of Carl Zeiss confocal microscope LSM700 using as excitation wavelength at 543 nm.

2.7.2 4',6-diamidino-2-phenylindole (DAPI) staining

Seedlings were equilibrated performing a washing step with phosphate-buffered saline (PBS). PBS was prepared as follows: 137 mM NaCl, 2.7 mM KCl, 10 mM Na_2HPO_4, 1.8 mM KH_2PO_4, pH 7.4 adjusted with HCl. 5 mg/ml DAPI stock solution was diluted in PBS to 300 nM final concentration. Samples were stained with 300 µl of diluted DAPI followed by 5 minutes incubation. Samples were rinse in PBS and visualised under CLSM exciting at 358 nm.

2.7.3 Ratiometric roGFP2 analysis

Radicles expressing roGFP2 were placed on a slide in a drop of sterile water and imaging was performed using a Carl Zeiss confocal microscope LSM700 equipped with 405 nm and 488 nm lasers for excitation. Images were taken with 40x/1.3 Oil DIC M27 lens in a multitrack mode. Ratiometric analyses were performed using ImageJ software (http://rsbweb.nih.gov/ij/). The fluorescence at 405 nm was corrected by subtraction of the background and the corrected image was divided by the 488 nm fluorescence image to give a ratio of threshold 3. The ratio image was converted to a "fire" look-up table for pseudo-colour visualization of the 405/488 nm merged image. The ratios obtained were very sensitive to changes of configuration hence

only the same parameters were used to compare different images. In addition a calibration of the probe was performed for every experiment.

2.7.4 Calibration of roGFP2 probe

A calibration of roGFP2 was performed at the end of each experiment. For full reduction of the probe, radicles were treated for 5 minutes with 2.5 mM dithiothreitol (DTT). For full oxidation of the probe, radicles were treated for 10-15 minutes with 2 mM hydrogen peroxide (H_2O_2). In all cases, a minimum of 8 samples per treatment were used.

2.7.5 Redox potential calculation

roGFP2 oxidation degree and roGFP2 redox potential were calculated as described by Meyer (2007). roGFP2 midpoint redox potential ($E°'_{roGFP2}$) is -280 mV while roGFP2 redox potential (E_{roGFP2}) depends on the oxidation degree of its disulphide bridge. roGFP2 oxidation degree is calculated as described in Figure 2.4 (A) where R is the 405/488 nm ratio of the sample, R_{red} is the 405/488 nm ratio of the reduced form of the probe, R_{ox} is the 405/488 nm ratio of the oxidised form of the probe, I_{488min} and I_{488max} are the minimum and maximum intensity of fluorescence at 488 nm respectively (Meyer et al 2007). Since roGFP2 and glutathione exchange electrons in a reversible way, the redox potential of glutathione can be calculated using the Nernst equation (Figure 2.4 B) where E_{GSH} is the glutathione redox potential, $E°_{GSH}$ is glutathione midpoint potential (-240 mV), R is the gas constant (8.315 J K^{-1} mol^{-1}), T is the temperature (298.15 K), z is the number of electrons exchanged (2) and F is the Faraday constant (9.648 10^4 C mol^{-1}).

A

$$OxD_{roGFP2} = \frac{R - R_{red}}{(I_{488min}/I_{488max})(R_{ox} - R) + (R - R_{red})}$$

B

$$E_{roGFP2} = E^{o'}_{roGFP2} - \frac{RT}{zF} \ln \frac{1 - OxD_{roGFP2}}{OxD_{roGFP2}} =$$

$$E^{o'}_{GSH} - \frac{RT}{zF} \ln \frac{2[GSH]_{total}(1 - OxD_{GSH})^2}{OxD_{GSH}} = E_{GSH}$$

Figure 2.4 Formulae used to calculate (A) roGFP2 oxidation degree and (B) glutathione redox potential (Meyer et al 2007).

roGFP2 probe equilibrates with glutathione allowing estimation of glutathione oxidation degree and glutathione redox potential by roGFP2 fluorescence measurements. (A) The oxidation degree (OxD_{roGFP2}) was calculated from roGFP2 fluorescence ratio of 405/488 nm for *in vivo* experiment using CLSM. R_{red} and R_{ox} are the ratios of the fully reduced and fully oxidised roGFP2 respectively while R is the fluorescence 405/488 ratio. I_{488min} and I_{488max} are the fluorescence intensity of the fully reduced and fully oxidised roGFP2. (B) Nernst equation used to calculate GSH potential from roGFP2 redox potential. In this equation E_{GSH}, E^{o}_{GSH}, OxD_{GSH} and E_{roGFP2}, E^{o}_{roGFP2} and OxD_{roGFP2} are the redox potential, midpoint potential and oxidation degree of glutathione and roGFP2 respectively, R is the gas constant (8.315 J K^{-1} mol^{-1}), T is the temperature (298.15 K), z is the number of electrons exchanged (2) and F is the Faraday constant (9.648 10^4 C mol^{-1}).

2.8 Histochemical β-Glucuronidase (GUS) staining

2.8.1 Acetone fixation

Arabidopsis radicles expressing *CYCB1;1::GUS* reporter were surface sterilised, stratified and synchronised with 3 mM HU as described in section 2.1.2.1. Seedlings were fixed at selected time points with 200 µl of ice-cold acetone 90% in 1,5 ml tube. Samples were washed 3 times with PBS prior to GUS staining.

2.8.2 GUS staining

Whole *CYCB1;1::GUS* seedlings were stained for GUS in 1,5 ml tubes and visualised by fluorescence Leica DM 2500 microscope. The reaction buffer was prepared as follows: 10 ml 1M NaH_2PO_4, 0.5 ml 0.1M K3[Fe(CN)^6], 0.5 ml 0.1M K_4[Fe(CN)^6], ml 0.5M EDTA, 1 ml 10% Triton dissolved in 86 ml dH_2O. Potassium ferricyanide (K_3[Fe(CN)^6]) and potassium ferrocyanide (K_4[Fe(CN)^6]) were included to prevent the diffusion of the substrate. Aliquots of the reaction buffer were frozen at -20 ºC until analysis.

GUS staining was performed by addition of 200 µl of 5-bromo-4-chloro-3-indolyl-β-D-glucuronide Na salt (50 mg/ml X-Gluc) to the reaction buffer. Samples were vacuum infiltrated until bubbles were formed followed by 4-5 hours incubation at 37ºC. A destaining step was performed with warm 70% ethanol until the blue GUS signal was clearly visible and visualized using a modular polarization microscope Leica DM2500 (http://www.leica-microsystems.com).

2.9 RNAseq analysis

RNAseq analyses were performed together with Dorothee Wozny and Natanael Viñegra in collaboration with Prof. Maarten Koornneef and Dr Wim Soppe lab (Max Planck Institute for Plant Breeding Research, Cologne, Germany). Dry and imbibed seeds were used to extract RNA as described in section 2.6.1 in three biological replicates. RNA sequencing was performed with Illumina sequencing method.

2.9.1 RNAseq processing analysis

The raw data processing procedures were carried out by Michael Wilson, University of Leeds, UK. Paired-end Illumina reads were aligned using TopHat (v2.0.10) against a Bowtie2 (v2.2.8) index built from the TAIR10 reference sequence to create SAM alignment files, which were then sorted and converted into BAM alignment files using Samtools (v1.3). Paired-end Illumina reads were aligned using TopHat (v2.0.10) against a Bowtie2 (v2.2.8) index built from the TAIR10 reference sequence to create SAM alignment files, which were then sorted and converted into BAM alignment files using Samtools (v1.3) (Langmead & Salzberg 2012) (Trapnell et al 2012). The aligned read replicates were then counted using featureCounts to create gene-count matrix, which was then tested for differential gene expression between all pairs using EdgeR in R/Bioconductor, genes were called as differentially expressed if they showed a fold change of greater than 2 and a FDR corrected p-value of 0.05 or less (Robinson et al 2010). Counts for heatmaps and principal component analysis were converted to Transcripts Per Kilobase Million (TPM), PCA was performed using the PCAMethods package in R/Biocondcuctor, using the ppca method, with centering (Stacklies et al 2007).

The quantitative visualization of the splice junctions was performed from the aligned date on IGV platform (https://www.broadinstitute.org).

2.9.2 GO slim analysis

The functional categorization by loci for the whole genome was obtained from the common differentially regulated genes using GO slim tool (https://www.arabidopsis.org/tools/bulk/go/index.jsp).
The % of loci is given as follow:

$$\frac{\text{Number of genes annotated in GO slim category x 100}}{N} = \%$$

Where N is the total number of genes from the input list of common differentially regulated transcripts annotated to any term of the ontology.

GO protein classification was obtained from the input list of common differentially regulated transcripts using GO slim tool on the *protein analysis through evolutionary relationships system* (Panther) platform.

Chapter 3. Characterization of the relationship between the cellular redox state and cell cycle

3.1 Introduction

Glutathione (GSH) is a low molecular weight redox buffer that is abundant in plant cells. GSH is found in all compartments of the plant cell and can reach concentrations of up to 10 mM in organelles such as mitochondria. In contrast, the levels of GSH in the apoplast/cell wall compartment are very low. GSH levels in cells are strictly regulated by synthesis, transport and degradation. GSH is synthesised in two steps (Figure 1.7). GSH synthesis is subject to both transcriptional and post transcriptional controls (Galant et al 2011). GSH synthesis is required for the growth of the post embryonic root meristem and for the maintenance of the stem cell niche (Vernoux 2000, Wang et al 2013). The *root meristemless1* (*rml1*) mutant carries a mutation in the *GSH1* gene and has only about 3% of the wild type levels of GSH. This mutant has a rootless phenotype due to an arrest of cells in the G1/S transition in the root apical meristem (Cheng et al 1995, Vernoux 2000). Moreover, treatment with L-buthionine (S,R)-sulfoximine (BSO), a specific inhibitor of GSH synthesis, slows cell division in the root apical meristem (Koprivova et al 2010, SanchezFernandez et al 1997). Furthermore, analysis of the *miao* mutant that lacks the plastid form of glutathione reductase (GR2) and displays defects in the root apical meristem showed that GSH is required for the downstream effectors of PLETHORA (PLT) (Yu et al 2013), the auxin-inducible master regulator of root development (Galinha et al 2007).

The structure of the root apical meristem is well characterised, particularly with regard to the quiescent centre and surrounding layers. The Arabidopsis primary root comprises of four zones; the root cap, the meristem, the transition zone and the elongation zone (Kumpf & Nowack 2015, Verbelen et al 2006). The expression patterns of marker

genes have been widely used to gain information concerning the structures of Arabidopsis roots, in which a small organizing centre, the quiescent centre (QC), maintains stem cell niche. For example, *PLETHORA3* (here called *PLT3*) is expressed in provascular cells, the quiescent centre and columella progenitor cells (Galinha et al 2007). The *PLETHORA* genes encode AP2 class putative transcription factors that are essential for QC specification and stem cell activity. In contrast to *PLT3*, *WUSCHEL-RELATED HOMEOBOX 5* (*WOX5*) is specifically expressed in the QC (Sarkar et al 2007). Conserved factors regulate signalling in Arabidopsis shoot and root stem cell organizers (Sarkar et al 2007). The *WOODEN LEG (WOL)* histidine kinase is a cytokinin-binding receptor that is required for proliferation of the vascular cylinder (Mahonen et al 2000). In the following experiments, GFP probes linked to the promoters of the *PET3*, *WOX5* and *WOL* were used to identify the different cell types in the root in order to determine the region of cell proliferation. Once this had been identified, roGFP2 was used to measure GSH ratio in the dividing cells (Meyer et al 2007). Moreover, this probe was used to monitor changes in the glutathione redox potential of the nucleus and cytosol of these cells in relation to the cell cycle.

Although progression through the cell cycle phases has been well characterized, the role of redox regulation in this process is poorly understood in plants (Considine & Foyer 2014). In animal cells, changes in oxidation are required for the activation of regulatory proteins involved in cell division. For example, a transient increase of ROS levels are linked to the transition G1/S in mouse embryos (Menon et al 2003). Moreover, the expression of *cyclin D1* that initiates the cell cycle is regulated by a redox-dependent mechanism (Burch & Heintz 2005). However, uncontrolled oxidation leads to an arrest of the cell cycle (Combettes et al 1999). In the following studies, the roGFP2 probe was used to determine the redox potential of the glutathione pool in the nuclei and cytosol of proliferating cells in the root apical meristem

in vivo. These measurements provide an estimation of the changes that occur in redox state during cell proliferation. However, the cells in the root meristem do not divide synchronously. Therefore, a low level of hydroxyurea (HU), which is an inhibitor of the ribonucleotide reductase and causes an arrest of the cell cycle at G1/S phase, was used to synchronise cells cycle progression (Cools et al 2010). Cell cycle markers were used to identify cells present in the different cell cycle stages. However, while G2/M specific markers such as *Cyclin B1-1* fused to either with GFP or GUS (Colon-Carmona et al 1999) are available, there are relatively few markers for other cell cycle stages. A dual core marker system that involves Cytrap expressing both S *pHTR2::CDT1a (C3)-RFP* and the G2/M *pCYCB1::CYCB1-GFP* specific marker was therefore used in the following studies. The first construct *pHTR2::CDT1a (C3)-RFP* is used as a marker for the S phase of the cell cycle. In the Cytrap system the *HISTONE THREE RELATED2* (*HTR2*) promoter, which shows S-specific transcription levels was fused to the *Cdt1* sequence to trigger active degradation of the RFP signal before metaphase (Yin et al 2014). The Cytrap system also uses a *pCYCB1::CYCB1-GFP* construct, in which *GFP* is expressed under the control the *CycB1;1* promoter at the G2/M phase of the cell cycle (Yin et al 2014). This system has successfully been used in cell cycle studies in Arabidopsis, where it was established that the cell cycle was 17 hours long, with 6 hours in G1, 8 hours for S/G2 and 3 hours for the M phase (Yin et al 2014). Cell cycle progression was also observed by following the incorporation of the thymidine analogue, ethynyldeoxyuridine (EdU), into newly synthesised DNA, which is detected with a fluorescent azide dye. The following studies used the *Cyclin B1-1:GUS* and the Cytrap systems, together with EdU labelling in the absence and presence of HU to characterise the progression of the cell cycle synchronization in wild type Arabidopsis roots. This information was used to identify cell cycle progression in roGFP2 roots, and so determine changes in the fluorescence of the probe during the cell cycle *in vivo*.

3.2 Results

3.2.1 Use of markers to identify cell types in the emerging Arabidopsis radicles

3.2.1.1 PLT3::GFP, WOX5::GFP, WOL::GFP

In the following experiments, seeds of different Arabidopsis genotypes were allowed to germinate and detection of the different cell types using cell type specific markers linked to GFP. In each case, seeds were imbibed for 48 hours at 4 ºC followed by incubation for 48 hours at 21ºC. GFP was then visualised in the radicles using confocal light scanning microscopy (CLSM). Propidium iodide was used to detect cell wall structures, as shown by the red staining in Figure 3.1. The fluorescence signal from the *PLT3::GFP* marker was used to identify the columella cells in the Arabidopsis roots (Figure 3.1 A). The fluorescence signal from *WOX5::GFP* was used to localise the QC (Figure 3.1 B) and *WOL::GFP* was used to identify the cells of the vascular system (Figure 3.1 C). Based on these observations, the area shown by the white box in Figure 3.1 B was designated as the area of cell proliferation that was monitored in the following studies using roGFP2.

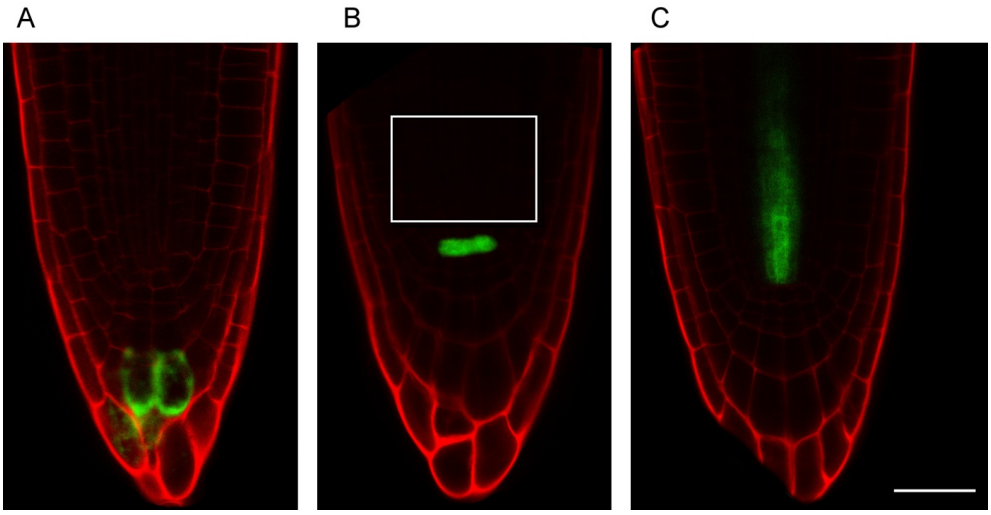

Figure 3.1 The distribution of GFP-tagged markers for in the different cell types in Arabidopsis roots

Arabidopsis root tips expressing GFP tagged to (A) *PLETHORA* (*PLT*) gene encoding AP2-domain transcription factors (*PLT3*), (B) *WUSCHEL*-related homeobox 5 (WOX5) and (C) *WOODEN LEG* (*WOL*). Roots were stained with PI on a microscope slide. Scale bar = 25 μm.

3.2.1.2 Analysis of roGFP2 fluorescence in radicles

Images of roGFP2 fluorescence were also obtained in Arabidopsis radicles at the same developmental stage as those used to determine different cell types as shown in Figure 3.1. The roGFP2 fluorescence was observed in all the cells of the Arabidopsis radicles including the root cap and the dividing cells of the meristematic zone, as indicated by the white box in Figure 3.2. roGFP2 florescence was observed in the nuclei and the cytosol of the cells (Figure 3.2). The fluorescence and the oxidation degree of roGFP2 redox couple were used to determine the redox potential of glutathione in the nuclei and the cytosol as described in the materials and methods section. In each case, values for the nuclei and the cytosol were obtained from 4-5 cells in the selected area of 2.5 mm the proliferation zone (1 technical replicate) indicated by the white boxes in Figure 3.2, with 3 technical replicates obtained per root sample per time point. For each time point, 3 biological replicates were performed. The dynamic range for the maximum change of the fluorescence ratio between the fully oxidized and fully reduced state of the roGFP2 chromophore was calculated from the fluorescence at 405 nm and 488 nm (Figure 3.3). The full reduction state of the probe was measured using 3 mM DTT and full oxidation of the probe was determined using 2 mM H_2O_2 (Figure 3.3 A and B). The formation of the disulphide bonds upon oxidation favours the protonated neutral form of the chromophore causing an increase in fluorescence at 405 nm while the 488 nm peak is decreased. Conversely, full reduction of the roGFP2 probe leads to a decrease in excitation at 405 nm while the peak at 488 nm is increased.

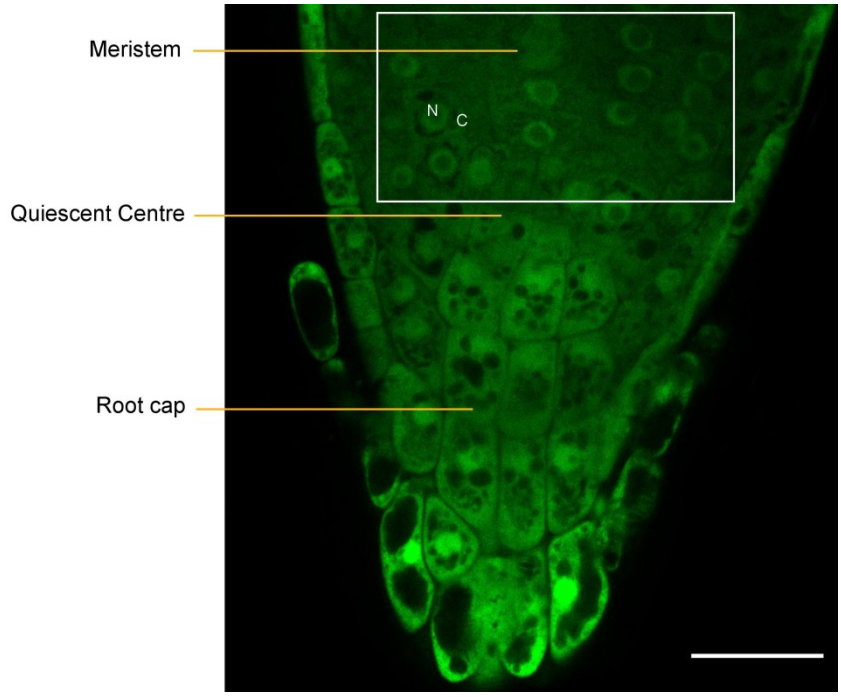

Figure 3.2 Image of roGFP2 fluorescence in the nuclei and cytosol of Arabidopsis radicle.

Cells of the meristem are shown by the white box above the quiescent centre and the root cap. Scale bar 25 µm.

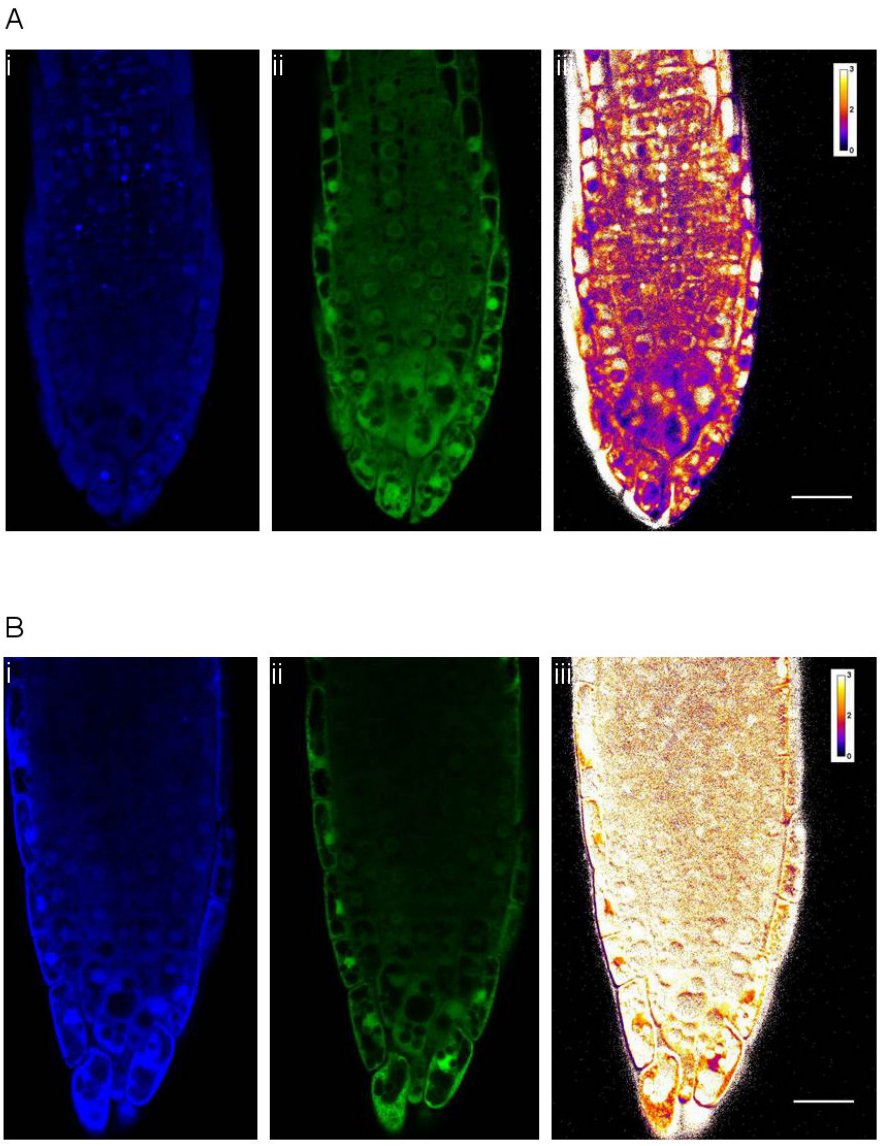

Figure 3.3 Images of roGFP2 fluorescence in the Arabidopsis radicle showing the calibration of the probe with (A) full reduction achieved in the presence of 3 mM DTT and (B) full oxidation of roGFP2 probe with 2 mM H_2O_2.

(i) Fluorescence of the oxidised form of roGFP2 excited at 405 nm is shown in blue, (ii) fluorescence of the reduced form of roGFP2 excited at 488 nm is shown in green and (iii) the ratios 405/488 nm are shown in a pseudo colour look-up scale. In the look-up scale lower values of 405/488 nm ratio indicate a more reduced state of roGFP2 and are shown in purple while higher value of 405/488 nm ratio indicating a more oxidised state of roGFP2 are shown in yellow. Scale bar 25 µm.

3.2.2 The glutathione redox potential of the nuclei and the cytosol of asynchronous cells

The fluorescence of roGFP2 was followed in the proliferating cells within the zone shown by the white the box in Figure 3.2 for 24 hours beginning at the 48 h time point after stratification. The roGFP2 fluorescence signal was measured in the nuclei and cytosol of this meristematic zone, using the 405/488 nm ratios to calculate the oxidation degree and glutathione redox potential as described in the materials and methods section. The 405/488 nm ratios in the nuclei and cytosol (Figure 3.4 A and B respectively) were generally between about 0.4 and 0.55 during the 24-hour time course of the experiment indicating that both compartments were highly reduced. Furthermore, the overall average 405/488 nm ratios in the nuclei was similar to that measured in the cytosol.

The oxidation degree (OxD) in the nuclei and cytosol, estimated from 405/488 nm ratios was between 20% and 35% for the nuclei (Figure 3.4 C) and between 20% and 40% for the cytosol (Figure 3.4 D). Again these differences were not statistically significant. The OxD was used to calculate the glutathione redox potential in the nuclei and cytosol (Figure 3.4 E and F respectively). The glutathione redox potential of the nuclei ranged from -287 to -307 mV and -280 to -300 mV in the cytosol (Figure 3.4 E and F respectively). The range of fluctuations in this parameter in both compartments was about 20 mV as shown by the red lines in Figure 3.4 (E and F). The average glutathione redox potentials measured in the nuclei and cytosol over the 24 hours of the experiment was -297.5 mV ± 0.7 in the nuclei and -292.8 mV ± 0.6 in the cytosol (Table 3).

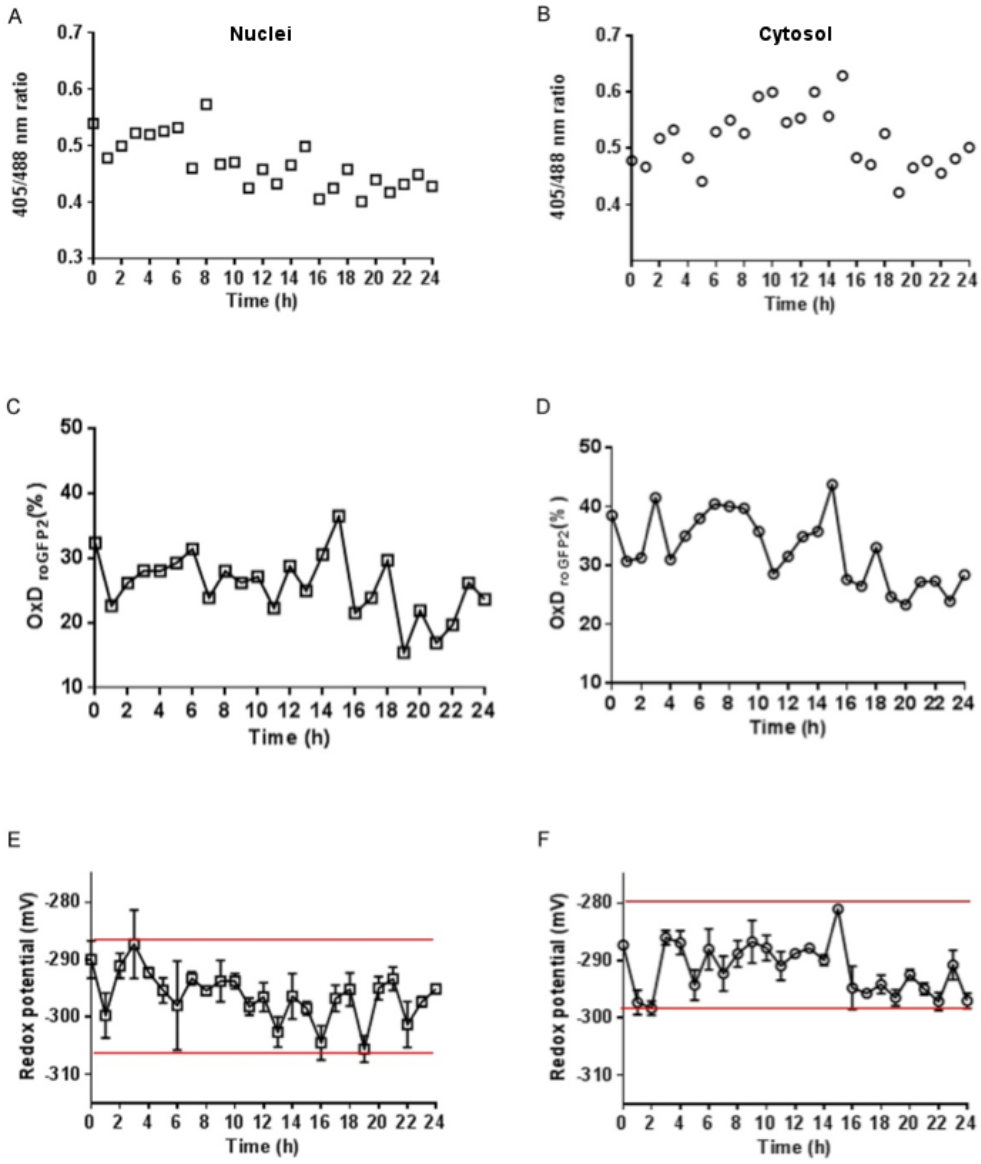

Figure 3.4 Quantification of roGFP2 fluorescence and determination of the glutathione redox potentials of the nuclei (left) and cytosol (right) of cells in the proliferation zone of Arabidopsis roots.

The 405/488 nm fluorescence ratios measured in the (A) nuclei and (B) the cytosol of cells in the proliferating zone of Arabidopsis roots measured from 48 to 72 hours after stratification. The oxidation degree in the (C) nuclei and (D) cytosol and of glutathione redox potential in (E) the nuclei and (F) cytosol were calculated from the 405/488 nm fluorescence ratios. The experiments were performed over 24-hour period. The red lines show the maximum, minimum and the range values of glutathione redox potential.

Table 3 Calculated glutathione redox potentials in the nuclei and cytosol of asynchronously dividing cells in the root meristem over a 24-hour time period.

Compartment	Glutathione redox potential (mV)
Nuclei	-297.5 ± 0.7
Cytosol	-292.8 ± 0.6

*Data are the mean values ± SEM (n ≥ 3).

3.2.3 Use of HU to synchronise the cell cycle

The data shown in Figure 3.4 and Table 3 were obtained from cells in the proliferation zone of the Arabidopsis root apical meristem, in which division of the cells is asynchronous. In order to determine whether the glutathione redox potentials of the cytosol and nuclei changes in the different cell cycle phases, the G1/S phase inhibitor HU was used to synchronise cell division in the proliferating zone, as defined by the white box in Figure 3.2. In these experiments, germinating seeds (48 hours after stratification) were transferred to new plates in the absence (Controls) or presence of 3 mM HU. This concentration has previously been shown in preliminary experiments to inhibit the cell cycle without causing cell death or permanent growth cessation. This finding is in agreement with the data reported by Cools et al (2010). The effect of HU treatment on cell cycle inhibition was visualised using the CYCB1:1-GUS marker and *in vivo* probes including a dual core marker system (Cytrap) and EdU labelling.

3.2.3.1 Root growth in presence of HU

In order to determine the effect of HU on root development, the growth of radicles emerging from seeds 48 hours after stratification was followed over 24 hours in the presence of 3 mM HU (Figure 3.5). After 5 hours exposure to HU, the length of radicles was significantly decreased compared to controls (Figure 3.5 A and B). However, the length of the primary roots was the same in the absence or presence of HU after 17 or 21 hours of treatment (Figure 3.5 B).

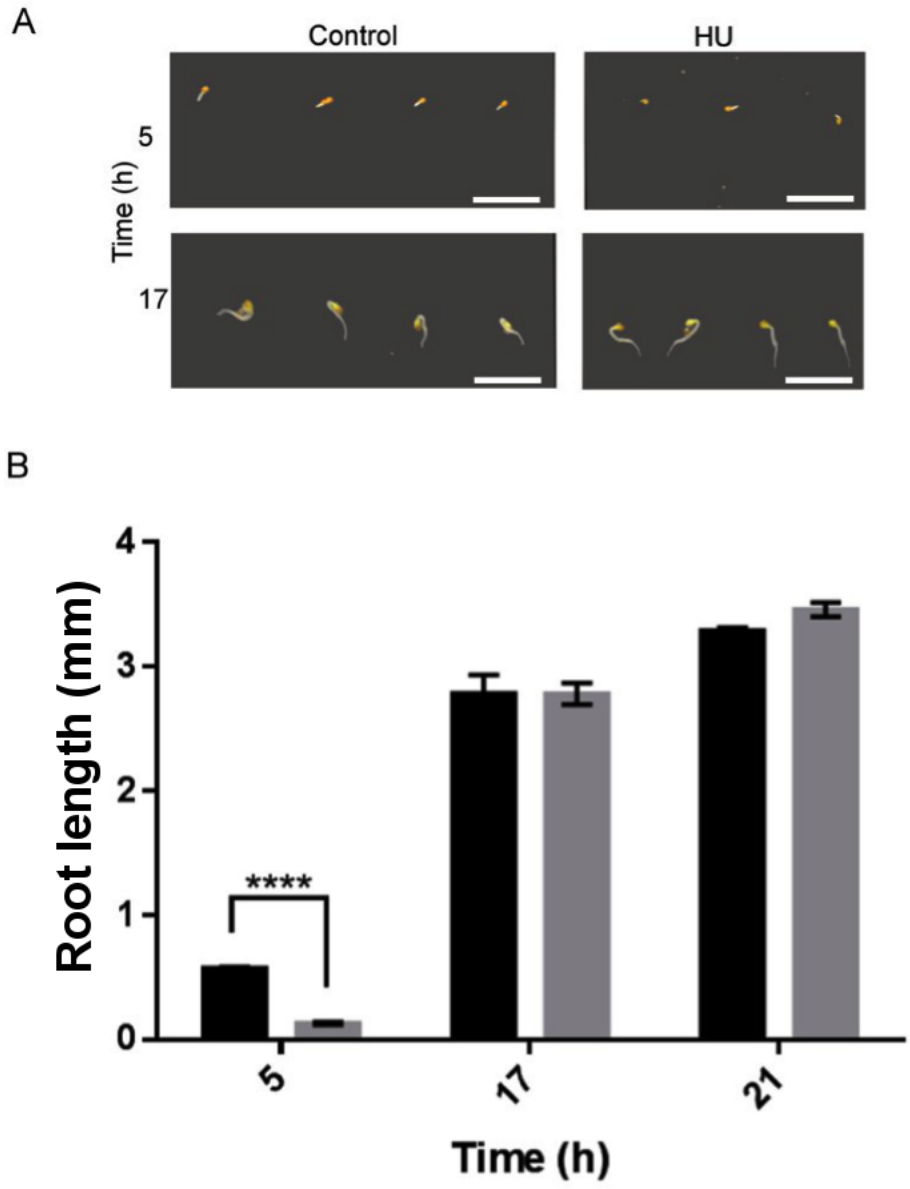

Figure 3.5 Effect of 3 mM HU on primary root growth.

(A) Germinating seeds were exposed for 5 hours (top right) or 17 hours (bottom right) to 3 mM HU. Control samples of germinating seeds in the absence of HU at the same time points (top and bottom left). (B) A comparison of the root length after 5, 17 and 21 hours of HU treatment (grey) with the length of radicles growing in the absence of the treatment (black). Values that were significant different between treated and untreated radicles, determined using one way ANOVA, P value < 0.0001, are indicated by asterisks. Scale bar 5 mm.

3.2.3.2 Effects of HU on cell growth

In order to investigate the effects of HU treatment on the progression of cell proliferation, the number of cells and the size of the nuclei were estimated in radicles that had been treated with HU for 24 hours (beginning at the 48 h time point after stratification) and compared to control samples in the absence of HU (Figure 3.6). The number of cells in the proliferation zone was significantly lower after 24 hours of HU treatment than in control samples (Figure 3.6 A). The size of the nuclei in the proliferation zone of the radicles that had been treated with HU for 24 hours was compared with that of the nuclei in this zone in control radicles that had not been subjected to the synchronization treatment. In the absence of HU, the nuclei had a uniform size of 3.8 +/- 0.012 (Figure 3.6 B). In comparison, size of the nuclei within the proliferation zone was increased at all the time points measured, increasing progressively from the first hour of treatment to maximum values between 10 and 15 hours after the onset of HU treatment. Thereafter, there was a decrease in the size of the nuclei but overall the nuclei were significantly larger as a result of HU treatment compared to controls (Figure 3.6 B).

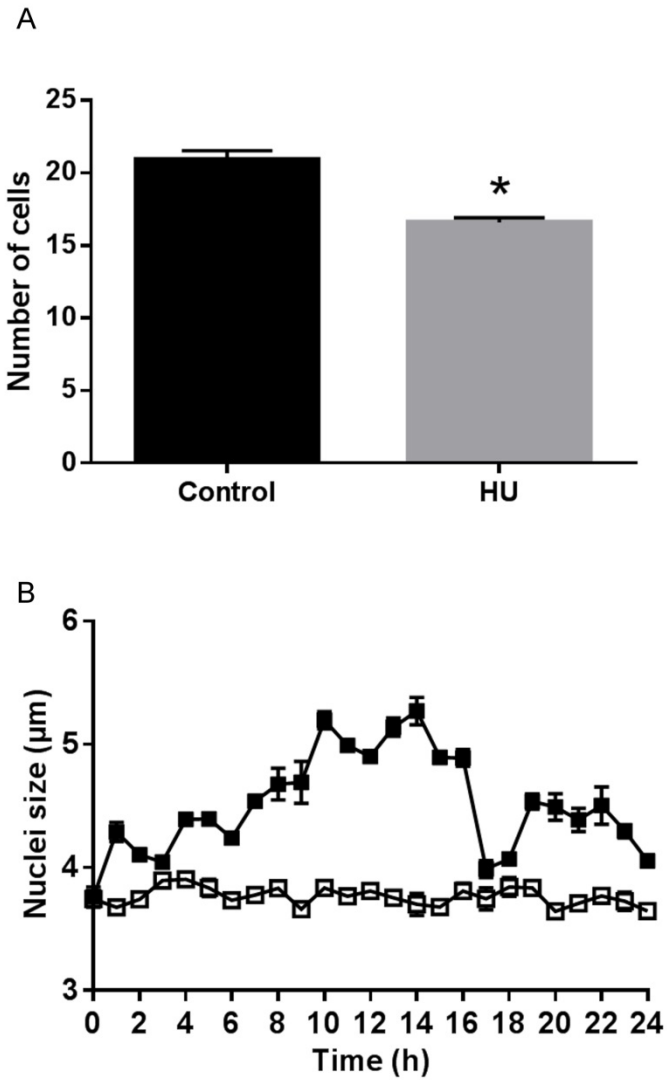

Figure 3.6 Effects of HU treatment on the number of cells and the size of the nuclei within the proliferation zone of the radicles of germinating seeds

(A) Number of cells in radicles treated up to 24 hours with HU (grey) and untreated (black). (B) Nuclear size in radicles treated up to 24 hours with HU (closed squares) and compared to control (open squares). Data are the mean values ± SE (n=3). *$p < 0.05$ in Significance given from analysis by Student's two tail *t*-test.

3.2.3.3 Expression of a *CYCB1:1-GUS* marker

Cyclin B1-1 (*CycB1;1*) is expressed in the G2/mitotic phase of the cell cycle (Himanen et al 2003). The expression of the gene can therefore be used as a specific marker for this phase of the cell cycle. The expression of a *CYCB1;1-GUS* reporter Arabidopsis line was used to analyse the effect of HU on cell cycle progression over a 24-hour period starting 48 hours after stratification. While patches of blue staining indicating GUS expression were observed in the control roots over the 24-hour period of the experiment, no significant accumulation was observed. In contrast, an accumulation of GUS staining was observed in the proliferation zone of the radicles treated with HU (Figure 3.7). Maximum staining in the HU radicles was observed between 17 and 18 hours after the start of HU treatment (Figure 3.7 HU). The GUS staining in the proliferation zone of the HU treated radicles had largely disappeared by 22 hours after the start of the treatment (Figure 3.7). These data indicate that cells in the proliferation zone were arrested at the G2/mitotic phase of the cell cycle between 17 and 18 hours after the onset of treatment. After this point; the cells were released from HU-mediated inhibition, suggesting that HU has only a temporary effect on cell cycle progression.

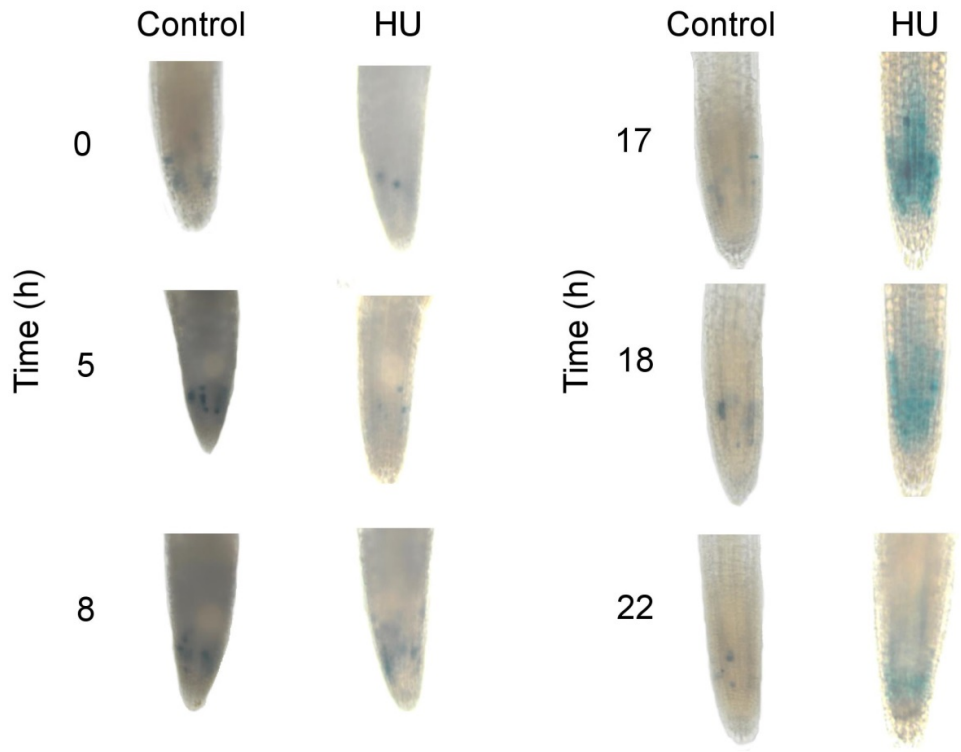

Figure 3.7 The effect of HU on the expression of a CYCB1;1::GUS marker in the proliferation zone of the root meristem in an Arabidopsis reporter line.

The accumulation of GUS staining in the roots was observed over a 24-hour period starting 48 hours after stratification in the absence (Control) or presence of hydroxyurea (HU).

3.2.3.4 The dual core marker system (Cytrap)

An Arabidopsis cell line expressing both S [*pHTR2::CDT1a (C3)-RFP*] and a G2/M (*pCYCB1::CYCB1-GFP*) markers was used to further analyse the effects of HU on cell cycle progression in the root apical meristem. As in the studies using the CYCB1;1-GUS marker, HU treatment was applied for 24 hours starting 48 hours after stratification to the line expressing the dual core marker system.

The appearance of the pink and green fluorescence associated with the expression of the S [pHTR2::CDT1a (C3)-RFP] and G2/M (pCYCB1::CYCB1-GFP) markers was random in the control roots over the 24-hour period of the experiment (Figure 3.8). After 5 hours of HU treatment the expression of the pHTR2::CDT1a (C3)-RFP and pCYCB1::CYCB1-GFP markers was similar to that in control radicles. In contrast, an accumulation of the pink fluorescence associated with the expression of the S [pHTR2::CDT1a (C3)-RFP] marker was observed 7 and 10 hours after the start of experiment in the roots treated with HU. Moreover, an accumulation of the green fluorescence associated with the expression of the G2/M marker (pCYCB1::CYCB1-GFP) was observed between 12 and 16 hours after the start of HU treatment (Figure 3.8). The larger area of the pink fluorescence associated with expression of the pHTR2::CDT1a (C3)-RFP marker in HU treated radicles (Figure 3.8 B) than in the control radicles (Figure 3.8 B) observed after 7 and 10 hours of the start of the treatment, suggests that a large number of cells present were in the S phase of the cell cycle. The difference in the expression of the G2/M cell cycle pCYCB1::CYCB1-GFP marker and controls at all the time points of the experiment indicates that HU induces synchronization from the first hours of HU treatment. However, between 12 and 16 hours, the area of cells expressing pCYCB1::CYCB1-GFP fluorescence in HU treated roots was much higher than in the controls indicating that most cells had reached the G2/M phase art this time point.

Taken together with the results obtained with the *CYCLIN B1-1* (*CycB1;1*) marker, these data suggest that most cells are in the G2/M phase of the cell cycle after 16 hours of HU treatment. Moreover, there is an accumulation of cells in the S phase between 7-10 hours after the start of the HU treatment.

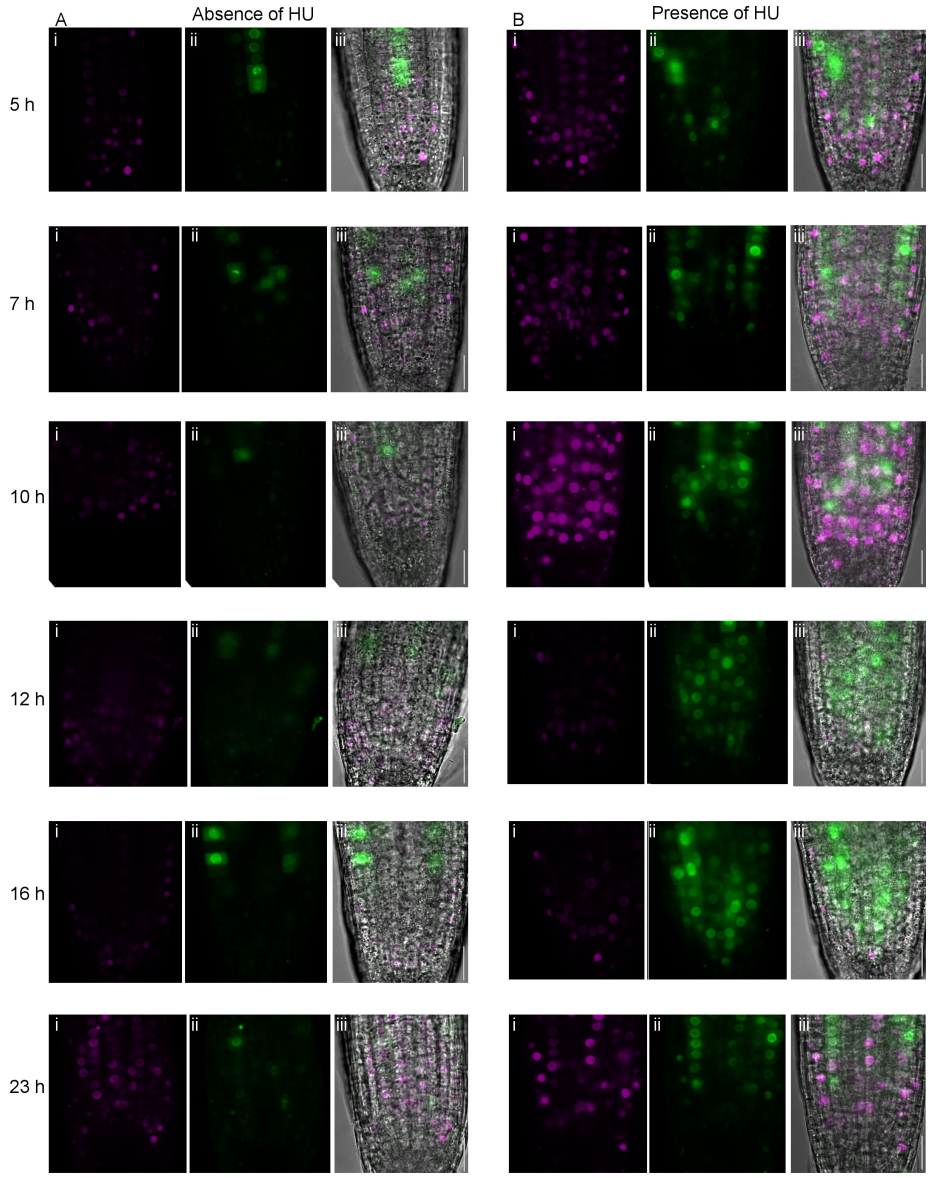

Figure 3.8 The effect of HU on the expression of (i) S (*pHTR2::CDT1a-RFP*) and (ii) G2/M (*pCYCB1::CYCB1-GFP*) markers in the proliferation zone of the root apical meristem in Arabidopsis reporter line.

The accumulation of (ii) GFP (green) and (i) RFP (pink) was followed in the root meristem over a 24-hour period starting 48 hours after stratification in (A) the absence or (B) presence of HU. (iii) The composite pictures were obtained by merging the GFP, RFP and the transmitted light pictures. Hours of treatment are indicated by numbers on the left. Scale bar 25 μm.

3.2.3.5 5-ethynyl-2'-deoxyuridine (Edu) Labelling

The data shown in Figure 3.7 and Figure 3.8 were obtained with Arabidopsis cell lines expressing cell cycle markers. To characterise the effects of HU on cell cycle progression in the root apical meristem further and to determine when cells were in the S phase of the cell cycle, the thymidine analogue, 5-ethynyl-2'-deoxyuridine (EdU) was used. EdU is incorporated into newly synthesised DNA. The extent of EdU accumulation can therefore be used as a marker for the S phase of the cell cycle. EdU incorporation was measured in the following studies using the fluorescent tag Alexa Fluo 594, which binds to EdU. Cells were stained with 4',6-diamidino-2-phenylindole (DAPI), which binds to chromatin and images were taken by CLSM exciting at 358 nm (Figure 3.9).

As in the studies using *in vivo* reporters of cell cycle progression, HU treatment was applied for 24 hours, starting 48 hours after stratification. Two hours after the onset of HU treatment, the roots were then incubated in EdU for 2 hours and stained with DAPI. Samples were also taken 17 hours after the onset of HU treatment and incubated in EdU for a further 2 hours, then stained with DAPI to visualise the nuclei (Figure 3.9).

After 2 hours of HU treatment the incorporation of EdU was similar to that in control radicles. However, after 17 hours of the start of the treatment there was an accumulation of EdU labelled nuclei suggesting that the replication of newly synthesised DNA driven by synchronization with HU had happened before this time point of HU incubation.

Taken together with the results obtained with the *in vivo* cell cycle markers (Figure 3.7 and Figure 3.8), the EdU staining procedures suggest that most cells are in the S phase of the cell cycle between 8 and 16 hours of HU treatment.

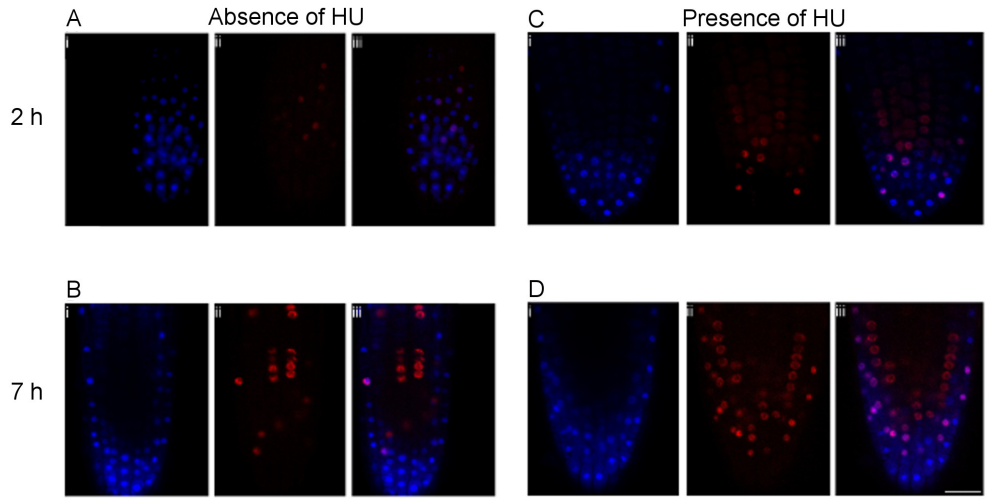

Figure 3.9 Incorporation of EdU and DAPI after treatment with HU.

(ii) Roots were incubated with EdU and stained with (i) DAPI for 2 hours after the onset of (C) HU treatment and (A) control. Samples were also incubated in EdU (ii) a further 2 hours and stained with DAPI (i) 17 hours after the onset of (D) HU treatment and (B) control. Scale bar 25 µm.

3.2.3.6 The abundance of transcripts encoding selected cell cycle markers (cyclins) in Arabidopsis roots in which the cell cycle had been synchronised using HU relative to unsynchronised controls.

Taken together, the above results suggest that HU treatment causes an accumulation of cells in G1/S phase between 6-8 hours, in the S phase between 10 and 16 hours and the G2/M phase between 16 and 23 hours. In order to explore the effect of HU on cell cycle progression further, the relative abundance of cell cycle marker transcripts was compared in whole roots treated with HU for 24 hours relative to untreated controls using qPCR (Figure 3.10). In these studies, cyclin *CYCA3.1* (Figure 3.10 A) was used as a marker for the G1/S phase of the cell cycle, *CYCD3.1* (Figure 3.10 B) and *CYCD5.1* (Figure 3.10 C) were used as S phase markers, and cyclins *CYCB2.1* (Figure 3.10 D) *CYCA1.1* (Figure 3.10 E) and *CYCB1.1 1* (Figure 3.10 F) were used as markers for the G2/M phase of the cell cycle (Culligan et al 2004, Menges & Murray 2002).

The abundance of *CYCA3.1* transcripts, which are used as a marker for the G1/S phase of the cell cycle, was low and relatively constant throughout the time course of the experiment in the absence of HU (Figure 3.10 A). The levels of *CYCA3.1* transcripts were much higher after 5 hours in the presence of HU than in the control roots (Figure 3.10 A). The *CYCA3.1* transcript levels remained high thereafter compared to the controls (Figure 3.10 A).

The levels of *CYCD3.1* (Figure 3.10 B) transcripts, which were used as an S phase marker were similar in the absence or presence of HU (Figure 3.10 B) over the 24-hour time course of the experiment, except that the abundance of *CYCD3.1* transcripts was significantly higher at 10 and 16 h time point points after the start of HU treatment than in untreated control roots (Figure 3.10 B).

The level of *CYCD5.1* transcripts, which was also used as an S phase marker, was low and relatively constant throughout the time course of

the experiment in the absence of HU (Figure 3.10 C). Incubation with HU had little effect on *CYCD5.*1 transcript levels, except for the 10 and 16 h time points, where the levels of these transcripts were significantly higher in the presence than the absence of HU (Figure 3.10 C).

The levels of *CYCA1.1*, *CYCB2.1* and *CYCB1.1* transcripts, which were used here as markers for the G2/M phase of the cell cycle, were low and relatively constant throughout the time course of the experiment in the presence of HU (Figure 3.10 D, E, F respectively). In contrast, roots incubated without synchronisation treatments showed two marked peaks in the levels of *CYCA1.1*, *CYCB2.1* and *CYCB1.1* transcripts, which occurred at 5 hours and 20 hours after the start of the experiment (Figure 3.10 D, E and F).

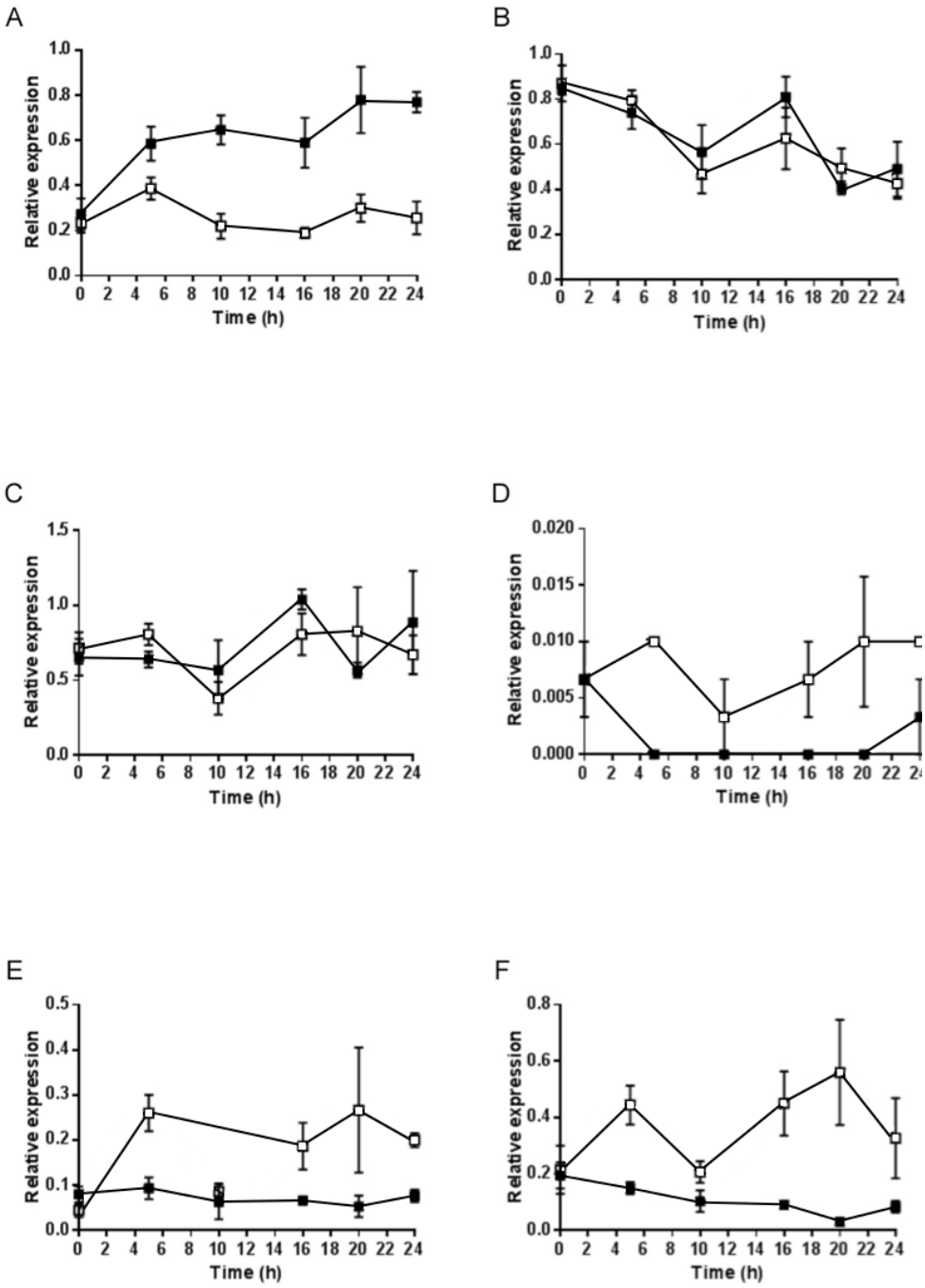

Figure 3.10 The relative expression of selected cell cycle markers in radicles incubated for 24 hours in either the absence of HU (open symbols) or presence of HU (closed symbols).

Transcripts analysed were: (A) G1/S phase marker *CYCA3.1*, (B and C) S phase markers *CYCD5.1* and *CYCD3.1* respectively, (D, E and F) G2/M phase markers *CYCB2.1*, *CYCA1.1* and *CYCB1.*1 respectively.

3.2.4 Measurements of the glutathione redox potentials of the nuclei and cytosol during cell cycle

In these experiments cell cycle progression was synchronised using 3 mM HU, as described above. Changes in roGFP2 fluorescence were determined in the proliferation zone of the germinating radicles over a 24-hour period in the absence or presence of HU. The 405/488 nm ratios were used to calculate the oxidation degree and glutathione redox potentials as described in the materials and methods section. Variations in the oxidation degree (OxD) and the glutathione redox potentials of the nuclei and cytosol in the proliferation zones of control and HU treated radicles were compared to determine whether there were changes in the redox state of these intracellular compartments during cell cycle progression.

3.2.4.1 Glutathione redox potentials of the nuclei and cytosol in the absence and presence of HU

Fluctuations in the 405/488 nm ratios were observed in the nuclei (Figure 3.11 A) and cytosol (Figure 3.11 B) of the proliferating cells in the absence and presence of HU. The presence of HU caused a shift in the 405/488 nm ratios of the nuclei between 2 and 8 hours of the onset of treatment being between as low as 0.40 in the HU treated samples compared to values of 0.50 in the absence of HU. Similarly, the 405/488 nm ratios of the cytosol were about 0.50 in the HU-treated roots between 18 and 24 hours of the treatment compared 0.40 in the absence of HU. There were no marked differences in the 405/488 nm ratios of the cytosol of the proliferating cells during the 24 hours incubation in the absence and presence of HU (Figure 3.11 B).

The OxD was between 20% and 40% in the nuclei (Figure 3.11 C) and between 20% and 55% in the cytosol (Figure 3.11 D) over the time course of the experiment cells in the absence and presence of HU.

There were no statistically significant differences in the data obtained in the absence compared to the presence of HU (Figure 3.1 C and D).

The OxD was used to calculate the glutathione redox potentials of the nuclei and cytosol (Figure 3.11 E and F respectively). The glutathione redox potentials of the control nuclei and those treated with HU were between -287 to -307 mV. Similarly the redox potentials of the cytosol of the unsynchronised and synchronised cells ranged between -280 to -307 mV (Figure 3.11 E and F respectively). The average glutathione redox potentials measured in synchronised cells over the 24-hour period of the experiment was -295.8 mV ± 0.8 for the nuclei and -293 mV ± 0.9 for the cytosol (Table 4). These values were not significantly different from those calculated in control samples (Table 4). However, the presence of HU resulted in significant differences in the glutathione redox potentials of the nuclei between 5 and 8 hours after the onset of treatment (Figure 3.11 E). At these time points the values obtained in the HU treated nuclei were as much 20 mV different from the values calculated in the controls in the absence of HU. Similarly, the glutathione redox potentials of the cytosol were significantly different in the cells with HU treatment compared to untreated controls between 1 and 5 hours after the onset of treatment. At these time points the values obtained in the cytosol of HU treated cells were as much 20 mV different from the values calculated in the controls in the absence of HU (Figure 3.11 F).

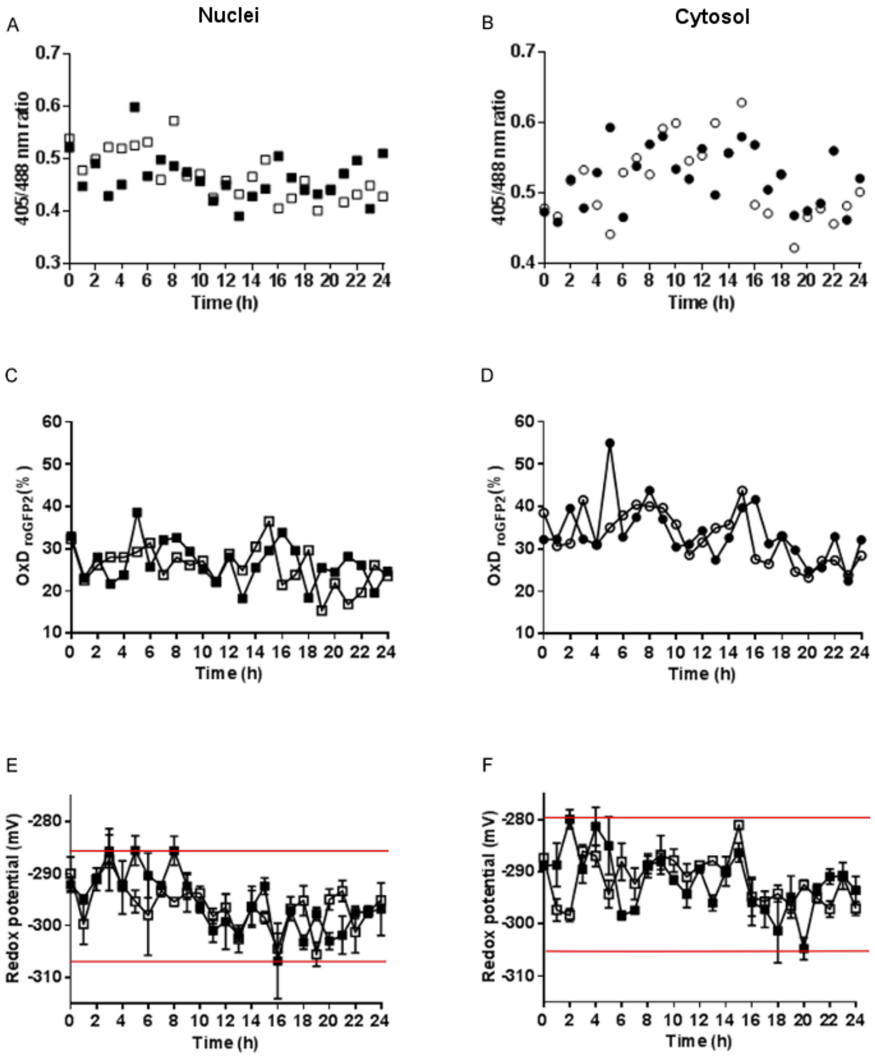

Figure 3.11 Analysis of roGFP2 fluorescence in the nuclei (left) and cytosol (right) of the proliferation zone of Arabidopsis roots in the absence (open symbols) or presence (closed symbols) of HU.

(A, B) The 405/488 nm fluorescence ratios, (C, D) the oxidation degree and (E, F) the glutathione redox potentials measured in the nuclei (A, C, E) and the cytosol (B, D, F), of cells in which the cell cycle was either unsynchronised controls (open symbols) or synchronised using HU (closed symbols). The red lines in E and F indicate the maximum and minimum values of the glutathione redox potentials. Experiments were repeated at least 3 times. Data are the mean values ± SE (n=3). **p < 0.01 in Significance given from analysis by Student's two tail t-test.

Table 4 A comparison of the glutathione redox potentials of the cytosol and nuclei of dividing cells in the proliferation zones of radicles in the absence (control) and presence of hydroxyurea (HU).

	Glutathione redox potential (mV)	
Compartment	**Control**	**HU**
Nuclei	-297.5 ± 0.7	-295.8 ± 0.8
Cytosol	-292.8 ± 0.6	-293 ± 0.9

*Data are the mean values ± SEM (n ≥ 3).

3.3 Discussion

The aim of the studies described in this chapter was to characterise the glutathione redox potentials of the cytosol and nuclei of cells in the proliferation zones of Arabidopsis roots, in order to determine whether changes in these parameters could be determined during the cell cycle progression. In these studies, hydroxyurea (HU) was used to synchronise cell cycle progression in the radicles of germinating Arabidopsis seeds. *In vivo* and *in vitro* techniques were used to identify the different phases of the cell cycle in the roGFP2 roots.

Taken together, the data presented in this chapter allow the determination of cell cycle progression in the proliferation zones of roots treated with HU relative to unsynchronised controls. The number of cells in the proliferation zones of the HU roots was significantly decreased compared to controls, demonstrating that HU limits cell division. However, this limitation was transient because root growth was only limited within the first hours of HU treatment.

3.3.1 Cell cycle progression in the presence of HU

HU has been widely used to synchronise the progression of cell cycle in whole tissues. It specifically inhibits the small subunit of ribonucleotide reductase decreasing deoxynucleotide triphosphate levels and decreasing replication progression, allowing synchronous mitosis. For example, cell cycle progression was followed in HU treated Arabidopsis root tips expressing a *CYCB1.1:DB-GUS* marker, 7 days after germination. In addition, HU was used to explore the expression of the dual-colour marker system called Cell Cycle Tracking in Plant Cells (Cytrap) that allows visualization of the S phase and G2 to M cell cycle stages. An analysis of the Cytrap data obtained in the present studies revealed an accumulation of cells in the G1/S phase between 6-8 hours

after the start of the HU treatment (Figure 3.8). Moreover, the abundance of *CYCA3.1* transcripts, which are used as a marker for the G1/S phase was high from 5 hours after the start of the HU treatment and remained high thereafter relative to the unsynchronised controls (Figure 3.10 A).

The data presented here show that the incorporation of EdU into new synthesised DNA, which was used as a marker for S phase occurred at 17 hours after the onset of HU treatment suggesting that there was a strong enrichment of S-phase cells at this time point. In agreement with this conclusion, the levels of *CYCD3.1* and *CYCD5.1* transcripts were maximal between the 8 and 17 h time point points after the start of HU treatment (Figure 3.10 B and C).

The levels of the *CYCB1.1*:*DB-GUS* marker for the G2 to M cell cycle stages measured in this study were highest between 17 and 19 hours after the transfer to media containing 3 mM HU, indicating a strong enrichment of M-phase cells at this time point. In agreement with these observations, the data presented in Figure 3.7 show that GUS staining arising from the *CYCB1.1:DB-GUS* marker was maximum between 17 and 18 hours after the start of HU treatment. Moreover, that data obtained using the dual-colour marker system, Cell Cycle Tracking in Plant Cells (Cytrap), which allows simultaneous monitoring of the S and G2/M phases of the cell cycle (Yin et al 2014), showed most cells were in the G2/M phase of the cell cycle after 16 hours of HU treatment. It is difficult to understand why the levels of *CYCA1.1*, *CYCB2.1* and *CYCB1.1* transcripts, which were also used here as markers for the G2/M phase of the cell cycle, were low and constant in the presence of HU (Figure 3.10 D, E, F). However, the levels of these transcripts were very low in all cases. Moreover, qPCR was performed on extracts from whole roots, rather than proliferating cells. Therefore, any changes in the levels of these transcripts in cells at the G2/M phase of the cell cycle were probably diluted to below detection in the qPCR analysis of extracts.

Taken together, these data show that the HU treatment used in the present studies led to a synchronisation of the progression of cell cycle in the proliferation zone of Arabidopsis roots, such that the majority of cells were in in the S phase between 6-8 hours after the start of the HU treatment, with an accumulation of cells in the S phase from 8 to 16 hours and in the G2/M phase from 16-19 hours of HU treatment, as illustrated in Figure 3.12. These finding are in agreement with the timing of cell cycle progression reported by Yin et al (2014).

3.3.2 Redox changes during cell cycle progression in the presence of HU

The nuclei and the cytosol of dividing cells in the Arabidopsis root tip had similar glutathione redox potentials, with values of -297.5 mV ± 0.7 in the nuclei and -292.8 mV ± 0.6 in the cytosol (Table 3). These values, which are similar to those measured in yeast using rxYFP (Dardalhon et al 2012), indicate that the nuclei and cytosol of root tip cells are in a highly reduced state and that the nuclear redox environment is not greatly different from that of the cytosol.

While there were large fluctuations in the measured 405/488 nm ratios in the nuclei and cytosol over the time course of the experiment in the absence and presence of HU, there was a significant increase in the ratios and consequently a significant change in the calculated glutathione redox potentials measured between 2 and 4 hours after the onset of treatment in the cytosol and between 5 and 8 hours in the nuclei. Thus the synchronisation treatment resulted in a significant oxidation of both the cytosol and nuclei within the first hours of HU treatment (Figure 3.11 E and F). The data presented in this chapter show that the majority of the cells in the proliferation zone were in the G1/S phase of the cell cycle between 6-8 hours after the start of the HU treatment (Figure 3.8 and Figure 3.10). Thus, the oxidation within the nuclei occurs within the G1/S phase, and is preceded by an oxidation in the cytosol. By the time there was a strong enrichment of cells at the S-phase, i.e. up to 16 hours after the start of HU treatment (Figure 3.10 B, C), the 405/488 nm ratios and calculated glutathione redox potentials had similar values in the presence or absence of HU. Moreover, the 405/488 nm ratios and calculated glutathione redox potentials were the same at the G2/M phases in synchronised cells and unsynchronised controls.

The data presented here showed that there is a transient oxidation of the cytosol and nuclei early in G1/S phase of the cell cycle (Figure 3.11 E and F). This finding is consistent with observations in animal cells, where an oxidation event at G1 phase is required to regulate the expression of Cyclin D1 (Menon et al 2003). The biphasic growth that takes place in proliferating animal cells is under the control of redox species regulation (Chiu & Dawes 2012). The perception of growth factors in mammalian cells triggers ROS production leading to cell gene transcription, protein synthesis, and cell cycle entry (Moreira et al 2015). This involves the AP-1 transcription factor, complex of Jun and Fos proteins, which controls the expression of genes for cell proliferation, particularly the *Cyclin D1*, which is critical for the transition of G1 to S (Klatt et al 1999). CYCLIN D1 has been suggested to contain redox-sensing cysteine residues that are susceptible to oxidation. Redox sensing involving reactive cysteine thiols that function as redox sensors in cell-cycle regulation ensuring that cell division is executed in an appropriate redox environment (Chiu & Dawes 2012).

In contrast to mild oxidation, which is required for mitogenic signalling in animal cells, excessive oxidation leads to arrest of the cell cycle in animals and plants. The presence of oxidative stress in mammalian cells, together with nitric oxide leads to a reaction between c-Jun and glutathione at Cys269 in the protein DNA-binding site (Klatt et al 1999). This glutathionylation of the protein at this domain inhibits DNA-binding activity, resulting in repression of gene expression (Klatt et al 1999). Glutathionylation of c-Jun can be reversed by a reducing agent such as dithiothreitol, indicating that upon restoration of redox homeostasis, c-Jun can activate cyclin expression to promote cell-cycle progression. While the factors that regulate cell cycle progression in animals are different from those that exist in plants, the observation that an oxidation of the cytosol and nuclei was observed at G1 phase in proliferating roots cells suggest that similar regulatory principles may apply to all eukaryotic cells.

The results presented in this chapter can be summarised as follows:

- In dividing cells of Arabidopsis radicles, the glutathione redox potential of the nuclei and cytosol is similar and highly reduced.
- Hydroxyurea does not cause oxidative stress. Therefore, it can be used to synchronise the proliferating cells of Arabidopsis radicles.
- A transient increase of oxidation in both the nuclei and cytosol is required in the G1 phase of the cell cycle for progression into the replicative S phase.

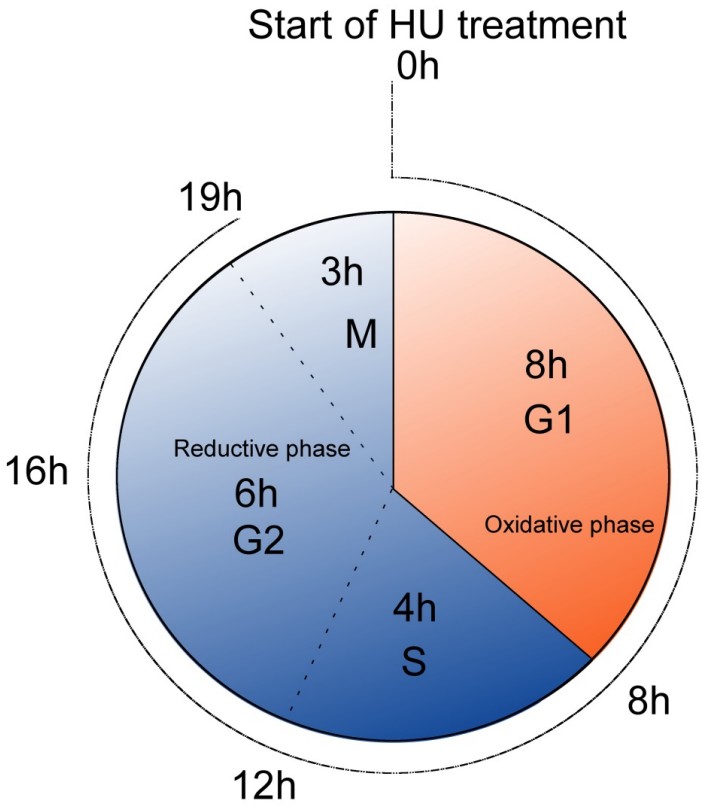

Figure 3.12 Schematic representation of redox cycle within cell cycle progression in the proliferation zone of Arabidopsis radicles.

The duration of oxidative reductive cell cycle phase in hours are indicated by numbers within the circle. Numbers outside the dashed line indicate the hours of HU treatment.

Chapter 4. Characterisation of the *vitamin C defective 2*, *vtc2-1* and *vtc2-4* mutant lines

Introduction

Ascorbic acid (vitamin C) is the most abundant low molecular weight antioxidant in plant cells, accumulating to high concentrations (20~50 mM) in chloroplasts and the cytosol (Foyer & Noctor 2011, Rautenkranz et al 1994). The major pathway for ascorbate biosynthesis in leaves is the GDP-mannose (galactose) pathway (Figure 1.4) (Dowdle et al 2008). However, ascorbate can be produced by a number of different pathways in other plant organs (Agius et al 2003, Gao et al 2011). The isolation and characterisation of Arabidopsis mutants that show impaired ascorbate accumulation was pivotal in elucidating the ascorbate biosynthesis pathway (Conklin et al 2000). Analysis of such mutants has shown that GDP-L-galactose phosphorylase catalyses the rate limiting step of the galactose pathway. This enzyme is encoded by the *VTC2* gene (Laing et al 2007, Linster et al 2007). However, a homologue of *VTC2, VTC5,* which also encodes a GDP-L-galactose phosphorylase is present in Arabidopsis plants (Dowdle et al 2008). The *vitamin C defective vtc2vtc5* double knockout mutants that are defective in both the *VTC2* and *VTC5* genes have a seedling lethal phenotype, which can be rescued by the addition of L-galactose or ascorbate (Dowdle et al 2008). The abundance of *VTC2* and *VTC5* transcripts and GDP-L-galactose phosphorylase activity is higher in the light than the dark (Dowdle et al 2008, Gao et al 2011, Yabuta et al 2008). Moreover, ascorbate accumulation in leaves increases in the light and decreases in the dark (Bartoli et al 2006, Pignocchi et al 2006). These findings demonstrate that the ascorbate synthesis pathway is regulated by light.

Ascorbate is considered to fulfil functions in the regulation of plant growth and development. For example, ascorbate has a regulatory role in cell cycle progression (Potters et al 2000). However, the mechanisms of ascorbate-dependent cell cycle regulation are not understood. Several types of mutants with defects in ascorbate synthesis are

available. Of these the *vtc2-1* and *vtc2-2* mutants that have only 20-30% of the wild ascorbate content were identified in an ethyl-methanesulfonate (EMS) mutagenesis screen for ozone sensitive mutants (Conklin et al 1996). These mutants have a slow growth phenotype as well as hypersensitivity to some abiotic stresses (Bartoli et al 2005, Conklin et al 2000, Jander et al 2002, Kerchev et al 2011, Kotchoni et al 2009, Pavet et al 2005). The *vtc1-1, vtc2-1, vtc3-1,* and *vtc4-1* mutants also show an altered flowering and senescence phenotype (Conklin et al 2000, Kotchoni et al 2009, Pavet et al 2005). The *vtc2-1* mutant has a single base substitution (from G to A) in the fifth intron of *VTC2* gene, introducing a splicing site and a premature stop codon (Muller-Moule 2008). Recently, several *vtc2* T-DNA insertion mutant lines have been identified. Of these, the *vitamin C defective 2 vtc2-4* (SAIL_769_H05) mutant line, which here will be called *vtc2-4*, was used in the following studies. In this T-DNA line, the T-DNA is inserted in intron 620 bp downstream the start codon. The vectors used to produce SAIL lines have a 1'2' bidirectional promoter, which in the case of SAIL_769_H05 mutant line, might lead to the transcription of the last four exons of the *VTC2* gene (Ulker et al 2008).

The following studies were performed to investigate the role of ascorbate on shoot growth under different light intensity and photoperiod conditions. Firstly, the *vitamin C defective 2* mutant lines, *vtc2-1* and *vtc2-4* were grown in parallel with wild type (Col-0) plants under short day (8-hour photoperiod) conditions at two light intensities, 180 µmol m^{-2} s^{-1} and 250 µmol m^{-2} s^{-1}. Secondly, the mutant and Col-0 plants were grown under continuous light (either 180 µmol m^{-2} s^{-1} or 250 µmol m^{-2} s^{-1}). Shoot biomass, rosette diameter and ascorbate contents were measured after 2-4 weeks of growth depending on the growth conditions. For example, the plants grown under continuous light were harvested after 2 weeks because of early flowering.

4.1 Results

4.1.1 Characterisation of shoot phenotype of Arabidopsis *vitamin C defective 2, vtc2-1* and *vtc2-4* mutant lines under short day conditions

In these studies, the shoot phenotypes and total leaf ascorbate contents were compared in the different lines grown under two different light intensities, 180 µmol m^{-2} s^{-1} and 250 µmol m^{-2} s^{-1} under short day (8-hour photoperiod) regime. Measurements of the number of leaves, rosette diameter and rosette fresh weights (biomass) were performed on four week-old plants.

4.1.1.1 Shoot phenotypes of Arabidopsis *vitamin C defective 2*, *vtc2-1* and *vtc2-4* mutant lines under short day condition

The rosettes of *vitamin C defective 2* mutant lines, *vtc2-1* and *vtc2-4* were visibly smaller than wild type, Col-0 when plants were grown under short day conditions either at 180 µmol m^{-2} s^{-1} light conditions (Figure 4.1) or 250 µmol m^{-2} s^{-1} (Figure 4.2).

Figure 4.1 Comparison of the rosette phenotypes of wild type (Col-0) Arabidopsis plants and *vitamin C defective 2* mutant lines, *vtc2-1* and *vtc2-4*, grown under 180 µmol m^{-2} s^{-1}.

Plants grown for four weeks under short day conditions (8-hour photoperiod).

Figure 4.2 Comparison of the rosette phenotypes of the wild type (Col-0) and *vitamin C defective 2* mutant lines, vtc2-1 and vtc2-4, grown under short day conditions (250 µmol m^{-2} s^{-1}).

Plants grown up to four weeks under short day conditions (8-hour photoperiod).

4.1.1.2 Comparisons of the number of leaves, rosette diameter and shoot biomass of Arabidopsis *vitamin C defective 2*, *vtc2-1* and *vtc2-4* mutant lines under short day conditions

The *vitamin C defective 2* mutant lines, *vtc2-1* and *vtc2-4*, had a significantly smaller rosette diameter with fewer leaves and lower biomass than Col-0, when plants were grown for four weeks under 180 µmol m^{-2} s^{-1} (Figure 4.3 A and C). Similarly, the *vtc2-1* plants had smaller rosettes with a significantly lower number of leaves and lower biomass than Col-0, when plants were grown for four weeks under 250 µmol m^{-2} s^{-1} (Figure 4.3 B). However, while the *vtc2-4* plants did not show statistically significant differences in these parameters to the wild type when grown under 250 µmol m^{-2} s^{-1}.

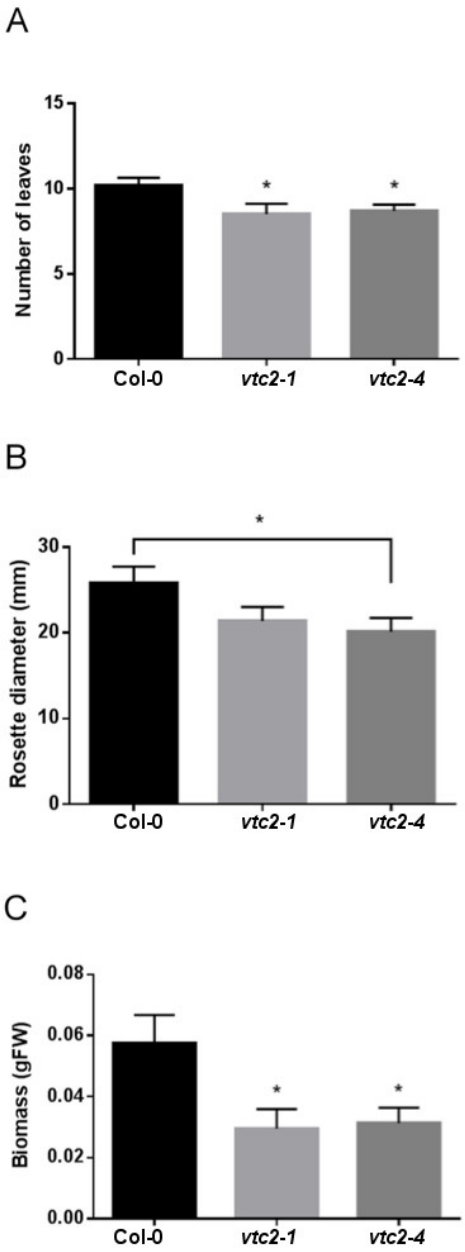

Figure 4.3 Comparison of the (A) number of leaves, (B) rosette diameter and (C) fresh weights of Col-0 plants and *vitamin C defective 2* mutant lines, *vtc2-1* and *vtc2-4*, grown under 180 µmol m^{-2} s^{-1} irradiance for four weeks.

Data are the mean values ± SE (n = 10). * $p < 0.05$, in significance given from analysis by Student's two tail *t*-test and One-Way ANOVA.

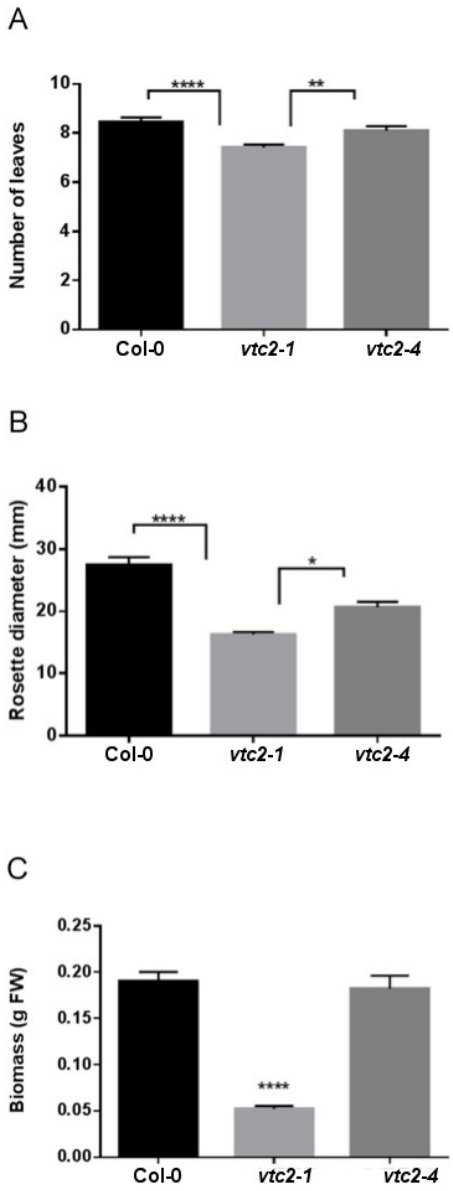

Figure 4.4 (A) Comparison of the number of leaves, (B) rosette diameter and (C) fresh weight of Col-0 and *vitamin C defective 2* mutant lines *vtc2-1* and *vtc2-4* grown under 250 µmol m^{-2} s^{-1} irradiance for three weeks.

Data are the mean values ± SE (n = 10). (* $p < 0.05$, ** $p < 0.01$ *** $p < 0.001$ and **** $p < 0.0001$) in significance given from analysis by Student's two tail *t*-test and One-Way ANOVA.

4.1.1.3 Total rosette ascorbate content in the wild type Col-0 *vitamin C defective 2* mutant lines under short day conditions

The total ascorbate content was determined in the rosettes of 2 week-old Col-0 and the *vitamin C defective 2* mutant lines, *vtc2-1* and *vtc2-4*, grown under 180 µmol m^{-2} s^{-1} and 250 µmol m^{-2} s^{-1} light. In these studies, samples were harvested 4 hours into the photoperiod. Both mutant lines, *vtc2-1* and *vtc2-4*, had a significantly lower total ascorbate content (about 20% of the wild type) when plants were grown under 180 µmol m^{-2} s^{-1} (Figure 4.5). This finding agrees with previously published data on the ascorbate content of the *vtc2-1* line (Jander et al 2002, Muller-Moule et al 2002).

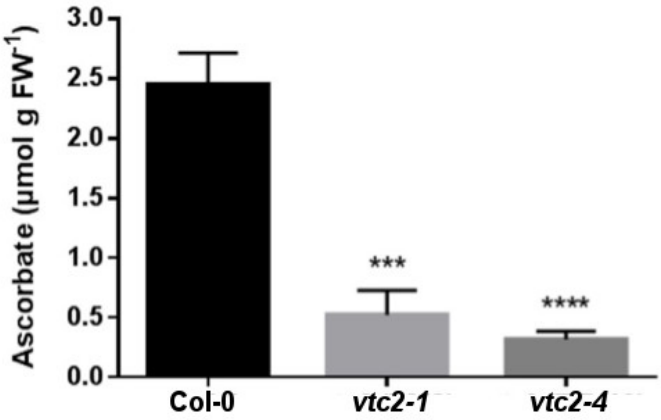

Figure 4.5 Rosette ascorbate contents of Col-0 and *vitamin C defective 2* mutant lines, *vtc2-1* and *vtc2-4*, grown under 180 µmol m^{-2} s^{-1} irradiance.

Data are the mean values ± SE (n=3). *** $p < 0.001$ and **** $p < 0.0001$ in significance given from analysis by Student's two tail *t*-test and One-Way ANOVA.

When the genotypes were grown under 250 µmol m^{-2} s^{-1} light conditions, the rosettes of the 2 week-old *vtc2-1* and *vtc2-4* lines had a significantly lower total ascorbate content (30%) than the wild type (Figure 4.6 A). There were no significant differences in the total ascorbate contents of the *vtc2-1* and *vtc2-4* rosettes under either light intensity (Figure 4.5 and Figure 4.6 A).

The above measurements were performed on rosette samples that had been harvested 4 hours into the photoperiod. Samples were harvested for the total rosette ascorbate at other selected times (0 i.e. 16 hours dark, and 2 and 7 hours into the photoperiod) in the different genotypes grown at 250 µmol m^{-2} s^{-1}. The *vtc2-1* and *vtc2-4* rosettes had significantly lower total ascorbate than Col-0 in all the time points (Figure 4.6 B). While the total ascorbate content of the Col-0 rosettes increased during the photoperiod, the ascorbate content of the *vtc2-1* and *vtc2-4* rosettes was low and constant over the photoperiod (Figure 4.6 B).

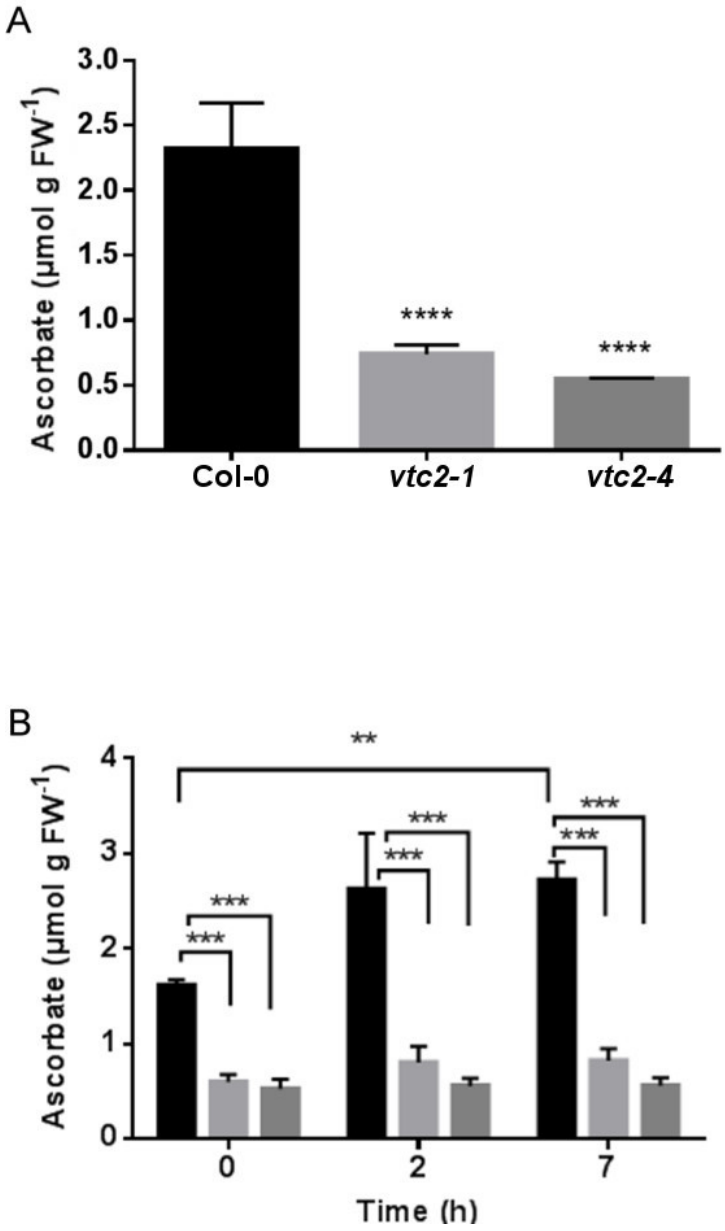

Figure 4.6 (A) Total ascorbate contents in the rosettes of *vitamin C defective 2* mutant, *vtc2-1* (light grey) and *vtc2-4* (dark grey) lines compared to the wild type (black) determined at 4 h into the photoperiod, after a (B) 16 hours dark period (0), and at 2 and 7 hours into the photoperiod.

Plants grown for two weeks under 250 µmol m^{-2} s^{-2}. (**p<0.01, *** p<0,001 and **** p<0,0001) in significance given from analysis by Student's two tail *t*-test and One-Way ANOVA comparison between the mutant lines and Col-0.

4.1.1.4 Expression of *VITAMIN C DEFECTIVE 2* homologue, *VITAMIN C DEFECTIVE 5* (*VTC5*) gene in plants grown under short day conditions

GDP-L-galactose phosphorylase, which is required for the phosphorylation of the GDP-L-galactose to L-galactose-1-P in ascorbate biosynthesis, is encoded by two genes in Arabidopsis, the *VITAMIN C DEFECTIVE 2 (VTC2)* and the *VITAMIN C DEFECTIVE 5* (*VTC5*) (Gao et al 2011). qRT-PCR was performed using primers for the *VTC5* gene in rosette leaves of the different genotypes grown for 2 weeks at 250 µmol m^{-2} s^{-1}. In these experiments samples were harvested after the 16 hours dark period (0), and at 1, 4 and 7 hours into the photoperiod in the different genotypes. The levels of *VTC5* transcripts were similar in all lines, except at the 4 time point, when *VTC5* transcript levels were significantly higher in the *vtc2-1* and *vtc2-4* mutants than the wild type (Figure 4.7).

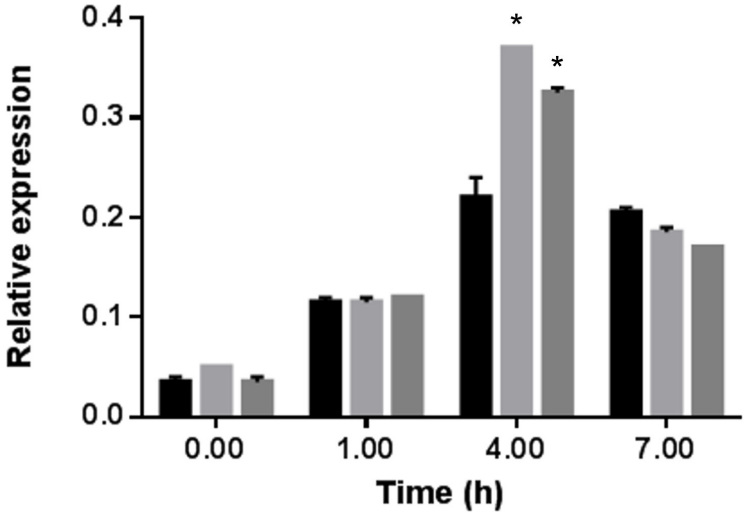

Figure 4.7 Relative expression level of *VITAMIN C DEFECTIVE 5* (*VTC5*) gene in *vtc2-1* (light grey), *vtc2-4* (dark grey) and wild type (black) measured at the end of the 16 hour dark period (0), and at 1, 4 and 7 hours into the photoperiod (250 µmol m^{-2} s^{-1}).

Data are the mean values ± SE (n=2).

4.1.1.5 Relationships between the rosette ascorbate content and biomass under short day conditions

The data shown above for total fresh weight and rosette ascorbate content were used to explore the relationships between shoot growth and rosette ascorbate levels further (Figure 4.8). The data presented in Figure 4.8 suggest that there is a strong relationship between these parameters in the different Arabidopsis genotypes when plants are grown under short day conditions at 180 µmol m^{-2} s^{-1}. However, when the data for plants grown under short days at 250 µmol m^{-2} s^{-1}, no relationship between biomass and leaf ascorbate was apparent.

On the contrary, *vtc2-1* plants grown under 250 µmol m^{-2} s^{-1} of light intensity, accumulate less biomass than Col-0 while *vtc2-4* mutant line presented a biomass similar to that measured in Col-0 (Figure 4.9).

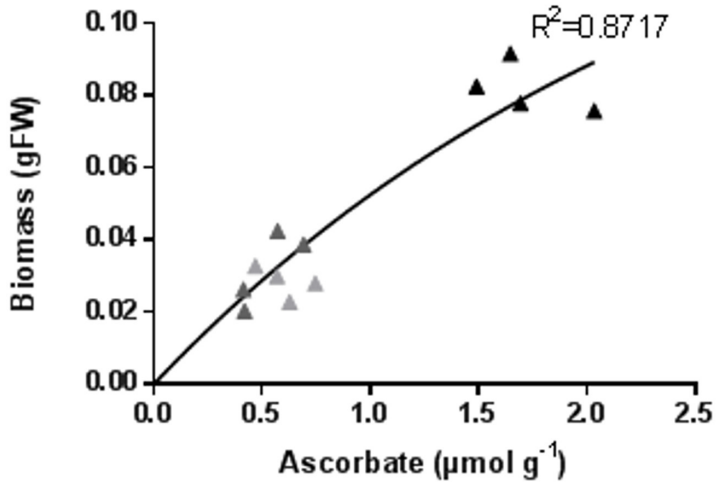

Figure 4.8 Relationships between biomass accumulation and ascorbate contents in Col-0 (black), *vtc2-1* (light grey) and *vtc2-4* (dark grey) in plants grown under short day (180 µmol m^{-2} s^{-1}) conditions.

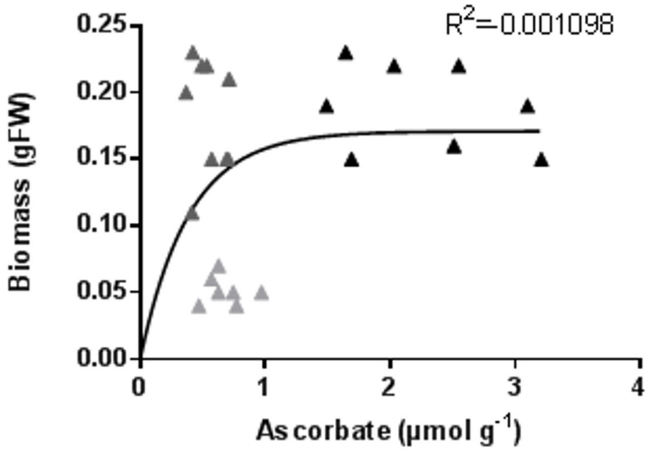

Figure 4.9 Relationships between biomass accumulation and ascorbate contents in Col-0 (black), *vtc2-1* (light grey) and *vtc2-4* (dark grey) in plants grown under short day (250 µmol m^{-2} s^{-1}) conditions.

4.1.2 Characterisation of the *vitamin C defective 2, vtc2-1* and *vtc2-4* mutant lines under continuous light

In parallel with the experiments performed under an 8-hour photoperiod regime, wild type (Col-0) and the *vitamin C defective 2* mutant lines, *vtc2-1* and *vtc2-4* were grown under a continuous light regime using two light intensities, 180 µmol m^{-2} s^{-1} or 250 µmol m^{-2} s^{-1}.

4.1.2.1 Shoot phenotypes of the wild type (Col-0) and vitamin *C defective 2, vtc2-1* and *vtc2-4* mutant lines grown under continuous light regimes

In these studies plants were grown until flowering, which occurred at three weeks under 180 µmol m^{-2} s^{-1} irradiance and two weeks at 250 µmol m^{-2} s^{-1} respectively. Under both irradiances, the *vitamin C defective 2* mutant line *vtc2-1* rosettes were visibly smaller than the Col-0 rosettes while the phenotype of *vtc2-4* was similar to that of Col-0 (Figure 4.10).

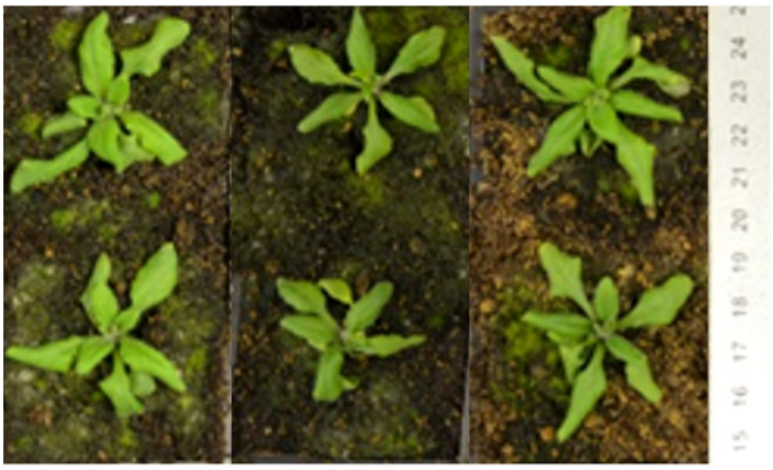

Figure 4.10 Comparison of the rosette phenotype of the wild type (Col-0) and *vitamin C defective 2* mutant lines, *vtc2-1* and *vtc2-4*, grown under 180 µmol m^{-2} s^{-1}.

Plants grown up to three weeks under continuous light conditions regime.

Figure 4.11 Comparison of the rosette phenotype of the wild type (Col-0) and *vitamin C defective 2* mutant lines, *vtc2-1* and *vtc2-4*, grown under 250 µmol m^{-2} s^{-1} irradiance.

Plants grown for two weeks under continuous light regime.

4.1.2.2 Comparisons of the number of leaves, rosette diameter and shoot biomass of Arabidopsis *vitamin C defective 2*, *vtc2-1* and *vtc2-4* mutant lines under continuous light conditions

Measurements of the number of leaves, rosette diameter and fresh weight (rosette) biomass were performed at week three in plants grown at 180 µmol m^{-2} s^{-1} of light intensity. Under these conditions, the number of leaves, rosette diameter and biomass of the *vtc2-1* plants were significantly smaller than the other 2 genotypes (Figure 4.12). These parameters were similar in the *vtc2-4* line to Col-0 (Figure 4.12).

Measurements of the number of leaves, rosette diameter and fresh weight (rosette) biomass were also performed on 2-week old plants grown at 250 µmol m^{-2} s^{-1}. At this irradiance, the *vtc2-1* plants had fewer leaves, a smaller rosette diameter and lower biomass than the wild type (Col 0). However, the *vtc2-4* mutant line also had significantly less rosette biomass than Col-0 under these conditions (Figure 4.13 C). While no significant differences in the number of leaves were found between the *vtc2-1* mutant and Col-0 plants, the number of leaves measured in the *vtc2-4* mutant line was significant higher than Col-0 (Figure 4.13 A).

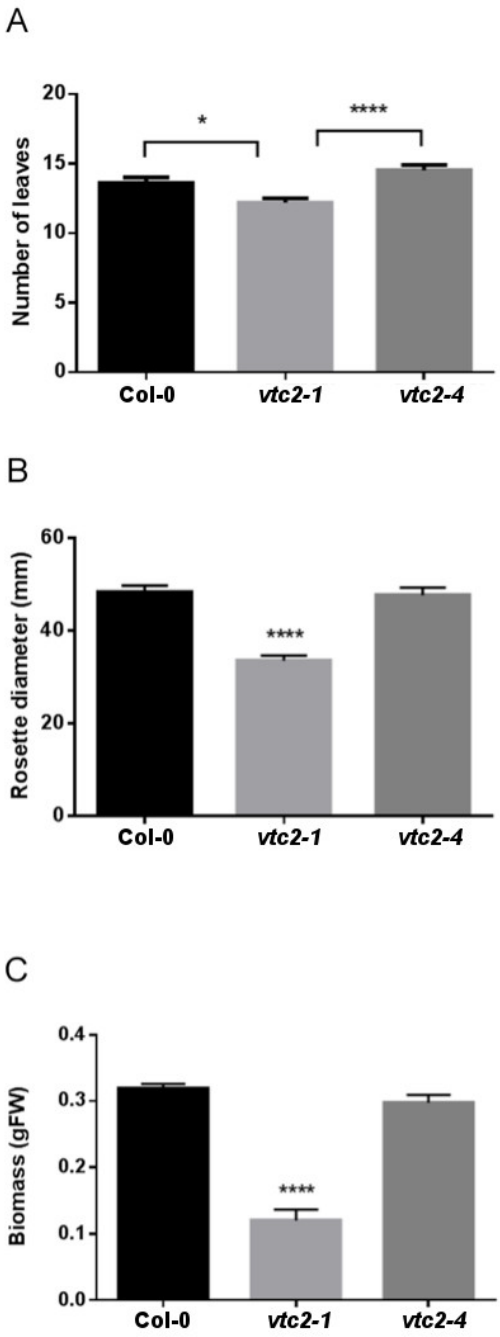

Figure 4.12 A comparison of (A) the number of leaves, (B) rosette diameter and (C) fresh weight of Col-0 rosettes and those of the *vitamin C defective 2, vtc2-1* and *vtc2-4* mutant lines, grown under 180 µmol m^{-2} s^{-1} light conditions.

Data are the mean values ± SE (n = 10). (* p< 0.05 and **** p< 0.0001) in significance given from analysis by Student's two tail *t*-test and One-Way ANOVA comparison between the mutant lines and Col-0.

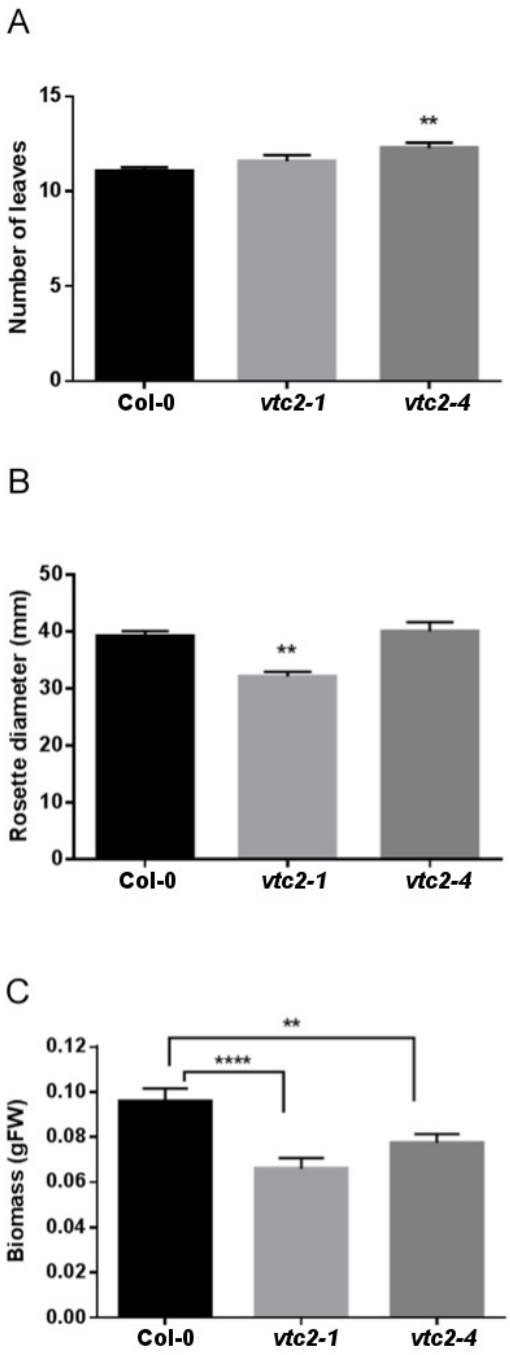

Figure 4.13 A comparison of the (A) number of leaves, (B) rosette diameter and (C) fresh weight in Col-0 plants and in *vitamin C defective 2* mutant lines, *vtc2-1* and *vtc2-4*, grown under 250 µmol m^{-2} s^{-1} irradiance.

Data are the mean values ± SE (n = 15). (** p< 0.01 and **** p< 0.0001) in significance given from analysis by Student's two tail *t*-test and One-Way ANOVA comparison between the mutant lines and Col-0.

4.1.2.3 Total ascorbate content of Arabidopsis *vitamin C defective 2* mutant lines

Total leaf ascorbate was measured in the rosettes of plants grown for two weeks under continuous light at either 180 or 250 µmol m^{-2} s^{-1} light intensity. In plants grown under continuous 180 µmol m^{-2} s^{-1} irradiance, the *vtc2-1* and *vtc2-4* rosettes had significantly lower total ascorbate, 20% of the wild type for *vtc2-1* and 30% for *vtc2-4* (Figure 4.14). Similarly, in plants grown under continuous irradiance at 250 µmol m^{-2} s^{-1}, the *vtc2-1* and *vtc2-4* rosettes had significantly lower total ascorbate levels compared to Col-0. In this case, *vtc2-1* had about 15% of the wild type ascorbate, while the value was 30% for *vtc2-4*. Hence, the *vtc2-1* rosettes had a significantly lower amount of ascorbate than the *vtc2-4* rosettes under these conditions (Figure 4.15).

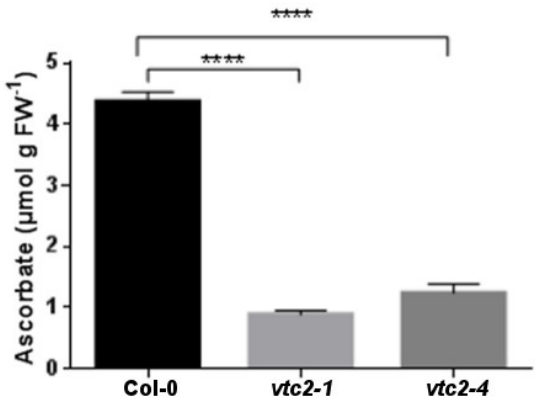

Figure 4.14 A comparison of rosette ascorbate contents in Col-0 plants and *vitamin C defective 2* mutant lines, *vtc2-1* and *vtc2-4*, grown under continuous light conditions (180 µmol m^{-2} s^{-1}).

Data are the mean values ± SE (n = 3). (**** p< 0.0001) in Significance given from analysis by Student's two tail *t*-test and One-Way ANOVA comparison between the mutant lines and Col-0.

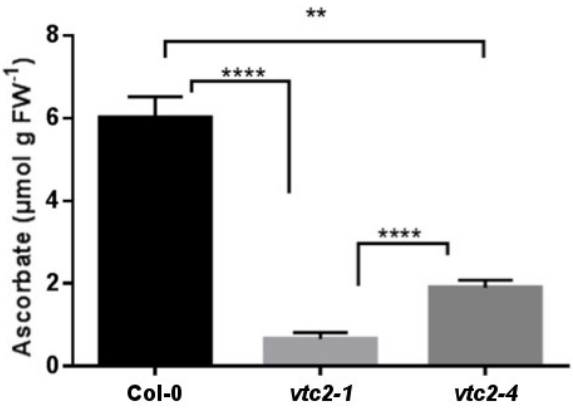

Figure 4.15 A comparison of rosette ascorbate contents in Col-0 and the *vitamin C defective 2* mutant lines, *vtc2-1* and *vtc2-4*, grown under continuous light conditions (250 µmol m^{-2} s^{-1}).

Data are the mean values ± SE (n = 3). (** p< 0.01 and **** p< 0.0001) in Significance given from analysis by Student's two tail *t*-test and One-Way ANOVA comparison between the mutant lines and Col-0

4.1.2.4 Correlation of ascorbate content and biomass

The data shown above for total fresh weight and rosette ascorbate content were used to explore the relationships between shoot growth and rosette ascorbate levels further (Figure 4.16 and Figure 4.17). The data presented in Figure 4.16 show that there is no marked relationship between these parameters in plants grown under continuous light at 180 µmol m^{-2} s^{-1}. However, in plants grown under continuous light at 250 µmol m^{-2} s^{-1}. There is relationship between rosette ascorbate contents and biomass (Figure 4.17). Taken together these findings indicate that correlation between rosette ascorbate contents and biomass accumulation is highly dependent on the growth conditions.

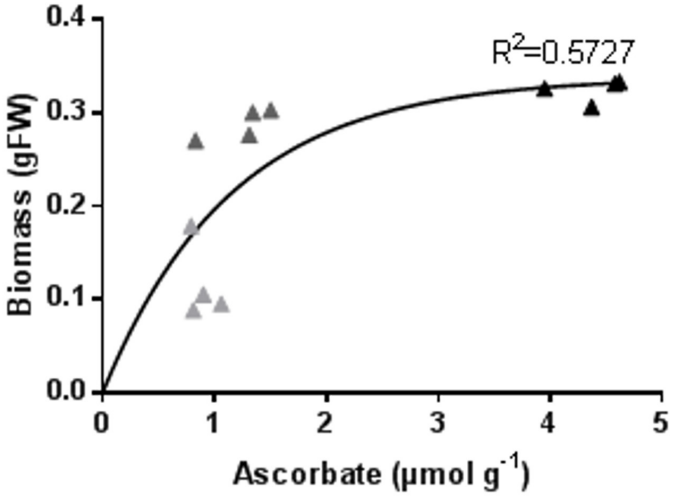

Figure 4.16 Relationships between biomass accumulation and ascorbate contents in Col-0 (black), *vtc2-1* (light grey) and *vtc2-4* (dark grey) in plants grown under continuous light (180 µmol m^{-2} s^{-1}).

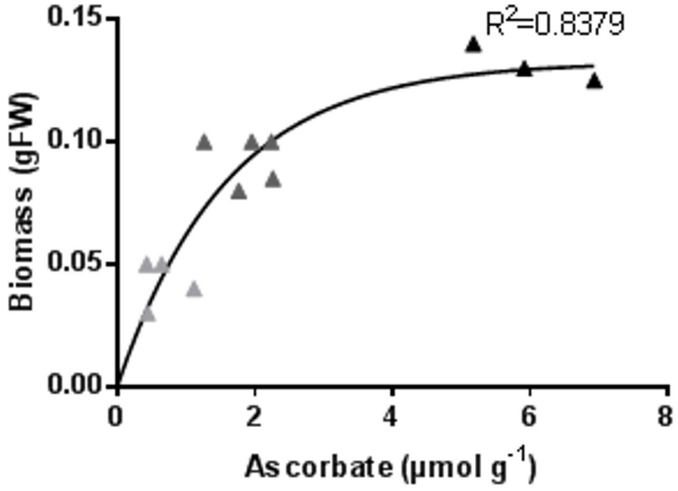

Figure 4.17 Relationships between biomass accumulation and ascorbate contents in Col-0 (black), *vtc2-1* (light grey) and *vtc2-4* (dark grey) in plants grown under continuous light (250 µmol m^{-2} s^{-1}).

4.2 Discussion

A large number of ascorbate-deficient mutants (*vtc1-2*, *vtc2-2*, *vtc2-3*, *vtc3-1*, *vtc4-1*) were identified in Arabidopsis (Conklin et al 2000). Of these mutants, *vtc1-1* and *vtc2-1* have been extensively studied to characterise ascorbate functions in plants, particularly with regard to plant growth and development (Dowdle et al 2008, Jander et al 2002, Kerchev et al 2011, Muller-Moule 2008, Wang et al 2013). The *vtc1-1* and *vtc2-1* mutants have a slow growth phenotype suggesting that ascorbate plays a role in the control of plant growth (Kerchev et al 2011, Kiddle et al 2003, Muller-Moule 2008, Pavet et al 2005, Veljovic-Jovanovic et al 2001). To explore the relationships between ascorbate and plant growth further, rosette growth and ascorbate contents were compared in the Arabidopsis wild type, the *vtc2-1* mutant, here called *vtc2-1* and a T-DNA insertion mutant, here called *vtc2-4* under either short day growth conditions at two irradiance levels (180 µmol m^{-2} s^{-1} or 250 µmol m^{-2} s^{-1}) or under continuous light at these same two irradiance levels. The results presented in this chapter regarding rosette biomass accumulation in the different genotypes are summarised in Table 5. Taken together, the data demonstrate that the *vtc2-1* and *vtc2-4* rosettes have about the same level of ascorbate relative to the wild type under all growth conditions. In addition the *vtc2-1* and *vtc2-4* rosettes show a similar slow growth phenotype relative to the wild type under most but not all short-day and continuous light growth conditions (Table 5).

The amount of ascorbate found in leaves is dependent on the light intensity experienced by the leaves (Bartoli et al 2005). Ascorbate synthesis and accumulation are higher in the light than in darkness. Moreover, ascorbate is rapidly turned over and degraded (Pallanca & Smirnoff 2000). The data shown in Figure 4.6 show that the ascorbate level in the wild type leaves was low in darkness and increased rapidly upon illumination in plants grown under short conditions. Moreover, a

comparison of the data shown in Figure 4.6 and that shown in Figure 4.15 suggests that the ascorbate contents of the wild type rosette leaves grown under continuous light is about double that of the leaves grown under short day conditions. However, in contrast to the wild type, the ascorbate contents of the *vtc2-1* and *vtc2-4* rosettes did not increase upon illumination when plants were grown under short day conditions (Figure 4.6). Nevertheless, the rosette ascorbate contents was higher in both mutant lines when plants were grown under continuous light compared to short day conditions. In the case of the *vtc2-4* mutants, the rosette ascorbate content in plants grown under continuous light (Figure 4.14 and Figure 4.15) was about double that measured under short day conditions (Figure 4.6).

The data presented here obtained by analysis of the growth of *vtc2-1* and *vtc2-4* genotypes suggest that there is a relationship between leaf ascorbate content and rosette growth but few conclusions can be drawn because there is a high dependence on the growth conditions, as discussed previously (De Simone et al 2015). A recent study has reported that the decreased growth phenotype of the *vtc2-1* mutants is not linked to ascorbate deficiency (unpublished data). These authors suggested that the *vtc2-1* (EMS) mutant shows a different grow the profile compared to the *vtc2-4* line. In addition, they suggested that after backcrossing *vtc2-1* (EMS) to wild type plants they were able to identify *vtc2-1* ascorbate-deficient plants that had a wild type growth phenotype (unpublished data). The data presented here show that in half of the four growth conditions used in these studies, the *vtc2-4* line had the same growth phenotype to the *vtc2-1* mutants. In the other two studies the phenotype of the *vtc2-4* line was more similar to the wild type than the *vtc2-1* mutants. It was suggested that the decreased growth phenotype of the *vtc2-1* line is caused by an additional mutation caused by the EMS mutagenesis process (Conklin et al 1996). This possibility is explored further in the following chapter, where the *vtc2-1* plants were

crossed with wild type plants and rosette ascorbate and diameter were determined in the T2 progeny.

The results presented in this chapter show that although leaf ascorbate content is important for rosette growth, plant development is strongly dependent on growth conditions. Further studies are required to investigate the possibility of a regulatory function of VTC2.

Table 5 Summary of the growth phenotypes and ascorbate contents of *vtc2-1* and *vtc2-4* mutant lines in relation to the wild type (Col-0).

Photoperiod	Light intensity (µmol m^{-2} s^{-1})	Mutant line	Rosette phenotype	Ascorbate content
8 h	180	*vtc2-1*	Dwarf	20%
	180	*vtc2-4*	Dwarf	20%
	250	*vtc2-1*	Dwarf	30%
	250	*vtc2-4*	Col-0	30%
24 h	180	*vtc2-1*	Dwarf	20%
	180	*vtc2-4*	Col-0	30%
	250	*vtc2-1*	Dwarf	15%
	250	*vtc2-4*	Dwarf	25%

Chapter 5. Characterization of the relationships between the cellular redox state and cell cycle of *vitamin C defective 2* (*vtc2-1)* mutant line in relation to the wild type

5.1 Introduction

In previous chapter the growth characteristics of the shoots of two *vtc2* mutant lines were characterised in relation to the wild type. Analysis of various parameters associated with shoot growth indicated that the two *vtc2* mutant lines tended to grow slower than the wild type, particularly under short day conditions. However, an earlier analysis of the seedling phenotypes showed that seedling development was similar to wild type in ascorbate-deficient mutants such as *vtc2-1* (Olmos et al 2006). Seed germination is a key developmental step in the plant life cycle. In orthodox seeds there is little or no ascorbate or ascorbate peroxidase (APX). Ascorbate is synthesised *de novo* within a few hours of imbibition (Tommasi et al 2001). Germination of wheat and rice seeds is suppressed by pre-treatment with ascorbate and it is hence used to prevent pre-harvest sprouting (Ishibashi & Iwaya-Inoue 2006) and also to prime seeds for improved stress tolerance (Fercha et al 2014).

Seed rehydration and germination are characterised by high metabolic rates, associated with protein, RNA and DNA synthesis. The shift from dry to germinated seeds is also defined by high respiration rates and the accumulation of reactive oxygen species (ROS), which are considered to function as positive signals for dormancy release (El-Maarouf-Bouteau & Bailly 2008, El-Maarouf-Bouteau et al 2013). Mutants lacking cytosolic ascorbate peroxidase 6 (APX6) showed reduced germination and altered responses to abscisic acid, suggesting that this enzyme plays a role in redox-hormone cross talk during seed germination (Chen et al 2014). Although a small amount of dehydroascorbate (DHA) is present in dry seeds its functions are uncertain (Tommasi et al 2001). Increases in the ascorbate pool are

considered to arise from ascorbate synthesis rather than regeneration (De Gara et al 1997, Tommasi et al 2001).

Seed rehydration is followed by cell expansion and elongation due to the uptake of water, leading to the protrusion of the radicle from the seed coat. It is thought that cell division in the cells of germinating seeds starts just before the protrusion of the radicle, DNA replication being initiated at the start of radicle protrusion and mitosis occurring only after protrusion (Masubelele et al 2005). However, the regulation and timing of these processes is not well defined.

Ascorbate is considered to be important in the regulation of cell cycle progression but its precise functions remain to be characterised. The addition of ascorbic acid led to cell division in the quiescent centre (QC) of *Allium cepa* root tips (Liso et al 1988). Cells of the QC, where ascorbate is mainly present as DHA, rarely divide and the cell cycle is arrested at the G1 phase. The accumulation of auxin in the QC of maize roots results in a high level of oxidation (Kerk & Feldman 1995, Kerk et al 2000). Moreover, ascorbate oxidase mRNAs and activity are high within the QC, ensuring depletion of ascorbic acid. Ascorbate is required for the G1 to S transition, and hence low ascorbate levels ensure the maintenance of the G1 state in the in the QC (Kerk & Feldman 1995, Kerk et al 2000). The addition of ascorbic acid to pea roots in which the cell cycle was arrested in the G1/S phase by hydroxyurea (HU) treatment resulted in more rapid release from inhibition (Citterio et al 1994). However, addition of ascorbic acid did not initiate proliferation of non-dividing cells in the meristem (Citterio et al 1994).

The addition of DHA to dividing *Allium cepa* cells shortened the G1 phase of the cell cycle (Decabo et al 1993). Similarly, DHA delayed cell cycle progression in synchronised tobacco BY-2 cells (Potters et al 2004). Taken together, these findings suggest that high levels of ascorbic acid are required for cell cycle progression within the root meristem (Citterio et al 1994, De Pinto et al 1999, De Tullio et al 1999, Liso et al 1988).

The leaves of the ascorbate deficient mutants such as *vtc2-1* have an increased level of glutathione, suggesting that glutathione may compensate for low ascorbate in terms of antioxidant capacity (Pavet et al 2005, Veljovic-Jovanovic et al 2001). However, the effect of low ascorbate on the distribution of glutathione between the nucleus and cytosol has not been studied. In the following experiments, cell cycle progression was measured in the dividing zone of *vitamin C defective 2, vtc2-1* roots expressing roGFP2. Changes in the glutathione redox potential of the cytosol and nuclei were compared in this line to those occurring in the wild type expressing roGFP2 over a 24-hour period in the absence or presence of hydroxyurea (HU).

5.2 Selection of *vtc2*-roGFP2 lines

The original crossing of the *vtc2-1* (EMS mutant), here called *vtc2-1* and roGFP2 (Col-0) lines, was performed by Till Pellny at Rothamsted Research. F2 Seeds of the cross *vtc2* x roGFP2 (Col-0) line, here called *vtc2*-roGFP2, provided by Dr Pellny were then selected and characterised to determine the effect of low antioxidant (ascorbate) availability on the cell cycle and the glutathione redox state of the nucleus and cytosol.

5.2.1 Selection of crosses lines homozygous for roGFP2

The *vtc2*-roGFP2 double crossed individuals were firstly selected on ½ MS supplemented with 50 µg/ml kanamycin because this antibiotic resistance marker was used in the roGFP2 construct. Wild type (Col-0) plants, which do not contain the antibiotic resistance marker and hence are not able to grow on ½ MS supplemented with kanamycin, were used as a negative control (Figure 5.1 A). However, all lines showed similar germination rates in the absence of kanamycin (Figure 5.1 B). The presence of the roGFP2 gene was verified by standard PCR using primers for GFP. Fluorescence at 405 nm and 488 nm for roGFP2 were confirmed for selected lines using confocal microscopy.

The F2 seeds were stratified for 48 hours at 4ºC. Seedlings were grown up to one week on ½ MS supplemented with 50 µg/ml kanamycin. About 65% of the *vtc2*-roGFP2 seeds germinated compared to 80% for the roGFP2 parent line (Figure 5.1 A). DNA was extracted from individuals that were able to germinate and sustain growth on kanamycin media and standard PCR was used to confirm the presence of roGFP2 gene (Figure 5.2). In total, 150 double crossed individuals were found to be resistant to kanamycin and to contain the roGFP2 sequence, as well as exhibiting fluorescence changes consistent with the presence of roGFP2 (Figure 5.3).

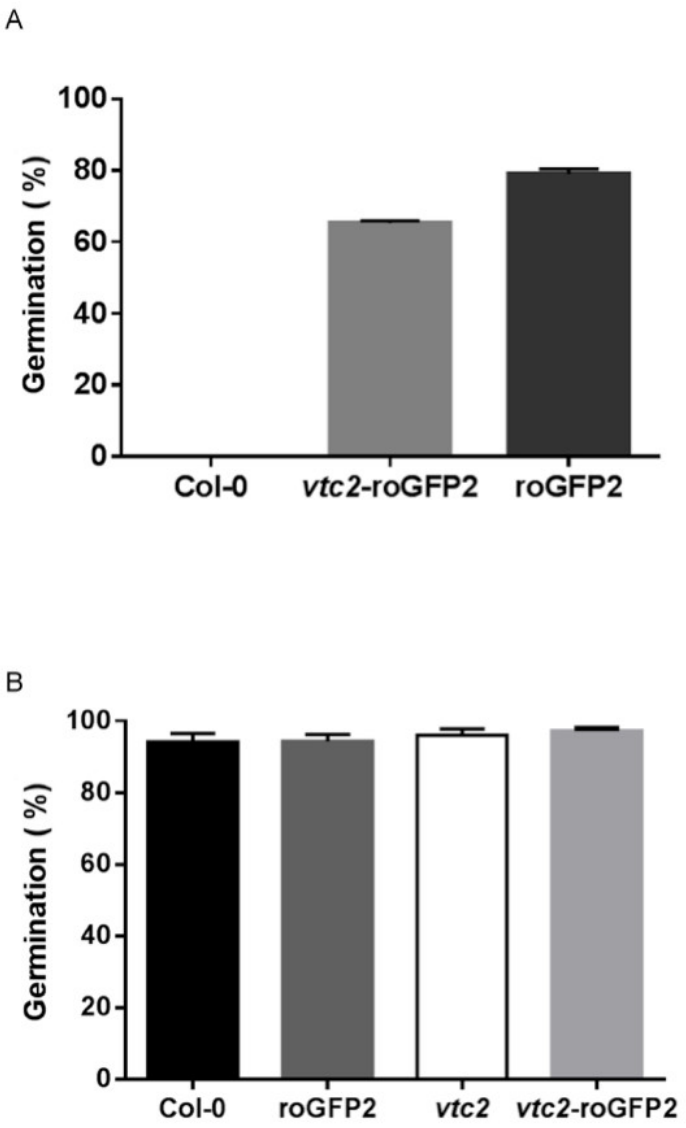

Figure 5.1 Selection of *vtc2*-roGFP2 crossed lines on ½MS supplemented with kanamycin.

Germination percentage of *vtc2*-roGFP2 individuals grown on ½MS in (A) the presence and (B) in the absence of kanamycin.

Figure 5.2 PCR products obtained using primers amplifying a region of roGFP2.

The numbers of the top and bottom lane show 520 bp bands corresponding to the amplified roGFP2 fragment in each of the *vtc2*-roGFP2 crosses. roGFP2 products in each individuals are confirmed by the absence of the band in wild type (WT),which is used as a positive control and by the absence of product in the negative control (-).

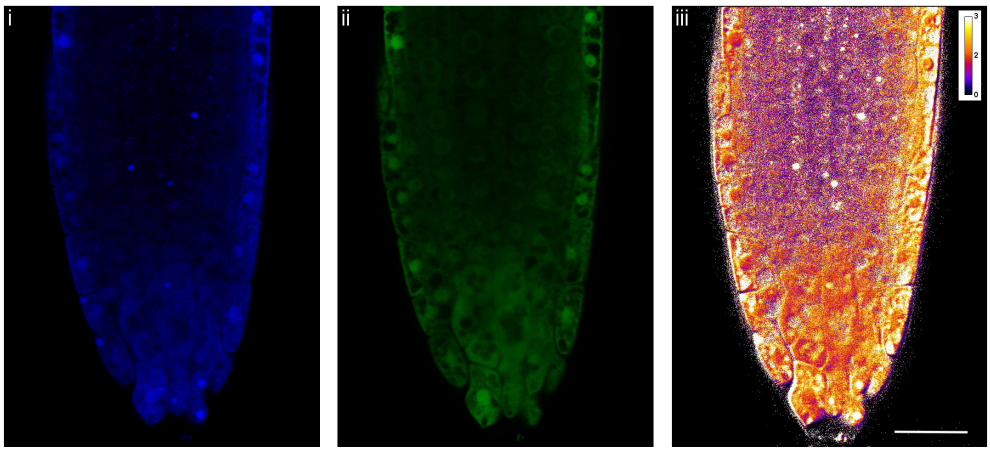

Figure 5.3 A typical image of roGFP2 fluorescence in the roots of one of the F3 generation *vtc2*-roGFP2 Arabidopsis crossed individuals.

(i) The fluorescence of the oxidised form of roGFP2 excited at 405 nm is shown in blue, (ii) the fluorescence of the reduced form of roGFP2 excited at 488 nm is shown in green and (iii) the 405/488 nm ratio is shown in a pseudo colour look-up scale used to visualise the relative redox state. Scale bar 25 μm.

5.2.2 Selection of double crosses lines roGFP2 with low ascorbate

The 150 *vtc2*-roGFP2 double crossed individuals found to be resistant to kanamycin and confirmed to contain roGFP2 were transferred to soil and grown under long day (16-hour photoperiod) conditions. The individuals were analysed for total ascorbate contents 2 weeks after transfer to soil. The total ascorbate content of the leaves of the roGFP2 parent line was between 4 and 6 µmol g^{-1} fresh weight (Figure 5.4 A). The rosette ascorbate contents of all F2 *vtc2*-roGFP2 double crossed individuals was similar to that of the *vtc2* parent line being not higher than 2 µmol g^{-1} fresh weight in any of the individuals (Figure 5.4 A) and was therefore only 50% or less of the leaf ascorbate measured in the roGFP2 parent line.

In parallel to the ascorbate content, the rosette diameter was measured in the two weeks old individuals (Figure 5.4 B). The roGFP2 parent line had a rosette diameter between 25 and 42 mm while in *vtc2* parent line it was between 7 and 9. In comparison the *vtc2*-roGFP2 line showed a smaller rosette diameter, which was between 12 and 30 mm (Figure 5.4 B). Of the 150 *vtc2*-roGFP2, two individuals were selected to perform measurements of the glutathione redox potential as shown in 5.3, 5.4 and 5.5 sections of this chapter.

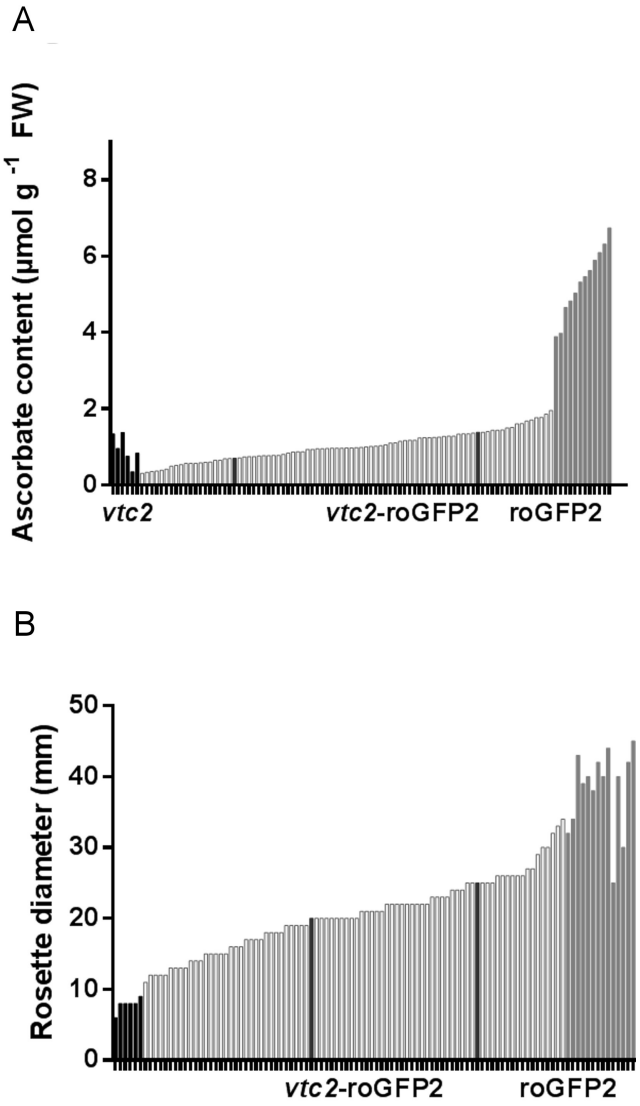

Figure 5.4 A comparison of (A) the rosette ascorbate content and (B) rosette diameter of individuals of the roGFP2 parent line (grey), the *vtc2* parent line (black) and the F3 *vtc2*-roGFP2 double crossed individuals (light grey) measured in 2 week-old seedlings grown under 250 µmol m^{-2} s^{-1}.

Dark grey columns indicate the *vtc2*-roGFP2 double crossed individuals used for glutathione redox potential measurements in 5.3, 5.4 and 5.5 sections of this chapter.

5.2.3 Shoot phenotype of *vtc2*-roGFP2 crossed line

vtc2-roGFP2 crossed lines showed a rosette phenotype visibly smaller than roGFP2 (Figure 5.5). The number of leaves and rosette diameters were also measured on the 2-week-old plants of the roGFP2 parent line and the *vtc2*-roGFP2 plants. The roGFP2 plants had between 10 and 17 leaves at this stage (Figure 5.6 A). In comparison the *vtc2*-roGFP2 crossed lines had between 2 and 12 leaves (Figure 5.6 A). At the 2-week-old stage, the diameters of the *vtc2*-roGFP2 plants varied between 12 and 30 mm. In comparison, the diameters of the roGFP2 rosettes were between 25 and 42 mm at this stage (Figure 5.6 B).

Figure 5.5 Comparison of the rosette phenotype in roGFP2 parent line (left) and in the *vtc2*-roGFP2 crossed individuals (right). Plants grown up to five weeks under long day photoperiod regime (16 hours light).

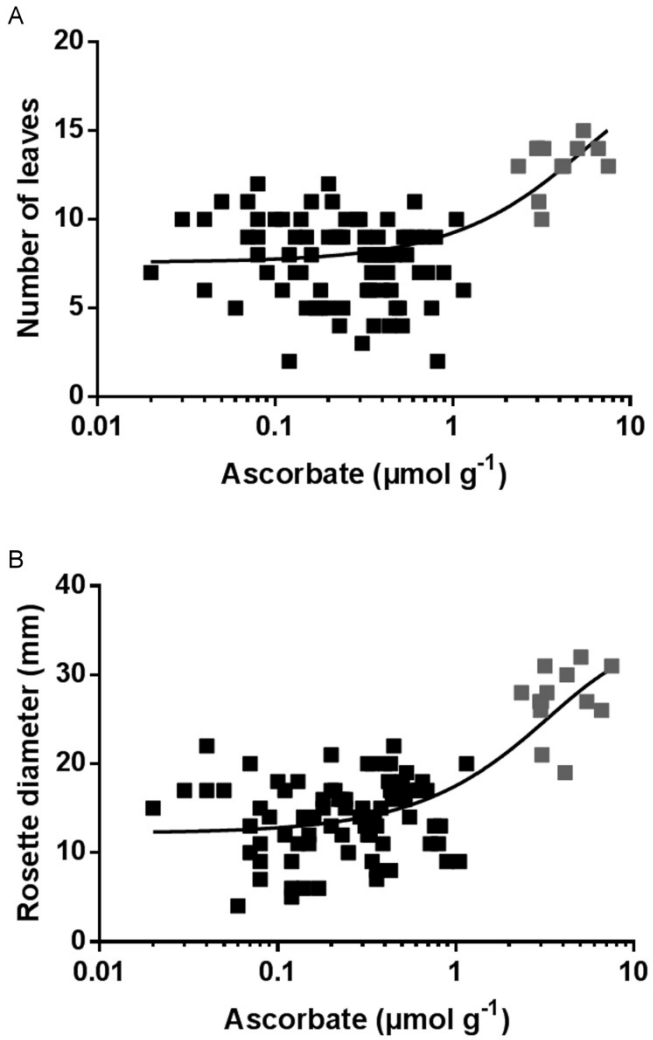

Figure 5.6 (A) Number of leaves and (B) rosette diameters relative to ascorbate content in individuals of the roGFP2 (grey) parent line and in the *vtc2*-roGFP2 crossed individuals (black).

Numbers of leaves and rosette diameters were measured on 2-week-old plants.

The numbers of leaves and rosette diameters of the roGFP2 parent and *vtc2*-roGFP2 crossed lines were measured over a period of 4 weeks after transfer to soil (Figure 5.7). The number of leaves and rosette diameters of the roGFP2 parent and *vtc2*-roGFP2 crossed lines were not significantly different over the first week of growth (Figure 5.7). However, at later stages of growth the roGFP2 parent plants had significantly more leaves with significantly greater rosette diameters than the *vtc2*-roGFP2 crossed plants (Figure 5.7).

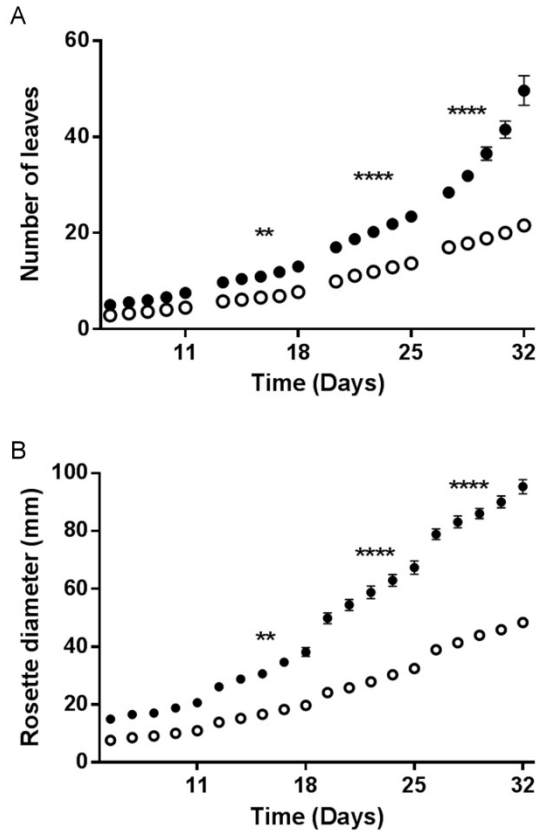

Figure 5.7 Comparison of the growth of the roGFP2 (close symbols) and *vtc2*-roGFP2 (open symbols) rosette in terms of (A) number of leaves and (B) rosette diameter.

Plants were grown for up to five weeks (** p< 0.01 up to 18 days and **** p< 0.0001 up to 32). Significance given from analysis by Student's two tail *t*-test and One-Way ANOVA comparison between the lines.

5.3 A comparison of roGFP2 fluorescence parameters measured in the nuclei and the cytosol of proliferating cells of roGFP2 and *vtc2*-roGFP2 roots in the absence of HU

F3 seeds of the *vtc2*-roGFP2 cross were germinated together with roGFP2 seeds, as described previously (Chapter 3). The 405/488 nm fluorescence ratios were measured in the nuclei and the cytosol of cells in the proliferating zones between 48 and 72 hours after stratification and these values were used to calculate the glutathione redox potentials. The 405/488 nm ratios in the nuclei and cytosol were higher in *vtc2*-roGFP2 cells than in roGFP2 (Figure 5.8 A and B). For example, the 405/488 nm ratios measured in the nuclei of the *vtc2*-roGFP2 cells were about 2.0, whereas values measured in the nuclei of the roGFP2 cells were about 0.5 (Figure 5.8 A). The OxD of the nuclei and cytosol of *vtc2*-roGFP2 cells was much higher than that of the roGFP2 cells (Figure 5.8 C and D). For example, the OxD of the nuclei of the *vtc2*-roGFP2 cells was about 50%, whereas values measured in the nuclei of the roGFP2 cells were about 25% (Figure 5.8 C). The OxD was used to calculate the glutathione redox potential in the nuclei and cytosol of the *vtc2*-roGFP2 plants and compared with that calculated for the roGFP2 cells (Figure 5.8 E and F respectively). The values for glutathione redox potentials of the nuclei in the *vtc2*-roGFP2 and roGFP2 cells were significantly different throughout the time course of the experiment. On average there was a 20 mV difference in values for the nuclei between the genotypes (Figure 5.8 E and F). Moreover, apart from a small number of individual time-points the glutathione redox potentials of the cytosol in *vtc2*-roGFP2 and roGFP2 cells were also significantly different throughout the time course of the experiment. On average, there was a 10 mV difference in values for the cytosol between the genotypes. (Figure 5.8 E and F). The average glutathione redox potential of the cytosol and nuclei calculated over the time course of the experiment were similar in the *vtc2*-roGFP2 plants (Table 6). However, these values were significantly lower than the average values calculated in the roGFP2 plants (Chapter 3).

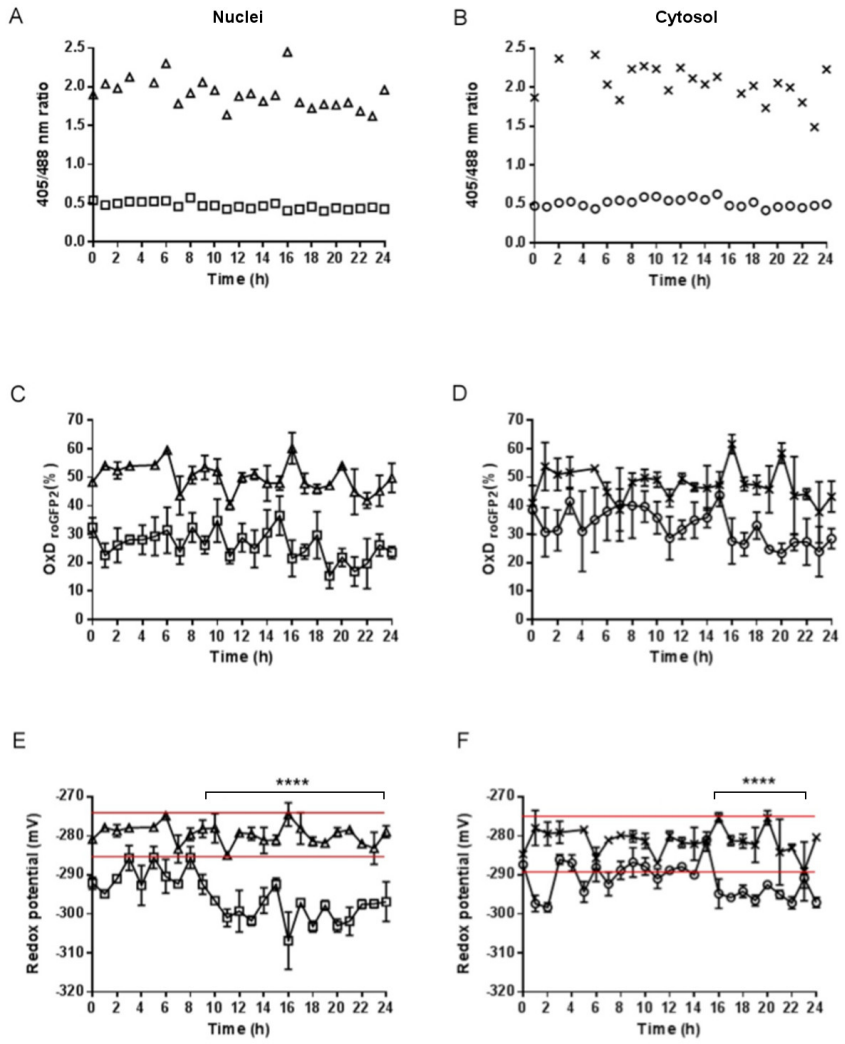

Figure 5.8 A comparison of roGFP2 fluorescence in the nuclei and cytosol of roGFP2 roots (open squares and open circles respectively) and the nuclei and cytosol of *vtc2*-roGFP2 line (open triangles and crosses respectively).

The 405/488 nm fluorescence ratios measured in (A) the nuclei and (B) the cytosol of cells in the proliferating zones measured between 48 and 72 hours after stratification. The oxidation degree in (C) the nuclei and (D) cytosol and the glutathione redox potentials determined for the (E) nuclei and (F) cytosol. The red lines indicate the maximum and minimum values for the glutathione redox potentials in *vtc2*-roGFP2 line. Data are the mean values (n=3) ****p < 0.0001 in Significance given from analysis by Student's two tail *t*-test.

Table 6 A comparison of the calculated glutathione redox potentials of the nuclei and cytosol dividing cells of the *vtc2*-roGFP2 root meristem averaged over the 24-hour period of the experiment.

Compartment	Glutathione redox potential (mV)
Nuclei	-279.7 ± 0.5
Cytosol	-281.2 ± 0.8

Data are the mean values ± SEM (n ≥ 3).

5.4 Cell cycle progression in the *vtc2*-roGFP2 root meristem

5.4.1 Effects of HU on cell numbers and nuclear size in the *vtc2*-roGFP2 root meristem

The effects of HU on the number of cells and the size of the nuclei were estimated in the proliferation zone of the *vtc2*-roGFP2 radicles as described in (Chapter 3). Measurements were made on roots in the absence or presence of HU over a 24-hour period (as described in Chapter 3). The number of cells in the proliferation zone of the *vtc2*-roGFP2 roots was significantly decreased after 24 hours in the presence of HU was compared to control samples in the absence of HU (Figure 5.9 A). The size of the nuclei was similar at all-time points in the absence of HU (Figure 5.9 B). In the presence of HU there was a rapid but transient increase in nuclear size in the *vtc2*-roGFP2 roots after the first 6 hours of treatment, reaching a maximum at 10 h (Figure 5.9 B). There was also a second more persistent increase in nuclear size between 18 and 22 hours after the onset of HU treatment (Figure 5.9 B).

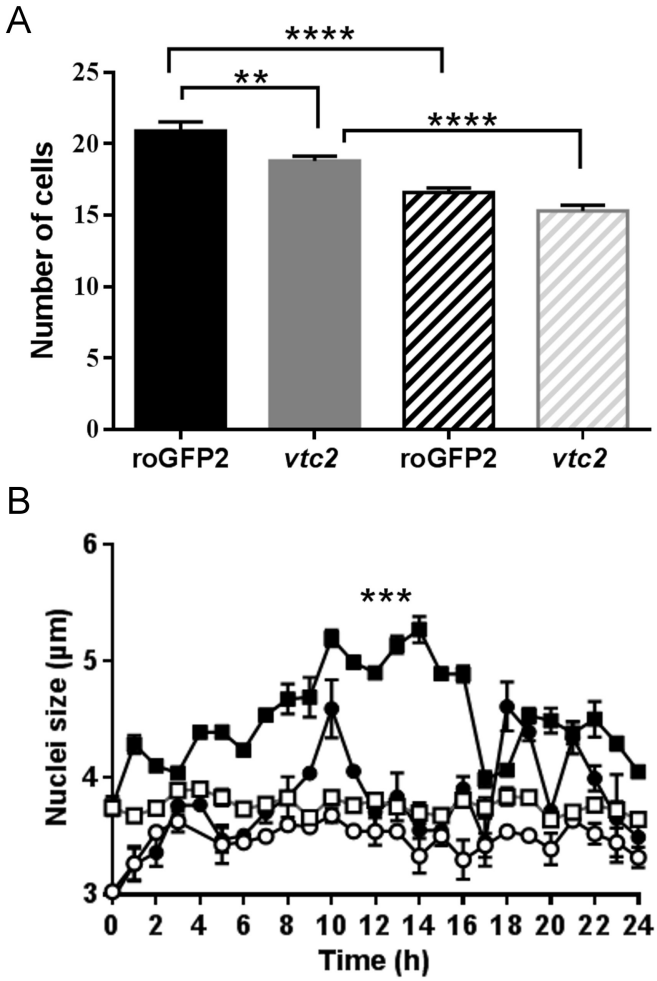

Figure 5.9 Effects of HU treatment on the number of cells and the size of the nuclei of *vtc2*-roGFP2 within the proliferation zone of the radicles of germinating seeds.

(A) Number of cells in roGFP2 (black) and *vtc2*-roGFP2 (grey) radicles treated up to 24 hours with HU (stripes) and untreated (block). (B) Nuclear size in roGFP2 (squares) and *vtc2*-roGFP2 (circles) radicles treated up to 24 hours with HU (closed symbols) and untreated (open symbols). Data are the mean values ± SE (n=3). **p < 0.01, ***p < 0.001, ***p < 0.0001 in Significance given from analysis by Student's two tail *t*-test.

5.4.2 The abundance of selected cell cycle markers transcripts (cyclins) in *vtc2*-roGFP2 roots in which the cell cycle had been synchronised using HU relative to unsynchronised controls.

The relative abundance of cell cycle marker transcripts was compared in the whole *vtc2*-roGFP2 roots treated with HU for 24 hours relative to untreated controls (Figure 5.10). The cyclin markers selected to elucidate the effects of HU on cell cycle progression in roGFP2 (Chapter 3) were also used in these studies. Cyclin *CYCA3.1* (Figure 5.10 A) was used as a marker for the G1/S phase of the cell cycle, *CYCD5.1* was used as a late G1/S-early S phase marker (Figure 5.10 B), *CYCD3.1* was used as S phase markers (Figure 5.10 C), and cyclins *CYCB2.1* (Figure 5.10 D) *CYCA1.1* (Figure 5.10 E) and *CYCB1.1* (Figure 5.10 F) were used as markers for the G2/M phase of the cell cycle (Culligan et al 2004, Menges & Murray 2002).

The abundance of G1/S phase cell cycle marker *CYCA3.1* transcripts was low and relatively constant throughout the time course of the experiment in the absence of HU (Figure 5.10 A). Conversely, the levels of *CYCA3.1* transcripts were significantly higher after 10 hours from the start of HU treatment (Figure 5.10 A).

The levels of *CYCD5.1* transcripts, which were used as a late G1/S or early S phase marker, were low and relatively constant throughout the time course of the experiment in the absence of HU (Figure 5.10 B). In the presence of HU, the levels of *CYCD5.1* transcripts increased after 10 hours from the start of HU treatment reaching a maximum at 16 hours and decreased thereafter (Figure 5.10 B).

The abundance of *CYCD3.1* transcripts, which was used as S phase marker, was low and relatively constant throughout the time course of the experiment in the absence of HU while in synchronised roots was significantly higher after 16 hours from the onset of HU treatment

reaching maximum values at 20 h time point and decreased thereafter (Figure 5.10 C).

The levels of transcripts of G2/M phase cell cycle markers, *CYCA1.1*, *CYCB2.1* and *CYCB1.1*, were low and relatively constant throughout the time course of the experiment in the presence of HU (Figure 5.10 D, E, F respectively). In contrast, unsynchronised roots, which were not treated with HU, showed two marked peaks in the levels of *CYCA1.1*, *CYCB2.1* and *CYCB1.1* transcripts, which occurred 5 hours and 20 hours after the start of the experiment (Figure 5.10 D, E and F). These are in accordance with the roGFP2 data shown in Chapter 3.

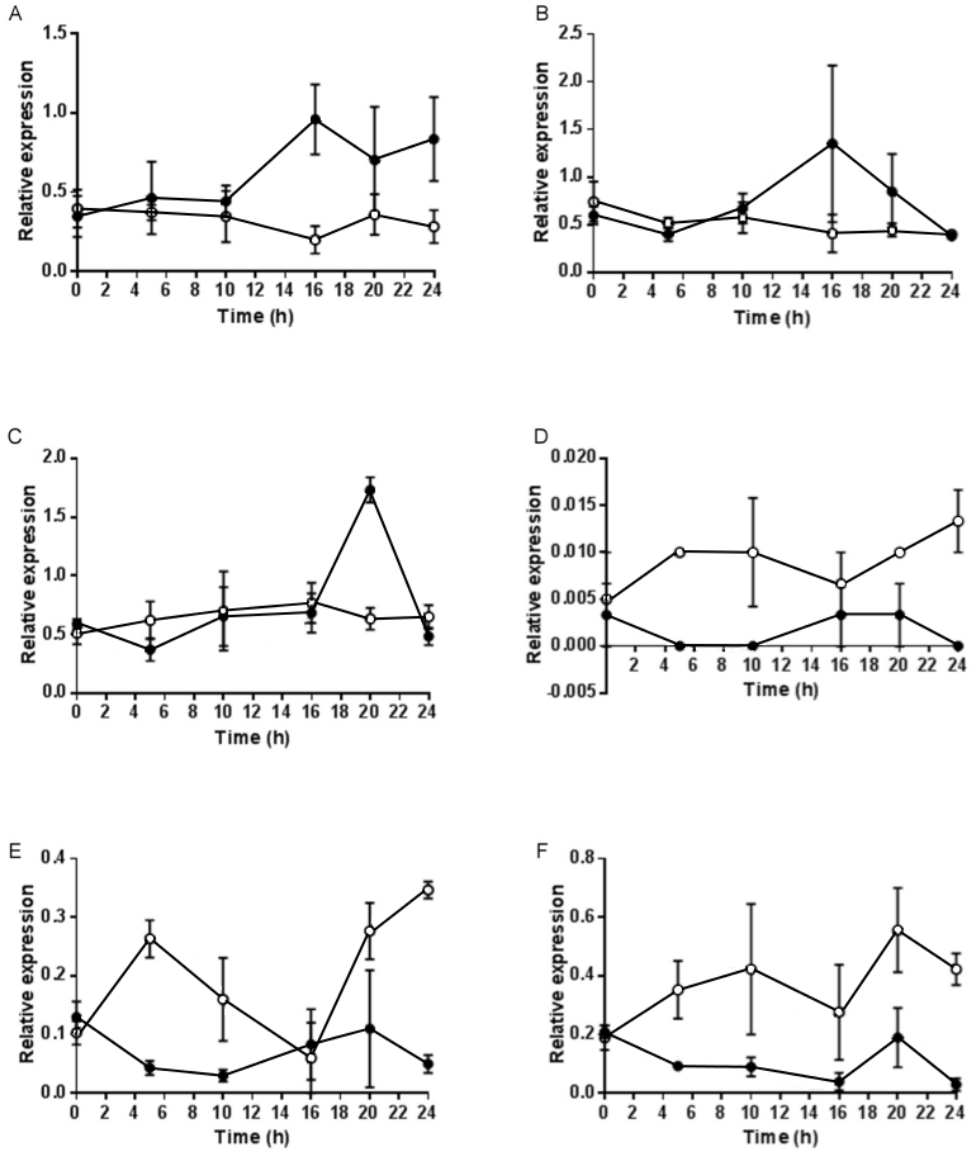

Figure 5.10 The relative expression of selected cell cycle markers of *vtc2*-roGFP2 radicles synchronised for 24 hours in presence of HU (closed symbols) relative to controls in the absence of HU (open symbols).

Transcripts measured were: (A) G1/S cell cycle marker *CYCA3.1*, (B, C) S cell cycle markers *CYCD5.1* and *CYCD3.1* respectively, (D, E, F) G2/M cell cycle markers *CYCB2.1*, *CYCA1.1* and *CYCB1.1* respectively.

5.5 A comparison of the effects of HU on roGFP2 fluorescence parameters measured in the nuclei and the cytosol of proliferating cells of roGFP2 and *vtc2-roGFP2* roots

Similar to the studies on the cell cycle progression performed using the roGFP2 seedlings (Chapter 3), 3mM HU was used to synchronise the cell cycle in the proliferation zone of the germinating radicles of *vtc2*-roGFP2 seedlings. Studies were performed over a 24-hour period in the presence or absence of HU, as described in Chapter 3. The 405/488 nm ratios measured in proliferation zones of the *vtc2*-roGFP2 root meristems were used to calculate the oxidation degree and glutathione redox potentials as described in the materials and methods section.

Overall, HU had no effect on the 405/488 nm ratios of the cytosol or nuclei in the *vtc2*-roGFP2 cells (Figure 5.11 A and B). However, OxD of the nuclei of the synchronised cells was significantly lower than that of the controls in the absence of HU samples at 9 h and between 15 and 20 hours after the start of the HU treatment (Figure 5.11 C). The OxD of the cytosol of the synchronised cells was not significantly different from than that of the controls in the absence of HU (Figure 5.11 D).

The oxidation degree (OxD) was used to calculate the glutathione redox potentials as described in the methods section. In cells of *vtc2*-roGFP2 roots that were synchronised with HU, the glutathione redox potentials of the nuclei were similar to those calculated for cytosol, having values between -285 and -277 mV (Figure 5.11 E and F respectively) over the whole time course of the experiment. The average glutathione redox potentials of the synchronised cells in the proliferation zones of the *vtc2*-roGFP2 roots measured over the whole 24-hour period of the experiment were -282.3 mV ± 0.5 for the nuclei and -282.9 mV ± 0.5 for the cytosol (Table 7). These values were not significantly different from those calculated in unsynchronised control samples over the whole time course (Table 7). The nuclear glutathione redox potentials in the proliferation zones of the *vtc2*-roGFP2 roots were only significantly

different in the presence of HU between 10 and 20 hours after the onset of treatment compared to unsynchronised controls (Figure 5.11 E). At these time points the values obtained in the HU treated nuclei were as much 10 mV different from the values calculated in the unsynchronised controls in the absence of HU. Similarly, the glutathione redox potentials of the cytosol of the *vtc2*-roGFP2 cells were significantly different in the presence of HU compared to untreated controls between 1 and 5 hours after the onset of treatment.

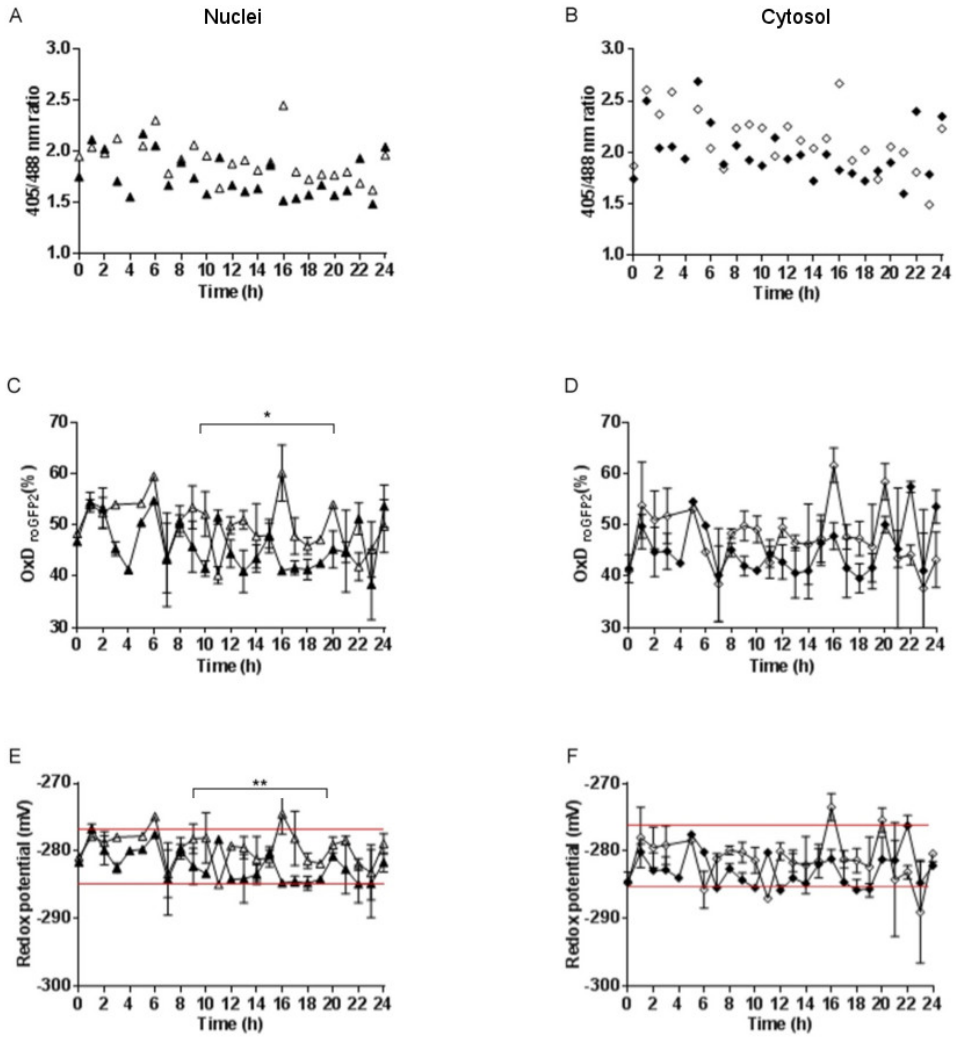

Figure 5.11 5.12 A comparison of roGFP2 fluorescence in the proliferation zones of *vtc2*-roGFP roots, in the absence (open triangles) and presence (closed triangles) of HU.

The 405/488 nm fluorescence ratios measured in the (A) nuclei and (B) the cytosol of cells in the proliferation zone. The oxidation degree in the (C) nuclei and (D) cytosol and the glutathione redox potentials determined for the (E) nuclei and (F) cytosol. The red lines indicate the maximum and minimum values for the glutathione redox potentials. Data are the mean values (n=3) *p < 0.05 and **p < 0.01 in Significance given from analysis by Student's two tail *t*-test Experiments were repeated at least 3 times. Data are the mean values ± SE (n=3). *p < 0.05 and **p < 0.01. Significance analysed by Student's two tail t-test.

Table 7 A comparison of the glutathione redox potentials of the cytosol and nuclei of dividing cells in the proliferation zones of *vtc2*-roGFP2 radicles in the absence (control) and presence of hydroxyurea (HU).

	Glutathione redox potential (mV)	
Compartment	**Control**	**HU**
Nuclei	-279.7 ± 0.5	-282.3 ± 0.5
Cytosol	-281.2 ± 0.8	-282.9 ± 0.5

Data are the mean values ± SEM (n ≥ 3).

5.6 Discussion

In the previous chapter, data presented were showing that the rosettes of the *vtc2-1* mutants had a slow growth phenotype compared to the wild type under most conditions analysed, as has been observed previously (Pavet et al 2005, Radzio et al 2003). However, this phenotype is not apparent in seedlings prior to 2 weeks (Olmos et al 2006, Pavet et al 2005); see Figure 5.7. The *vtc2-1* rosette leaves has similar or even higher levels of leaf glutathione than the wild type, with higher GSH to GSSG ratios, particularly later in rosette development (Pavet et al 2005). A previous study has shown that the roots of 12 days old *vtc2-1* seedlings had a similar phenotype to the wild type (Olmos et al 2006). However, the 12 days old *vtc2-1* seedlings had longer roots than the wild type plants, as illustrated in Figure 5.13. The experiments described in this chapter were undertaken to determine whether low antioxidant (ascorbate) buffering capacity in the *vtc2-1* mutants altered the cell cycle in the emerging radicles of germinating seeds.

The number of cells in the 2.5 mm selected area of the proliferation zone of the *vtc2*-roGFP2 roots (Figure 5.9 A) was significantly lower than that in the roGFP2 roots (Figure 5.9 A), suggesting that cell expansion increases to compensate the decrease in cell number (Olmos et al 2006). The addition of HU to synchronise the cell cycle significantly decreased the number of cells in the proliferation zone of the *vtc2-1* (Figure 5.9 A) and roGFP2 roots (Figure 5.9 A).

There were marked differences in the ability of the nuclei in the proliferation zone of the *vtc2*-roGFP2 roots (Figure 5.9 B) and roGFP2 roots (Figure 5.9 B) to increase in size during the cell cycle. These data strongly suggest that low antioxidant capacity severely impairs the ability of the nuclei to increase in size, perhaps through the inhibition of histone gene expression and/or translation, or the ability to accumulate sufficient nucleotides or amino acids to synthesise RNA and proteins.

However, the diminished ability of the *vtc2*-roGFP2 nuclei to increase in size does not appear to inhibit progression through the cell cycle. The expression of markers used to identify the different phases of the cell cycle was not greatly changed in the *vtc2*-roGFP2 roots (Figure 5.10) compared to roGFP2 roots (Figure 5.10).

The effect of low ascorbate on the distribution of glutathione between the nucleus and cytosol has not been studied previously. The data presented here shows that low ascorbate had a marked effect of the glutathione redox potentials of the nuclei and cytosol of the *vtc2*-roGFP2 roots compared to roGFP2 roots (Table 8). The nuclei and cytosol of the *vtc2*-roGFP2 roots were significantly more oxidised than the roGFP2 roots in the absence or presence of HU (Table 8). The addition of HU did not change the OXD or glutathione redox potentials in the nuclei and cytosol of either genotype. The failure of the *vtc2*-roGFP2 nuclei to increase in size except in a transient manner is likely to be linked to the increased levels of oxidation measured in the cytosol/nuclear compartments of the *vtc2*-roGFP2 roots compared to roGFP2 roots. In addition, the fluctuations in the glutathione redox potentials of the nuclei and cytosol measured during cell cycle progression in the roGFP2 roots were absent from the *vtc2*-roGFP2 roots. The small changes in the glutathione redox potentials of the cell cycle observed in G1 might therefore be required to generate an increase in nuclear size prior to DNA replication. RNA seq analysis was therefore performed to explore the effects of low ascorbate on gene expression in germinating seedlings (Chapter 6).

The results presented in this chapter can be summarised as follows:

- Low antioxidant capacity delays cell cycle progression in the proliferating zone of Arabidopsis radicle.
- The nuclei and cytosol of the radicle of low ascorbate mutants are significantly more oxidised than those of the wild type.
- The redox rhythms, which were present in Col-0 radicles, are impaired in low ascorbate mutant lines.

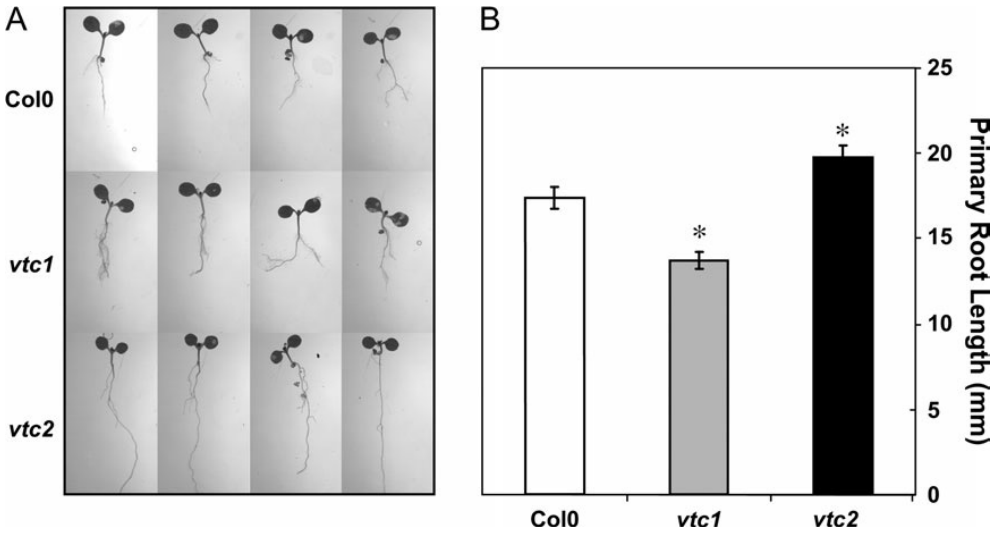

Figure 5.13 A comparison of wild type, *vtc1*, and *vtc2* (A) seedling phenotypes and (B) primary root length. The data are means 6 SE, where an asterisk defines significant differences at P=0.05, with reference to wild-type values. Figure taken from Olmos et al (2006).

Table 8 Summary of the glutathione redox potential of the nuclei and cytosol in the absence and presence of HU in the radicles of roGFP2 and vtc2-roGFP2 lines.

Glutathione redox potential

Compartment	**Genotype**	**(mV) Absence of HU**	**(mV) Presence of HU**
Nuclei	roGFP2	-297.5 ± 0.7	-295.8 ± 0.8
	vtc2-roGFP2	-279.7 ± 0.5	-282.3 ± 0.5
Cytosol	roGFP2	-292.8 ± 0.6	-293 ± 0.9
	vtc2-roGFP2	-281.2 ± 0.8	-282.9 ± 0.5

Chapter 6. Defining the low ascorbate transcriptome of dry and imbibed Arabidopsis seeds using the *vtc2-1* and *vtc2-4* lines

6.1 Introduction

In chapter 5, it was shown that low ascorbate in the *vtc2-1*-roGFP2 lines caused significant changes in the glutathione redox potentials of the nuclei and cytosol of proliferating cells in the root apical meristem of germinating seeds. However, there was no effect on seed germination or the growth of the roots. In contrast, the data in chapter 4 show that the *vtc2-1* and *vtc2-4* mutant rosettes tend to be smaller than the wild type, particularly at later stages of vegetative development when plants were grown under short day conditions. Transcriptome analysis has previously been performed on *vtc1* and *vtc2-1* rosette leaves (Kerchev et al 2011, Kiddle et al 2003). Analysis of the *vtc1* mutants provided the first molecular signature of ascorbate deficiency in Arabidopsis leaves (Kiddle et al 2003). In this study 171 genes were differentially expressed in *vtc1* leaves compared with the wild type. A second analysis of the *vtc1* transcriptome using an improved Arabidopsis microarray revealed that 510 transcripts were differentially expressed relative to the wild type. These studies revealed that many transcripts involved in plant defences, particularly pathogenesis-related proteins and related hormone signalling, particularly transcripts related to abscisic acid (ABA) and salicylic acid (SA) were increased in abundance as a result of low ascorbate. Moreover, these changes were reversed by feeding ascorbate (Kiddle et al 2003). The leaves of the *vtc1* and *vtc2-1* mutants were show to have higher levels of ABA than the wild type (Kerchev et al 2011). All of the *vtc* mutants were later shown to have higher SA levels than the wild type and enhanced disease resistance (Mukherjee et al 2010, Pavet et al 2005).

Microarray analysis of the *vtc2-1* leaf transcriptome reported that 963 transcripts were differentially expressed as a result of the low ascorbate

in the mutant compared to the wild type (Kerchev et al 2011). Many of the genes identified in the *vtc2-1* leaf transcriptome were the same as those described in the *vtc1* leaves. Moreover, a proteome analysis of *vtc* leaves revealed that accumulation of a number of proteins was changed relative to the wild type including Fe-SODs, a Cu,Zn-SOD, HSP70, PsbS, and a chloroplast-localized glyoxalate I (Giacomelli et al 2006). Moreover, unlike the wild type significant increases in the levels of cpHSP70-1 and cpHSP70-2 proteins were observed in the *vtc2* leaves following high light treatment (Giacomelli et al 2006).

A previous analysis of *vtc1* transcriptome data revealed that transcripts encoding proteins involved in the G1 phase of the cell cycle and the G2/S transition were differentially expressed in rosette leaves as a result of low ascorbate (Bartoli et al 2006). While these data provide insights into how low ascorbate may influence leaf functions, no information is available on the effects of low ascorbate on seed development or germination. The following studies were performed to address this issue, and to understand how low ascorbate might influence the cell cycle in germinating seedlings.

In the following studies, next generation sequencing (RNAseq analysis) of the *vtc2-1*, *vtc2-4* and wild type lines was used to analyse the effect of low ascorbate on gene expression in dry and imbibed seeds. For the dry seed samples used in this analysis, seeds were harvested from plants of all the lines that had been grown at the same time, in the same controlled environment chambers under long day conditions. Harvested seeds were dried at room temperature and stored in the dark for up to 4 weeks before analysis. Dry seeds were sent to Dr Wim Soppe in the Department of Plant Breeding and Genetics at the Max Planck Institute for Plant Breeding Research in Cologne, Germany. Seed imbibition and germination tests were performed at the Max Planck Institute, together with the RNAseq analysis. Raw RNAseq data were obtained from the Max Planck Institute and analysed in Leeds in collaboration with Michael Wilson, who is the bioinformatician of the Plant Centre. The RNAseq reads were mapped to the Arabidopsis reference genome

using the TopHat/Bowtie pipeline. The Subread package was used for quantification of transcript abundances. Identification of significant changes and transcripts per kilobase (TPM) values were obtained using EdgeR. Only genes that were differentially expressed at a 2 fold cut-off and FDR<0.05, are discussed in the following analysis.

6.2 Results

6.2.1 Global overview of transcriptomic analysis of the dry and imbibed seeds of *vtc2-4* and *vtc2-1* mutants

Sample variation was estimated using principal component analysis (PCA). The PCA plot shows clear separation of the samples in the different treatments, i.e. dry and imbibed seeds (Figure 6.1). The first dimension (x-axis) shows that 94.12% of the variance is explained by the treatment while the second dimension (y-axis) is (3.59%) is related to differences between the biological samples (Figure 6.1). The PCA analysis reveals that the biological replicates for each genotype studied here cluster together (Figure 6.1). In dry seeds, the data from the *vtc2-1* and *vtc2-4* dry seeds overlap and are separated from Col-0 (Figure 6.1). While the data for the imbibed seed samples also cluster together, the *vtc2-1* samples are separated from the *vtc2-4* samples but both overlap with Col-0 (Figure 6.1).

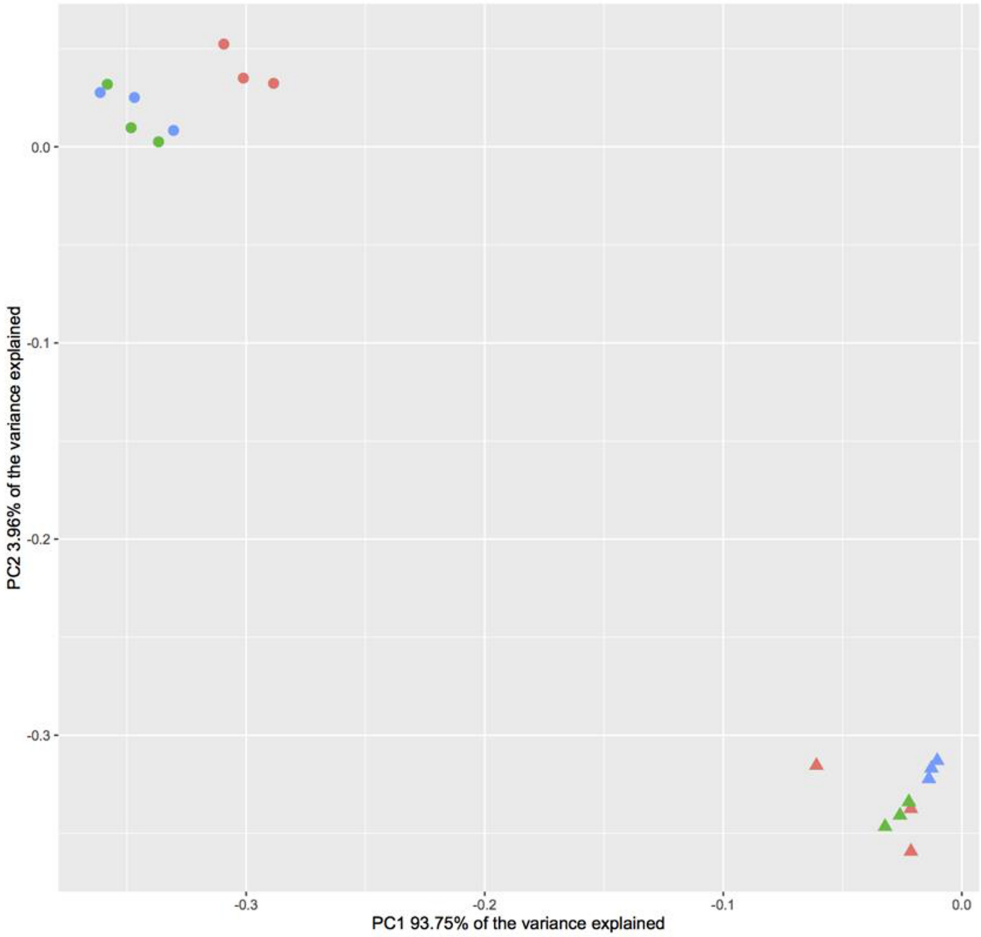

Figure 6.1 Principal component analysis (PCA) of the transcript profiles of dry (circle) and imbibed (triangle) seeds of the Col-0 (red), *vtc2-1* (green) and *vtc2-4* (blue) mutants.

6.2.1.1 Quantitative visualization of *VTC2* gene in Col-0, *vtc2-4* and *vtc2-1* mutants

The number of reads of the *VTC2* transcript of Col-0, *vtc2-1* and *vtc2-4* seeds are shown in Figure 6.2. *VTC2* gene comprises 7 exons and 5 introns (Figure 6.2). In Col-0 seeds *VTC2* gene is fully transcribed to about 156 reads (Figure 6.2 green), while this number decreases to 46 in the *vtc2-1* (Figure 6.2 blue). On the contrary, the transcription of *VTC2* gene was restricted to 328 reads of the first 4 exons in the *vtc2-4* seeds (Figure 6.2 red).

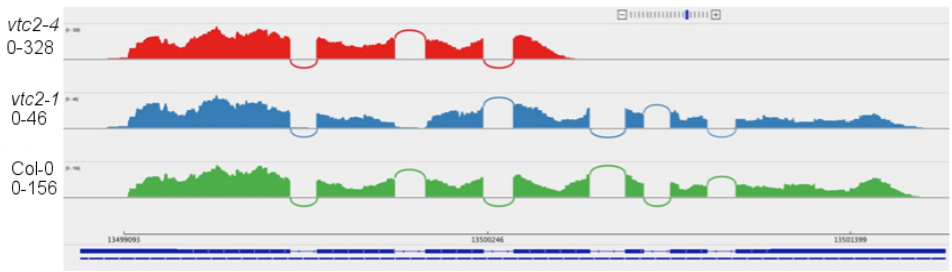

Figure 6.2 Sashimi plot showing the splice junctions of the *VTC2* gene in Col-0 (green), *vtc2-4* (red) and *vtc2-1* (blue). Numbers on the left shows the number of reads.

6.2.2 Transcriptome profiling analysis of dry seeds of the *vtc2-4* and *vtc2-1* mutant lines

In the dry seeds of the *vtc2-1* mutant there were 1049 differentially regulated transcripts compared to Col-0 (Figure 6.3 A). Of these, 536 were unique to *vtc2-1* while 513 were in common with the *vtc2-4* mutant seeds (Figure 6.3 A). The total number of differentially regulated transcripts in the dry seeds of the *vtc2-4* mutant was 1272 relative to Col-0, of which 759 were unique for this genotype (Figure 6.3 A).

The total number of transcripts whose abundance was increased in dry *vtc2-4* seeds was about the double of that of the *vtc2-1* genotype (Figure 6.3 B). Of these, 630 of the 970 transcripts that were differentially changed were unique to the *vtc2-4* seeds (Figure 6.3 B). Moreover, 214 transcripts whose abundance was increased relative to Col-0 were unique to the *vtc2-1* seeds. In total, 340 transcripts that were increased relative to Col-0 were common in both lines (Figure 6.3 B).

In total, 495 transcripts were decreased in abundance in the dry seeds of the *vtc2-1* mutants (Figure 6.3 C). Similarly, 302 transcripts were decreased in abundance in the dry seeds of the *vtc2-4* mutants (Figure 6.3 C). Of these, 153 were common to both mutant lines (Figure 6.3 C). It is important to note that 20 of the total number of transcripts, which were differentially changed in both mutants (Figure 6.3 A), did not cluster together in either the increased (Figure 6.3 B) or in the decreased abundant transcript groups (Figure 6.3 C). These 20 genes were inversely regulated in the mutants and for this reason do not appear in Figure 6.3 (B, C).

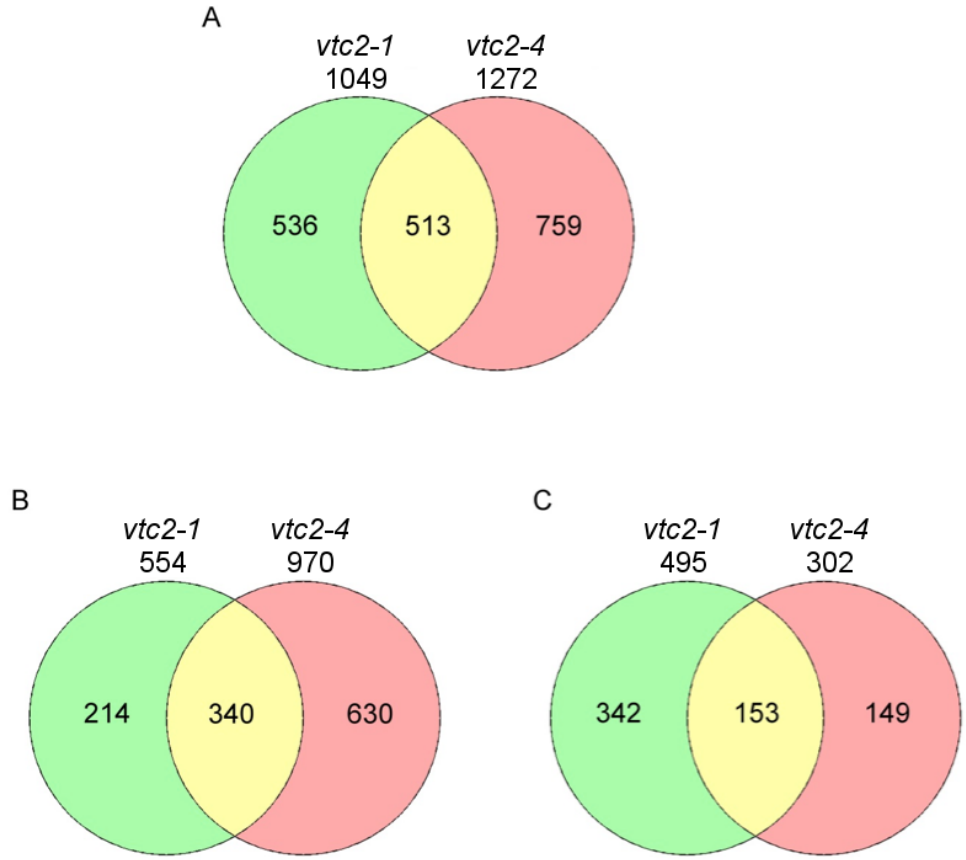

Figure 6.3 Common and unique differentially regulated transcripts in the dry seeds of the *vtc2-1* and *vtc2-4* mutants relative to Col-0.

(A) Total differentially expressed transcripts in *vtc2-1* and *vtc2-4* relative to Col-0. (B) Common and unique differentially transcripts, whose abundance was increased in *vtc2-1* and *vtc2-4* in relation to Col-0. (C) Common and unique transcripts, whose abundance was decreased in in *vtc2-1* and *vtc2-4* in relation to Col-0.

6.2.2.1 Global functional categorization of differentially regulated transcripts in the dry seeds of *vtc2-4* and *vtc2-1* relative to Col-0

The transcripts that were differentially changed in the dry seeds of the *vtc2-1* and *vtc2-4* mutants relative to Col-0 were first analysed using GO slim tool analysis (Figure 6.4). The general overview of the targeting of the transcripts within the cells revealed that the most represented category was the nucleus. In addition, a large number of differentially expressed transcripts were targeted to the mitochondria and chloroplasts (Figure 6.4 A). The transcripts that were differentially changed in the dry *vtc2-1* and *vtc2-4* seeds relative to Col-0 encode proteins that are involved in metabolism and stress responses, as well as signal transduction and gene expression (Figure 6.4 B). Consistent with this analysis, many of the transcripts that were differentially expressed in the dry seeds of the *vtc2-1* and *vtc2-4* mutants were identified as having transcription factor or DNA/RNA binding properties (Figure 6.4 C).

A further analysis of protein classes performed using *protein analysis through evolutionary relationships system* (Panther) showed that genes encoding large numbers (13%) of hydrolases, transferases and oxidoreductases were differentially expressed in the dry seeds of the *vtc2-1* and *vtc2-4* mutants (Figure 6.5 A). Similarly about 8% of the transcripts encoded proteins with nucleic acid binding properties. Within the oxidoreductase subcategory, 40% of total number of transcripts encoded proteins with oxygenase functions while about 20% had reductase/dehydrogenase and oxidase activities. Within the nucleic acid binding subcategory, 60% encoded proteins with DNA binding properties and 30% was RNA binding proteins (Figure 6.5 C).

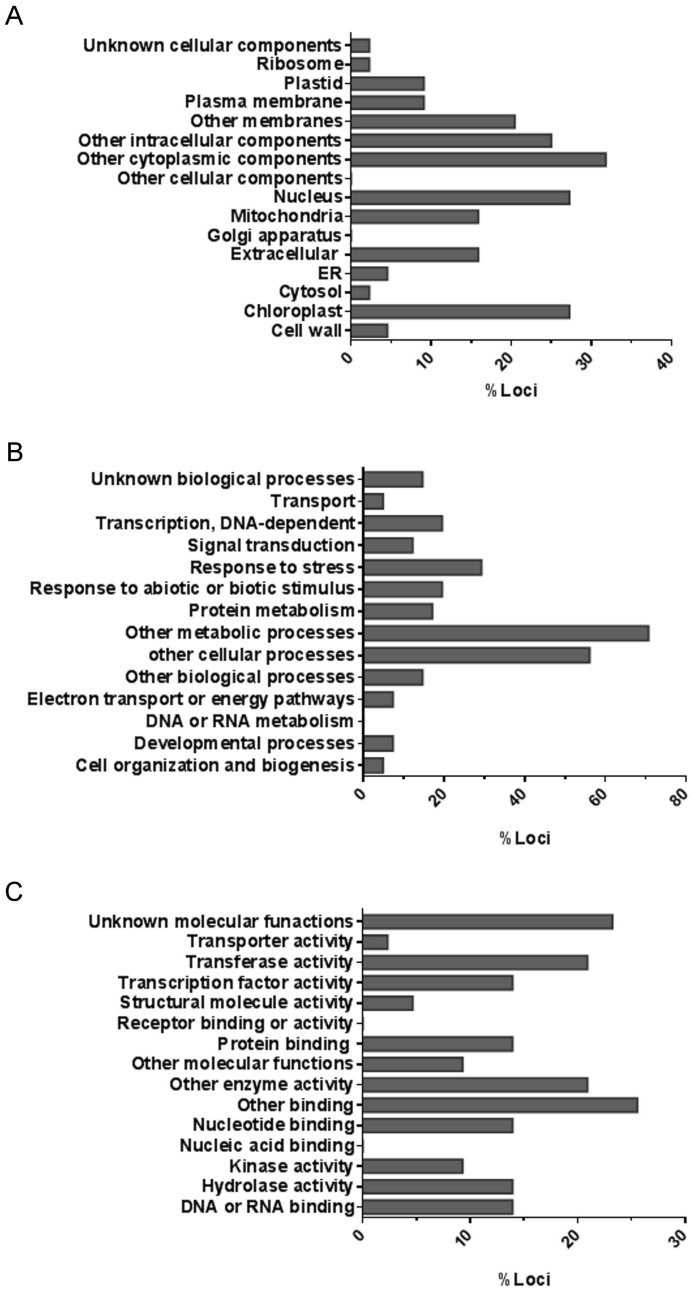

Figure 6.4 Functional classification by loci based on GO slim of the (A) cellular component, (B) biological processes and (C) molecular function in the dry seeds of *vtc2-1* and *vtc2-4* mutants relative to Col-0.

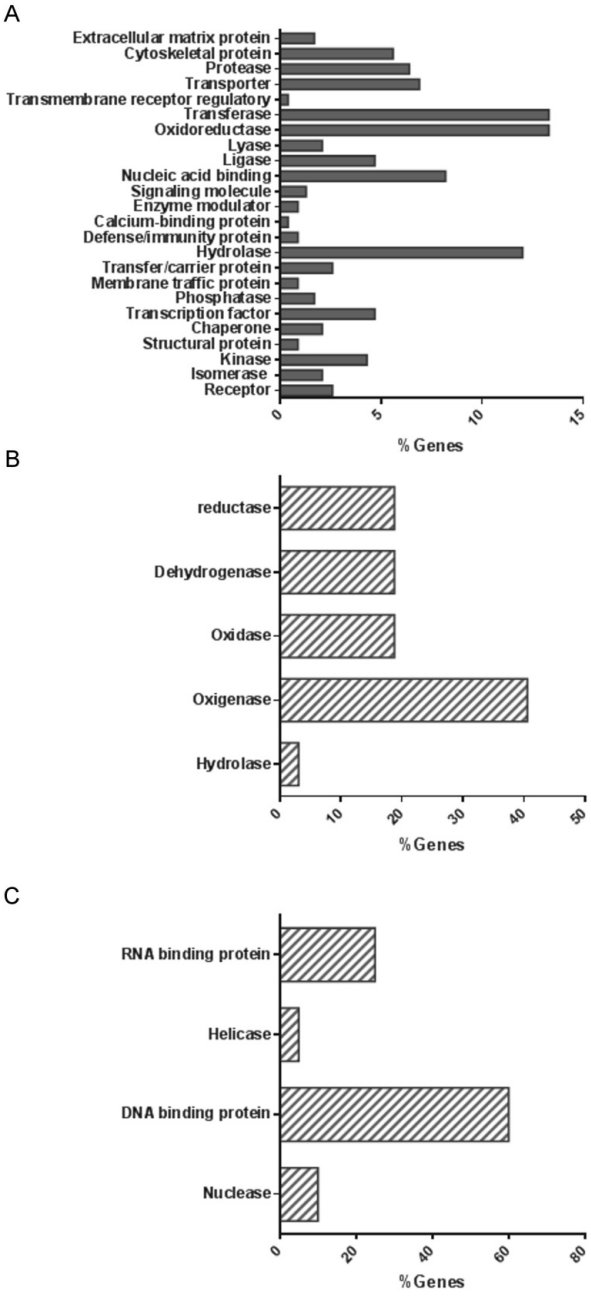

Figure 6.5 Analysis of protein classifications in terms of (A) the number of genes (B) Sub-categorization of oxidoreductase and (C) nucleic acid functions in the dry seeds of *vtc2-1* and *vtc2-4* mutants relative to Col-0.

6.2.2.2 Transcripts that were highly expressed in dry seeds of the *vtc2-4* and *vtc2-1* mutants relative to Col-0

The 10 transcripts showing the highest levels of differential regulation in the dry seeds of the *vtc2-1* and *vtc2-4* mutants are shown in Figure 6.6. The transcripts that are highly expressed in the *vtc2-1* and *vtc2-4* mutants are important in plant adaptation to stressful environmental conditions. For example, the transcripts whose abundance was most increased in the dry seeds of both mutants relative to the wild type was *FLAVIN-CONTAINING MONOXYGENASE 1* (*FMO1*; Figure 6.6) mutants, which is an important component in systemic acquired resistance (SAR) (Mishina and Zeier, 2006). *FMO1* controls a salicylic acid (SA) independent branch of the *ENHANCED DISEASE SUSCEPIBILY 1* (*EDS1*) and *PHYOALEXIN-DEFICIENT 4* (*PAD4*) pathway that regulates immunity and cell death, particularly in response to virulent pathogens (Bartsch et al 2006). Recently, however, SA and a second immune-regulatory metabolite (pipecolic acid) were shown to regulate SAR and defence priming in an *FMO1*-dependent manner (Bernsdorff et al 2016, Mishina & Zeier 2006). Moreover, transcript encoding cytochrome P450 monooxygenase (CYP82C2) was highly expressed in the dry seeds of the *vtc2-1* (Figure 6.6 A) and the *vtc2-4* mutants (Figure 6.6 B). CYP82C2 is involved in indole glucosinolate metabolism. In particular, it is important in the accumulation of jasmonate-induced indole glucosinolates and in jasmonate-induced defence gene expression as well as root growth inhibition (Liu et al 2010). The function of JA in responses to biotic stresses is well documented while his role in responses to abiotic is less clear. The data presented here show transcripts associated to calcium signalling were increased in both mutants. A CaM-like protein, calcium binding 19 protein (CML19) also known as CENTRIN 2, is highly expressed in the dry seeds of the *vtc2-1* and *vtc2-4* mutants (Figure 6.6 A and B). This protein was shown to move from the cytosol to the nucleus in plants subjected to stress (Liang et al 2006). Functioning as a putative calcium

sensor, this protein is important in nucleotide excision repair during homologous recombination (Molinier et al 2004). Calcium signals are also sensed by CPKs. The data presented here show that *CPK25* transcripts accumulate in both mutants (Figure 6.6). CPK25 has an unknown function, however like all the CPKs, CPK25 is involved in calcium signalling pathways in responses to stress (Kanchiswamy et al 2010). Interestingly, CPK25 lacks of the calcium-binding site, which it has been shown to affect calcium sensitivity (Boudsocq & Sheen 2013, Hrabak et al 2003).

Together with transcripts associated to adaptation to stressful environmental conditions the abundance of several cell division and DNA repair related transcripts was also increased in both mutants (Figure 6.6). ARR7 has a role in cell expansion and development repressing the expression expansin genes, which are induced by cytokinins (Lee et al 2007). Cytokinins are plant hormones that play a central role in mediating cell cycle and development. ARR7 is involved in the two components signalling mediating H_2O_2 and ethylene induced stomata closure (Marchadier & Hetherington 2014)

Transcripts encoding the MYB transcription factor, MYB56 were also much higher in the dry seeds of *vtc2* (EMS; Figure 6.6 A) and in the *vtc2-4* mutant (Figure 6.6 B) relative to the wild type. The R2R3-MYBs are a major transcription factor family in plants, with 126 members in *Arabidopsis*. MYB56 is a substrate for CRL3BPM E3 ligases, which mark specific proteins for degradation. MYB56 is negative regulator of flowering, controlling the expression of the *FLOWERING LOCUS T* (*FT*) (Chen et al 2015). MYB56 is predominantly expressed in developing seeds, regulating the expression of genes involved in cell wall metabolism, as well as cell division and expansion, in a manner that controls seed size (Wang et al 2013). On the other hand, *SOLO DANCER* transcript (SDS) with high levels in the dry seeds of the *vtc2-1* and *vtc2-4,* encodes a meiotic cyclin-like protein (Figure 6.6 A and B). This meiosis-specific novel cyclin-like protein is required for homologue

synapsis and bivalent formation, and may regulate the timing of sister chromatid separation (Azumi et al 2002).

The levels of *CDC7* and *CDKB1;2* transcripts were high in both mutants relative to the wild type (Figure 6.6 A). *CDC7* was first identified in S. cerevisiae where it is expressed at the G1 to S transition (Jares et al 2000). The CDC7 protein, which is related to the MAP kinase kinase kinases, recruits the enzymes required for replication on DNA replication site. CDC7 expression is restricted to the hypocotyl and cotyledons in Arabidopsis and cabbage and it is also weakly expressed at the early stages of seedling development (Barroco et al 2005). As in yeast CDC7 expression begins at the G1 to S transition and it is constant thereafter throughout the cell cycle.

CDKs are required for cyclin activity. While A-type CDK are also present in mammals and yeast, B-type CDK, (CDKB1;1 and CDKB1;2) are plant specific and regulate the G2 to M transition interacting with A2-type cyclins and preventing endoreplication (Boudolf et al 2009).

Transcripts encoding farnesoic acid carboxyl-O-methyltransferase (FAMT), which uses *S*-adenosyl methionine in the methylation of sesquiterpene farnesoic acid (FA), were higher in *vtc2-4* than *vtc2-1* mutants. The methylated product of FA(MeFA) is a precursor insect juvenile hormones III, and its presence perturbs insect growth and development (Yang et al 2006). Interestingly, *FAMT* expression is regulated by a microRNA (miRNA), MIR163, suggesting that low ascorbate might alter miRNA expression leading to increased defence responses through effects on FAMT (Ng et al., 2015)

Redox associated transcripts encoding glutathione S-transferases (GST) and gluaredoxins (GRX) were also more highly expressed in both mutants than the wild type (Figure 6.6). In particular, transcripts encoding 2 Tau class GSTs (GSTU8 and GSTU12) were abundant in the *vtc2-1* (Figure 6.6 A) and in the *vtc2-4* (Figure 6.6 B). GSTU8 was shown to a glutathione-associated gene that was highly expressed in catalase-deficient (cat2) and catalase plus glutathione reductase-deficient Arabidopsis mutants (Mhamdi et al 2010). GSTU8 had high

peroxidase activity (Dixon & Edwards 2010) and can form glutathione-oxylipin conjugates, linking this GST to jasmonate signalling (Mueller et al 2008). Like GSTU8, GSTU12 is a hydrogen peroxide-responsive gene that localises entirely to the nucleus. GSTU12 co-purifies with ribosomal proteins but it has no peroxidase activity, and has been suggested to function as a transcriptional regulator in the nucleus (Dixon & Edwards 2010). GST8 encodes a TAU GST with peroxidase activity that is induced by drought and auxins (Bianchi et al 2002).

Of the transcripts that are highly expressed in the seeds of *vtc2-1* and *vtc2-4* mutants relative to the Col-0 only one encodes a protein associated with metabolism, the levels of GLU1 transcripts that encode the major ferredoxin-dependent glutamate synthase (GOGAT) (Feraud et al 2005) (Figure 6.6). This key enzyme of primary nitrogen assimilation is usually highly expressed in leaves in response to factors such as light intensity and sucrose availability (Kissen et al 2010). Expression of this gene in dry seeds may be required to support amino acid production associated with rapid metabolism

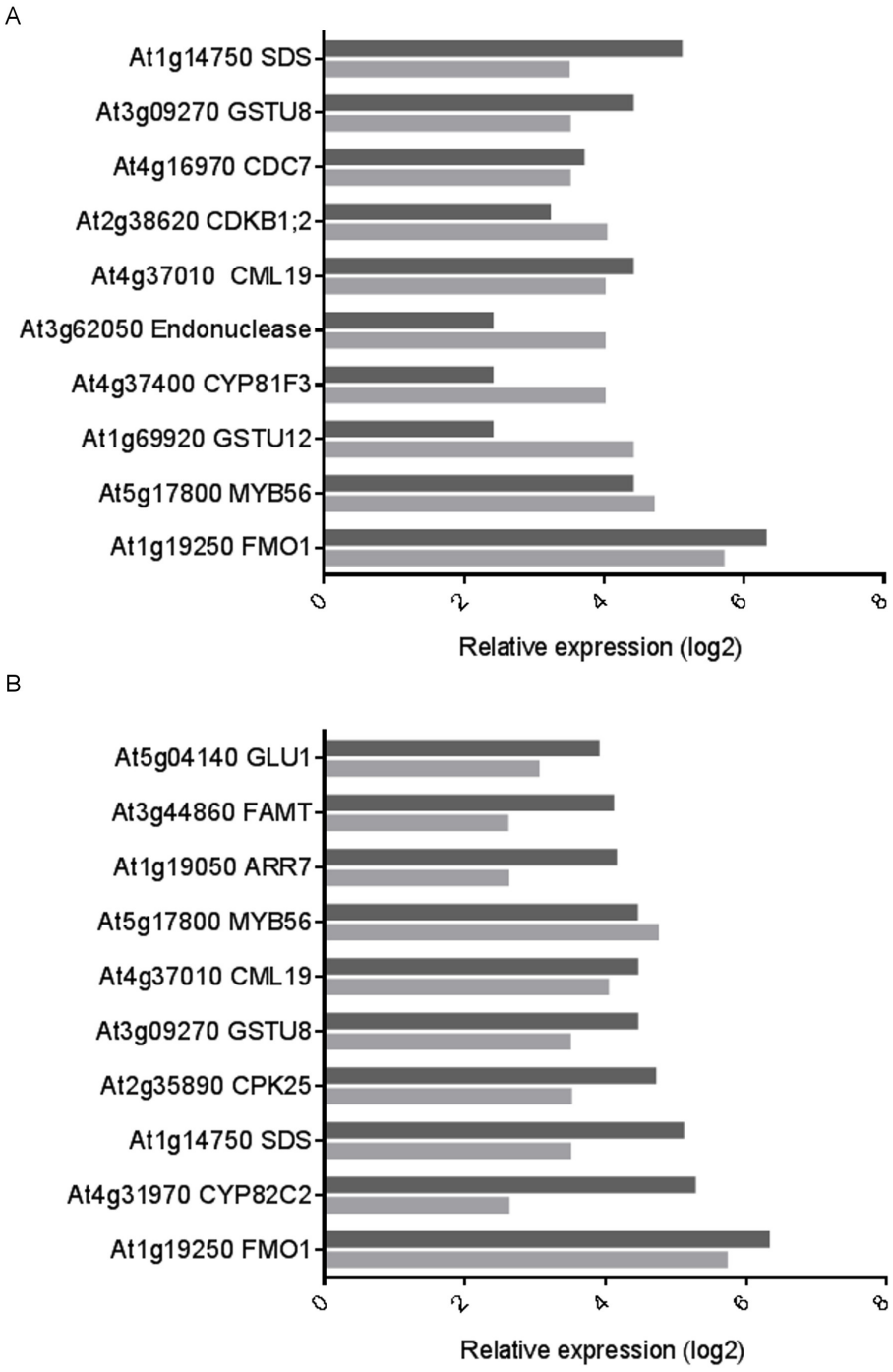

Figure 6.6 Top ten most induced transcripts in the dry seeds of (A) *vtc2-1* and (B) *vtc2-4* mutants relative to Col-0.

In both cases the data for *vtc2-1* are shown as the lighter bars, while the data for the *vtc2-4* mutants are shown as the darker bars.

6.2.2.3 Transcripts that were decreased in abundance in *vtc2-4* and *vtc2-1* relative to Col-0

The 10 transcripts showing the lowest levels of differential regulation in the dry seeds of the *vtc2-1* and *vtc2-4* mutants are shown in Figure 6.7. The transcripts that are most decreased in expression in the *vtc2-1* and *vtc2-4* mutants are related to plant secondary metabolism and cell division. Transcript with lowest levels of expression in the dry seeds of the *vtc2-1* relative to the wild type encodes 4-Coumarate-CoA ligase (Figure 6.7 A) while in the *vtc2-4* mutant the lowest abundant transcript encodes transcription factor involved in the production of anthocyanin pigment 2 protein (PAP2; AtMYB90). The 4-coumarate-CoA ligase has a key role in the secondary compound synthesis at the point where phenylpropanoid metabolism diverges into several major branch pathways (Hamberger & Hahlbrock 2004). This enzyme catalyses the activation of 4-coumarate and some related substrates to the respective CoA esters, channelling common, metabolites into different branches of general phenylpropanoid metabolism, such as lignin, flavones, flavonols (Li et al 2015). PAP2 (AtMYB90) is also involved in the regulation of secondary metabolism. This MYB protein is a regulator of flavonoid biosynthesis, which plays a major role in the induction of anthocyanin biosynthesis in response to high light stress (Bac-Molenaar et al 2015). While the role of PAP2 is less clear that that of PAP1, it may have a specific role for in the UV-A/blue light signal transduction pathway mediated by CRY1 (Bulley et al 2012).

Transcripts encoding two stress inducible glycosyltransferases (UGT79B5 and UGT72B2) were lower in the dry seeds of both mutants than Col-0 (Figure 6.7). In mammals, UGTs have an important role in detoxification of xenobiotics catalysing the transfer of glucuronic acid to a variety of substrates. The glucuronidation of hydrophobic compounds such as xenobiotics leads to changes in the solubility of the substrate facilitating their elimination and hence reducing the toxicity (Radominska-Pandya et al 2010). While the functions of UGT79B5

remain to be characterised, UGTs catalyse the glycosylation of small molecules in the biosynthesis of secondary metabolites. These metabolites comprise signalling molecules and defence compounds in plants which act on the JA-SA cross talk (Von Saint Paul et al 2011).

A putative member of the S-adenosyl-L-methionine-dependent methyltransferases superfamily, F16P17.4, was decreased in both mutants (Figure 6.7 A and B). O-Methyltransferases (OMTs) like glycosyltransferases (GTs) mediate the pathways of secondary metabolites, in particularly it has been shown that OMTs regulate the biosynthesis of flavonoids (Seguin et al 1998).

The levels of *BUD2* transcripts, which encode S-adenosylmethionine decarboxylase 4 (SAMDC4) were decreased in both mutants relative to the wild type. *BUD2* is involved in the biosynthesis of polyamines (Figure 6.7 A and B), which function in environmental stress responses and regulate root and shoot growth (Bartoli et al 2006, Watson et al 1998). For example, *BUD2* mediates root branching through a mechanism that involves auxin (Bartoli et al 2006). Moreover, *bud2* mutants show a bushy and dwarf phenotype as a consequence of impaired transport of auxins (Bartoli et al 2006). The *bud2* mutants are insensitive to exogenous auxins and in contrast to the wild type; they do not show altered lateral root formation in the presence of auxin (Cui et al 2010).

Transcripts encoding a cytochrome P450 (CYP71B29) were decreased in both mutants. CYP71B29 belongs to the CYP71 family and is thought to be involved in secondary metabolism but its functions have not yet been characterised (Figure 6.7). However, many of the proteins within the CYP gene family are involved in the biosynthesis of different metabolites, hormones such as GA, ABA and IAA, and signalling molecules such as JA and SA, as well as plant defence molecules like lignin and flavonoids (Liu et al 2010, Pfalz et al 2011).

The accumulation of transcription factors involved in anthocyanin biosynthesis and responses to environmental stress were decreased in both mutants (Figure 6.7 A and B). These include two basic helix-loop-

helix (bHLH114) DNA-binding, the auxin-responsive transcription factors (IAA20) and the ethylene responsive transcription factor (ERF039) were down regulated in both mutants (Figure 6.7 A and B). 133 BHLH genes are present in Arabidopsis, which are divided in twelve families containing conserved amino acid sequence. Only few BHLH genes have been characterised in plants. *BHLH114* has been associated to the anthocyanin biosynthesis in a mechanism that involves interaction with transcription factors of the R2R3MYB class (Goff et al 1992). IAA proteins are transcriptional factors that function as strong repressors of early auxin response (Tiwari et al 2004). IAA20 is expressed in the quiescent centre cells of the root apical meristem and also in the columella cells of the root cap (Sato and Yamamoto, 2008). Overexpression IAA20 resulted in a semi-dwarf phenotype. In particular, the primary root stopped growing soon after germination because of collapse of root apical meristem (Sato and Yamamoto, 2008). Aux/IAA family of auxin responsive transcriptional repressors that acts by binding to TIR1-related F-box proteins to activate auxin signalling by freeing ARFs that regulate the expression of auxin-responsive genes. TIR1 is a component of SCF ubiquitin ligase, which is responsible for Aux/IAA degradation by proteasome. However, IAA20 lacks of the TIR1 binding domain and it might represent a novel role in auxin signalling (Dreher et al 2006). Moreover, it has been shown that IAA induced CC-type GRS6 in Oryza (Garg et al 2010).

Transcripts encoding the ethylene responsive transcription factor, ERF039 which belongs to the DREB sub-group of the AP2/ERF family that regulates primary and secondary metabolism as well as stress responses, were decreased in both mutants. The DREB subfamily plays a role in responses to abiotic stresses in a process mediated by the dehydration-responsive element (DRE; (Liu et al 1998). Group VII transcription factors are particularly important in seed germination because they are involved in sensing of molecular oxygen and nitric oxide and they are partners of DELLA proteins that control plant growth, for example in cell division in the apical hook (Marin-de la Rosa et al

2014). Another member of the ethylene-responsive transcription family, AtERF98, is involved in the regulation of ascorbate biosynthesis and influences the expression of *VTC1* in Arabidopsis (Zhang et al 2012). Knock out *aterf98-1* mutants have lower ascorbate synthesis rates and lower salt resistance. However, overexpressing *aterf98-1* in *vtc1* did not lead to salt (Zhang et al 2012).

The cell cycle associated transcripts *CUL1* and *NPR6* were also decreased in both mutants relative to Col-0 (Figure 6.7). Transcripts encoding for *CUL1* were much lower in the *vtc2-1* seeds than in the *vtc2-4* seeds (Figure 6.7 A). CUL1 is part of the cullin-RING ubiquitin ligase complex (SCF complex) and it is mainly localised in the nucleus during interphase. Mutants in the *AtCUL1* gene fail to progress into the S phase of the cell cycle in yeast (Schwob et al 1994). Null *AtCUL1* mutations in plants are embryo lethal (Shen et al 2002).

NPR6 belongs to BTB-ankryin protein transcriptional co-activator family. The first BTB-ankryin protein to be identified was NON-EXPRESSOR OF PATHOGENESIS-RELATED GENES1 (NPR1), which is associated to SA-dependent defence responses to pathogen attack (Conklin et al 2013). NPR6 is also known as BLADE-ON-PETIOLE 1 *gene* (BOP1), which promotes and maintains cell division in the petioles of the cotyledon and rosette leaves in Arabidopsis, probably through regulation of class I *KNOX* genes (Bartoli et al 2004). NPR6 also plays a role in plant defences induced by methyl jasmonate (Canet et al 2012).

The abundance of peroxidases (*PER*26 and *PER64*) was also decreased in both mutants relative to Col-0 (Figure 6.7 A and B). Arabidopsis contains 73 genes encoding peroxidases, all of which have a high degree of homology. Although the heme-containing peroxidase, *PER*26 is not well characterised, it is known that heme-containing peroxidases are able to produce H_2O_2 and are involved in responses to abiotic and biotic stresses and in auxin signalling. Some peroxidases are required for the oxidative burst associated with resistance to bacteria and fungi (Bindschedler et al 2006). *PER64* has a role in

responses to environmental stresses such as wounding, pathogen attack and oxidative stress. Moreover, *PER64* is a homologue of the ZPO-C gene of *Z. elegans* and it is specifically involved in the lignification of sclerenchyma (Sato et al 2006).

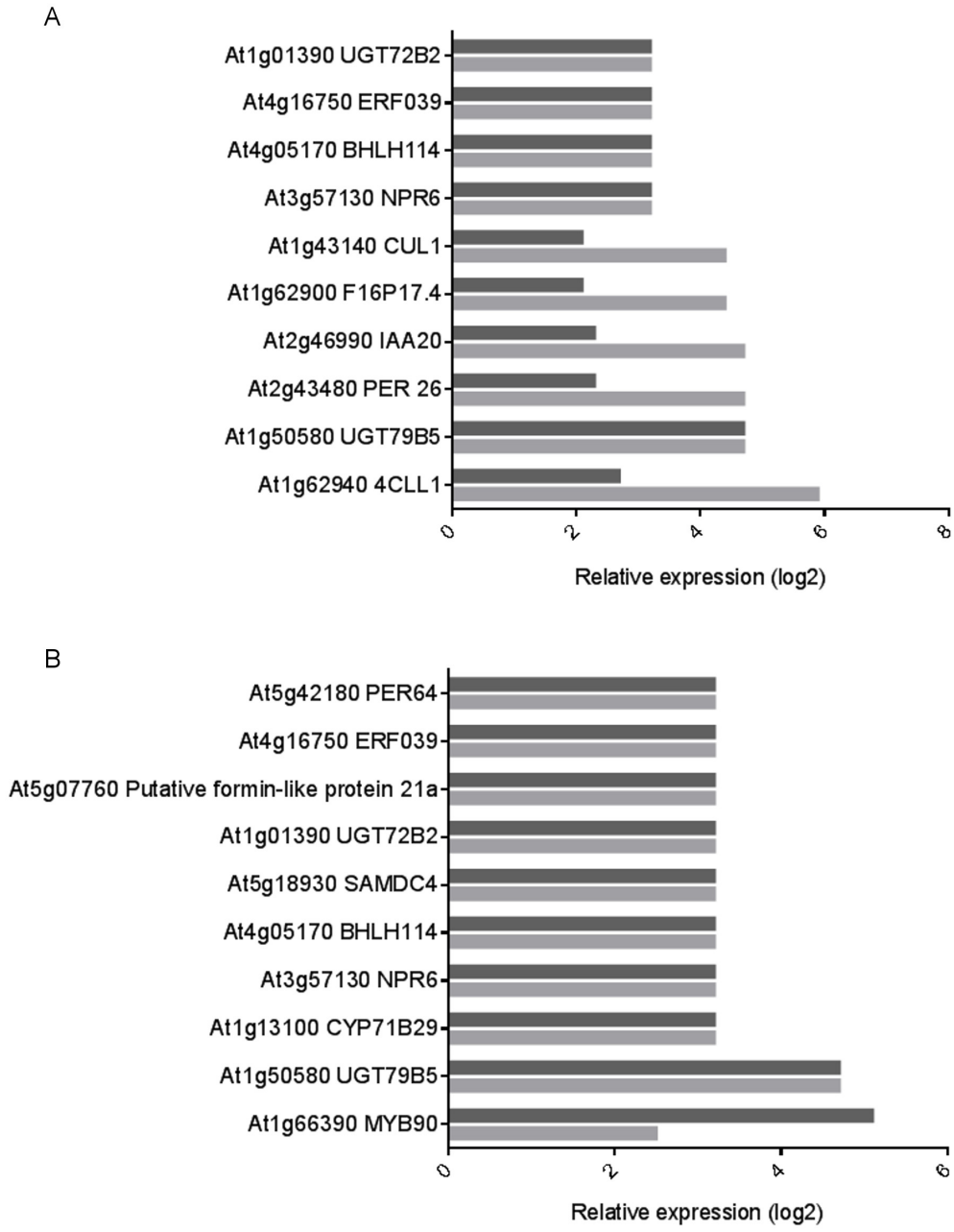

Figure 6.7 Top ten most repressed transcripts in the dry seeds of (A) *vtc2-1* and (B) *vtc2-4* mutants relative to Col-0.

In both cases the data for *vtc2-1* are shown as the lighter bars, while the data for the *vtc2-4* mutants are shown as the darker bars.

6.2.2.4 Redox associated transcripts

The *vtc2-1* and *vtc2-4* mutants contain only 20-30% of the wild type ascorbate. Since low ascorbate will result in a low redox buffer capacity environment, a gene by gene analysis of function was used to identify the genes with redox functions that were differentially expressed in the low ascorbate mutants relative to Col-0 shown in Table 9. On the genes listed in Table 9, the possible functions of *FMO1*, *GSTU12* and *GSTU8* and *CYP82C2* in dry seeds have been discussed above. Of the other 31 redox related transcripts that are increased in abundance seven encode cytochrome P450 proteins: *CYP82C2*, *CYP705A9*, *CYP708A2*, *CYP71A12*, CYP71B20, *CYP71B15* and *CYTB5-C*. Moreover, a further three cytochrome P450 proteins (cytochrome P450-like protein *CYP71B29* and *CYP705A20*) were repressed (Table 9). As discussed above, *CYP82C2* and CYP79B2 are involved in glucosinolate metabolism and *CYP70* and *CYP71* encode oxidosqualene cyclases involved in the biosynthesis of terpenes (Mizutani & Ohta 2010).

In addition to *GSTU12* and *GSTU8*, only one glutathione-related transcript *GRX-C8* was increased in both mutants relative to the wild type (Table 9). Transcripts encoding *GRXS9* and a GRX-like protein (At5g01420) were lower in the ascorbate-deficient mutants relative to the wild type (Table 9). At5g01420 is a 4CxxC type GRX, which is localised in the cytosol. It has been shown that the CxxC type Grx-1 has DHA reductase activity and it is involved in the reduction of DHA to ascorbate (Flandrin et al 2015, Washburn & Wells 1999). The CCxS type monothiol glutaredoxin-S9 thioredoxin (GRX9/ROXY7). Although GRX9 is not well characterised, but it shows high homology with the two isoforms of GRX13 (GRXS13.1 and GRXS13.2) (Laporte et al 2012). GRX9 is activated by SA through a mechanism that involves TGA transcription factors (Blanco et al 2009) while the expression of GRX9 suppresses the defence response mediated by JA (Ndamukong et al 2007).

Transcripts encoding *SKU5* were increased in both mutants relative to the wild type (Table 9). *SKU5* encodes an extracellular glycosyl phosphatinylinositol–anchored glycoprotein that controls directional root growth. It belongs to family comprising of 19 members, which are localised in the cell wall and are related to multiple-copper oxidases, ascorbate oxidase and laccase. The *sku5* mutants show impaired directional growth in roots and hypocotyls (Sedbrook et al 2002). Transcripts encoding an UDP-glucuronic acid decarboxylase (*UXS6)* were increased in both mutants relative to the wild type but no information is available on the specific functions of this protein (Table 9).

The accumulation of *GDP-L-Galactose-Phosphorylase* (*VTC2*) transcripts were not significantly different in the *vtc2-1* mutants compared to the wild type seeds (Figure 6.8 A) but the abundance of *VTC2* transcripts was significantly decreased (2.5 fold) in the *vtc2-4* mutant (Figure 6.8 A). Furthermore, no changes in the expression of the *VTC2* homologue, *VTC5,* were found in either mutant (Figure 6.8 A).

Interestingly, other two transcripts that encode L-gulono-1,4-lactone oxidases, *GulLO2* and *GulLO6,* were decreased in both mutants (Figure 6.8 B). In animals L-gulono-1,4-lactone is oxidised to ascorbate in the biosynthetic pathway (Davey et al 1999).

Table 9 Differentially expressed redox-related regulated transcripts in dry seeds.

Accession	Description	LogFC	
		vtc2-1	*vtc2-4*
At1g19250	Flavin-containing monooxygenase, 1 FMO1	5.7	6.3
At1g69920	Glutathione S-transferase U12, GSTU12	4.4	2.4
At4g37400	Cytochrome-P450 monooxygenase-like protein	4	2.4
At3g09270	Glutathione S-transferase U8, GSTU8	3.5	4.4
At5g04140	Ferredoxin-dependent glutamate synthase1	3	3.9
At4g37980	Cinnamyl alcohol dehydrogenase 7	2.8	3.2
At4g38420	Protein SKU5 similar 9	2.6	2.4
At4g31970	Cytochrome P450 CYP82C2	2.6	5.3
At2g27010	Cytochrome P450, CYP705A9	2.6	3.2
At5g14070	Glutaredoxin-C8 GRX-C8	2.6	3.2
At2g28760	UDP-glucuronic acid decarboxylase 6 UXS6	2.6	2.4
At5g48000	Cytochrome P450 CYP708A2	2.6	2.4
At4g39950	Cytochrome P450 CYP79B2	2.5	3.3
At2g30750	Cytochrome P450 CYP71A12	2.5	3.4
At3g26180	Cytochrome P450 CYP71B20	2.4	3.8
At3g26830	Cytochrome P450 CYP71B15	2.4	3.7
At2g46650	Cytochrome B5 isoform C CYTB5-C	2.3	2.5
At2g37540	Putative oxidoreductase	2.4	3
At5g06470	Electroncarrier/disulphide oxidoreductase related	-2.3	-2.3
At5g01420	Glutaredoxin family protein	-2.3	-2.3
At4g15300	Cytochrome P450 like protein	-2.3	-2.3
At3g20110	Cytochrome P450 CYP705A20	-2.3	-2.3
At2g30540	Monothiol glutaredoxin-S9 thioredoxin	-2.3	-2.3
At1g62580	Flavin-containing monooxygenase FMO GS-OX-like 7	-2.3	-2.3
At1g36580	Uncharacterized protein	-2.3	-2.3
At1g13100	Cytochrome P450 71B29	-3.2	-3.2

\

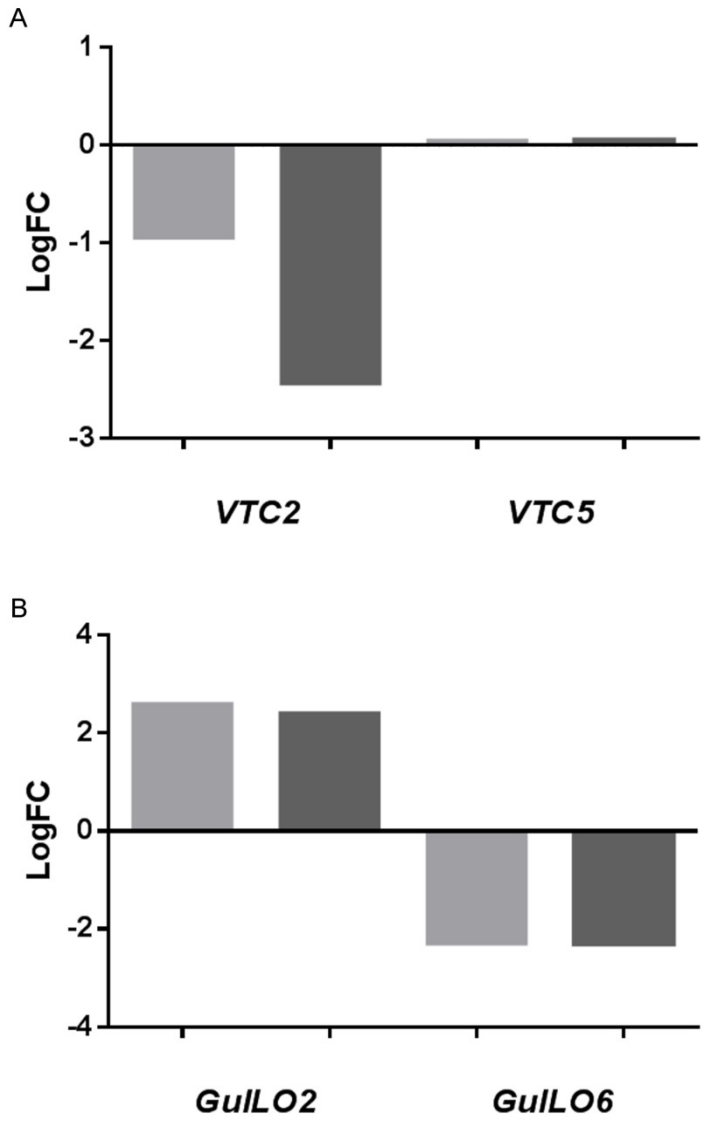

Figure 6.8 Abundance of transcripts encoding L-gulono-1,4-lactone oxidases that are related to ascorbate biosynthesis in animals in the *vtc2-1* (light grey) and *vtc2-4* (dark grey) mutants.

(A) Fold change in *VTC2* and *VTC5* transcripts in the D-Mannose/ L-galactose pathway. (B) Fold change in L-gulono-1,4-lactone oxidases *GulLO2* and *GulLO6* transcripts in the D-glucuronic acid pathway.

6.2.2.5 Transcripts that localise to the nucleus

Differentially expressed transcripts that encode nuclear proteins were compared in the *vtc2-1* and *vtc2-4* dry seeds compared to the wild type. As discussed previously, the most abundant transcript that was differentially changed was the *MYB56* transcription factor, which controls seeds size. *MYB56* (also called BRAVO), which is expressed predominantly in developing seeds, is a member of the R2R3 gene family. It is a central stem cell specific regulator that controls cell division. It counteracts brassinosteroid (BR)-mediated cell division in the primary root meristem to protect the stem cell niche (Vilarrasa-Blasi et al 2014). *MYB56* expression is regulated by the BR-regulated BES1 in the vascular cells and initials. Other R2R3 MYB transcription factors whose abundance was increased in the ascorbate-deficient mutant seeds relative to Col-0 were *MYB84*, *MYB124* and *MYB Like 2* (*MYBL2*) (Table 10). *MYB84*, also called *REGULATOR OF AXILLARY MERISTEMS* (*RAX*)3 belongs to a large family of transcription factors involved in the axillary meristem formation during postembryonic development (Muller et al 2006). *MYB124* is encoded by *FOUR LIPS* gene and regulates cell division to form stomata (Lai et al 2005). *FLP* is expressed in the shoots and also in roots, particularly the root tip (Lai et al 2005). All *flp* mutants show impaired stomatal phenotypes that are either characterized by stomata that are in direct contact with each other or with increased numbers of cells. In stomata, *FLP* acts as a repressor of the mitosis-inducing factor CDKB1;1. However, it may also regulate the E2F-DP pathway because of binding to overlapping regions with *CDKB1;1* (Xie et al 2010).

Several transcripts that are differentially accumulated in the ascorbate-deficient mutants such as *CDKB1;2, CDC7* and *SDS* are related to cell cycle regulation. As discussed above, *SDS* transcript levels were greatly increased in the ascorbate-deficient mutants transcripts as described in 6.2.2.2 section. Other transcripts that were greatly increased in the ascorbate-deficient mutants relative to Col-0 include

CTF18, which is required for cohesion in the replication fork. The replicative fork complex is essential for the correct cohesion of the sister chromatid (Hanna et al 2001). However, *ORC2* transcripts where significantly decreased in the ascorbate-deficient mutants. ORC2 is an essential component of the origin recognition complex. The *orc2* mutants in yeast show arrest of the cell cycle at the G1/S phase (Bell et al 1993). Furthermore, *orc2* mutation in Arabidopsis causes a zygotic lethal phenotype, the seeds aborting early. Moreover nuclear division is arrested and the nuclear size is greatly increased (Collinge et al 2004).

Transcripts related to DNA repair such as CEN2, cell cycle check point regulator, RAD1, and two breast cancer like proteins (BRCA2A and BRCA2B) were also increased in the ascorbate-deficient mutants (Table 10). Transcripts encoding CEN2 and RAD1-like are both involved in responses to DNA damage through the pathway that includes Cullin4 (CUL4) signalling to the proteasome (Molinier et al 2008). Breast cancer proteins (BRCA2A and BRCA2B) form a complex with RAD51 and mediate DNA repair in humans (Jensen et al 2010). Furthermore, it has been shown that this complex mediates responses to stress through a process, which involves SA (Cui et al 2010).

The levels of *MYB LIKE 2* (MYBL2), *MYB28* and *MYB90* transcripts were decreased in the ascorbate-deficient mutants. *MYBL2* is highly expressed in the embryo, and encodes a protein that regulates flavonoid synthesis. Loss of MYBL2 functions leads to increased accumulation of anthocyanins in the seed coat (Dubos et al 2008). MYB28 and MYB90 fulfil roles in response to stresses such as high light and are induced by hormones such as JA, SA and GA (Bac-Molenaar et al 2015). Over-expression of *MYB28* leads to hypersensitivity to ABA during seed germination, cotyledon greening and early seedling growth (Yu et al 2016).

Table 10 Differentially expressed transcripts that encode nuclear proteins in dry seeds.

Accession	Description	LogFC	
		vtc2-1	***vtc2-4***
At5g17800	MYB56 transcription factor BRAVO	4.7	4.4
At1g69920	Glutathione S-transferase U12 GSTU12	4.4	2.4
At3g62050	Endonuclease	4.0	2.4
At4g37010	CML 19/CEN2	4.0	4.4
At2g38620	CDKB1;2	4.0	3.2
At4g16970	CDC7	3.5	3.7
At1g14750	SDS	3.5	5.1
At4g17760	Cell cycle checkpoint RAD1	3.5	2.4
At3g09270	Glutathione S-transferase U8	3.5	4.4
At1g14350	MYB transcription factor related MYB124	3.5	3.8
At5g06510	Nuclear transcription factor Y subunit A-10	3.5	3.2
At1g71030	Arabidopsis MYBL2	2.6	2.9
At4g00020	Breast cancer protein 2 like 2A BRCA2A	2.6	3.2
At1g04730	Chromosome transmission fidelity protein 18 CTF18	2.5	2.6
At2g37560	Origin recognition complex subunit 2 ORC2	-2.3	-2.3
At3g49690	Transcription factor MYB84/RAX3	-2.3	-2.3
At5g01630	Breast cancer susceptibility protein 2b BRCA2B	-2.3	2.1
At5g61420	Transcription factor MYB28	-2.3	-2.3
At1g66390	Transcription factor MYB90	-2.5	-5.1

6.2.3 Transcriptome profiling analysis of imbibed seeds of the *vtc2-4* and *vtc2-1* mutant lines

In contrast to dry seeds of the *vtc2-1* and *vtc2-4* mutants where over 1000 transcripts were differentially regulated relative to Col-0 (Figure 6.3 A), the total number of transcripts whose abundance was changed in the imbibed seeds of the ascorbate-deficient mutants relative to Col-0 was only about 100. The number of transcripts, whose abundance was increased in the imbibed *vtc2-4* seeds, was about the same that of *vtc2-1* seeds (Figure 6.9 B). Moreover, 37 of the 80 transcripts that were differentially increased were unique to the *vtc2-4* mutants (Figure 6.9 B) while 44 transcripts were unique to the *vtc2-1* imbibed seeds. In total, 43 of the transcripts that were increased relative to Col-0 were common to both genotypes (Figure 6.9 B).

Only 16 transcripts were decreased in abundance in the imbibed seeds of the *vtc2-1* mutants (Figure 6.9 C). In contrast, 46 transcripts were decreased in abundance in the imbibed seeds of the *vtc2-4* mutants (Figure 6.9 C). Of these, only 2 were common to both mutant lines (Figure 6.9 C).

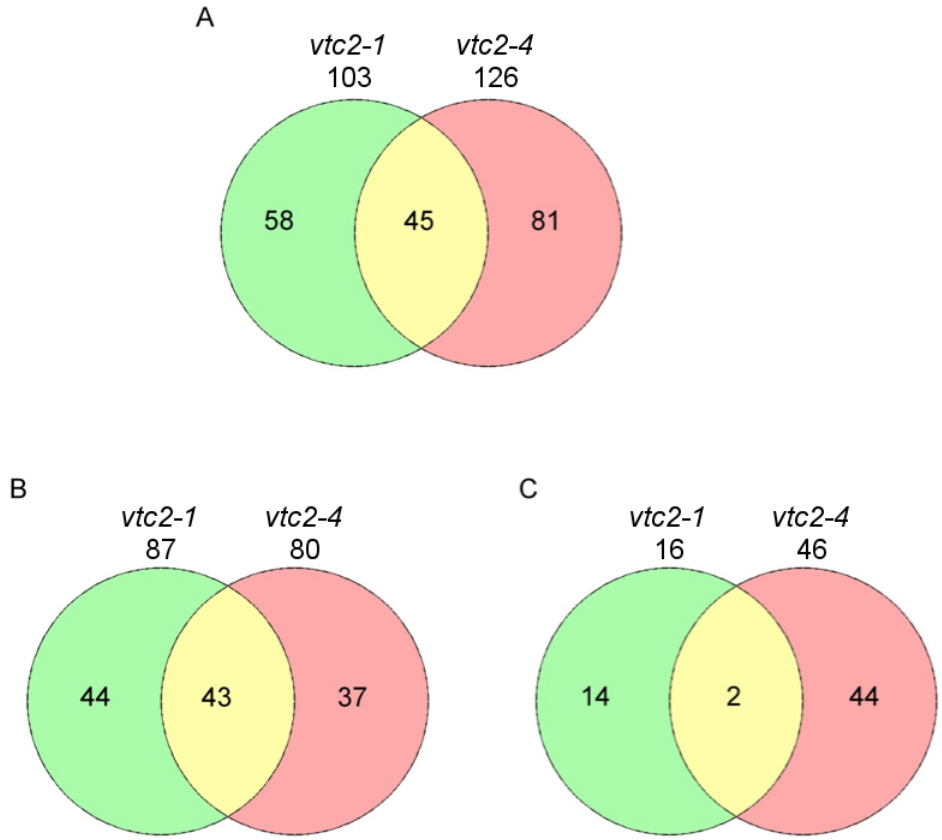

Figure 6.9 Venn diagrams showing common and unique differentially expressed transcripts in imbibed seeds of the *vtc2-1* and *vtc2-4* mutants relative to Col-0.

(A) Total common and unique differentially regulated genes in *vtc2-1* and *vtc2-4* in relation to Col-0. (B) Common and unique differentially up regulated genes in *vtc2-1* and *vtc2-4* in relation to Col-0. (C) Common and unique differentially down regulated genes in *vtc2-1* and *vtc2-4* in relation to Col-0.

6.2.3.1 Global functional categorization of differentially regulated transcripts in imbibed *vtc2-4* and *vtc2-1* seeds relative to Col-0

GO slim tool analysis showed that transcripts localised in the chloroplasts and in the nucleus were the most highly represented categories in imbibed seeds (Figure 6.10 A). Similar to dry seeds, the transcripts that were differentially changed in imbibed seeds relative to Col-0 encode proteins that are involved in metabolism and stress responses, as well as in transcription and DNA-dependent processes (Figure 6.10 B). These transcripts largely encode transcription factors transferases and nucleotide-binding proteins, as well as proteins involved in DNA and RNA processing (Figure 6.10 C).

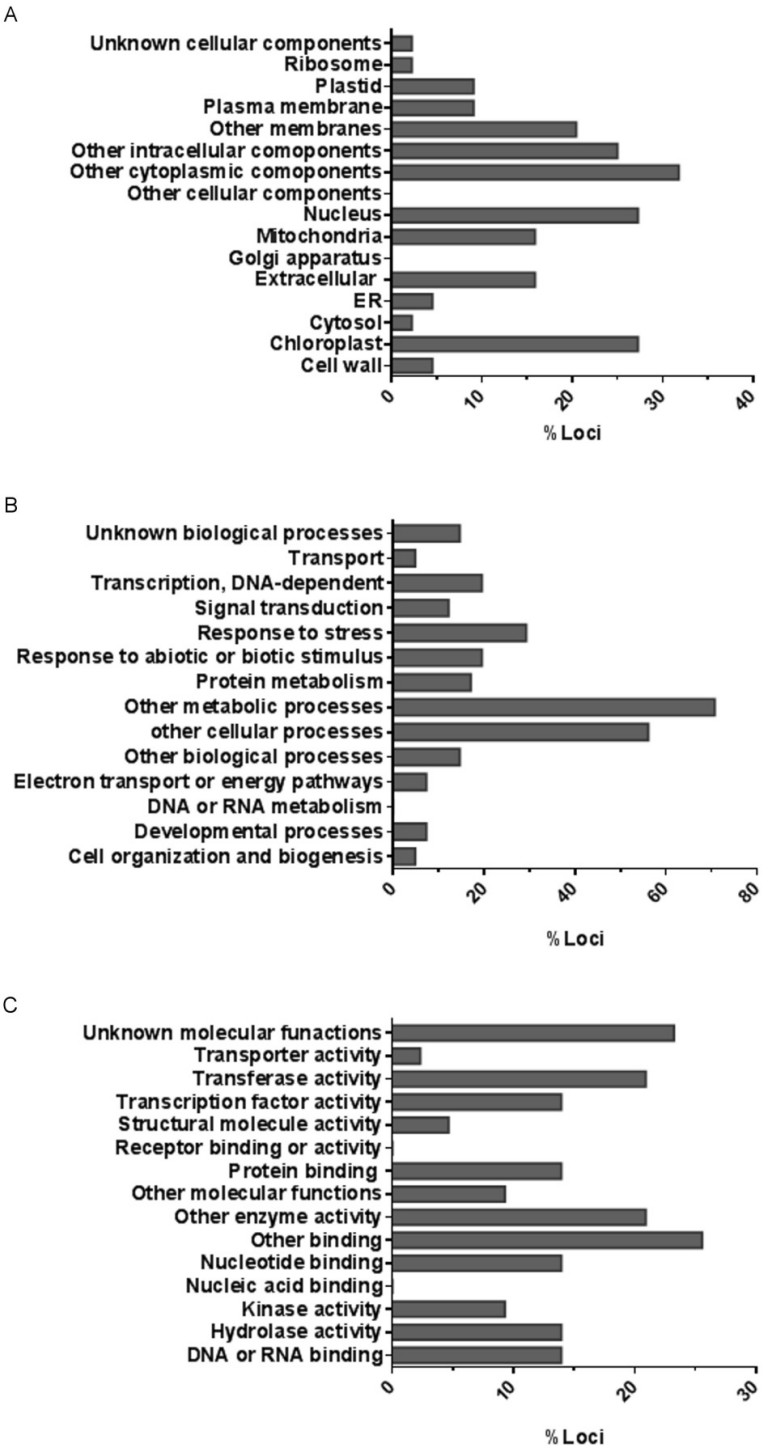

Figure 6.10 Functional classification by loci based on GO slim of the (A) cellular component, (B) biological processes and (C) molecular function in imbibed *vtc2-1* and *vtc2-4* seeds relative to Col-0.

6.2.3.2 Transcripts that were highly expressed in *vtc2-4* and *vtc2-1* imbibed seeds relative to Col-0

The transcripts whose levels were most decreased in the *vtc2-1* and *vtc2-4* mutants relative to Col-0 encode proteins associated with the photosynthetic electron transport chain. For example, *psbJ* encodes a photosystem II core protein. *psbJ* mutants show hypersensitivity to high light. In addition, petD encodes a subunit of the cytochrome b6-f complex.

The transcript (*CEP1*) whose abundance was most increased in the imbibed seeds of the *vtc2-1* and *vtc2-4* mutants is usually expressed only in flowers (Figure 6.11 A). *CEP1* encodes a papain-like cysteine protease that is involved in flower development regulating pollen fertility via PCD (Zhang et al 2014). The *cep1* mutants have impaired pollen development with abnormal pollen shape and number (Zhang et al 2014). Similarly, *CPK17* transcripts were greatly increased in the ascorbate-deficient mutants relative to Col-0. *CPK17* is also expressed in flowers and is involved in the development of the pollen tube (Myers et al 2009).

Transcripts encoding a peroxisomal ligase (*AAE12*) were increased in the imbibed seeds of the *vtc2-1* and *vtc2-4* mutants relative to Col-0 (Figure 6.11 B). Although the functions of AAE12 are not well characterised, it is considered to have a role in lipid and secondary metabolism (Hooks et al 2012). Other transcripts related to secondary metabolism are also increased in the imbibed seeds of the *vtc2-1* and *vtc2-4* mutants relative to Col-0. These include *CYP71B22,* which belongs to the CYP71 family (Figure 6.11 A). Although *CYP71B22* functions remain to be characterised, many of the proteins in the CYP71 gene family are involved in the biosynthesis of hormones such as GA, ABA, IAA, as well as in the synthesis of JA and SA and flavonoids (Liu et al 2010, Pfalz et al 2011). Transcripts encoding *FLAVIN-DEPENDENT OXIDOREDUCTASE* (*FOX3*), which has electron carrier activity were increased in the imbibed seeds of the *vtc2-*

1 and *vtc2-4* mutants relative to Col-0 in both mutants (Figure 6.11). Although *FOX3* is not well characterised, another *FOX* gene (*FOX1*) has been shown to be co-expressed with *CYP71A12* in response to pathogen attack (Rajniak et al 2015).

As in the case of dry seeds, the levels of several JA associated transcripts including *CORI3, JAZ5* and *JAZ8* were increased in the imbibed seeds of both mutants relative to Col-0 (Figure 6.11). *CORI3* encodes a cysteine lyase that mediates defence responses in *gulliver3-D*/*dwarf4-D* mutants (Kim et al 2013). The levels of *TIFY 5A* and *TIFY 11A* were increased in the imbibed seeds of both mutants relative to Col-0. These jasmonate ZIM-domain (JAZ) transcription factors repress growth and defence responses through a mechanism that involves direct binding of JA to repressors such as *NINJA* and *TOPLESS* (Pauwels et al 2010, Shyu et al 2012).

The levels of *ERF 109* (also called *REDOX RESPONSIVE TRANSCRIPTION FACTOR 1*) transcripts were also increased in the imbibed seeds of both mutants relative to Col-0 (Figure 6.11). The expression of this redox sensitive transcription factor, which contains an APETALA2 (AP2) domain, is induced by JA. This transcription factor regulates shoot and root development as well as plant defence responses through the propagation of ROS signals and regulation of redox homeostasis under stress (Matsuo et al 2015). The RRTF1 transcription factor also mediates cross talk between JA signalling and auxin biosynthesis in the regulation of the lateral root formation (Cai et al 2014). The levels of transcripts encoding another TF, NAC063 were increased in the imbibed seeds of both mutants relative to Col-0 (Figure 6.11). This transcription factor has been implicated in cell wall development and expansion but its precise function are not well characterised (Conklin et al 2013)

Similar to dry seeds, farnesoic acid carboxyl-O-methyltransferase (FAMT) transcripts were increased in both ascorbate-deficient mutants relative to Col-0 (Figure 6.11). This enzyme is thought to be involved in plant defences against insect attack (Yang et al 2006). Transcripts

encoding mitochondrial Complex I subunit NADH-ubiquinone oxidoreductase chain 1 (ND1) were also increased in both ascorbate-deficient mutants relative to Col-0 (Figure 6.11). The mitochondrial-encoded *ND1,* which was one of the 10 most increased transcripts in both ascorbate-deficient mutants (Figure 6.11), is a subunit of Complex I in the mitochondrial membrane respiratory chain, playing a major role in the transfer of electrons from NADH to the respiratory chain (Heazlewood et al 2003).

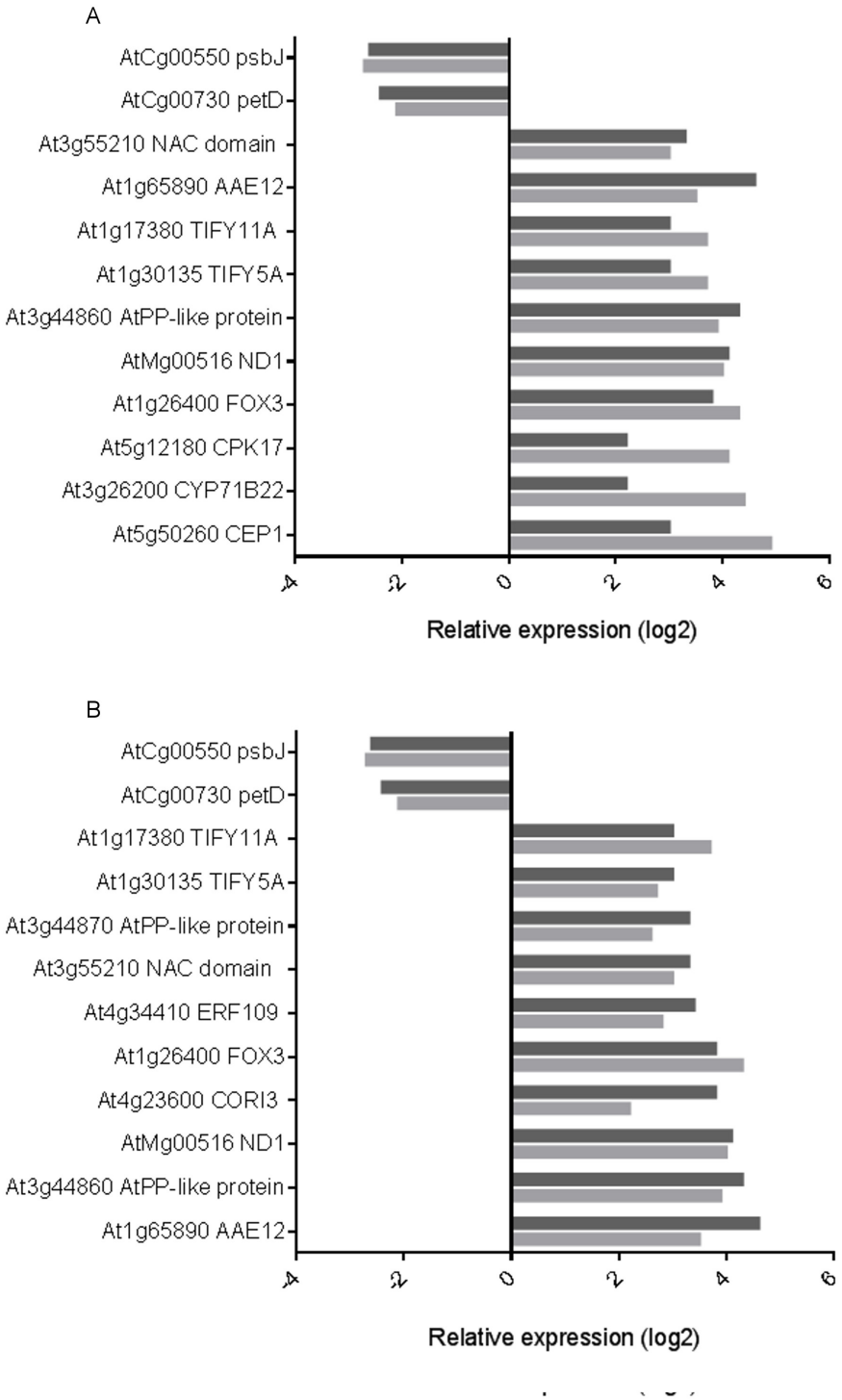

Figure 6.11 Most induced or repressed transcripts in the imbibed seeds of (A) *vtc2-1* and (B) *vtc2-4* mutants relative to Col-0.

In both cases the data for *vtc2-1* are shown as the lighter bars, while the data for the *vtc2-4* mutants are shown as the darker bars.

6.2.3.3 Redox associated transcripts

A number of transcripts associated with cellular redox homeostasis were also greatly increased in the imbibed seeds of the *vtc2-1* and *vtc2-4* mutants relative to Col-0 (Table 3). These include transcripts that encode the nuclear proteins FOX3, RRTF1 and CYP71B22, and the mitochondria-localised ND1 (Table 11). Like ND1, NADH dehydrogenase (ND2) forms part of the hydrophobic core of the membrane arm of Complex I that transfers electrons from NADH to ubiquinone in the respiratory electron transport chain. Transcripts encoding ND2 were also increased in the imbibed seeds of the ascorbate-deficient mutants suggesting that low ascorbate has a strong effect on genes encoding the mitochondrial membrane respiratory chain NADH dehydrogenase (Table 11). This might be important because the enzyme L-galactono-1,4-lactone dehydrogenase (GLDH), which catalyses the last step of ascorbate biosynthesis, is bound to CI (Pineau et al 2008). Moreover, *gldh* mutants are deficient in CI, indicating that this enzyme is essential for CI assembly (Pineau et al 2008).

Table 11 Differentially regulated redox associated transcripts.

Accession	Description	LogFC	
		vtc2-1	***vtc2-4***
AtMg00516	NADH-ubiquinone oxidoreductase chain 1 ND1	4	4.1
AtMg00285	NADH-ubiquinone oxidoreductase chain 2 ND2	2.2	2.7
At1g26400	FAD-binding Berberine family protein FOX3	4.3	3.8
At3g26200	CYP450 71B22	4.4	2.2
At4g34410	Ethylene-responsive transcription factor ERF109, RRTF1	2.8	3.4
At1g70680	Probable peroxygenase 5	2.1	2.3
AtCg00730	Cytochrome b6-f complex subunit 4 petD	-2.1	-2.4
AtCg00550	Photosystem II reaction center protein J psbJ	-2.7	-2.6

6.2.3.4 Transcription factors

As discussed above, a number of transcripts encoding transcription factors were greatly increased in the imbibed seeds of the *vtc2-1* and *vtc2-4* mutants relative to Col-0 (Table 3). These include WRKY40, FAMT, RRTF1, TIFY 5A and TIFY 11A as well as 2 AtPP like proteins (Table 12). As already discussed, the TIFY 5A and TIFY 11A proteins function as repressors of jasmonate responses in response to abiotic and biotic stresses (Fonseca et al 2009). WKRY40 is required for the regulation of responses to both biotic and abiotic stresses, it functions antagonistically to WRKY60. WRKY60 and inhibits seed germination and root development. WKRY40 is a positive regulator of ABA sensitivity. The ABA-mediated induction of WRKY60 is abolished in *wrky40* mutants suggesting that WKRY40 acts as a regulator for WRKY60 (Chen et al 2010).

Table 12 Transcription factors.

Accession	Description	LogFC	
		vtc2-1	*vtc2-4*
At3g44860	AtPP-like protein, methyltrnasferase FAMT	3.9	4.3
At4g34410	Ethylene-responsive transcription factor ERF109	2.8	3.4
At3g55210	NAC domain containing protein 63	3.0	3.3
At1g30135	Repressor of jasmonate responses, negative regulation of nucleic acid-templated transcription TIFY 5A	3.7	3
At1g17380	TIFY 11A JASMONATE-ZIM-DOMAIN PROTEIN 5, JAZ5	2.2	2.8
At1g80840	WRKY transcription factor 40 Pathogen-induced transcription factor.	2.1	2.3
At3g44870	AtPP-like protein, methyltrnasferase	2.6	3.3

6.3 Discussion

The data presented in chapters 3 and 5 showed that the nuclei and cytosol of the proliferating cells in the root apical meristem were more oxidized in the low ascorbate *vtc2-1* mutants than in Col-0. Moreover, the ability of the nuclei to gain mass in G1 was changed in *vtc2-1* root apical meristem and the progression through the cell cycle was slower than in the wild type.

The transcript profiling studies presented in this chapter focused largely on transcripts that were differentially changed in both the *vtc2-1* mutant and *vtc2-4* mutants relative to the wild type to ensure that the observed effects were due to low ascorbate and not to other genes that might have been altered in either of the mutants. While the germination rates of the *vtc2-1* mutant and *vtc2-4* seeds were similar to Col-0, the transcriptome profiles of dry seeds of the low ascorbate mutants was very different to that of the wild type. This is surprising but it reflects the redox state of the cells in the mother plants during seed production. Moreover, transcripts present in the dry seeds are critical to the processes occurring during imbibition and the transition from the quiescent to the metabolically active state. Also interesting is the observation that the levels of many more transcripts were altered as a result of low ascorbate in the dry seeds than the imbibed seeds. The number of differentially regulated transcripts was 10 times higher in the dry seeds (Figure 6.3) than the imbibed seeds (Figure 6.9) of the *vtc2-1* and *vtc2-4* mutants relative to the wild type.

The transcripts synthesised during seed development on the mother plant are stored in dry seeds, ready to be engaged at the early stages of seed development as water is imbibed. The dry seeds of the *vtc2-1* and *vtc2-4* mutants are rich in transcripts that encode proteins associated with redox processes, jasmonate and salicylic acid-dependent pathways of plant defence and the cell cycle but decreased in transcripts related to secondary metabolism. For example, MYB56, which encodes a seed-specific protein that regulates cell division and

expansion as well seed size was highly expressed in dry seeds with low ascorbate. Similarly, transcripts encoding cell division regulative proteins, CDC7 and CDKB1;2 were also highly expressed in both mutants relative to Col-0. Since the expression of CDC7 occurs early in the G1/S transition (Jares et al 2000) and CDKB1;2 is associated to the regulation of the G2/M transition, it would appear that the low ascorbate mutants already have high levels of transcripts that can initiate the cell cycle once hydration occurs. These findings also suggest that the low ascorbate environment of the mother plant leads to a significant rearrangement in the transcriptome to prepare the seed for prompt initiation of high cell division rates once the cells return to the metabolically active state. Moreover, the high abundance of *GSTU8* and *GSTU12* transcripts in the low ascorbate mutants suggests that these proteins might have an important role in nuclear processes upon imbibition. GSTU8 and GSTU12 are localised in the nucleus, both have peroxidase functions and are associated with cell signalling. They are highly expressed in plants subjected to oxidative stress suggesting a role in protection of the nucleus from oxidation.

No changes in transcripts involved in ascorbate biosynthesis were observed in the dry seeds of either of the *vtc2* mutants. This is consistent with previous studies, which have shown that there is little or no ascorbate in dry seeds. Ascorbate synthesis and the expression of enzymes associated with the regeneration of ascorbate such as DHAR activity starts only following imbibition and upon germination (Arrigoni 1994).

In contrast to the dry seeds, the imbibed seeds of the *vtc2-1* and *vtc2-4* mutants did not show differential regulation of transcripts associated with the cell cycle or glutathione metabolism. The marked differences in the low ascorbate signatures of the dry and imbibed seeds means that there is either rapid turnover degradation of transcripts upon the transition to the metabolically active state that prevents an early onset of the cell cycle in the low ascorbate mutants. However, the imbibed seeds of the low ascorbate mutants had higher levels of transcripts

encoding core subunits of mitochondrial Complex I and transcripts involved in jasmonate signalling. The increase in mitochondrial Complex I associated transcripts might be related to the function of the mitochondrial electron transport chain in ascorbate synthesis in particular the association of galactono-lactone dehydrogenase with Complex I (Miller et al., 2003). The increase in transcripts associated with jasmonate signalling in imbibed seeds is interesting because these transcripts tend to be repressed in ascorbate deficient leaves (Kerchev et al 2011). Relatively few transcripts associated with the signalling of hormones other than jasmonate were differentially expressed in the imbibed seeds of the low ascorbate mutants. Despite a marked increase in the accumulation of transcripts encoding *WRKY40*, which is a positive regulator of ABA sensitivity, the germination rates were the same in all genotypes. Hence, the expression of transcripts involved in the signalling of hormones that regulate seed germination is not influenced by low ascorbate, at least in a way that alters seed germination (Figure 6.12).

Taken together, the transcriptome data obtained from dry and imbibed seeds of *vtc2-1* and *vtc2-4* mutant lines reported here suggest that low ascorbate content in the mother plant leads to large changes in transcripts associated to cell cycle and stress responses when compared to wild type. In contrast, the germination percentage is unaffected by low ascorbate (Figure 6.12.), a finding that is consistent with the absence of ascorbate in dry seeds. However, further studies are required to determine the role of ascorbate on the break of dormancy and germination rate.

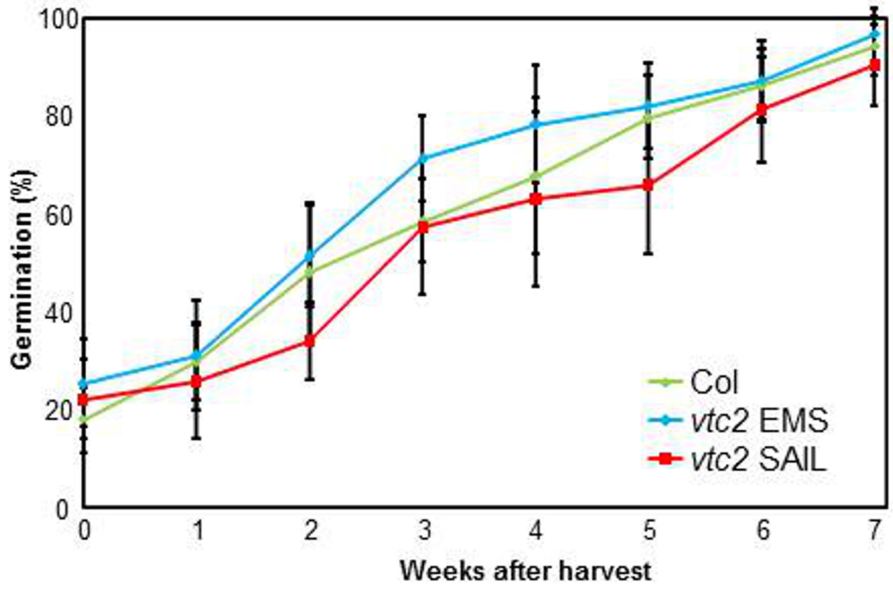

Figure 6.12 Comparison of the germination rate of Col-0 (green), *vtc2-1* (blue) and *vtc2-4* (red).

Germination test was performed each week for 7 weeks after harvest by Dr Wim Soppe at the Max Planck Institute for Plant Breeding Research in Cologne, Germany.

Chapter 7. General discussion

Seeds are plant reproductive organs that ensure plant survival. They connect the end of one generation to the beginning of next, seed germination being the beginning of a new life cycle, in which the emerging plant has to be equipped with all the genomic information required for survival. Seeds are also the basis of much of the life on earth, being an essential part of food supply for animals and in the human diet. Seeds are also used for many other processes such as oil production. High quality seeds are not only essential for human food and animal needs, but also for plant propagation and breeding, underpinning food and protein security worldwide. Germplasm preservation relies on the availability of high quality seeds, capable of withstanding environmental pressures and climate change. Seed development and maturation start on the flowering mother plant. Hence, environmental stresses such as drought and high temperatures, which are experienced by the mother plant during seed set, are likely to have an impact on the seed. Maternal processes alter seed gene expression, particularly during dormancy and germination (Donohue & Schmitt 1998). In addition, the synthesis of nutrients and hormones by the mother plant during seed development has a profound impact on dormancy and germination (Finch-Savage & Leubner-Metzger 2006, Holdsworth et al 2008). However, the ways in which maternal stresses affect seed properties particularly seed quality are poorly understood. Understanding how the stresses experienced during seed production alter seed quality and germination, as well as the survival of the seedlings is therefore crucial in order to improve seed quality traits and avoid economic losses.

The transition from seed dormancy to germination, which is regulated by external factors and internal stimuli, is crucial to seed quality and development. Hormones such as ABA and gibberellic acid play a key role in this transition. ABA, which is required for dormancy maintenance, is synthesised during seed development on the mother

plant. ABA gradually degrades during seed storage in the dry state leading to after-ripening and loss of dormancy. This phytohormone inhibits the accumulation of *DELAY OF GERMINATION 1* (*DOG1*), which in turns requires ABA to maintain dormancy (Holdsworth et al 2008). Similar to ABA insensitive mutants, *dog1* mutants lack dormancy (Bentsink et al 2006). The *DOG1* promoter contains motifs required for seed-specific gene expression and for ABA responses (Bentsink et al 2006). *DOG1* expression is highest during seed development, high *DOG1* transcript levels persisting during dry seed storage, but then disappearing upon imbibition.

Plant perception of environmental stresses generally involves enhanced oxidation leading to changes in cellular redox state that trigger redox signalling pathways that alter plant growth and defence. In dry seeds however, which are in a metabolically inactive state, enhanced oxidation has only a limited capacity to influence gene expression and is hence usually linked to loss of seed quality rather than acclimation to stress. While many studies have focused on enhanced oxidation as a regulator of seed quality, very few have used plants with low antioxidant capacity to study effects on seed production, quality or germination. In the present study, the effects of low ascorbate, a major plant antioxidant, on seed quality (i.e. germination), the transcript profiles of dry and imbibed seeds, and the regulation of the cell cycle in the proliferating cells of the emerging radical were determined by comparisons of these parameters in the *vtc2-1* and *vtc2-4* mutants to the wild type. While dry seeds have little or no ascorbate, *APX6* plays an important role in seed vigour and stress tolerance, particularly in the dry state (Chen et al 2014). *APX6* activity is involved with ABA signalling, in particular the induction of *ABI4* transcription in the control of seed dormancy (Chen et al 2014).

Taken together, the studies reported in this thesis report several novel findings regarding the role of cellular redox processes in the control of the cell cycle and seed germination. These can be summarised as follows:

- The nuclei and cytosol of proliferating cells in the Arabidopsis root apical meristem are in a highly reduced state (-297.5 mV ± 0.7 and -292.8 mV ± 0.6). However, a transient oxidation of about 15 mV occurred in both compartments in G1 (to values of -286.4 mV ± 0.8 in the nuclei and -280 mV ± 0.6 in the cytosol), in roots where the cell cycle had been synchronised using hydroxyurea.
- Low antioxidant buffering capacity in the ascorbate-deficient mutants results in a stable higher cellular oxidation state in both the nuclei (282.3 mV ± 0.5) and cytosol (282.9 mV ± 0.5) of the proliferating cells in the root apical meristem. A sustained oxidation in the nuclei and cytosol (of only about 15 mV) leads to alterations in nuclear size and cell cycle marker gene expression in roots where the cell cycle has been synchronised using hydroxyurea.
- Low antioxidant buffering capacity in the ascorbate-deficient mutants has a marked effect on the dry seed transcript profile, with increased expression of redox-related and cell cycle marker genes. Since it is generally accepted that ascorbate levels are very low in dry seeds, these data suggest that this antioxidant still plays an important role in the redox control of gene expression.

7.1 Dynamic changes in glutathione redox potential occur during cell division in the root apical meristem

Determination of the redox state of a cell is far to be trivial. While there are currently few probes that can be used to make accurate measurements of this important parameter, redox sensitive probes that provide an estimate of the glutathione redox potential in specific cell compartments such as roYFP and roGFP have been developed and widely used. For example, roGFP1 targeted to the mitochondria of HeLa cells showed that the mitochondrial matrix is highly reduced, with a glutathione redox potential of about -360 mV (Hanson et al 2004). Moreover, expression of roGFP1 in brain cells was used to elucidate the redox communication between the mitochondria and cytosol of mice neurons (Wagener et al 2016). Studies in plat cells have shown that the cytosolic glutathione pool is much more highly reduced than can be estimated from measurements of GSH/GSSG ratios in cell extracts (Noctor et al 2012). In agreement with previous observations, the measurements of the glutathione redox potential reported here for the cytosol of proliferating cells in the Arabidopsis root apical meristem show that the cytosol is highly reduced (-292.8 mV ± 0.6). Studies in yeast using rxYFP reported similar (-291 mV) values (Dardalhon et al 2012). These authors showed that the glutathione redox potentials of the nuclei and cytosol were similar under most conditions measured. This was also the case for the glutathione redox potentials of the nuclei and cytosol measured in plant cells. It was only possible to demonstrate the transient oxidation that occurred in both compartments in G1 by synchronisation of the cell cycle with hydroxyurea.

An oxidative event is required at G1 for animal fibroblast cells to enter into the S phase of the cell cycle; this process involves oxidative activation of *CYCLIN D1* expression (Menon et al 2003). The redox regulation of cell cycle proteins in the fibroblasts has been known for a number of years (Conour et al 2004). In this system, GSH contents oscillate during the cell cycle, with lowest levels at G1. GSH levels then

increased though S phase with the highest levels at the G2/M phase (Conour et al 2004). Similarly, the GSH content of proliferating Arabidopsis cells in culture increases gradually until cell division when the GSH is re-distributed to the daughter cells (Pellny et al 2009). Most of the redox sensitive proteins associated to cell cycle regulation in Chinese hamster fibroblasts were found at G2/M (Conour et al 2004). Relatively few studies have been performed in intact tissues because of lack of synchronisation of the cell cycle in animal tissues organs. Similarly, there is little or no synchronisation in the proliferating cells of plants. The data presented here show that redox changes occur during cell cycle in plants as they do in animals. However, while the basic principles of cell cycle regulation are similar in animal and plants, the components such as cyclins, CDK s and other factors involved are very different.

Consistent with the data in animal cells, measurements of roGFP2 fluorescence in synchronised Arabidopsis roots show a significant increase of oxidation in the G1 phase. However, this oxidation is transient and is rapidly followed by a re-reduction that appears to be concomitant with entry into the S phase of the cell cycle (Chapter 3). While the mechanisms of redox regulation of the cell cycle in plants still have to be determined, it is like that they involve proteins such as thioredoxins, GRX, GSTs and nucleoredoxins. It is important to remember that changes in the glutathione redox potentials are only used as an indicator or marker of the wider redox changes occurring in the cytosol and nuclei of proliferating cells. Hence, the redox regulation of the cell cycle may not directly involve the GSH or GSH/GSSG ratios. However, if GSH is involved in cell cycle regulation it is likely to occur via intermediates such as GRX, GSTs or peroxiredoxins or through protein glutathionylation. For example, in animals, a reversible glutathionylation of Cys269 in the DNA binding site of the c-Jun transcription factor is important in cell cycle regulation. Together with Fos, Jun is part of the AP-1 transcription factor complex, which regulates the expression of genes associated with cell proliferation and

apoptosis (Klatt et al 1999). In addition, glutathionylation of HISTONE 3 (H3) has been suggested to regulate gene expression and the replication machinery in fibroblasts (Garcia-Gimenez et al 2014). Furthermore, glutathionylation of the 20S proteasome in yeast modulates the response to oxidative stress, including the degradation of cell cycle-related proteins (Demasi et al 2014). While glutathionylation of chloroplast and cytosolic proteins such as the glyceraldehyde 3-phosphate dehydrogenases has been reported in plants, no proteins associated with cell cycle regulation have as yet been reported to be glutathionylated. However, a number of proteins associated with cell cycle regulation are putative thioredoxin targets (Montrichard et al 2009) and are hence likely to also be sensitive to glutathionylation. Moreover, the data presented here show that cell cycle progression is altered in cells with low antioxidant buffering capacity (i.e. ascorbate), suggesting that the cell cycle is subject to redox regulation, as discussed below.

7.2 Cell cycle regulation is altered in plants with low ascorbate

Literature evidence supports a role for ascorbate in the regulation of the cell cycle in animals and plants. While mild oxidation is required for cell cycle operation excessive oxidation leads to an inhibition of the cell cycle in animals and plants. However, very few studies have focussed on redox regulation of the cell cycle in plants, particularly in recent years. The accumulation of ascorbate in proliferating Arabidopsis cells in culture follows a different pattern from that of GSH (Pellny et al 2009). Ascorbate levels are very high at the early phases of growth, while GSH levels are low (Pellny et al 2009). Moreover, the addition of ascorbate promoted cell division in tobacco BY-2 cells, while the addition of DHA decreased the mitotic index (Kato & Esaka 1999). Changes in the uptake of DHA and ascorbate have been observed during the different phases of growth in tobacco BY-2 cells in culture, such that DHA uptake was maximal during the exponential growth phase, being maximal at the M phase and M/G1 transition (Horemans et al 2003). The addition of GSH did not prevent the DHA-dependent delay cell cycle progression in synchronised BY-2 cells (Potters et al

2004). Taken together, these data suggest that ascorbate and GSH fulfil different roles in the cell cycle and that these antioxidants act largely independently of each other in their functions during the cell cycle.

The addition of DHA led to a shortening of the G1 phase in QC cells in maize roots (Decabo et al 1993). The activity of ascorbate oxidase, which catalyses the breakdown of ascorbate, is high in QC cells, leading to the hypothesis that low ascorbate and high oxidation states are required to maintain stem cells in the G1 phase (Kerk & Feldman 1995, Kerk et al 2000). While the addition of ascorbate will stimulate the cell cycle in competent cells, it was not able to re-start the cell cycle in non-competent cells (Crichton et al 1978). Taken together, these data show that ascorbate levels change during cell proliferation and that high ascorbate/DHA ratios are required for cell cycle progression in plant cells, the roles of ascorbate in the cell cycle are far from clear. The data presented here show that mutants with impaired ascorbate synthesis have low levels of ascorbate in their leaves and they show altered patterns of vegetative growth to the wild type. However, seed germination rates and the growth of the emerging radicles are similar in the low ascorbate mutants and the wild type. These data show that low ascorbate accumulation alone does not impair seed germination or seedling growth relative to the wild type. However, the proliferation zones of the root apical meristems of the low ascorbate mutants has fewer cells than the wild type. This was the first indication that cell division was impaired in the low ascorbate mutants relative to the wild type. A closer investigation showed that the nuclei in the cells in the proliferation zone of the *vtc2-1* roots did not show the same increases in size during the cell cycle as those of the wild type suggesting that high ascorbate levels are required to facilitate the changes in nuclear size that occur during G1 and S. The relationship between nuclear volume and the cell cycle is far from understood. Cell cycle progression is coupled to cell growth at the transition from the G1 to S-phases of the cell cycle. In budding yeast, cyclin Cln3, which complexes with the

cyclin-dependent kinase Cdk1 to activate Start by phosphorylating and thereby inactivating the Start repressor Whi5, is considered to act as a reporter of cell size (De Bruin et al 2004).

While it is generally accepted that cells do not commit to division until they have grown to a certain critical size, the mechanisms that underpin size control remain poorly understood. Similarly, it is not known how the volume of the cell nucleus is set, nor how the ratio of nuclear volume to cell volume is determined. It has been proposed that the cell can measure the volume of the cytoplasm relative to the nucleus in such a way that cell division is triggered when the cytoplasm has a sufficient size (Csikasz-Nagy et al 2006). However, the volume of nucleus is not constant and increases during the G1 phase. If we assume that it is the increase in nuclear size that triggers the G1 to S transition, as suggested for S-phase entry in mammalian cells (Yen & Pardee 1979), then it would appear that low ascorbate has a profound effect on the ability of the nuclei to increase in size and hence pass through G1 to S. The size of the nuclei in the roots with low ascorbate is only the same as that of the wild type at the later stages of cell proliferation. The nuclei of the ascorbate-deficient roots are smaller throughout G1, the only increase in size occurring transiently at 10 h, in contrast to a much longer period in the wild type. If the size of the nucleus is set directly by the physical bulk of the chromatin, then the DNA content must only increase in a transient manner in the ascorbate-deficient mutants.

The expression of markers is crucial to understanding cell cycle progression in the presence of hydroxyurea, which was used to synchronize cell division in root apical meristem (Figure 7.1). The expression of the G1/S phase marker CYCA3.1 was significantly lower in the proliferating cells of the low ascorbate roots than the wild type 5 and 10 hours after the onset of hydroxyurea treatment suggesting that G1 was delayed in cells with low ascorbate. However, the S and S/G2 markers were more highly expressed in the low ascorbate mutants than the wild type at later stages on the treatment, suggesting that S and S/G2 phases occur later in the low ascorbate roots than the wild type.

Taken together, these data suggest that a sustained change in redox potential of about -15 mV is sufficient to have a major effect on the nuclei, such that cell progression is delayed relative to the wild type. However, the increase in cellular oxidation is not sufficient to cause an arrest in the cell cycle in the *vtc2-1* mutants (Figure 5.11) just delay it. It is perhaps worthy of note that the nuclei and cytosol of the *vtc2-1* mutants were much more oxidised in the S and S/G2 phases than the wild type (Figure 5.11) The transient oxidation observed in the nuclei and cytosol of the wild type roots was absent from the low ascorbate mutants.

7.3 Low ascorbate alters the transcript profile of dry seeds

The data presented here suggests that the redox state of the cells in the root apical meristem that is protected against prolonged oxidation by antioxidants such as ascorbate exerts a strong influence on progression through the cell cycle. However, little is known about the mechanisms involved in the redox regulation of the cell cycle or how the altered cellular redox state observed in the low ascorbate mutants influences gene expression. While there has been extensive characterisation of the effects of low ascorbate on the leaf transcript profiles (Pavet et al 2005), there have been no studies on the effects of low ascorbate on seed development or seed transcript profiles.

The dry seeds contain the transcripts that were produced during seed development on the mother plant. It is generally accepted that the environmental conditions experienced by the mother plant can influence seed quality and vigour, in part due to the transcript profile of the dry seeds. Ascorbate is present in the developing embryos early in seed development but the ascorbate pool becomes progressively oxidised as the embryo develops, so that only DHA predominates in the mature embryo (Tommasi et al 2001). Environmental stresses increase the level of oxidation experienced during seed production on the mother plant. Assuming that low ascorbate can mimic this increase in oxidation by limiting the capacity to buffer ROS accumulation, the low ascorbate

mutants can be used as a model for processes that might occur in such situations. The increased oxidation observed in the low ascorbate mutants might therefore trigger similar signalling responses and changes in transcript abundance to those occurring in the seeds of plants exposed to environmental stresses. Transcripts stored in the dry seeds are essential to the success of germination following imbibition.

The levels of ascorbate in the developing seed have been linked to polyembryony and polycotyly (Chen & Gallie 2012). Overexpression of DHAR expression in tobacco led to increased monozygotic twinning, the twin progeny in the seeds being genetically identical. However, while the ascorbate level in the developing seed affects this first zygotic division, it does not induce a premature initiation of this division prior to the correct positioning of the plane of cell division (Chen & Gallie 2012). The studies described here indicate that regardless of the effects of ascorbate on these processes, seed viability and germination are unaffected by the ability to synthesis or accumulate ascorbate. Moreover, the transcriptome profiles of the dry seed indicated that while low ascorbate had a large effect on the seed transcriptome profile, relative few of the transcripts that were changed in abundance in the low ascorbate mutants were related to hormone-mediated processes that might impact on germination. However, several transcription factors of the MYB, bHLH and AUX/IAA families, which are associated with ABA-sensitivity, cell division and secondary metabolism were highly expressed in the ascorbate-deficient seeds. For example, the levels of *MYB28* and *WRKY40* transcripts, which are related to changes in sensitivity to ABA (Figure 6.6) were increased in the low ascorbate seeds, as were the transcripts encoding CYP71B29, which is involved in ABA synthesis (Figure 6.6). Transcripts encoding nuclear proteins that directly involved in the regulation of cell cycle progression such as *CDKB1;2* and *CDC7* were greatly increased in the low ascorbate seeds. The functions of these transcripts in the processes that occur during seed imbibition are unknown but it is possible that these proteins are

translated early in seed germination to stimulate the G2/M and G1/S transitions. However, the levels of *CDKB1;2* and *CDC7* transcripts were similar in the imbibed seeds of all genotypes.

The large increase in the levels of transcripts encoding the nuclear GSTs, *GSTU8* and *GSTU12* in the dry seeds of both *vtc2-1* and *vtc2-4* suggests that these proteins are important in maintaining key redox functions in the nuclei (Table 9). The increases in these transcripts together with transcripts involved in cell cycle regulation in the dry of the *vtc2-1* and *vtc2-4* mutants, might suggest a co-ordination of the pathways that involve these components. However, further work is required to identify whether any functional relationships exist between the GSTU8/ GSTU12 and CDKB1;2 and CDC7 proteins.

7.4 Perspectives and future work

The findings discussed in this thesis provide a firm foundation for future studies. Possible lines of future work include further studies on the *vtc2-1* and *vtc2-4*:

1. Crossing *vtc2-4* with roGFP2 to confirm the redox changes obtained for *vtc2-1* mutants. Both low ascorbate mutant lines show impaired cell cycle progression and growth. Establishing whether *vtc2-1* and *vtc2-4* show similar redox patterns will confirm the role of ascorbate on cell regulation. Moreover, synchronization treatment with hydroxyurea of the *vtc2-4* roGFP2 cross line will solidify the role of ascorbate in cell cycle regulation.
2. Characterization of seed properties in ascorbate-deficient mutants. Seed size and weight are crucial traits for plant establishment and seed yields. Preliminary data in our lab bring up evidence of altered seed size in *vtc2-1* and *vtc2-4* mutants. Phenotype measurements of low ascorbate mutant seeds such as seed size and weight might provide prospects for seed production improvement.
3. Measurements of cell number and cell size in *vtc2-1* and *vtc2-4* mutants. The nuclei of *vtc2-1* line are not able to sustain nuclear

growth size during synchronization treatments. Although these mutants have altered cell cycle progression, cell division is not stopped. Investigating whether ascorbate alters the nucleus/cytoplasm ratio and the overall cell size cells will elucidate the mechanisms of cell size modulation and cell cycle progression regulation imposed by ascorbate.

In addition to the studies on ascorbate-deficient mutants, further work will cover:

4. Confirmation of the differential expression of GSTU8 and GSTU12 by qRT-PCR. RNAseq analysis has brought evidence that the nuclear GSTU8, GSTU12 are related to cell cycle regulation in the ascorbate-deficient mutants. However, before performing further experiments the differential accumulation of the transcripts levels of GSTU8 and GSTU12 needs to be confirmed using primers specific to these target genes.
5. Once this is confirmed, availability of either transposon or T-DNA insertion *gstu8* and *gstu2* mutants can be checked. *gstu8* and *gstu2* mutants will be obtained and characterised. Moreover, expression studies of cell cycle regulators will allow the evaluation of the GSTU8 and GSTU12 target protein.
6. Proteomic analysis of the CDKB1;2 and CDC7 proteins to explore whether the sequences of the CDKB1;2 and CDC7 proteins contain redox sensitive cysteines, which can be target of redox regulation. These experiments would provide more in depth knowledge of the redox control of specific cell cycle phases.
7. Obtain the DHAR expressing tobacco plants or similar transformed plants with altered levels of ascorbate-recycling enzymes. Coupling biochemical assay to measure the changes in ascorbate and glutathione content will be performed together with cell cycle synchronization in plants overexpressing DHAR will be also a possible path to follow in the examination of the cell cycle regulation by ascorbate.

8. Characterise mutants impaired in vernalisation process. Vernalisation pathways play an important role in response to changes in temperature during flowering and share common signalling mechanisms to dormancy and germination. During the course of my studies I selected several vernalisation mutants. Among them there are mutants for *SHORT VEGETATIVE PHASE* (*SVP*) and *FLOWERING LOCUS T* (*FT*). Expressing roGFP2 in vernalisation mutants could help elucidating how stresses experienced by the mother plant are inherited by seeds. Stress treatments such as drought and high temperature will be performed on the mother plant during seed development and changes in the redox state of the next generation seeds will allow the improvement of quality traits, particularly dormancy and germination.
9. Epigenetic studies on histone modifications. Experiments involving treatment with glutathionylation inducers and other histones modification such as carbonylation and polyADP ribosylation, will give an insight on the role of the redox regulation in epigenetics and the involvement of glutathione in chromatin structure modification.
10. Further transcriptomic analysis to associate a set of TF with known modification to the transcriptomic data that were accumulated here. DNA affinity purification sequencing (DAP-seq) identified a whole set of TF binding site and the relative chemical modification allowing to predict an entire set of enriched transcripts (O'Malley et al 2016). Associating differentially expressed TF transcripts with known modification to transcripts, which are differentially expressed in the ascorbate-deficient mutants will give precious information concerning the complex pathways in which selected transcripts are involved.

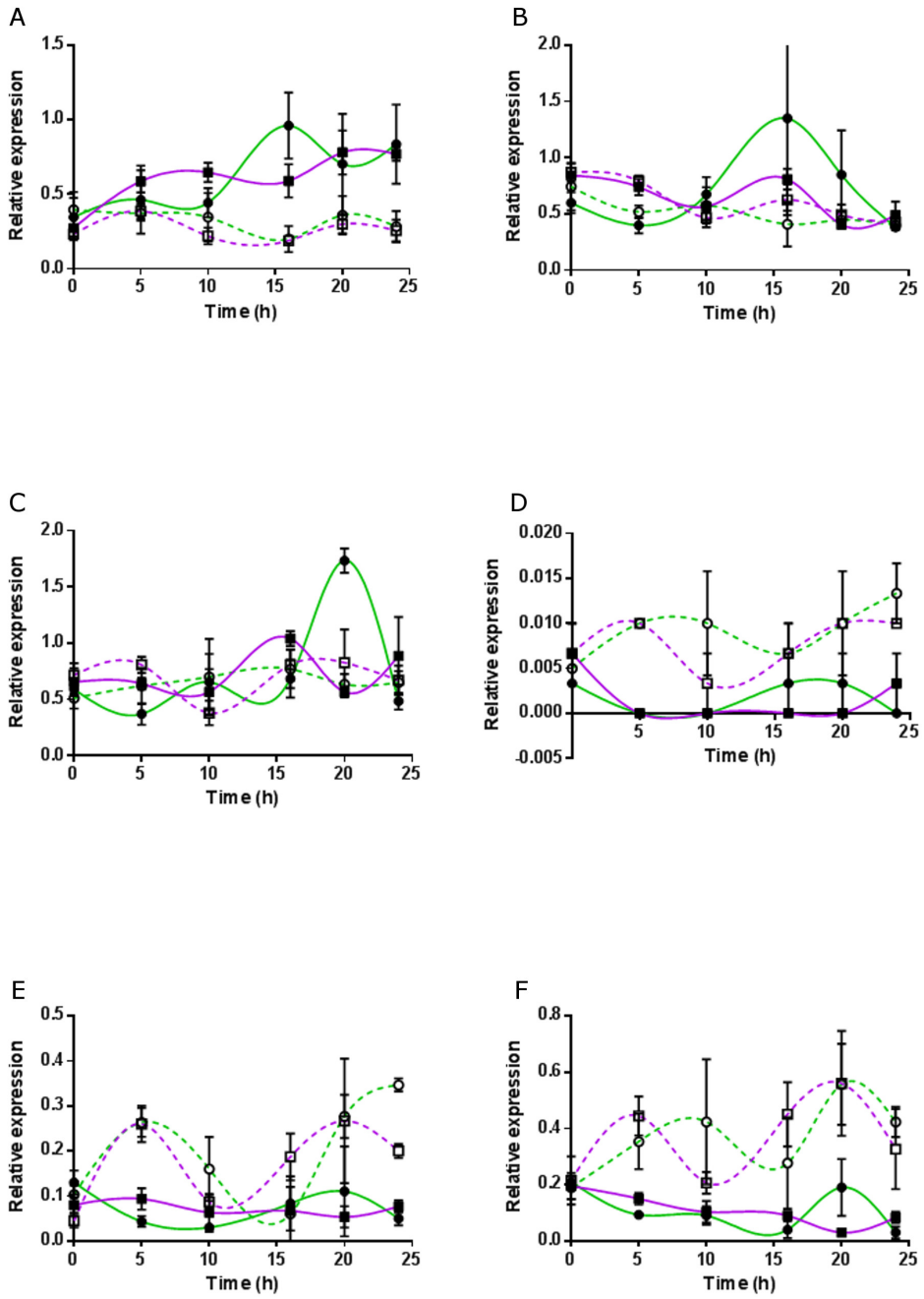

Figure 7.1 The relative expression of selected cell cycle markers of Col-0 (purple) and *vtc2*-roGFP2 radicals (green) synchronised for 24 hours in presence of HU (closed symbols) relative to controls in the absence of HU (open symbols).

Transcripts measured were: (A) G1/S cell cycle marker *CYCA3.1*, (B and C) S phase cell cycle markers *CYCD5.1* and *CYCD3.1* respectively, (D, E and F) G2/M markers *CYCB2.1*, *CYCA1.1* and *CYCB1.1* respectively**.**

Chapter 8. References

Agius F, Gonzalez-Lamothe R, Caballero JL, Munoz-Blanco J, Botella MA, Valpuesta V. 2003. Engineering increased vitamin C levels in plants by overexpression of a D-galacturonic acid reductase. *Nat Biotechnol* 21: 177-81

Alkhalfioui F, Renard M, Vensel WH, Wong J, Tanaka CK, et al. 2007. Thioredoxin-linked proteins are reduced during germination of Medicago truncatula seeds. *Plant Physiol* 144: 1559-79

Arrigoni O. 1994. Ascorbate System in Plant Development. *J Bioenerg Biomembr* 26: 407-19

Azumi Y, Liu D, Zhao D, Li W, Wang G, et al. 2002. Homolog interaction during meiotic prophase I in Arabidopsis requires the SOLO DANCERS gene encoding a novel cyclin-like protein. *EMBO J* 21: 3081-95

Bac-Molenaar JA, Fradin EF, Rienstra JA, Vreugdenhil D, Keurentjes JJ. 2015. GWA Mapping of Anthocyanin Accumulation Reveals Balancing Selection of MYB90 in Arabidopsis thaliana. *Plos One* 10: e0143212

Bailly C. 2004. Active oxygen species and antioxidants in seed biology. *Seed Science Research* 14: 93-107

Bailly C, Audigier C, Ladonne F, Wagner MH, Coste F, et al. 2001. Changes in oligosaccharide content and antioxidant enzyme activities in developing bean seeds as related to acquisition of drying tolerance and seed quality. *J Exp Bot* 52: 701-08

Barboule N, Demeter K, Benmeradi N, Larminat F. 2009. Bcl-2 is an integral component of mitotic chromosomes. *Cell Biol Int* 33: 572-7

Barroco RM, Van Poucke K, Bergervoet JHW, De Veylder L, Groot SPC, et al. 2005. The role of the cell cycle machinery in resumption of postembryonic development. *Plant Physiol* 137: 127-40

Bartoli CG, Gomez F, Fernandez L, Foyer CH. 2004. Regulation of ascorbic acid synthesis in plants. *Free Radical Bio Med* 36: S127-S27

Bartoli CG, Guiamet JJ, Kiddle G, Pastori GM, Di Cagno R, et al. 2005. Ascorbate content of wheat leaves is not determined by maximal L-galactono-1,4-lactone dehydrogenase (GalLDH) activity under drought stress. *Plant Cell Environ* 28: 1073-81

Bartoli CG, Yu JP, Gomez F, Fernandez L, McIntosh L, Foyer CH. 2006. Inter-relationships between light and respiration in the control of ascorbic acid synthesis and accumulation in Arabidopsis thaliana leaves. *J Exp Bot* 57: 1621-31

Bartsch M, Gobbato E, Bednarek P, Debey S, Schultze JL, et al. 2006. Salicylic acid-independent ENHANCED DISEASE SUSCEPTIBILITY1 signaling in Arabidopsis immunity and cell death is regulated by the monooxygenase FMO1 and the nudix hydrolase NUDT7. *The Plant cell* 18: 1038-51

Bashandy T, Guilleminot J, Vernoux T, Caparros-Ruiz D, Ljung K, et al. 2010. Interplay between the NADP-linked thioredoxin and glutathione systems in Arabidopsis auxin signaling. *The Plant cell* 22: 376-91

Baskin TI, Wilson JE, Cork A, Williamson RE. 1994. Morphology and Microtubule Organization in Arabidopsis Roots Exposed to Oryzalin or Taxol. *Plant & cell physiology* 35: 935-42

Bell SP, Kobayashi R, Stillman B. 1993. Yeast origin recognition complex functions in transcription silencing and DNA replication. *Science* 262: 1844-9

Bentsink L, Jowett J, Hanhart CJ, Koornneef M. 2006. Cloning of DOG1, a quantitative trait locus controlling seed dormancy in Arabidopsis. *Proc Natl Acad Sci U S A* 103: 17042-7

Berjak P, Pammenter NW. 2013. Implications of the lack of desiccation tolerance in recalcitrant seeds. *Front Plant Sci* 4: 478

Bernsdorff F, Doring AC, Gruner K, Schuck S, Brautigam A, Zeier J. 2016. Pipecolic Acid Orchestrates Plant Systemic Acquired

Resistance and Defense Priming via Salicylic Acid-Dependent and -Independent Pathways. *The Plant cell* 28: 102-29

Bianchi MW, Roux C, Vartanian N. 2002. Drought regulation of GST8, encoding the Arabidopsis homologue of ParC/Nt107 glutathione transferase/peroxidase. *Physiol Plant* 116: 96-105

Bindschedler LV, Dewdney J, Blee KA, Stone JM, Asai T, et al. 2006. Peroxidase-dependent apoplastic oxidative burst in Arabidopsis required for pathogen resistance. *Plant J* 47: 851-63

Blanco F, Salinas P, Cecchini NM, Jordana X, Van Hummelen P, et al. 2009. Early genomic responses to salicylic acid in Arabidopsis. *Plant Mol Biol* 70: 79-102

Boudolf V, Lammens T, Boruc J, Van Leene J, Van Den Daele H, et al. 2009. CDKB1;1 forms a functional complex with CYCA2;3 to suppress endocycle onset. *Plant Physiol* 150: 1482-93

Boudsocq M, Sheen J. 2013. CDPKs in immune and stress signaling. *Trends Plant Sci* 18: 30-40

Bryant G, Koster KL, Wolfe J. 2001. Membrane behaviour in seeds and other systems at low water content: the various effects of solutes. *Seed Science Research* 11: 17-25

Bulley S, Wright M, Rommens C, Yan H, Rassam M, et al. 2012. Enhancing ascorbate in fruits and tubers through over-expression of the l-galactose pathway gene GDP-l-galactose phosphorylase. *Plant Biotechnol J* 10: 390-97

Bulley SM, Rassam M, Hoser D, Otto W, Schunemann N, et al. 2009. Gene expression studies in kiwifruit and gene over-expression in Arabidopsis indicates that GDP-L-galactose guanyltransferase is a major control point of vitamin C biosynthesis. *J Exp Bot* 60: 765-78

Burch PM, Heintz NH. 2005. Redox regulation of cell-cycle re-entry: Cyclin D1 as a primary target for the mitogenic effects of reactive oxygen and nitrogen species. *Antioxid Redox Sign* 7: 741-51

Cacas JL. 2010. Devil inside: does plant programmed cell death involve the endomembrane system? *Plant Cell Environ* 33: 1453-73

Cai XT, Xu P, Zhao PX, Liu R, Yu LH, Xiang CB. 2014. Arabidopsis ERF109 mediates cross-talk between jasmonic acid and auxin biosynthesis during lateral root formation. *Nat Commun* 5: 5833

Canet JV, Dobon A, Fajmonova J, Tornero P. 2012. The BLADE-ON-PETIOLE genes of Arabidopsis are essential for resistance induced by methyl jasmonate. *BMC Plant Biol* 12: 199

Caron MM, De Frenne P, Brunet J, Chabrerie O, Cousins SAO, et al. 2015. Interacting effects of warming and drought on regeneration and early growth of Acer pseudoplatanus and A. platanoides. *Plant Biology* 17: 52-62

Carrera E, Holman T, Medhurst A, Dietrich D, Footitt S, et al. 2008. Seed after-ripening is a discrete developmental pathway associated with specific gene networks in Arabidopsis. *Plant J* 53: 214-24

Chen CM, Letnik I, Hacham Y, Dobrev P, Ben-Daniel BH, et al. 2014. ASCORBATE PEROXIDASE6 Protects Arabidopsis Desiccating and Germinating Seeds from Stress and Mediates Cross Talk between Reactive Oxygen Species, Abscisic Acid, and Auxin. *Plant Physiol* 166: 370-83

Chen H, Lai Z, Shi J, Xiao Y, Chen Z, Xu X. 2010. Roles of arabidopsis WRKY18, WRKY40 and WRKY60 transcription factors in plant responses to abscisic acid and abiotic stress. *BMC Plant Biol* 10: 281

Chen LY, Bernhardt A, Lee J, Hellmann H. 2015. Identification of Arabidopsis MYB56 as a Novel Substrate for CRL3(BPM) E3 Ligases. *Mol Plant* 8: 242-50

Chen Z, Gallie DR. 2012. Induction of monozygotic twinning by ascorbic acid in tobacco. *Plos One* 7: e39147

Cheng JC, Seeley KA, Sung ZR. 1995. Rml1 and Rml2, Arabidopsis Genes Required for Cell-Proliferation at the Root-Tip (Vol 107, Pg 365, 1995). *Plant Physiol* 108: 881-81

Chioda M, Spada F, Eskeland R, Thompson EM. 2004. Histone mRNAs do not accumulate during S phase of either mitotic or

endoreduplicative cycles in the chordate Oikopleura dioica. *Mol Cell Biol* 24: 5391-403

Chiu J, Dawes IW. 2012. Redox control of cell proliferation. *Trends Cell Biol* 22: 592-601

Chory J. 1997. Light modulation of vegetative development. *The Plant cell* 9: 1225-34

Citterio S, Sgorbati S, Scippa S, Sparvoli E. 1994. Ascorbic-Acid Effect on the Onset of Cell-Proliferation in Pea Root. *Physiologia Plantarum* 92: 601-07

Collinge MA, Spillane C, Kohler C, Gheyselinck J, Grossniklaus U. 2004. Genetic interaction of an origin recognition complex subunit and the Polycomb group gene MEDEA during seed development. *The Plant cell* 16: 1035-46

Colon-Carmona A, You R, Haimovitch-Gal T, Doerner P. 1999. Spatio-temporal analysis of mitotic activity with a labile cyclin-GUS fusion protein. *Plant J* 20: 503-08

Combettes B, Reichheld JP, Chaboute ME, Philipps G, Shen WH, Chaubet-Gigot N. 1999. Study of phase-specific gene expression in synchronized tobacco cells. *Methods Cell Sci* 21: 109-21

Conklin PL, De Paolo D, Wintle B, Schatz C, Buckenmeyer G. 2013. Identification of Arabidopsis VTC3 as a putative and unique dual function protein kinase::protein phosphatase involved in the regulation of the ascorbic acid pool in plants. *J Exp Bot* 64: 2793-804

Conklin PL, Saracco SA, Norris SR, Last RL. 2000. Identification of ascorbic acid-deficient Arabidopsis thaliana mutants. *Genetics* 154: 847-56

Conklin PL, Williams EH, Last RL. 1996. Environmental stress sensitivity of an ascorbic acid-deficient Arabidopsis mutant. *P Natl Acad Sci USA* 93: 9970-74

Conour JE, Graham WV, Gaskins HR. 2004. A combined in vitro/bioinformatic investigation of redox regulatory mechanisms governing cell cycle progression. *Physiol Genomics* 18: 196-205

Considine MJ, Foyer CH. 2014. Redox Regulation of Plant Development. *Antioxid Redox Sign* 21: 1305-26

Cools T, Iantcheva A, Maes S, Van den Daele H, De Veylder L. 2010. A replication stress-induced synchronization method for Arabidopsis thaliana root meristems. *Plant J* 64: 705-14

Cordoba-Pedregosa MD, Gonzalez Reyes JA, Canadillas MD, Navas P, Cordoba F. 1996. Role of apoplastic and cell-wall peroxidases on the stimulation of root elongation by ascorbate. *Plant Physiol* 112: 1119-25

Costigan SE, Warnasooriya SN, Humphries BA, Montgomery BL. 2011. Root-Localized Phytochrome Chromophore Synthesis Is Required for Photoregulation of Root Elongation and Impacts Root Sensitivity to Jasmonic Acid in Arabidopsis. *Plant Physiol* 157: 1138-50

Crichton RR, Ponceortiz Y, Koch MHJ, Parfait R, Stuhrmann HB. 1978. Isolation and Characterization of Phytoferritin from Pea. *Biochemical Journal* 171: 349-56

Csikasz-Nagy A, Battogtokh D, Chen KC, Novak B, Tyson JJ. 2006. Analysis of a generic model of eukaryotic cell-cycle regulation. *Biophys J* 90: 4361-79

Cui X, Ge C, Wang R, Wang H, Chen W, et al. 2010. The BUD2 mutation affects plant architecture through altering cytokinin and auxin responses in Arabidopsis. *Cell Res* 20: 576-86

Culligan K, Tissier A, Britt A. 2004. ATR regulates a G2-phase cell-cycle checkpoint in Arabidopsis thaliana. *The Plant cell* 16: 1091-104

Dardalhon M, Kumar C, Iraqui I, Vernis L, Kienda G, et al. 2012. Redox-sensitive YFP sensors monitor dynamic nuclear and cytosolic glutathione redox changes. *Free Radic Biol Med* 52: 2254-65

Davey MW, Gilot C, Persiau G, Ostergaard J, Han Y, et al. 1999. Ascorbate biosynthesis in Arabidopsis cell suspension culture. *Plant Physiol* 121: 535-43

De Bruin RA, McDonald WH, Kalashnikova TI, Yates J, 3rd, Wittenberg C. 2004. Cln3 activates G1-specific transcription via phosphorylation of the SBF bound repressor Whi5. *Cell* 117: 887-98

De Gara L, De Pinto MC, Arrigoni O. 1997. Ascorbate synthesis and ascorbate peroxidase activity during the early stage of wheat germination. *Physiologia Plantarum* 100: 894-900

De Pinto MC, Francis D, De Gara L. 1999. The redox state of the ascorbate-dehydroascorbate pair as a specific sensor of cell division in tobacco BY-2 cells. *Protoplasma* 209: 90-97

De Schutter K, Joubes J, Cools T, Verkest A, Corellou F, et al. 2007. Arabidopsis WEE1 kinase controls cell cycle arrest in response to activation of the DNA integrity checkpoint. *The Plant cell* 19: 211-25

De Simone A, Pellny TK, Foyer CH. 2015. Accumulation of ascorbate in the leaves of Arabidopsis thaliana wildtype and vtc2 mutants under continuous light and short photoperiod conditions. *Aspects of Applied Biology* 124: 123-30

De Tullio MC, Paciolla C, Dalla Veechia F, Rascio N, D'Emerico S, et al. 1999. Changes in onion root development induced by the inhibition of peptidyl-prolyl hydroxylase and influence of the ascorbate system on cell division and elongation. *Planta* 209: 424-34

Decabo RC, Gonzalezreyes JA, Navas P. 1993. The Onset of Cell-Proliferation Is Stimulated by Ascorbate Free-Radical in Onion Root Primordia. *Biol Cell* 77: 231-33

Demasi M, Hand A, Ohara E, Oliveira CL, Bicev RN, et al. 2014. 20S proteasome activity is modified via S-glutathionylation based on intracellular redox status of the yeast Saccharomyces cerevisiae: implications for the degradation of oxidized proteins. *Arch Biochem Biophys* 557: 65-71

Dewitte W, Murray JA. 2003. The plant cell cycle. *Annual review of plant biology* 54: 235-64

Di Donato RJ, Arbuckle E, Buker S, Sheets J, Tobar J, et al. 2004. Arabidopsis ALF4 encodes a nuclear-localized protein required for lateral root formation. *Plant J* 37: 340-53

Dion M, Chamberland H, St-Michel C, Plante M, Darveau A, et al. 1997. Detection of a homologue of bcl-2 in plant cells. *Biochem Cell Biol* 75: 457-61

Dixon DP, Edwards R. 2010. Glutathione transferases. *Arabidopsis Book* 8: e0131

Dolan L, Janmaat K, Willemsen V, Linstead P, Poethig S, et al. 1993. Cellular-Organization of the Arabidopsis-Thaliana Root. *Development* 119: 71-84

Dolezel J, Cihalikova J, Weiserova J, Lucretti S. 1999. Cell cycle synchronization in plant root meristems. *Methods Cell Sci* 21: 95-107

Dong K, Zhen SM, Cheng ZW, Cao H, Ge P, Yan YM. 2015. Proteomic Analysis Reveals Key Proteins and Phosphoproteins upon Seed Germination of Wheat (Triticum aestivum L.). *Front Plant Sci* 6

Donohue K, Schmitt J. 1998. Maternal environmental effects in plants - Adaptive plasticity? *Maternal Effects as Adaptations*: 137-58

Dowdle J, Ishikawa T, Gatzek S, Rolinski S, Smirnoff N. 2008. Two genes in Arabidopsis thaliana encoding GDP-L-galactose phosphorylase are required for ascorbate biosynthesis and seedling viability (vol 52, pg 673, 2007). *Plant J* 53: 595-95

Dreher KA, Brown J, Saw RE, Callis J. 2006. The Arabidopsis Aux/IAA protein family has diversified in degradation and auxin responsiveness. *The Plant cell* 18: 699-714

Dubos C, Le Gourrierec J, Baudry A, Huep G, Lanet E, et al. 2008. MYBL2 is a new regulator of flavonoid biosynthesis in Arabidopsis thaliana. *Plant J* 55: 940-53

El-Maarouf-Bouteau H, Bailly C. 2008. Oxidative signaling in seed germination and dormancy. *Plant Signal Behav* 3: 175-82

El-Maarouf-Bouteau H, Meimoun P, Job C, Job D, Bailly C. 2013. Role of protein and mRNA oxidation in seed dormancy and germination. *Front Plant Sci* 4

Feraud M, Masclaux-Daubresse C, Ferrario-Mery S, Pageau K, Lelandais M, et al. 2005. Expression of a ferredoxin-dependent glutamate synthase gene in mesophyll and vascular cells and functions of the enzyme in ammonium assimilation in Nicotiana tabacum (L.). *Planta* 222: 667-77

Fercha A, Capriotti AL, Caruso G, Caualiere C, Samperi R, et al. 2014. Comparative analysis of metabolic proteome variation in ascorbate-primed and unprimed wheat seeds during germination under salt stress. *J Proteomics* 108: 238-57

Finch-Savage WE, Leubner-Metzger G. 2006. Seed dormancy and the control of germination. *New Phytol* 171: 501-23

Flandrin A, Allouche S, Rolland Y, McDuff FO, Richard Wagner J, Klarskov K. 2015. Characterization of dehydroascorbate-mediated modification of glutaredoxin by mass spectrometry. *J Mass Spectrom* 50: 1358-66

Fonseca S, Chini A, Hamberg M, Adie B, Porzel A, et al. 2009. (+)-7-iso-Jasmonoyl-L-isoleucine is the endogenous bioactive jasmonate. *Nat Chem Biol* 5: 344-50

Foyer C, Rowell J, Walker D. 1983. Measurement of the Ascorbate Content of Spinach Leaf Protoplasts and Chloroplasts during Illumination. *Planta* 157: 239-44

Foyer CH, Noctor G. 2009. Redox Regulation in Photosynthetic Organisms: Signaling, Acclimation, and Practical Implications. *Antioxid Redox Sign* 11: 861-905

Foyer CH, Noctor G. 2011. Ascorbate and glutathione: the heart of the redox hub. *Plant Physiol* 155: 2-18

Foyer CHNG. 2005. Redox Homeostasis and Antioxidant Signaling: A Metabolic Interface between Stress Perception and Physiological Responses. *The Plant cell* 17: 1866-75

Galant A, Preuss ML, Cameron JC, Jez JM. 2011. Plant glutathione biosynthesis: diversity in biochemical regulation and reaction products. *Front Plant Sci* 2

Galen C, Rabenold JJ, Liscum E. 2007. Functional ecology of a blue light photoreceptor: effects of phototropin-1 on root growth enhance drought tolerance in Arabidopsis thaliana. *New Phytol* 173: 91-99

Galinha C, Hofhuis H, Luijten M, Willemsen V, Blilou I, et al. 2007. PLETHORA proteins as dose-dependent master regulators of Arabidopsis root development. *Nature* 449: 1053-57

Gao Y, Badejo AA, Shibata H, Sawa Y, Maruta T, et al. 2011. Expression Analysis of the VTC2 and VTC5 Genes Encoding GDP-L-Galactose Phosphorylase, an Enzyme Involved in Ascorbate Biosynthesis, in Arabidopsis thaliana. *Biosci Biotech Bioch* 75: 1783-88

Garcia-Gimenez JL, Ibanez-Cabellos JS, Seco-Cervera M, Pallardo FV. 2014. Glutathione and cellular redox control in epigenetic regulation. *Free Radical Bio Med* 75: S3-S3

Garg R, Jhanwar S, Tyagi AK, Jain M. 2010. Genome-wide survey and expression analysis suggest diverse roles of glutaredoxin gene family members during development and response to various stimuli in rice. *DNA Res* 17: 353-67

Garnczarska M, Bednarski W, Jancelewicz M. 2009. Ability of lupine seeds to germinate and to tolerate desiccation as related to changes in free radical level and antioxidants in freshly harvested seeds. *Plant physiology and biochemistry : PPB / Societe francaise de physiologie vegetale* 47: 56-62

Giacomelli L, Rudella A, Van Wijk KJ. 2006. High light response of the thylakoid proteome in arabidopsis wild type and the ascorbate-deficient mutant vtc2-2. A comparative proteomics study. *Plant Physiol* 141: 685-701

Goff SA, Cone KC, Chandler VL. 1992. Functional analysis of the transcriptional activator encoded by the maize B gene: evidence

for a direct functional interaction between two classes of regulatory proteins. *Genes Dev* 6: 864-75

Gomes MP, Garcia QS. 2013. Reactive oxygen species and seed germination. *Biologia* 68: 351-57

Griffith OW. 1999. Biologic and pharmacologic regulation of mammalian glutathione synthesis. *Free Radical Bio Med* 27: 922-35

Grill UKaD. 1993. Content of low-molecular-we^ht thiols during the imbibition of pea seeds. *Physiologia plantarum* 88: 557-62

Gutierrez C. 2009. The Arabidopsis Cell Division Cycle. *American society of plants biologists* e0120: 10.1199/tab.0120

Hamberger B, Hahlbrock K. 2004. The 4-coumarate:CoA ligase gene family in Arabidopsis thaliana comprises one rare, sinapate-activating and three commonly occurring isoenzymes. *Proc Natl Acad Sci U S A* 101: 2209-14

Hanna JS, Kroll ES, Lundblad V, Spencer FA. 2001. Saccharomyces cerevisiae CTF18 and CTF4 are required for sister chromatid cohesion. *Mol Cell Biol* 21: 3144-58

Hanson GT, Aggeler R, Oglesbee D, Cannon M, Capaldi RA, et al. 2004. Investigating mitochondrial redox potential with redox-sensitive green fluorescent protein indicators. *The Journal of biological chemistry* 279: 13044-53

Harrison SJ, Mott EK, Parsley K, Aspinall S, Gray JC, Cottage A. 2006. A rapid and robust method of identifying transformed Arabidopsis thaliana seedlings following floral dip transformation. *Plant Methods* 2

Haughn GW, Western TL. 2012. Arabidopsis Seed Coat Mucilage is a Specialized Cell Wall that Can be Used as a Model for Genetic Analysis of Plant Cell Wall Structure and Function. *Front Plant Sci* 3: 64

Heazlewood JL, Howell KA, Millar AH. 2003. Mitochondrial complex I from Arabidopsis and rice: orthologs of mammalian and fungal components coupled with plant-specific subunits. *Biochim Biophys Acta* 1604: 159-69

Himanen K, Reuzeau C, Beeckman T, Melzer S, Grandjean O, et al. 2003. The arabidopsis locus RCB mediates upstream regulation of mitotic gene expression. *Plant Physiol* 133: 1862-72

Holdsworth MJ, Bentsink L, Soppe WJJ. 2008. Molecular networks regulating Arabidopsis seed maturation, after-ripening, dormancy and germination. *New Phytol* 179: 33-54

Hooks KB, Turner JE, Graham IA, Runions J, Hooks MA. 2012. GFP-tagging of Arabidopsis acyl-activating enzymes raises the issue of peroxisome-chloroplast import competition versus dual localization. *J Plant Physiol* 169: 1631-8

Horemans N, Potters G, De Wilde L, Caubergs RJ. 2003. Dehydroascorbate uptake activity correlates with cell growth and cell division of tobacco bright yellow-2 cell cultures. *Plant Physiol* 133: 361-67

Hoyle GL, Steadman KJ, Daws MI, Adkins SW. 2008. Pre- and post-harvest influences on seed dormancy status of an Australian Goodeniaceae species, Goodenia fascicularis. *Annals of botany* 102: 93-101

Hrabak EM, Chan CW, Gribskov M, Harper JF, Choi JH, et al. 2003. The Arabidopsis CDPK-SnRK superfamily of protein kinases. *Plant Physiol* 132: 666-80

Inze D, De Veylder L. 2006. Cell cycle regulation in plant development. *Annu Rev Genet* 40: 77-105

Ishibashi Y, Iwaya-Inoue M. 2006. Ascorbic acid suppresses germination and dynamic states of water in wheat seeds. *Plant Prod Sci* 9: 172-75

Ishikawa T, Tanimoto M, Dowdle J, Smirnoff N. 2007. VTC2 encodes GDP-L-galactose phosphorylase, an enzyme involved in plant ascorbate biosynthesis. *Plant & cell physiology* 48: S32-S32

Jander G, Norris SR, Rounsley SD, Bush DF, Levin IM, Last RL. 2002. Arabidopsis map-based cloning in the post-genome era. *Plant Physiol* 129: 440-50

Jares P, Donaldson A, Blow JJ. 2000. The Cdc7/Dbf4 protein kinase: target of the S phase checkpoint? *EMBO Rep* 1: 319-22

Jensen RB, Carreira A, Kowalczykowski SC. 2010. Purified human BRCA2 stimulates RAD51-mediated recombination. *Nature* 467: 678-83

Jez JM, Cahoon RE, Chen SX. 2004. Arabidopsis thaliana glutamate-cysteine ligase - Functional properties, kinetic mechanism, and regulation of activity. *J Biol Chem* 279: 33463-70

Jiang K, Schwarzer C, Lally E, Zhang S, Ruzin S, et al. 2006. Expression and characterization of a redox-sensing green fluorescent protein (reduction-oxidation-sensitive green fluorescent protein) in Arabidopsis. *Plant Physiol* 141: 397-403

Job C, Rajjou L, Lovigny Y, Belghazi M, Job D. 2005. Patterns of protein oxidation in Arabidopsis seeds and during germination. *Plant Physiol* 138: 790-802

Kanchiswamy CN, Takahashi H, Quadro S, Maffei ME, Bossi S, et al. 2010. Regulation of Arabidopsis defense responses against Spodoptera littoralis by CPK-mediated calcium signaling. *BMC Plant Biol* 10: 97

Kato N, Esaka M. 1999. Changes in ascorbate oxidase gene expression and ascorbate levels in cell division and cell elongation in tobacco cells. *Physiologia Plantarum* 105: 321-29

Kerchev PI, Pellny TK, Vivancos PD, Kiddle G, Hedden P, et al. 2011. The Transcription Factor ABI4 Is Required for the Ascorbic Acid-Dependent Regulation of Growth and Regulation of Jasmonate-Dependent Defense Signaling Pathways in Arabidopsis. *The Plant cell* 23: 3319-34

Kerk NM, Feldman LJ. 1995. A Biochemical-Model for the Initiation and Maintenance of the Quiescent Center - Implications for Organization of Root-Meristems. *Development* 121: 2825-33

Kerk NM, Jiang KN, Feldman LJ. 2000. Auxin metabolism in the root apical meristem. *Plant Physiol* 122: 925-32

Kiddle G, Pastori GM, Bernard S, Pignocchi C, Antoniw J, et al. 2003. Effects of leaf ascorbate content on defense and photosynthesis gene expression in Arabidopsis thaliana. *Antioxid Redox Sign* 5: 23-32

Kim B, Fujioka S, Kwon M, Jeon J, Choe S. 2013. Arabidopsis brassinosteroid-overproducing gulliver3-D/dwarf4-D mutants exhibit altered responses to jasmonic acid and pathogen. *Plant Cell Rep* 32: 1139-49

Kissen R, Winge P, Tran DH, Jorstad TS, Storseth TR, et al. 2010. Transcriptional profiling of an Fd-GOGAT1/GLU1 mutant in Arabidopsis thaliana reveals a multiple stress response and extensive reprogramming of the transcriptome. *BMC Genomics* 11: 190

Klatt P, Molina EP, De Lacoba MG, Padilla CA, Martinez-Galisteo E, et al. 1999. Redox regulation of c-Jun DNA binding by reversible S-glutathiolation. *Faseb J* 13: 1481-90

Kondou Y, Nakazawa M, Kawashima M, Ichikawa T, Yoshizumi T, et al. 2008. RETARDED GROWTH OF EMBRYO1, a new basic helix-loop-helix protein, expresses in endosperm to control embryo growth. *Plant Physiol* 147: 1924-35

Koprivova A, Mugford ST, Kopriva S. 2010. Arabidopsis root growth dependence on glutathione is linked to auxin transport. *Plant Cell Rep* 29: 1157-67

Kotchoni SO, Larrimore KE, Mukherjee M, Kempinski CF, Barth C. 2009. Alterations in the Endogenous Ascorbic Acid Content Affect Flowering Time in Arabidopsis. *Plant Physiol* 149: 803-15

Kucera B, Cohn MA, Leubner-Metzger G. 2005. Plant hormone interactions during seed dormancy release and germination. *Seed Science Research* 15: 281-307

Kumpf RP, Nowack MK. 2015. The root cap: a short story of life and death. *J Exp Bot* 66: 5651-62

Lai LB, Nadeau JA, Lucas J, Lee EK, Nakagawa T, et al. 2005. The Arabidopsis R2R3 MYB proteins FOUR LIPS and MYB88 restrict

divisions late in the stomatal cell lineage. *The Plant cell* 17: 2754-67

Laing WA, Wright MA, Cooney J, Bulley SM. 2007. The missing step of the L-galactose pathway of ascorbate biosynthesis in plants, an L-galactose guanyltransferase, increases leaf ascorbate content. *P Natl Acad Sci USA* 104: 9534-39

Langmead B, Salzberg SL. 2012. Fast gapped-read alignment with Bowtie 2. *Nat Methods* 9: 357-9

Laporte D, Olate E, Salinas P, Salazar M, Jordana X, Holuigue L. 2012. Glutaredoxin GRXS13 plays a key role in protection against photooxidative stress in Arabidopsis. *J Exp Bot* 63: 503-15

Lee DJ, Park JY, Ku SJ, Ha YM, Kim S, et al. 2007. Genome-wide expression profiling of ARABIDOPSIS RESPONSE REGULATOR 7(ARR7) overexpression in cytokinin response. *Mol Genet Genomics* 277: 115-37

Li Y, Kim JI, Pysh L, Chapple C. 2015. Four Isoforms of Arabidopsis 4-Coumarate:CoA Ligase Have Overlapping yet Distinct Roles in Phenylpropanoid Metabolism. *Plant Physiol* 169: 2409-21

Liang L, Flury S, Kalck V, Hohn B, Molinier J. 2006. CENTRIN2 interacts with the Arabidopsis homolog of the human XPC protein (AtRAD4) and contributes to efficient synthesis-dependent repair of bulky DNA lesions. *Plant Mol Biol* 61: 345-56

Linster CL, Gomez TA, Christensen KC, Adler LN, Young BD, et al. 2007. Arabidopsis VTC2 encodes a GDP-L-galactose phosphorylase, the last unknown enzyme in the Smirnoff-Wheeler pathway to ascorbic acid in plants. *J Biol Chem* 282: 18879-85

Liso R, Innocenti AM, Bitonti MB, Arrigoni O. 1988. Ascorbic Acid-Induced Progression of Quiescent Center Cells from G1-Phase to S-Phase. *New Phytol* 110: 469-71

Liu F, Jiang H, Ye S, Chen WP, Liang W, et al. 2010. The Arabidopsis P450 protein CYP82C2 modulates jasmonate-induced root

growth inhibition, defense gene expression and indole glucosinolate biosynthesis. *Cell Res* 20: 539-52

Liu Q, Kasuga M, Sakuma Y, Abe H, Miura S, et al. 1998. Two transcription factors, DREB1 and DREB2, with an EREBP/AP2 DNA binding domain separate two cellular signal transduction pathways in drought- and low-temperature-responsive gene expression, respectively, in Arabidopsis. *The Plant cell* 10: 1391-406

Logan DC, Millar AH, Sweetlove LJ, Hill SA, Leaver CJ. 2001. Mitochondrial biogenesis during germination in maize embryos. *Plant Physiol* 125: 662-72

Lorence A, Chevone BI, Mendes P, Nessler CL. 2004. myo-inositol oxygenase offers a possible entry point into plant ascorbate biosynthesis. *Plant Physiol* 134: 1200-05

Mahonen AP, Bonke M, Kauppinen L, Riikonen M, Benfey PN, Helariutta Y. 2000. A novel two-component hybrid molecule regulates vascular morphogenesis of the Arabidopsis root. *Gene Dev* 14: 2938-43

Maia J, Dekkers BJW, Provart NJ, Ligterink W, Hilhorst HWM. 2011. The Re-Establishment of Desiccation Tolerance in Germinated Arabidopsis thaliana Seeds and Its Associated Transcriptome. *Plos One* 6

Maleki S, Sepehr R, Staniszewski K, Sheibani N, Sorenson CM, Ranji M. 2012. Mitochondrial redox studies of oxidative stress in kidneys from diabetic mice. *Biomed Opt Express* 3: 273-81

Marchadier E, Hetherington AM. 2014. Involvement of two-component signalling systems in the regulation of stomatal aperture by light in Arabidopsis thaliana. *New Phytol* 203: 462-8

Marin-de la Rosa N, Sotillo B, Miskolczi P, Gibbs DJ, Vicente J, et al. 2014. Large-scale identification of gibberellin-related transcription factors defines group VII ETHYLENE RESPONSE FACTORS as functional DELLA partners. *Plant Physiol* 166: 1022-32

Markovic J, Borras C, Ortega A, Sastre J, Vina J, Pallardo FV. 2007. Glutathione is recruited into the nucleus in early phases of cell proliferation. *The Journal of biological chemistry* 282: 20416-24

Masubelele NH, Dewitte W, Menges M, Maughan S, Collins C, et al. 2005. D-type cyclins activate division in the root apex to promote seed germination in Arabidopsis. *P Natl Acad Sci USA* 102: 15694-99

Matsuo M, Johnson JM, Hieno A, Tokizawa M, Nomoto M, et al. 2015. High REDOX RESPONSIVE TRANSCRIPTION FACTOR1 Levels Result in Accumulation of Reactive Oxygen Species in Arabidopsis thaliana Shoots and Roots. *Mol Plant* 8: 1253-73

Maughan SC, Pasternak M, Cairns N, Kiddle G, Brach T, et al. 2010. Plant homologs of the Plasmodium falciparum chloroquine-resistance transporter, PfCRT, are required for glutathione homeostasis and stress responses. *P Natl Acad Sci USA* 107: 2331-6

Maulucci G, Pani G, Labate V, Mele M, Panieri E, et al. 2009. Investigation of the spatial distribution of glutathione redox-balance in live cells by using Fluorescence Ratio Imaging Microscopy. *Biosens Bioelectron* 25: 682-7

May MJ, Vernoux T, Leaver C, Van Montagu M, Inze D. 1998. Glutathione homeostasis in plants: implications for environmental sensing and plant development. *J Exp Bot* 49: 649-67

Menges M, Murray JA. 2002. Synchronous Arabidopsis suspension cultures for analysis of cell-cycle gene activity. *Plant J* 30: 203-12

Menon SG, Sarsour EH, Spitz DR, Higashikubo R, Sturm M, et al. 2003. Redox regulation of the G1 to S phase transition in the mouse embryo fibroblast cell cycle. *Cancer Res* 63: 2109-17

Merad-Saidoune M BE, Nicole A, Marsac C, Martinou JC, Sola B, Sinet PM, Ceballos-Picot I. 1999. Overproduction of Cu/Zn-superoxide dismutase or Bcl-2 prevents the brain mitochondrial respiratory dysfunction induced by glutathione depletion. *Exp Neurol* 158: 428-36

Meyer AJ, Brach T, Marty L, Kreye S, Rouhier N, et al. 2007. Redox-sensitive GFP in Arabidopsis thaliana is a quantitative biosensor for the redox potential of the cellular glutathione redox buffer. *The Plant journal : for cell and molecular biology* 52: 973-86

Meyerowitz EM. 2002. Plants compared to animals: the broadest comparative study of development. *Science* 295: 1482-5

Mhamdi A, Hager J, Chaouch S, Queval G, Han Y, et al. 2010. Arabidopsis GLUTATHIONE REDUCTASE1 Plays a Crucial Role in Leaf Responses to Intracellular Hydrogen Peroxide and in Ensuring Appropriate Gene Expression through Both Salicylic Acid and Jasmonic Acid Signaling Pathways. *Plant Physiol* 153: 1144-60

Mishina TE, Zeier J. 2006. The Arabidopsis flavin-dependent monooxygenase FMO1 is an essential component of biologically induced systemic acquired resistance. *Plant Physiol* 141: 1666-75

Mizutani M, Ohta D. 2010. Diversification of P450 genes during land plant evolution. *Annual review of plant biology* 61: 291-315

Molas ML, Kiss JZ, Correll MJ. 2006. Gene profiling of the red light signalling pathways in roots. *J Exp Bot* 57: 3217-29

Molinier J, Lechner E, Dumbliauskas E, Genschik P. 2008. Regulation and role of Arabidopsis CUL4-DDB1A-DDB2 in maintaining genome integrity upon UV stress. *PLoS Genet* 4: e1000093

Molinier J, Ramos C, Fritsch O, Hohn B. 2004. CENTRIN2 modulates homologous recombination and nucleotide excision repair in Arabidopsis. *The Plant cell* 16: 1633-43

Montrichard F, Alkhalfioui F, Yano H, Vensel WH, Hurkman WJ, Buchanan BB. 2009. Thioredoxin targets in plants: the first 30 years. *J Proteomics* 72: 452-74

Moreira JD, Peres S, Steyaert JM, Bigan E, Pauleve L, et al. 2015. Cell cycle progression is regulated by intertwined redox oscillators. *Theor Biol Med Model* 12

Mueller S, Hilbert B, Dueckershoff K, Roitsch T, Krischke M, et al. 2008. General detoxification and stress responses are mediated by oxidized lipids through TGA transcription factors in Arabidopsis. *The Plant cell* 20: 768-85

Mukherjee M, Larrimore KE, Ahmed NJ, Bedick TS, Barghouthi NT, et al. 2010. Ascorbic acid deficiency in arabidopsis induces constitutive priming that is dependent on hydrogen peroxide, salicylic acid, and the NPR1 gene. *Mol Plant Microbe Interact* 23: 340-51

Muller D, Schmitz G, Theres K. 2006. Blind homologous R2R3 Myb genes control the pattern of lateral meristem initiation in Arabidopsis. *The Plant cell* 18: 586-97

Muller-Moule P. 2008. An expression analysis of the ascorbate biosynthesis enzyme VTC2. *Plant Mol Biol* 68: 31-41

Muller-Moule P, Conklin PL, Niyogi KK. 2002. Ascorbate deficiency can limit violaxanthin de-epoxidase activity in vivo. *Plant Physiol* 128: 970-77

Myers C, Romanowsky SM, Barron YD, Garg S, Azuse CL, et al. 2009. Calcium-dependent protein kinases regulate polarized tip growth in pollen tubes. *Plant J* 59: 528-39

Ndamukong I, Abdallat AA, Thurow C, Fode B, Zander M, et al. 2007. SA-inducible Arabidopsis glutaredoxin interacts with TGA factors and suppresses JA-responsive PDF1.2 transcription. *Plant J* 50: 128-39

Nelson DM, Ye X, Hall C, Santos H, Ma T, et al. 2002. Coupling of DNA Synthesis and Histone Synthesis in S Phase Independent of Cyclin/cdk2 Activity. *Molecular and Cellular Biology* 22: 7459-72

Nguyen TP, Cueff G, Hegedus DD, Rajjou L, Bentsink L. 2015. A role for seed storage proteins in Arabidopsis seed longevity. *J Exp Bot* 66: 6399-413

Noctor G, Foyer CH. 1998. Ascorbate and glutathione: Keeping active oxygen under control. *Annu Rev Plant Phys* 49: 249-79

Noctor G, Mhamdi A, Chaouch S, Han Y, Neukermans J, et al. 2012. Glutathione in plants: an integrated overview. *Plant, cell & environment* 35: 454-84

Nurse CNaP. 2003. ANIMAL CELL CYCLES AND THEIR CONTROL. *Annual Reviews Biochemistry* 61: 441-70

O'Malley RC, Huang SS, Song L, Lewsey MG, Bartlett A, et al. 2016. Cistrome and Epicistrome Features Shape the Regulatory DNA Landscape. *Cell* 165: 1280-92

Ogawa K, Tasaka Y, Mino M, Tanaka Y, Iwabuchi M. 2001. Association of glutathione with flowering in Arabidopsis thaliana. *Plant & cell physiology* 42: 524-30

Olmos E, Kiddle G, Pellny TK, Kumar S, Foyer CH. 2006. Modulation of plant morphology, root architecture, and cell structure by low vitamin C in Arabidopsis thaliana. *J Exp Bot* 57: 1645-55

Pajaud J, Ribault C, Ben Mosbah I, Rauch C, Henderson C, et al. 2015. Glutathione transferases P1/P2 regulate the timing of signaling pathway activations and cell cycle progression during mouse liver regeneration. *Cell Death Dis* 6

Pallanca JE, Smirnoff N. 2000. The control of ascorbic acid synthesis and turnover in pea seedlings. *J Exp Bot* 51: 669-74

Pauwels L, Barbero GF, Geerinck J, Tilleman S, Grunewald W, et al. 2010. NINJA connects the co-repressor TOPLESS to jasmonate signalling. *Nature* 464: 788-91

Pavet V, Olmos E, Kiddle G, Mowla S, Kumar S, et al. 2005. Ascorbic acid deficiency activates cell death and disease resistance responses in Arabidopsis. *Plant Physiol* 139: 1291-303

Pellny TK, Locato V, Vivancos PD, Markovic J, De Gara L, et al. 2009. Pyridine nucleotide cycling and control of intracellular redox state in relation to poly (ADP-ribose) polymerase activity and nuclear localization of glutathione during exponential growth of Arabidopsis cells in culture. *Mol Plant* 2: 442-56

Petersson SV, Johansson AI, Kowalczyk M, Makoveychuk A, Wang JY, et al. 2009. An Auxin Gradient and Maximum in the Arabidopsis

Root Apex Shown by High-Resolution Cell-Specific Analysis of IAA Distribution and Synthesis. *The Plant cell* 21: 1659-68

Pfalz M, Mikkelsen MD, Bednarek P, Olsen CE, Halkier BA, Kroymann J. 2011. Metabolic engineering in Nicotiana benthamiana reveals key enzyme functions in Arabidopsis indole glucosinolate modification. *The Plant cell* 23: 716-29

Pignocchi C, Kiddle G, Hernandez I, Foster SJ, Asensi A, et al. 2006. Ascorbate oxidase-dependent changes in the redox state of the apoplast modulate gene transcript accumulation leading to modified hormone signaling and orchestration of defense processes in tobacco. *Plant Physiol* 141: 423-35

Pineau B, Layoune O, Danon A, De Paepe R. 2008. L-galactono-1,4-lactone dehydrogenase is required for the accumulation of plant respiratory complex I. *J Biol Chem* 283: 32500-5

Potters G, De Gara L, Asard H, Horemans N. 2002. Ascorbate and glutathione: guardians of the cell cycle, partners in crime? *Plant Physiol Bioch* 40: 537-48

Potters G, Horemans N, Bellone S, Caubergs RJ, Trost P, et al. 2004. Dehydroascorbate influences the plant cell cycle through a glutathione-independent reduction mechanism. *Plant Physiol* 134: 1479-87

Potters G, Horemans N, Caubergs RJ, Asard H. 2000. Ascorbate and dehydroascorbate influence cell cycle progression in a tobacco cell suspension. *Plant Physiol* 124: 17-20

Pyo CW, Choi JH, Oh SM, Choi SY. 2013. Oxidative stress-induced cyclin D1 depletion and its role in cell cycle processing. *Bba-Gen Subjects* 1830: 5316-25

Queval G, Noctor G. 2007. A plate reader method for the measurement of NAD, NADP, glutathione, and ascorbate in tissue extracts: Application to redox profiling during Arabidopsis rosette development. *Analytical Biochemistry* 363: 58-69

Radominska-Pandya A, Bratton SM, Redinbo MR, Miley MJ. 2010. The crystal structure of human UDP-glucuronosyltransferase 2B7 C-

terminal end is the first mammalian UGT target to be revealed: the significance for human UGTs from both the 1A and 2B families. *Drug Metab Rev* 42: 133-44

Radzio JA, Lorence A, Chevone BI, Nessler CL. 2003. L-Gulono-1,4-lactone oxidase expression rescues vitamin C-deficient Arabidopsis (vtc) mutants. *Plant Mol Biol* 53: 837-44

Rajniak J, Barco B, Clay NK, Sattely ES. 2015. A new cyanogenic metabolite in Arabidopsis required for inducible pathogen defence. *Nature* 525: 376-9

Ramirez-Parra. E, Gutierrez. C. 2000. Characterization of wheat DP, a heterodimerization partner of the plant E2F transcription factor which stimulates E2F-DNA binding. *FEBS Lett.* 486: 73-78

Rautenkranz AAF, Li LJ, Machler F, Martinoia E, Oertli JJ. 1994. Transport of Ascorbic and Dehydroascorbic Acids across Protoplast and Vacuole Membranes Isolated from Barley (Hordeum-Vulgare L Cv Gerbel) Leaves. *Plant Physiol* 106: 187-93

Riechheld JP, Vernoux, T., Lardon, F., Vanmontagu, M., and Inze, D. 1999. Specific checkpoints regulate plant cell cycle progression in response to oxidative stress. *Plant J* 17: 647–56

Robinson MD, McCarthy DJ, Smyth GK. 2010. edgeR: a Bioconductor package for differential expression analysis of digital gene expression data. *Bioinformatics* 26: 139-40

Running JA, Burlingame RP, Berry A. 2003. The pathway of L-ascorbic acid biosynthesis in the colourless microalga Prototheca moriformis. *J Exp Bot* 54: 1841-49

Sabatini S, Beis D, Wolkenfelt H, Murfett J, Guilfoyle T, et al. 1999. An auxin-dependent distal organizer of pattern and polarity in the Arabidopsis root. *Cell* 99: 463-72

SanchezFernandez R, Fricker M, Corben LB, White NS, Sheard N, et al. 1997. Cell proliferation and hair tip growth in the Arabidopsis root are under mechanistically different forms of redox control. *P Natl Acad Sci USA* 94: 2745-50

Sarkar AK, Luijten M, Miyashima S, Lenhard M, Hashimoto T, et al. 2007. Conserved factors regulate signalling in Arabidopsis thaliana shoot and root stem cell organizers. *Nature* 446: 811-14

Sato Y, Demura T, Yamawaki K, Inoue Y, Sato S, et al. 2006. Isolation and characterization of a novel peroxidase gene ZPO-C whose expression and function are closely associated with lignification during tracheary element differentiation. *Plant Cell Physiol* 47: 493-503

Schindelin J, Arganda-Carreras I, Frise E, Kaynig V, Longair M, et al. 2012. Fiji: an open-source platform for biological-image analysis. *Nat Methods* 9: 676-82

Schwob E, Bohm T, Mendenhall MD, Nasmyth K. 1994. The B-type cyclin kinase inhibitor p40SIC1 controls the G1 to S transition in S. cerevisiae. *Cell* 79: 233-44

Sedbrook JC, Carroll KL, Hung KF, Masson PH, Somerville CR. 2002. The Arabidopsis SKU5 gene encodes an extracellular glycosyl phosphatidylinositol-anchored glycoprotein involved in directional root growth. *The Plant cell* 14: 1635-48

Seguin J, Muzac I, Ibrahim RK. 1998. Purification and immunological characterization of a recombinant trimethylflavonol 3'-O-methyltransferase. *Phytochemistry* 49: 319-25

Setterdahl AT, Chivers PT, Hirasawa M, Lemaire SD, Keryer E, et al. 2003. Effect of pH on the oxidation-reduction properties of thioredoxins. *Biochemistry* 42: 14877-84

Sharma P, Jha AB, Dubey RS, Pessarakli M. 2012. Reactive Oxygen Species, Oxidative Damage, and Antioxidative Defense Mechanism in Plants under Stressful Conditions. *Journal of Botany* 2012: 1-26

Shen WH, Parmentier Y, Hellmann H, Lechner E, Dong A, et al. 2002. Null mutation of AtCUL1 causes arrest in early embryogenesis in Arabidopsis. *Mol Biol Cell* 13: 1916-28

Shyu C, Figueroa P, Depew CL, Cooke TF, Sheard LB, et al. 2012. JAZ8 lacks a canonical degron and has an EAR motif that

mediates transcriptional repression of jasmonate responses in Arabidopsis. *The Plant cell* 24: 536-50

Stacklies W, Redestig H, Scholz M, Walther D, Selbig J. 2007. pcaMethods--a bioconductor package providing PCA methods for incomplete data. *Bioinformatics* 23: 1164-7

Stals HaI, D. . 2001. When plant cells decide to divide. *Trends in Plant Sci.* 6: 359-64.

Swarup R, Kramer EM, Perry P, Knox K, Leyser HMO, et al. 2005. Root gravitropism requires lateral root cap and epidermal cells for transport and response to a mobile auxin signal. *Nat Cell Biol* 7: 1057-65

Tiwari SB, Hagen G, Guilfoyle TJ. 2004. Aux/IAA proteins contain a potent transcriptional repression domain. *The Plant cell* 16: 533-43

Tolleter D, Hincha DK, Macherel D. 2010. A mitochondrial late embryogenesis abundant protein stabilizes model membranes in the dry state. *Bba-Biomembranes* 1798: 1926-33

Tommasi F, Paciolla C, De Pinto MC, De Gara L. 2001. A comparative study of glutathione and ascorbate metabolism during germination of Pinus pinea L. seeds. *J Exp Bot* 52: 1647-54

Trapnell C, Roberts A, Goff L, Pertea G, Kim D, et al. 2012. Differential gene and transcript expression analysis of RNA-seq experiments with TopHat and Cufflinks. *Nat Protoc* 7: 562-78

Ulker B, Peiter E, Dixon DP, Moffat C, Capper R, et al. 2008. Getting the most out of publicly available T-DNA insertion lines. *Plant J* 56: 665-77

vandenBerg C, Willemsen V, Hendriks G, Weisbeek P, Scheres B. 1997. Short-range control of cell differentiation in the Arabidopsis root meristem. *Nature* 390: 287-89

Vandepoele K. 2002. Genome-Wide Analysis of Core Cell Cycle Genes in Arabidopsis. *The Plant Cell Online* 14: 903-16

Veljovic-Jovanovic SD, Pignocchi C, Noctor G, Foyer CH. 2001. Low ascorbic acid in the vtc-1 mutant of arabidopsis is associated

with decreased growth and intracellular redistribution of the antioxidant system. *Plant Physiol* 127: 426-35

Verbelen JP, De Cnodder T, Le J, Vissenberg K, Baluska F. 2006. The Root Apex of Arabidopsis thaliana Consists of Four Distinct Zones of Growth Activities: Meristematic Zone, Transition Zone, Fast Elongation Zone and Growth Terminating Zone. *Plant Signal Behav* 1: 296-304

Vernoux T, Wilson, R.C., et al. 2000. The root meristemless1/cadmium sensitive2 gene defines a glutathione-dependent pathway involved in initiation and maintenance of cell division during postembryonic root development. *The Plant cell* 12: 97-109

Vilarrasa-Blasi J, Gonzalez-Garcia MP, Frigola D, Fabregas N, Alexiou KG, et al. 2014. Regulation of Plant Stem Cell Quiescence by a Brassinosteroid Signaling Module. *Dev Cell* 30: 36-47

Vivancos PD, Dong Y, Ziegler K, Markovic J, Pallardó FV, et al. 2010. Recruitment of glutathione into the nucleus during cell proliferation adjusts whole-cell redox homeostasis in Arabidopsis thaliana and lowers the oxidative defence shield. *The Plant Journal* 64: 825-38

Von Saint Paul V, Zhang W, Kanawati B, Geist B, Faus-Kessler T, et al. 2011. The Arabidopsis glucosyltransferase UGT76B1 conjugates isoleucic acid and modulates plant defense and senescence. *The Plant cell* 23: 4124-45

Wachter A, Wolf S, Steininger H, Bogs J, Rausch T. 2005. Differential targeting of GSH1 and GSH2 is achieved by multiple transcription initiation: implications for the compartmentation of glutathione biosynthesis in the Brassicaceae. *Plant J* 41: 15-30

Wagener KC, Kolbrink B, Dietrich K, Kizina KM, Terwitte LS, et al. 2016. Redox Indicator Mice Stably Expressing Genetically Encoded Neuronal roGFP: Versatile Tools to Decipher Subcellular Redox Dynamics in Neuropathophysiology. *Antioxid Redox Signal*

Waines JG, Ehdaie B. 2007. Domestication and crop physiology: Roots of green-revolution wheat. *Annals of botany* 100: 991-98

Wang J, Yu YW, Zhang ZJ, Quan RD, Zhang HW, et al. 2013. Arabidopsis CSN5B Interacts with VTC1 and Modulates Ascorbic Acid Synthesis. *The Plant cell* 25: 625-36

Wani R, Tsang AW, Furdui CM. 2011. Oxidation of Akt2 kinase promotes cell migration and regulates G(1)-S transition in the cell cycle. *Cell Cycle* 10: 3263-68

Washburn MP, Wells WW. 1999. The catalytic mechanism of the glutathione-dependent dehydroascorbate reductase activity of thioltransferase (glutaredoxin). *Biochemistry* 38: 268-74

Watson MB, Emory KK, Piatak RM, Malmberg RL. 1998. Arginine decarboxylase (polyamine synthesis) mutants of Arabidopsis thaliana exhibit altered root growth. *Plant J* 13: 231-9

Weitbrecht K, Muller K, Leubner-Metzger G. 2011. First off the mark: early seed germination. *J Exp Bot* 62: 3289-309

Wolucka BA, Van Montagu M. 2003. GDP-mannose 3 ',5 '-epimerase forms GDP-L-gulose, a putative intermediate for the de novo biosynthesis of vitamin C in plants. *J Biol Chem* 278: 47483-90

Xiao LM, Koster KL. 2001. Desiccation tolerance of protoplasts isolated from pea embryos. *J Exp Bot* 52: 2105-14

Xie Z, Lee E, Lucas JR, Morohashi K, Li D, et al. 2010. Regulation of cell proliferation in the stomatal lineage by the Arabidopsis MYB FOUR LIPS via direct targeting of core cell cycle genes. *The Plant cell* 22: 2306-21

Yabuta Y, Maruta T, Nakamura A, Mieda T, Yoshimura K, et al. 2008. Conversion of L-Galactono-1,4-lactone to L-Ascorbate Is Regulated by the Photosynthetic Electron Transport Chain in Arabidopsis. *Biosci Biotech Bioch* 72: 2598-607

Yabuta Y, Mieda T, Rapolu M, Nakamura A, Motoki T, et al. 2007. Light regulation of ascorbate biosynthesis is dependent on the photosynthetic electron transport chain but independent of sugars in Arabidopsis. *J Exp Bot* 58: 2661-71

Yan D, Duermeyer L, Leoveanu C, Nambara E. 2014. The functions of the endosperm during seed germination. *Plant & cell physiology* 55: 1521-33

Yang Y, Yuan JS, Ross J, Noel JP, Pichersky E, Chen F. 2006. An Arabidopsis thaliana methyltransferase capable of methylating farnesoic acid. *Arch Biochem Biophys* 448: 123-32

Yano H, Wong JH, Cho MJ, Buchanan BB. 2001. Redox changes accompanying the degradation of seed storage proteins in germinating rice. *Plant & cell physiology* 42: 879-83

Yen A, Pardee AB. 1979. Role of nuclear size in cell growth initiation. *Science* 204: 1315-7

Yin K, Ueda M, Takagi H, Kajihara T, Sugamata Aki S, et al. 2014. A dual-color marker system for in vivo visualization of cell cycle progression in Arabidopsis. *Plant J* 80: 541-52

Yoshimura K, Nakane T, Kume S, Shiomi Y, Maruta T, et al. 2014. Transient expression analysis revealed the importance of VTC2 expression level in light/dark regulation of ascorbate biosynthesis in Arabidopsis. *Biosci Biotech Bioch* 78: 60-66

Yu X, Pasternak T, Eiblmeier M, Ditengou F, Kochersperger P, et al. 2013. Plastid-Localized Glutathione Reductase2-Regulated Glutathione Redox Status Is Essential for Arabidopsis Root Apical Meristem Maintenance. *The Plant cell* 25: 4451-68

Yu YT, Wu Z, Lu K, Bi C, Liang S, et al. 2016. Overexpression of the MYB transcription factor MYB28 or MYB99 confers hypersensitivity to abscisic acid in arabidopsis. *J Plant Biol* 59: 152-61

Zhai QZ, Li CB, Zheng WG, Wu XY, Zhao JH, et al. 2007. Phytochrome chromophore deficiency leads to overproduction of jasmonic acid and elevated expression of jasmonate-responsive genes in Arabidopsis. *Plant & cell physiology* 48: 1061-71

Zhang D, Liu D, Lv X, Wang Y, Xun Z, et al. 2014. The cysteine protease CEP1, a key executor involved in tapetal programmed

cell death, regulates pollen development in Arabidopsis. *The Plant cell* 26: 2939-61

Zhang YZ, Jiao Y, Liu ZH, Zhu YX. 2015. ROW1 maintains quiescent centre identity by confining WOX5 expression to specific cells. *Nat Commun* 6

Zhang Z, Wang J, Zhang R, Huang R. 2012. The ethylene response factor AtERF98 enhances tolerance to salt through the transcriptional activation of ascorbic acid synthesis in Arabidopsis. *Plant J* 71: 273-87

Zimmermann K. FAL, Emily K. Schroeder, Ron J. Bouchard,Kenneth L. Tyler, and Daniel A. Linseman. 2007. Glutathione Binding to the Bcl-2 Homology-3 Domain Groove. *J Biol Chem.* October 5: 29296–304

Zuelke KA, Jeffay SC, Zucker RM, Perreault SD. 2003. Glutathione (GSH) concentrations vary with the cell cycle in maturing hamster oocytes, zygotes, and pre-implantation stage embryos. *Mol Reprod Dev* 64: 106-12